# High-resolution spatial analysis of morphodynamics and habitat changes in the Wadden Sea (SE North Sea)

DISSERTATION

zur Erlangung des Doktorgrades
der Mathematisch-Naturwissenschaftlichen Fakultät
der Christian-Albrechts-Universität
zu Kiel

vorgelegt von

**Tobias Dolch**

Kiel
2008

| | |
|---|---|
| Referent: | Prof. Dr. Horst Sterr |
| Korreferent: | Prof. Dr. Karsten Reise |
| | |
| Tag der mündlichen Prüfung: | 06. Juni 2008 |
| Zum Druck genehmigt: | 06. Juni 2008 |

# Contents

# Summary

The Wadden Sea is a coastal sea which is an ecologically important part of the shallow and sedimentary south-eastern North Sea. It offers large intertidal areas behind a chain of barrier islands and as these unconsolidated sediments are continuously driven by tides, wind and waves, the Wadden Sea is a highly dynamic ecosystem.

The main objective of this study is the analysis and quantification of the variability and development of the Wadden Sea ecosystem. Therefore, both biodynamics and morphodynamics in the northern Wadden Sea at the islands Sylt and Rømø have been taken into consideration on different time scales. Shorelines, surface sediments and megaripples were utilised as the morphodynamic study targets while seagrass beds and mussel beds were taken as biodynamic parameters. Furthermore, the interactions that exist between these study objects were identified and the factors driving their development analysed. Data were collected by remote sensing of high-resolution aerial photographs with a Geographic Information System (GIS) as well as in ground-truth surveys and sampling campaigns.

1) The study on changes of shorelines and other morphological features shows that different processes and diverging developments can be observed within a small coastal area. Increased hydrodynamics caused by rising sea levels and a consequent reduction in tidal catchment areas were identified as having the most extensive and dominant effects, primarily resulting in erosion. Beach replenishment has been noted to successfully restore the balance in coastal erosion, but the artificial input of sediment significantly affects depositional system. Longshore and tidal currents transport the sand, which is replenished at the western shore of Sylt, to the Ellenbogen, which is an area of prevailing sedimentation in the north of the island. Increased accumulation rates are observed here since the beginning of beach replenishments.

2) Coarsening of intertidal sediments is observed throughout the entire European Wadden Sea. It can be ascribed to increased hydrodynamics which cause severe long-term depletion of mud by increasing its resuspension and removal. While exposed areas are most affected by the depletion of fine-grained sediments, medium-term accumulation of fine deposits in sheltered inner areas is also apparent. However, tidal flats are also characterised by constant and considerable short-term variability in the grain size composition and distribution pattern of their surface sediments, which are driven by

weather events and changes in tidal patterns. Considerable changes are observed within a few tidal cycles.

3) A long-term analysis of megaripple populations east of the islands Sylt and Rømø reveals that their extent has almost doubled over the past six decades. This may be related to increased hydrodynamics, which facilitate the formation of megaripples.

4) A significant increase in seagrass bed area has been observed in the northern Wadden Sea since the mid-1990s. This is thought to have occurred due to decreased storm surge levels resulting in sediment stability. However, seagrass beds in the study area do not develop in synchrony and are characterised by considerable short-term fluctuations in bed area. On the other hand, they show recurring overall spatial distribution patterns as they primarily establish at sheltered sites and on high-lying tidal flats. Furthermore, general trends are also observed as they tend to either decline in areas in close vicinity to tidal channels or the beds are shifting away from them entirely. This is indicative of the impact of increased hydrodynamics and it can be assumed that this, associated with sediment instability, will become a major problem for seagrass habitats.

5) Mussel beds can be divided into persistent and temporal beds. Persistent beds are located at sheltered sites and form stable features with consistent spatial distribution patterns that can be observed over several decades. Temporal beds can form in rather exposed areas where they are vulnerable to extreme events, like storms and severe ice scouring, which may result in their abrupt disappearance. Persistent beds dominate in the study area and changes in bed area are primarily caused by their expansion or contraction.

These five study parameters are affected by global climate change, which is among other things indicated in the Wadden Sea by increased hydrodynamics. However, there are also close interactions between them which can serve to amplify the effects of climate change. For example, increased hydrodynamics cause a reduction in vegetation cover, mainly seagrass, resulting in fewer sheltered sites where muddy sediments can establish. This promotes the depletion of mud, in turn enlarging the proportion of sandy tidal areas. Here, the formation of megaripples is facilitated, which interfere with the occurrence of seagrass and mussel beds by their migration.

It is assumed that in the future the Wadden Sea faces substantial change brought about by erosion and the inundation of tidal flats together with the degradation of important habitats, as a consequence of global climate change. It can be expected that morphodynamic and biodynamic processes will accelerate and variability increase. Therefore, continuous

monitoring of a combination of selected abiotic and biotic factors is recommended in order to assess the complex Wadden Sea ecosystem and to detect developmental trends early. The methods introduced in this study are demonstrated to be highly suitable for monitoring, especially in the case of surveillance of high-resolution aerial photographs with GIS, which allows multi-purpose data collection from one information source and analysis within one system.

# Zusammenfassung

Das Wattenmeer ist ein Küstenmeer, welches einen ökologisch äußerst bedeutsamen Teil der flachen Sedimentküste der süd-östlichen Nordsee bildet. Ein Hauptbestandteil sind seine ausgedehnten Gezeitenflächen, die sich hinter einer Kette von sandigen Barriereinseln befinden. Diese unverfestigten Sedimente werden durch ein Zusammenspiel aus Gezeiten, Wind und Wellen gesteuert, wodurch das Wattenmeer ein hochdynamisches Ökosystem darstellt.

Hauptziele der vorliegenden Untersuchung sind die Analyse und die Quantifizierung der Variabilität und der Entwicklung des Ökosystems Wattenmeer. Zu diesem Zweck wurde sowohl die Biodynamik als auch die Morphodynamik im nördlichen Wattenmeer um die Inseln Sylt und Rømø auf verschiedenen Zeitskalen betrachtet. Küstenlinien, Oberflächensedimente des Watts und Megarippel wurden als Untersuchungsobjekte der Morphodynamik herangezogen, während Seegraswiesen und Muschelbänke die Biodynamik repräsentieren. Darüber hinaus wurde untersucht, welche dynamischen Interaktionen zwischen diesen fünf Untersuchungsobjekten bestehen und welche Faktoren ihre Entwicklung steuern. Die hierzu benötigten Daten wurden durch die visuelle Auswertung hoch-aufgelöster Luftbilder mittels eines Geographischen Informations Systems (GIS) sowie durch Mess- und Beprobungskampagnien im Feld erhoben.

1) Die Untersuchung der Veränderung der Küstenlinien und anderer morphologischer Merkmale ergab, dass innerhalb eines kleinräumigen Gebietes verschiedene küstenformende Prozesse und gegensätzliche Entwicklungenstendenzen ablaufen können. Eine verstärkte Hydrodynamik, die durch einen steigenden Meeresspiegel und die Verkleinerung des Einzugsgebietes von Tidebecken hervorgerufen wird, weist die weitreichendsten und dominantesten Effekte auf. Diese äußern sich primär in Form von Erosion. Es konnte gezeigt werden, dass Sandvorspülungen Küstenerosion erfolgreich ausgleichen, aber diese künstliche Sedimentzufuhr auch das Ablagerungssystem signifikant beeinflusst. Während der Sand an der Westküste Sylts vorgespült wird, werden seit Beginn dieser Küstenschutzmaßnahme deutlich erhöhte Akkumulationsraten am Ellenbogen, im Norden Sylts, verzeichnet. Küstenparallele und Tidenströmungen verbringen den Sand von der Westküste in dieses Akkumulationsgebiet.
2) Die Vergröberung der Wattsedimente ist ein Prozess, der im gesamten Wattenmeer verfolgt werden kann. Dieses Phänomen ist ebenfalls in einer ansteigenden Hydrodynamik

begründet, welche zu einer selektiven Erosion der Schlickanteile im Sediment führt. Ton- und Schluffteilchen werden verstärkt resuspensiert und mit der Strömung forttransportiert, wobei exponierte Wattflächen von diesem langfristigen Prozess primär betroffen sind. Trotz der im Watt dominierenden Verarmung an Feinsedimenten, verzeichnen geschützt-liegende Wattflächen eine mittelfristige Schlickakkumulation. Neben diesen langzeitlichen Entwicklungen sind Wattflächen auch durch eine starke kurzfristige Dynamik ihrer Sedimente gekennzeichnet. Diese wird durch die jeweils vorherrschenden Wetter- und Tidebedingungen gesteuert und deutliche Veränderungen können innerhalb weniger Tidenzyklen erfolgen.

3) Eine Langzeituntersuchung von Megarippelfeldern östlich der Inseln Sylt und Rømø ergab nahezu eine Verdopplung ihrer Fläche innerhalb der letzten sechs Jahrzehnte. Dies kann wiederum auf eine verstärkte Hydrodynamik zurückgeführt werden, welche für die Entstehung von Megarippeln vorausgesetzt ist.

4) Im nördlichen Wattenmeer wird seit Mitte der 1990er Jahre eine signifikante Steigerung der Seegraswiesenfläche beobachtet. Dieser Zuwachs wird mit einer Abnahme der Sturmhäufigkeit und einer damit verbundenen Sedimentstabilität erklärt. Dennoch haben sich die Seegraswiesen im Untersuchungsgebiet nicht synchron entwickelt und zeichnen sich durch eine beträchtliche kurzfristige Variabilität ihrer Fläche aus. Anderseits zeigen sie jedoch auch ein generelles räumliches Verteilungsmuster, wonach sich Seegraswiesen vornehmlich in geschützten Lagen und auf höher-gelegenen Wattflächen etablieren. Zudem lassen Seegraswiesen die weit verbreitete Tendenz erkennen, sich in Prielnähe aufzulösen oder sich im Ganzen von Prielen zu entfernen, was auf den Einfluss einer verstärkten Hydrodynamik hindeutet. Diese muss, verbunden mit einer erhöhten Sedimentinstabilität, als wesentlicher Faktor angesehen werden, der zu einem Rückgang von Seegraswiesen im Wattenmeer führen kann.

5) Muschelbänke können in beständige und temporäre Bänke unterschieden werden. Beständige Muschelbänke befinden sich in geschützten Lagen und zeichnen sich durch eine hohe Stabilität aus, wobei ihr generelles räumliches Muster über Jahrzehnte nahezu gleichbleibend ist. Temporäre Muschelbänke können sich in exponierten Lagen bilden. Hier sind sie allerdings Extremereignissen, wie Stürmen und schwerem Eisgang ausgesetzt, die diese Muschelbänke abrupt verschwinden lassen können. Beständige Muschelbänke machen den Hauptbestandteil des Muschelvorkommens im Untersuchungsgebiet aus. Veränderungen in der Gesamtfläche der Muschelbänke im

Untersuchungsgebiet werden somit auch primär durch Ausdehnung und Rückgang bestehender Bänke hervorgerufen. Aufgrund ihres geringeren Anteils an der Gesamtfläche sind großskalige Veränderungen nur selten auf die Dynamik temporärer Muschelbänken zurückzuführen.

Die fünf aufgeführten Untersuchungsobjekte stehen unter dem Einfluss des globalen Klimawandels, der sich im Wattenmeer u. a. durch eine verstärkte Hydrodynamik auswirkt. Aufgrund der engen Interaktionen der Untersuchungsobjekte können sich Effekte des Klimawandels durch Rückkopplungen verstärken. Zum Beispiel führt eine verstärkte Hydrodynamik zu einer Abnahme der Seegrasbestände. Diese wiederum fördern die Ablagerung schlickiger Sedimente. Eine Abnahme der Seegraswiesen begünstigt die Verarmung an Feinmaterial in den Wattsedimenten, wodurch der Anteil an gröberen Sandwatten zunimmt. Sandige Sedimente sind zur Bildung von Megarippeln notwendig. Diese wiederum können durch ihre Wanderung und Dynamik die Existenz von Seegraswiesen und Muschelbänke negativ beeinflussen.

Es ist davon auszugehen, dass das Wattenmeer mit dem Klimawandel beträchtlichen Veränderungen unterworfen ist. Wahrscheinlich sind eine zunehmende Erosion und Überflutung der Wattflächen sowie die Degradation wichtiger Habitate. Zudem werden ein beschleunigter Ablauf und eine gestiegene Variabilität morpho- und biodynamischer Prozesse erwartet. Aus diesen Gründen empfiehlt sich ein kontinuierliches Beobachtungsprogramm. Dieses sollte aus einer Kombination ausgesuchter abiotischer and biotischer Faktoren bestehen, um eine Bewertung des komplexen Ökosystems Wattenmeer vornehmen und Entwicklungstrends frühzeitig erkennen zu können. Die Methoden, die in dieser Studie vorgestellt wurden, erweisen sich hierzu als besonders geeignet. Eine Auswertung hoch-aufgelöster Luftbilder mittels eines Geographischen Informationssystems ermöglicht eine vielseitige Datenerhebung sowie eine Datenanalyse innerhalb desselben Systems.

# 1 General introduction

Approximately two-thirds of the world's coastline consists of sedimentary shores (Reise 2001) and it is estimated that chains of sand barrier islands occupy about eight percent (Postma 1996). The largest, uninterrupted tidal flat and barrier island depositional system in the world is located in the Wadden Sea, which is the shallow and sedimentary coastal zone of the south-eastern North Sea (CWSS 2008). This is the focal region of the present study on morpho- and biodynamics.

The Wadden Sea is a land-sea transition consisting of a network of tidal channels, sandbars, tidal flats, salt marshes and islands (Essink et al. 2005). It forms the largest unbroken system of tidal sand and mud flats and represents one of the most important international wetland habitats. The Wadden Sea ecosystem is characterised by an exceptionally high biological productivity, a unique species composition and a high degree of ecological specialisation and potential for adaptation. It serves as an essential spawning, feeding and nursery area for a wide range of species and sustains birds, fish, crustaceans and seals well beyond its borders (Dittmann 1999, Gätje and Reise 1998, CWSS 2008). Furthermore, it is of great significance as an essential feeding ground for migratory water birds (Nacken and Reise 2000). With regard to the high ecological importance of the Wadden Sea, mussel beds and seagrass beds are two features of major ecological relevance as they are both hotspots of biodiversity and productivity (Riesen and Reise 1982, Fonseca 1996, Asmus 1987, Buschbaum and Saier 2001, Cunha et al. 2005). However, there has been considerable temporal and spatial variability in bed area observed for both habitats on a short and long-term scale (Dankers et al. 1999, Frederiksen 2004a, 2004b, de Vlas et al. 2005, Reise et al. 2005b, Nehls et al. 2006, Reise and Kohlus 2008).

The Wadden Sea is not only a constantly changing system with respect to morphodynamics and biodynamics, but is an outstanding example of ongoing Holocene development of a sandy coast in the face of rising sea levels. The Wadden Sea is characterised by unconsolidated sediments and its natural processes result in a highly dynamic morphology. These include shoreline changes, the dynamics of intertidal sediments, salt marsh erosion and megaripple migrations. The main driving forces for these continuous changes are the tides, waves and wind (CPSL 2001), which also affect tidal flat flora and fauna. However, since its formation this area of coastline has been inhabited by people, resulting in the natural pattern being increasingly disrupted (Reise 2005, Lotze 2005, Lotze et al. 2005). Generally, the Wadden Sea's geological and geomorphological

features are closely related to biophysical processes and these biogeomorphological interactions are notably strong and unique at all scales (CWSS 2008). This can be seen for example in mussel and seagrass beds which interact with sediments (Ward et al. 1984, Philippart et al. 1992, Kröncke 1994, Widdows et al. 2002, Gacia et al. 2003, Mills and Fonseca 2003, Cabaço and Santos 2007).

Furthermore, the Wadden Sea provides valuable insights into the ongoing dynamic adaptation of coastal environments to global change with respect to both morphological and biological aspects and thus can be regarded as a perfect showcase for a changing sedimentary coastal system. As a corollary of global warming, sea level rise is expected to accelerate (IPCC 2007, Rahmstorf 2007). This global process will presumably exacerbate the dynamics of morphological and biological features in the Wadden Sea. This study endeavours to analyse the changes that have occurred over the course of the last century in order to provide lessons for a troubling future.

The overall objective of this study is the analysis and quantification of the variability and development of the islands and backbarrier coastal configurations. Both morphodynamics and biodynamics were taken into consideration on different time scales. Shorelines, surface sediments and megaripples were the morphodynamic study targets, while seagrass and mussel beds were utilised as the biodynamic parameters. The interactions between these morphological and biological parameters were analysed and the factors driving their development identified. A particular emphasis was placed on long-term data in order to distinguish real developmental trends from dynamic equilibriums. In terms of the methodology of the study, the data were obtained through field surveys and samplings as well as by remote sensing of high-resolution aerial photographs. Using these methods, the potential of aerial photographs for the survey of coastal features could be explored. All data were analysed using one Geographic Information System. The combination of remote sensing data with Digital Elevation Models and model data in GIS enabled extensive analysis.

The study is composed of the following chapters:

**Chapter 2** introduces the study area, namely the Wadden Sea and in particular a tidal basin in the northern Wadden Sea, where several representative processes can be observed.

**Chapter 3** reports on long-term changes of shorelines and other morphological features as well as on the effect of sand nourishment on the depositional system.

**Chapter 4** presents the dynamics of intertidal surface sediments and quantifies their changes from one tidal cycle to a 75-year period.

**Chapter 5** combines field and remote sensing data to analyse the dynamics of megaripple populations and individual megaripples and their effect on epibenthic structures.

**Chapter 6** reports on the long and short-term variability and the spatial distribution pattern of seagrass beds.

**Chapter 7** presents the quantitative and qualitative long-term development and the spatial distribution pattern of mussel beds.

In the final chapter, a general discussion combines the results from the individual studies presented in the chapters 3 to 7. It is concluded that, in addition to inherent variability, trends in the morphology and biotic habitats of the seabed surrounding Sylt and Rømø Islands serve as indicators of the expected outcomes for the entire Wadden Sea area over the coming decades if the scenarios of global warming and raised sea levels eventuate.

# 2 Study area

This study was conducted in the Wadden Sea, which represents an accumulative sedimentary tidal coast (Kelletat 1989). The survey area is the List tidal basin, which is located in the northern Wadden Sea. Several coastal processes, which are representative for this type of coast, can be observed here. In this study, shorelines changes were examined on the islands Sylt, Rømø and Jordsand. The dynamic of intertidal surface sediments was analysed in the tidal bay Königshafen, where also populations of megaripples were investigated. A comparative study on another megaripple field was conducted in the Blidselbucht (Fig. 2.2). The biological parameters of this study, namely seagrass and mussel beds, were analysed in the entire List tidal basin.

## 2.1 North Sea and Wadden Sea

The North Sea is a semi-enclosed, epi-continental, large marine ecosystem in northern Europe (Fig. 2.1a). It compromises a part of the North Atlantic and is a marginal sea, which covers an area of 750 000 $km^2$ (Sterr 2003). The present-day North Sea has been formed after the last glaciation. Its southern one-third was formerly a land basin which has been inundated through the Holocene transgression. This basin is relatively shallow (average depth of 94 m) and heavily sedimented (Ducrotoy et al. 2000, Sterr 2003). Especially the south-eastern North Sea coast is shallow and sedimentary. Sand beaches and dunes prevail here. This coastal zone is called the Wadden Sea (Fig. 2.1b). It is a coastal sea which offers large intertidal areas behind a chain of barrier islands. The Wadden Sea is an ecologically important part of the North Sea and covers 1 % of its total area where about half of it are tidal flats.

The Wadden Sea consists of a network of tidal channels, sandbars, tidal flats, salt marshes and islands and creates a transition zone between land and sea (Essink et al. 2005). It forms a narrow strip stretching over 450 km along the North Sea coast from Den Helder in the Netherlands along Germany up to Blåvandshuk in Denmark (de Jong et al. 1999) (Fig. 2.1b). This sedimentary environment covers 14 700 $km^2$ (11 200 $km^2$ are allotted to a conservation area) which makes it one of the largest wetlands worldwide (Essink et al. 2005). In cross-section, the Wadden Sea extends from the shoreline to the 10 m depth contour including estuaries like the Ems, Elbe and Weser estuary.

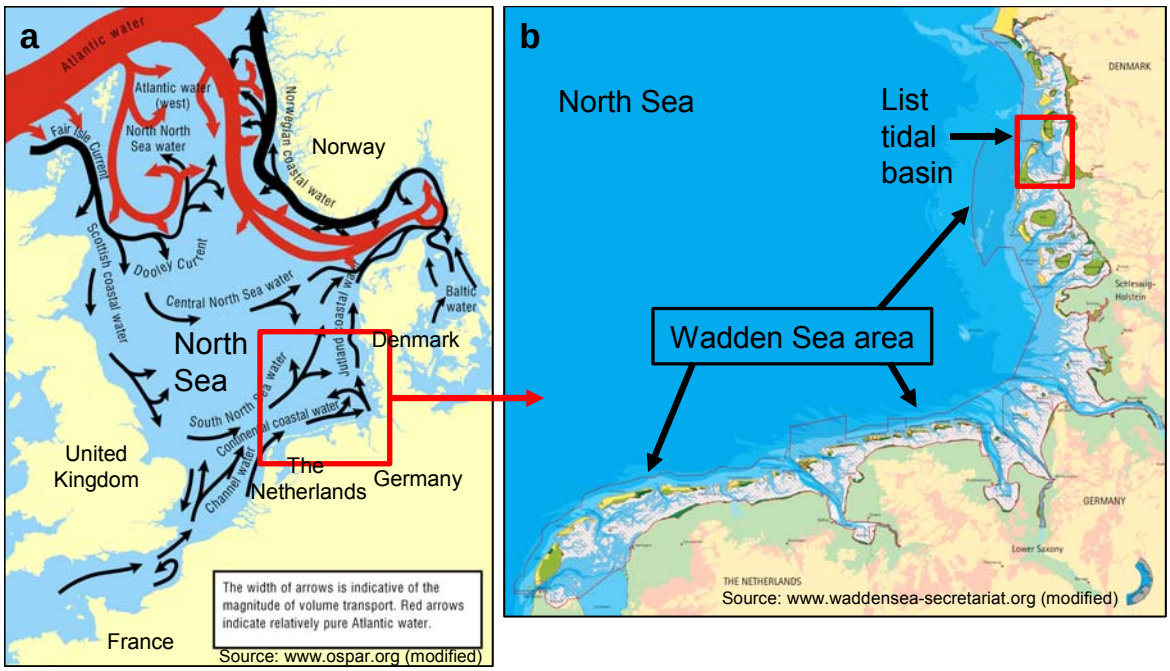


**Fig. 2.1:** The North Sea (a) and Wadden Sea area (b). The Wadden Sea is the shallow sedimentary coast of the south-eastern North Sea. The study area List tidal basin (b) is located in the northern Wadden Sea at the German-Danish border.

The Wadden Sea is characterized by unconsolidated sediments and a highly dynamic morphology. The main driving forces for the continuous changes are tides, waves and wind, and sediment transport is the main linking factor between these forces (CPSL 2001). Some changes lead to new conditions, like the shoreline changes, but more often dynamic equilibriums, like seasonal changes in the sedimentary system (Andersen and Pejrup 2001, Chang et al. 2006), are observed.

The Wadden Sea is further characterized by high dynamics in salinity, light, oxygen and temperature caused by daily changing flood and ebb tides. This has resulted in a complex system which is habitat for a unique flora and fauna. Productivity and size of the Wadden Sea provide a basis for the reproduction of North Sea fish stocks (Ducrotoy et al. 2000) and for its function as a turntable of bird migration (Essink et al. 2005). It is an open system interacting with the adjacent North Sea and functioning as a large filter for suspended matter from marine and riverine sources (CWSS 2008).

The List tidal basin is the survey area of the present study. It is located in the northern Wadden Sea at the German-Danish border (54° 50' - 55° 09' N and 8° 20' - 8° 42' E). Reise and Gätje (1997) found tidal basins to be the most suitable units for monitoring and research in the Wadden Sea. As the List tidal basin has a long and continuous history of research and well-defined borders, it is an ideal survey area (Reise and Gätje 1997). Ecological research was already conducted here by Möbius in 1869 and continued as well

as complemented e.g. by Nienburg (1927), Wohlenberg (1935, 1937), Hagmeier (1941), Kornmann (1952) and Reise (1985) (Reise and Lackschewitz 1998).

## 2.2 List tidal basin

The List tidal basin has a size of approx. 18 km (E-W) by 30 km (N-S) and a total area of 406 km$^2$ (Fig. 2.2). It forms a spatially almost closed system as it is framed by the German island Sylt and the Danish island Rømø, as well as the German and Danish mainland and two causeways that connect the islands with the mainland (Gätje and Reise 1998). The mainland is protected by the two barrier islands and borders directly the tidal flats. Dikes are constructed along most of the mainland shore except of the centre where a Pleistocene cliff has formed. Groins are often built in front of the dikes. Larger salt marshes also established in front of the dike in the north-eastern and south-eastern part of the List tidal basin.

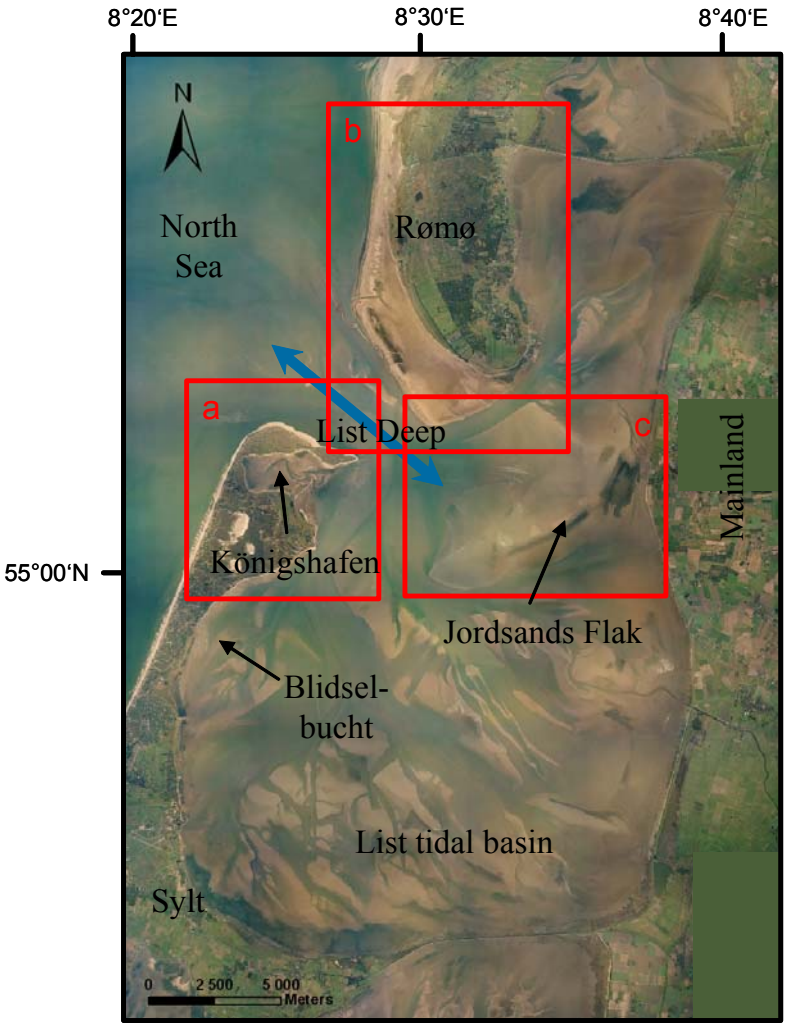


**Fig. 2.2:** The study area List tidal basin in the northern Wadden Sea. A special focus is laid on the northern part of the island of Sylt with the bay Königshafen (a), the southern part of the island of Rømø (b) and the former island of Jordsand with the spacious tidal flat area Jordsands Flak (c). The blue double-headed arrow symbolises the water flows through the tidal inlet List Deep.

The List tidal basin was formed after the last glaciation about 5500 years ago. Severe human impact can be recorded since the medieval times (Reise 1998, Bayerl and Köster 1998) but most man-made changes occurred in the 20$^{th}$ century. Notable are the constructions of the Hindenburg causeway (1927) (Wohlenberg 1953) and the Rømø causeway (1948) (Jespersen and Rasmussen 1984) as well as land claim measures along the Danish mainland shore from 1954 to 1972 and the formation of the Margrethe-Koog from 1979 to 1982 (Jespersen and Rasmussen 1989). Until today the tidal catchment area was reduced by about 200 km$^2$ mainly by successive embankment (Bayerl and Köster 1998).

The basins only connection to the open North Sea is the tidal inlet List Deep, which has a maximum depth of 40 m and a width of 2.8 km at its narrowest section (Fig. 2.2). Strong currents with maximum velocities of about 1.3 m s$^{-1}$ can be observed in the inlet (Backhaus et al. 1998) caused by 550 million m$^3$ water which are passing it with every tide. Three tidal channels diverge from the List Deep: the Rømø Dyb runs towards north-east while the Højer Dyb flows in south-east and the Lister Ley in southward direction. They reach a maximum depth of 20 m (Bayerl and Köster 1998) and show maximum current velocities of 0.6 m s$^{-1}$.

The tides are semi-diurnal and the mean tidal range is 1.8 m (Backhaus et al. 1998). The size of the water body in the List tidal basin varies considerably from 1120 million m$^3$ at high tide to 570 million m$^3$ at low tide whereas the salinity remains close to 30 - 32 psu. Water levels, as well as current velocities, are affected by wind direction and wind force. Westerly winds lead to higher water levels. This is further amplified with increasing wind speed. On the other hand, lower water levels are caused by easterly winds (Backhaus et al. 1998, Behrens et al. 1997). In the long-term view there is a rising trend in the high tide level recorded at the gauge List. While the mean low tide level remained relatively stable at 402.9 cm (average 1936 – 2005, data refers to gauge List), the mean high tide level rose from 567.81 cm (1936 – 1945) to 585.23 cm (1996 – 2005) with an average of 575.4 cm (1936 - 2005) (data from WSA Tönning, Waterways and Shipping Board Tönning) (Fig. 2.3). Regarding the period 1936 to 2005, the mean high tide level rose about 2.5 mm yr$^{-1}$, while the rise was even 3.0 mm yr$^{-1}$ from 1956 to 2005. As the mean low tide level remained relatively stable, this increased the tidal range which has a direct effect on the current velocities in the basin, resulting in an increased water exchange.

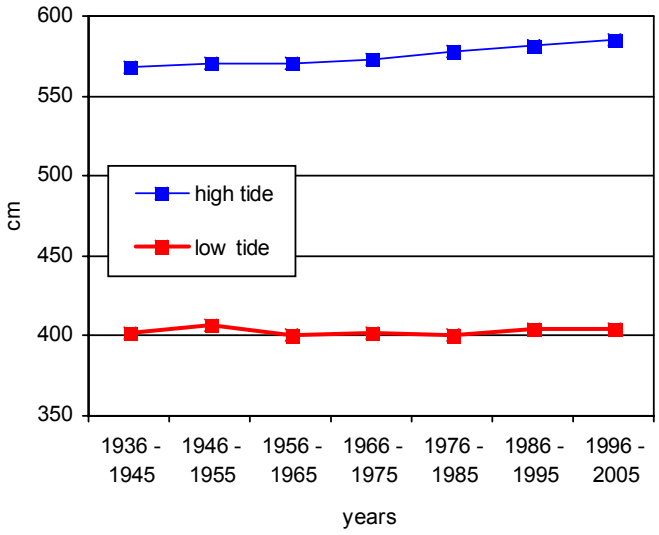


**Fig. 2.3:** Development of the high and low tide water level in the List tidal basin shown in 10-year averages from 1936 to 2005 (data from the gauge List).

Due to the shallow terrain, 40 % of the bight (159 $km^2$) are emerged during low tide (Bayerl and Köster 1998). The shallowness goes also along with rather slow current velocities which are often below 0.1 m $s^{-1}$ on the tidal flats (Backhaus et al. 1998). Sand is predominant on the tidal flats as it covers 72 % of the intertidal area (114.7 $km^2$). Mixed sediments occur as narrow belts close to the shore along the two islands and the dykes making up 25 % of the intertidal area (39 $km^2$). Muddy sediments form only 3 % (5.3 $km^2$) (Bayerl et al. 1998). The List tidal basin shows a typical spatial distribution of sediments with an increasing share of fine-grained sediments from the sandy centre towards its margins. The median grain size ranges from less than 2 φ (Phi) in vicinity to the Lister Deep to more than 3 φ at the margins of the basin (Bayerl et al. 1998).

Megaripples are morphological bedforms that occur along the entire width of the basin (east-west direction) but their north-south extent is limited and their occurrence focused on the centre of the basin. They can develop adjacent to the tidal inlet and the tidal channels where the sediment is sandy and the currents are sufficient to form them. The Blidselbucht east of the island of Sylt is an area where distinct megaripple populations established (Fig. 2.2).

The annual average water temperature in the List tidal basin is 9.0°C, with 5.3°C in winter and 13.7°C in summer. The air temperature is close to these data with an annual average of 8.4°C, with 4.8°C in winter and 12.8°C in summer (Backhaus et al. 1998). Ice cover was usually recorded during wintertime but became less in recent years. Just 13 years with no ice cover were registered from 1955 to 1997. However, for the last 10 years already 7 ice free winters are reported. Furthermore, the periods of ice cover are considerably shorter

and the measured ice layers are less thick compared to the earlier years (data from BSH, Federal Maritime and Hydrographic Agency, Hamburg).

Seagrass beds and mussel beds are primarily located in the parts of the intertidal that offer shelter from westerly storms. While the dwarf eelgrass *Zostera noltii* grows mainly in the upper intertidal area (+0.3 to 0.0 m), the eelgrass *Zostera marina* occurs primarily in the lower intertidal (0.0 to -0.5 m). Today, seagrass beds cover 19.8 % of the intertidal area which is a high value compared to other tidal basins in the Wadden Sea (Reise and Lackschewitz 1998). Mussel beds are located from the mid to the lower intertidal and cover 0.8 % of the intertidal area.

## 2.3 Königshafen

The Königshafen is part of the List tidal basin. It is a sheltered tidal bay in the northern part of the island of Sylt (55° 02' N, 8° 25' E) with an extent of 3.5 km (E-W) by 1.4 km (N-S) (Fig. 2.4). The Königshafen is almost completely enclosed except for a 650 m wide opening in the east and water is mainly exchanged through a central tidal creek.


**Fig. 2.4:** The Königshafen at the northern top of the island of Sylt. The bay was created by the formation of the sand spit Ellenbogen and is divided in an inner and outer part.

The Königshafen exists as a sheltered, almost enclosed bay since the formation of the large sandy spit (Ellenbogen) at its north at least 1300 years ago (Lindhorst et al., in prep.). Today, the Königshafen is not in its original state as it experienced man-made changes. The changes with the greatest impact are in regard of the reduction of the tidal catchment

area by the construction of a dike at the southern shoreline of the Königshafen (Mövenberg dike in 1937) and the artificial landfill of the island Uthörn (in the early 1940s) (Bayerl and Köster 1998).

The area is divided into the shallow, inner Königshafen which is located west of the island Uthörn and the outer Königshafen east of it. The outer Königshafen forms the transition to the open List tidal basin and borders one of its main tidal channels, Lister Ley. Due to this vicinity to the tidal channel the outer Königshafen is much more exposed to stronger currents than the sheltered inner Königshafen. Maximum current velocities of 0.6 m $s^{-1}$ are measured in the tidal channel while the current velocities on the tidal flats are often below 0.1 m $s^{-1}$ (Backhaus et al. 1998). Generally at low tide, the entire inner Königshafen falls dry except of the central tidal creek, while most of the outer Königshafen is subtidal and always covered with water at water depths between 2 and 8 m. The Königshafen seems to be ebb-dominated as this can be derived from the shapes of the megaripples.

Like in the List tidal basin the sediments in the Königshafen consist primarily of medium sand (80 %). Mud and fine sands can be found in sheltered locations such as the inner part of the Königshafen and in the lee-side of a sandy hook in the outer Königshafen. The sandy hook is a remarkable morphological feature of the Königshafen. It is characterised by a highly dynamic development. Other interesting morphological features are megaripples, which cover larger parts of the predominantly sandy Königshafen. Their occurrence is concentrated on the outer Königshafen and on the vicinity of the central tidal creek in the inner Königshafen.

Epibenthic biogenic structures such as mussel beds and seagrass beds can also be found in the Königshafen (Reise et al. 1989). Reise et al. (1994) estimate the seagrass beds in Königshafen to amount to 59.7 ha and the mussel beds to 4.6 ha in 1990. Recent results are presented in this study in Chapters 6.3.2 and 7.3.2.

## 2.4 Island of Sylt

The German island of Sylt has a north-south extent of 35 km and a maximum of 12 km in east-west direction in the centre of the island. The northern and southern sandy elongations are rather narrow with widths of 1 km and 1.3 to 4 km respectively. The broadened centre of the island is its backbone consisting of three cores of glacial deposits which were formed in the Saale Ice Age. With the post-glacial sea-level rise, mainly the western Pleistocene core has been eroded by wave action. It served as a supplier of sand for the

southwards and northwards directed sandy spits which were formed by longshore currents (Bayerl and Higelke 1994).

Compared to neighbouring islands the position of Sylt is more offshore (Fig. 2.1b) and therefore more exposed, making it more vulnerable, e.g. to sea level change or extreme weather events.

Sylt receives strong winds and westerly winds are prevailing. They make up to 50 % of the annual frequency even though a northward shift is observed in recent years. The average mean wind force is 7.2 ± 1.1 m $s^{-1}$ (January 1980 to June 2007), at which the average of the maximum wind force is 26.2 ± 5.6 m $s^{-1}$ (January 1991 to July 2007) (all data from DWD).

Northern Sylt can be divided into three parts: the western, northern and eastern shores (Fig. 2.5).


**Fig. 2.5:** The northern part of the island of Sylt with its west, north and east shore.

The western shore is characterised by sandy beaches with an adjoining belt of sand dunes. It is facing the open North Sea and is exposed to a consistent westerly wave wash as well as strong, primarily north-directed longshore currents. The western shore is strongly controlled by high wave energy and westerly winds amplify the waves. Wave height and wave period on Sylt varied from 3 m with 9 s and 0.1 m with 4 s, mean wave height 0.7 ± 0.5 m (Menn 2002). As a result, the western shore undergoes high erosion rates (Ahrendt and Thiede 2001) caused by a combination of waves and strong currents (hydrodynamics).

The western beaches of Sylt are eroding, coarse grained and steep. The beach sand shows a median diameter of 0.84 φ ranging from 2.12 to 0.17 φ (0.56 ± 0.33 mm). Regarding a cross-shore profile from the beach to the sea, the -7 m depth contour line is reached about 1 km west of the mean high water line. The beachface is steep with a slope of 2 to 4° (Menn 2002) which results in a horizontal distance of 25 to 30 m between mean high and low tide marks (Fig. 2.6). The slope shows a clear seasonality as it is flatter during winter and steeper during summer (Menn 2001). During winter the western shore tends more towards "longshore bar-through" and "rhythmic bar and beach" types and during summer it resembles more "transverse bar and rip" and "low tide terrace" beach types (see Short 1999 for more details).

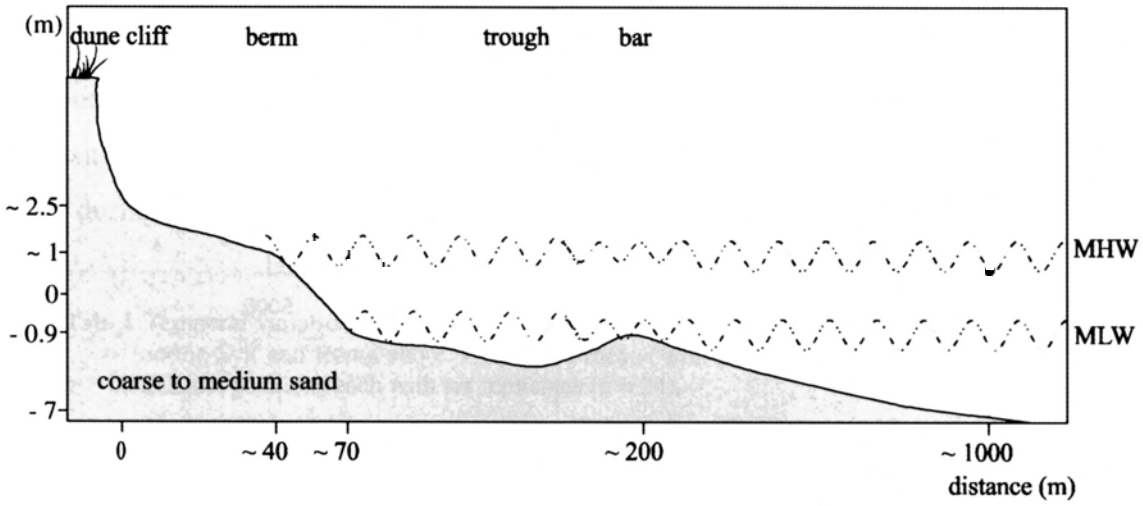


**Fig. 2.6:** A cross-profile of the western beach of the island of Sylt showing the steep beachface (from Menn 2001).

The northern shore is formed by a 4.3 km long, narrow sandy spit which runs in west- east direction. The beaches are sandy and partly wide (up to 160 m). The northern shore adjoins the tidal inlet List Deep with its strong currents.

The eastern shore is in a sheltered position by the island of Sylt and adjoins the shallow List tidal basin with its tidal flats. It has narrow beaches (15 m) and mainly borders the tidal flats directly. Compared to the western shore, it receives low wave energy. Current velocities at the eastern shoreline depend on the distance to the nearest tidal channel. The eastern shore is petrified by stone revetments to a large extent (Reise and Lackschewitz 2003).

The impressive landscape and the long sandy beaches of Sylt attract many tourists over the entire year. The island has 22 000 inhabitants and the number of tourist beds amounts to

50 000. Approximately 600 000 tourists are visiting the Sylt each year and tourism is the most important economical factor (www.syltinfo.de 2008).

## 2.5 Island of Rømø

Just like Sylt is Rømø part of the barrier island chain west of the mainland coast. Rømø is located just north of Sylt but positioned closer to the mainland. The two islands are separated by the tidal inlet List Deep, which has a minimum width of 2.8 km (Fig. 2.2).

Rømø has a north-south extent of 16 km and a width of 6 km (E-W), including the extensive Havsand at the western shore (Fig. 2.7). Climatic conditions are similar to Sylt.


**Fig. 2.7:** The southern part of the island of Rømø with the high sand Havsand at its western shore.

The late period (2900 BP to today) of the Holocene transgression is characterized by a slow rise in mean sea level. The pleistocene landscape inundated by the rising sea consisted primarily of gently sloping sandy outwash plains. This was the precondition for the formation of barrier islands (Bartholdy and Pejrup 1994). The formation started with the creation of a beach ridge system. The continuous arrival of high quantities of sediment has further led to the development of Rømø and other Danish barrier islands (Jacobsen 1998).

Rømø still receives material from two sources. The island is located south of a south-going littoral drift compartment, deriving its sand from coastal attack of the moraine deposits in the northern part of Jutland (0.5 to 1 mill $m^3$ $yr^{-1}$). Furthermore, it is located north of a smaller north-going littoral drift compartment originating at the island of Sylt (Bartholdy and Pejrup 1994). A certain amount of this volume is eroded by hydrodynamics but Rømø is a typical example for a prograding coastline. This means that the island is actually accreting during a transgression because a surplus of sand at present reverses the erosive tendency of the "transgressive" barrier-system (Bartholdy and Pejrup 1994).

The western shore is accreting, fine-grained and flat profiled. The median diameter of the beach sediments is 2.32 φ (Phi) ranging from 2.74 to 2.0 φ (0.20 ± 0.05 mm) (Menn 2002). Regarding a cross-shore profile from the beach to the sea, the -7 m depth contour line is reached about 5 to 5.5 km west of the mean high water line (Fig. 2.8). This beach is wide with a flat beachface (slope ≤ 1°) and a horizontal distance of 150 to 200 m. The mean beach profile is constant during the year. Compared to Sylt, the island proper of Rømø receives less wave energy and is not strongly controlled by it because much wave energy dissipates at the broad and flat offshore profile. This can also be derived from the finer grain size of the beach sediments. According to the characteristics described by Short (1999), the western beach resembles a dissipative beach type throughout the year. The term 'dissipative' is related to the wave energy which abates along the flat beach profile.

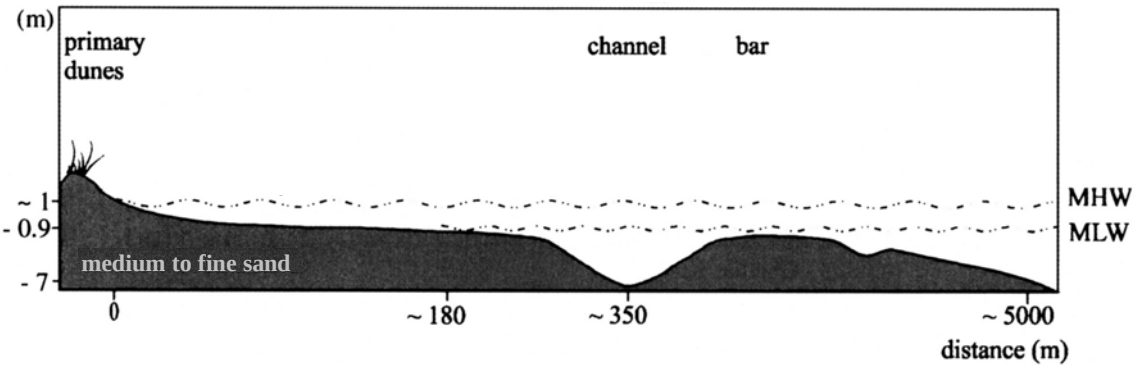


**Fig. 2.8:** A cross-profile of the western beach of the island of Rømø. In contrast to the western shore of the island of Sylt, beachface is flat (from Menn 2001).

The Havsand is part of Rømø (Fig. 2.7). It is a high sand situated south-west off the vegetated island proper. It has a width of 600 to 2500 m and a size of 3 $km^2$. As a high sand, the Havsand remains uncovered at normal high tides and forms a bridge between the tidal flats and the island proper. According to the classification by Jacobsen (1998),

Havsand is a high sand of the second category which means that it lies exposed in the tidal channel area. The Havsand is unvegetated except for newly developed primary dunes.

In the south of the island, Havsand adjoins the tidal inlet List Deep.

The south-eastern and eastern shore of Rømø borders mainly directly the tidal flats, sometimes with a narrow beach (up to 10 m width) as transition. The conditions are similar to the eastern shore of Sylt: the nearshore current velocities, which the island proper is exposed to, depend on the vicinity of the tidal channel to the shore.

Like on Sylt, Rømø is a popular tourist spot and tourism is a very important economical factor. Even though the island has only 850 inhabitants, Rømø shows a large capacity for tourism, expressed in hotels, holiday homes, hostels and camping sites (www.romo.dk 2008).

## 2.6 Jordsand

The island of Jordsand was first mentioned in 1231 and located in the centre of the shallow List tidal basin. It was at a minimum of 5 km away from the next shoreline. According to historical documents, it must have had a considerable size of 3 by 3 km in late medieval times. The island was large enough for two farms and pastures but it was already a low-lying area then. Therefore, erosion and loss of land is long-known as the first written evidence is from 1613. Numerous storm events which led to further loss of the island are recorded (Jespersen and Rasmussen 1975, 1989). As the buildings were abandoned, Jordsand gained more ecological importance, especially as a flood-free breeding area for many shore birds and as a resting area for thousands of migrating birds (Jepsen 1977). However, the island sank presumably in the mid to late 1990s.

Jordsand was Denmark's only holm and situated at the top front of Jordsands Flak – a spacious (30 $km^2$), wedge-shaped tidal flat area (Jespersen and Rasmussen 1989) (Fig. 2.9). Starting from the Danish mainland, Jordsands Flak protrudes still far into the tidal basin and is flanked by two tidal channels: Rømø Dyb in the north and Højer Dyb in the west and south. Jordsands Flak also experiences severe attacks from the sea, especially at the north-west front as the open North Sea lies in this direction.

In its centre, Jordsands Flak has a rather large (5 $km^2$) lengthwise elevated sand accretion that runs in northeast - southwest direction. The island Jordsand was situated at the south-western end of this sand accretion.

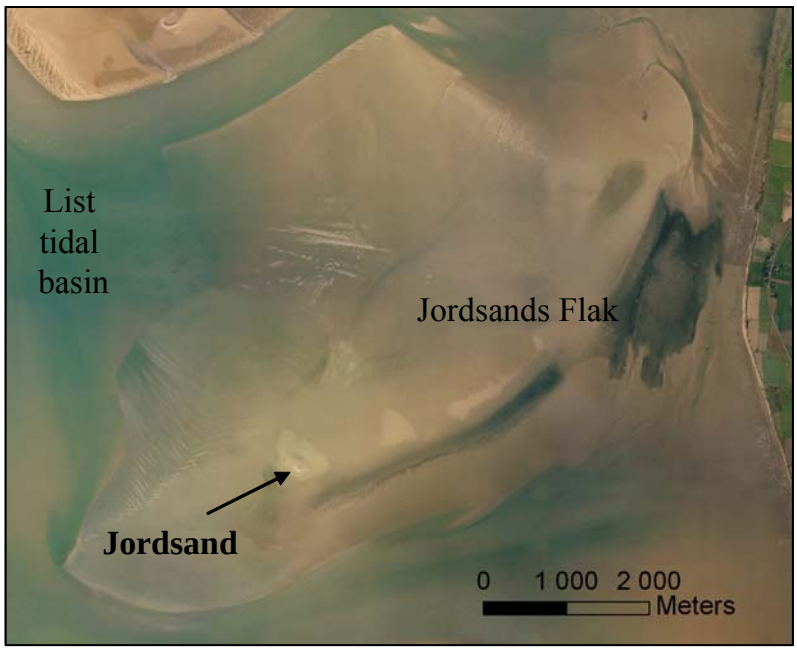


**Fig. 2.9:** The former island of Jordsand at the top front of the spacious tidal flat area Jordsands Flak.

It is hypothesised that Jordsand – together with the Danish islands Langli and Mandø north of it –is a remnant of formerly active barrier islands. These three are regarded to be part of an older barrier coastline, perhaps the "original" one left over after the sea reached the present level for the first time about 2900 years ago (Bartholdy and Pejrup 1994).

# 3 Analysis of long-term changes of sandy island shorelines utilising high-resolution aerial photography

## 3.1 Introduction

Sandy beaches occur on all sedimentary shorelines exposed to waves, wherever there is sufficient sediment for the waves to deposit it above sea level. It is estimated that sandy beaches cover 11 % (53 000 km) to 34 % (170 000 km) and chains of sand barrier islands, like e.g. found in the European Wadden Sea, occupy about 8 % of the world's coastline (Postma 1996, Short 1999).

Coasts are dynamic in nature and this applies especially to sandy shores as they consist of unconsolidated sediments. With increasing human population in coastal areas, the study of changing shorelines has become more and more important. Especially when shoreline retreat occurs on a human time scale, the quantification of erosion rates is essential for many reasons, e.g. land use decisions, efficiency check of shoreline protection structures, identification of erosion 'hotspots' and determination of possible hazards for constructions and people (Moore 2000, Moore and Griggs 2002). Most of the world's shorelines are in a state of erosion. More than 70 % by length of beach-fringed shorelines retreated over the past few decades, while less than 10 % prograded and the remaining 20 to 30 % having shown no measurable change (Bird 2000). Net erosion happens for different and often multiple reasons as several factors contribute to it and erosion is expected to increase as a result of global warming (Bird 2000, Pilkey and Cooper 2004). The global sea level rose about 0.2 meters from 1880 to 1990 and a further rise of 0.5 to 1.4 meters above the 1990 level is projected until 2100 (Rahmstorf 2007).

Climate change is also holding great risk to densely populated coastal zones of Germany. The overall damage potential as a result of sea level rise and increased erosion is estimated for Germany at 330 to 410 billon €, in which the impact is greater on the North Sea coast than on the Baltic Sea coast due to more low-lying areas (Sterr 2000b, 2002).

The sedimentary coast of the south-eastern North Sea is one of the world's largest continuous sandy shores. According to Kelletat (1995), it is classified as a sandy tidal coast, characterised by barrier sands, barrier islands and sandy spits. This combination of loose sands and tides result in a highly dynamic ecosystem, which is formed and constantly changed by wind, waves and currents. Therefore, surveys of shorelines are essential. In the study area of this survey, many coastal processes are observed which can be regarded as

representative for the Wadden Sea as e.g. the island Jordsand and the western shore of the island of Sylt are retreating while the western shore of the island of Rømø is prograding. Prograding beaches are rather infrequent and occur in areas of high sediment supply whereas retreating beaches tend to be the rule. According to the descriptions given by Bird (2000) the western shore of Sylt is a typical example for an eroding beach which can be recognized by its morphology with a concave beach slope backed by a cliff cut into backshore dunes (Fig. 2.6). The retreat of this shoreline can be retraced for the last 7500 years (Thiede and Ahrendt 2000) and estimations of its current annual retreat rate are ranging from 1.0 to 1.75 m (Larson et al. 1999, Thiede and Ahrendt 2000, CPSL 2005). All estimates confirm that the retreat rate increased in the last decades. The main causes for this are the rising sea level and storm surge frequency since 1960 (Hofstede 1997, CPSL 2001). Especially storms and waves in combination with high water levels are causing erosion and retreat of dunes and cliffs. The eroded material is temporarily deposited in the nearshore area after which it gets transported northwards by longshore currents (Larson et al. 1999). Estimates of annual sand losses along the entire western shore of Sylt are varying from 1.1 to 1.5 million $m^3$ (Larson et al. 1999, Ahrendt and Thiede 2001, CPSL 2005). However, the northern part of the island is particularly affected as it is angled 20° eastwards which facilitates erosion (Ahrendt 1993). Sand losses are estimated to be twice as much than in the southern part of the western shore of Sylt (Larson et al. 1999). In order to compensate losses and to stabilise shorelines, sand replenishment is carried out at Sylt almost annually since 1972. Sand replenishment is carried out along the outer shore of sandy barrier islands in the entire European Wadden Sea (Ahrendt 1993, Postma 1996, Eitner 1996 CPSL 2001). For example, the total amount of replenished sand from 1970 to 2002, is amounted 47.6 million $m^3$ in the Dutch Wadden Sea and 33 million $m^3$ for the island of Sylt (CPSL 2005). Even though this measure is costly, time-consuming and its benefit temporal, it successfully balances coastal erosion, turned out to be the best environmental practice and is recommended to be applied wherever feasible (CPSL 2001, CPSL 2005).

Sand replenishment is one among many other human measures, which modify coastal areas. Today, ‘natural coasts’ are rare and the ‘modern coast’ is a combination of stabilising and / or compensating human measures as well as natural adjusting coastal processes (Reise 2005). The Wadden Sea has undergone radical changes and transformations, which are ascribed to human interactions and often resulted in severe decline of habitats and biodiversity for at least 2000 years (Reise 1998, Lotze 2005, Lotze

et al. 2005, Reise 2005). The List tidal basin in the northern Wadden Sea has also been affected. Reise (1998) estimates that over the last 500 years one third of this basin has been converted into land by embankment and its tidal flat area decreased from approx. 66 to 40 % within the 20th century. Several human interactions have taken place during the survey period of this study: the tidal catchment area of the List tidal basin was considerably reduced by the construction of the Hindenburg causeway (1927) and the Rømø causeway (1948), the formation of the Lister Koog (1937) and Margrethe-Koog (1979 - 1982) by embankment, the artificial landfill of the island Uthörn (early 1940s) and land claim measures along the Danish mainland shore (1954 - 1972) (Wohlenberg 1953, Jespersen and Rasmussen 1984, 1989, Bayerl and Köster 1998) (Fig. 3.1).

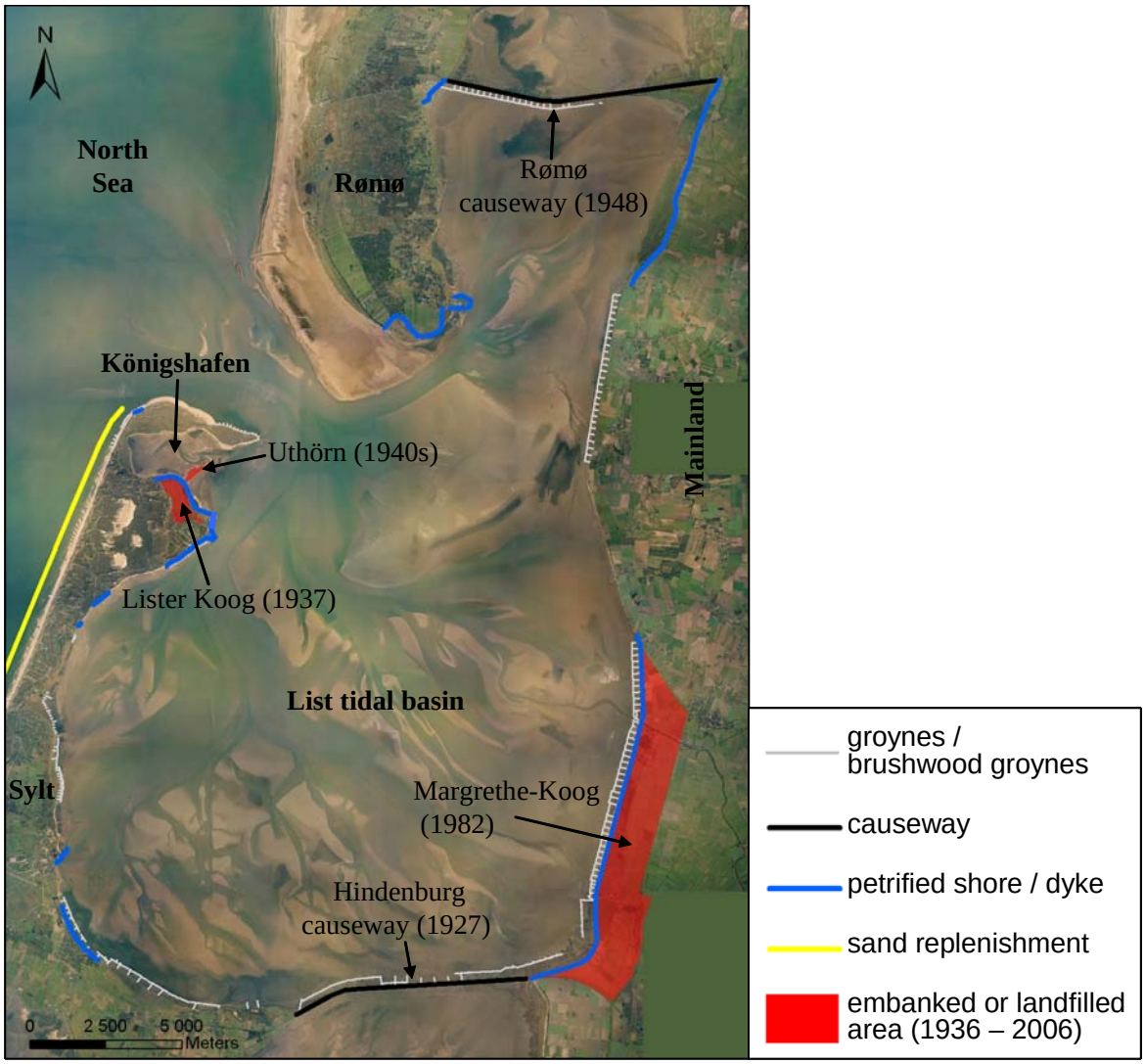


**Fig. 3.1:** Human modifications of the List tidal basin. This overview is compiled based on CPSL 2001, Reise and Lackschewitz 2003, ALR 2007 and own observations.

However, in order to survey the effects of coastal protection measures, especially of sand replenishment, Anders and Byrnes (1991) found the analysis of aerial photographs most suitable, also to develop cost/benefit analyses. Shoreline monitoring on the basis of aerial photographs and a Geographic Information System (GIS) was also conducted in this study. This method is a common technique carried out in various regions, e.g. California (Moore and Griggs 2002, Hapke 2005), Malaysia (Li et al. 1998), China (Chen et al. 2005), Jamaica (Robinson 2004), Bahamas (Rankey and Morgan 2002), Peru (Rogers et al. 2004) and Baltic Sea (Röber and Rudolphi 2004). It was beneficial for this study that a long-term set (dating back to 1928) of high-resolution aerial photographs was available for this sandy environment. Meaningful shoreline change data can only be developed for areas undergoing rapid change or where a long history of shoreline position data is available (Anders and Byrnes 1991). Besides exploring the potential of aerial photographs, an aim of the study was to reconstruct and to forecast the diverging developments of shorelines in the area. The use of Digital Elevation Models (DEM) enabled 3D-analyses and allowed the quantification of volumes of shoreline changes. Furthermore, the efficiency of beach replenishment was monitored and the consequences for the depositional system determined. It was also examined how dynamic morphological features in the Wadden Sea are and if hints for sea level rise and increased hydrodynamics can be detected from their development.

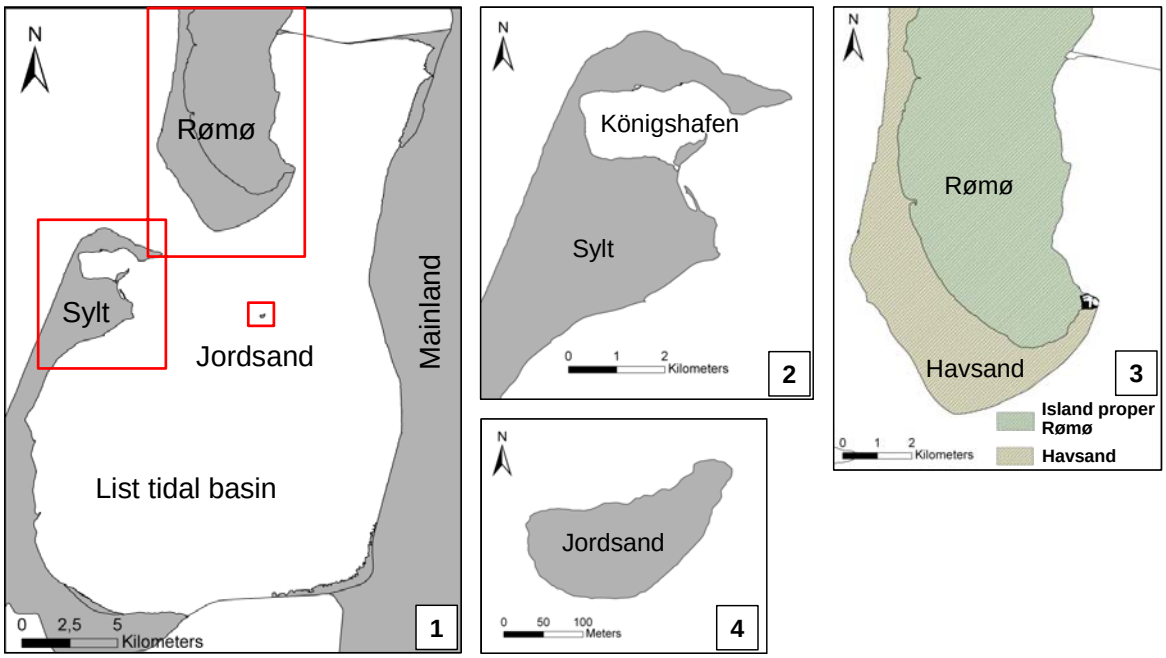


**Fig. 3.2:** The List tidal basin (1) with the focus areas northern Sylt (2), southern Rømø (3) and Jordsand (4).

A preselection of focus areas was made after visual analysis of shorelines: the northern part of the island of Sylt, the southern half of the island of Rømø including Havsand and Jordsand on Jordsands Flak were chosen (Fig. 3.2). These shorelines were selected because they turned out to be most interesting, as they are highly dynamic and develop divergently. They are subject to natural coastal processes, which can be regarded as representative for the Wadden Sea region, albeit often to some degree modified by human interferences

## 3.2 Materials and methods

The base of this study is a set of high-resolution aerial photographs and Digital Elevation Models (DEM) from different years. The aerial photographs were used to derive shoreline positions and volume changes were calculated on the base of the DEMs. The aerial photographs cover at maximum a period of 79 years. This long-term view has the advantage to level out omnipresent short-term fluctuations of shorelines, and to detect and quantify directional developments (Dolan et al. 1991, Anders and Byrnes 1991).

### 3.2.1 Aerial photographs

The aerial photographs are partly from the Alfred-Wegener-Institute for Polar and Marine Research (AWI) but most of them are from external sources. They were provided by the Regional State Office for the Rural Areas (ALR) in Husum, the Regional Office of the Schleswig-Holstein Wadden Sea National Park (NPA) in Tönning, but now united as LKN, and the Sønderjyllands Amt (SJA) in Tønder / Denmark. The photographs were taken at low tide and cover a time period from 1928 to 2006. In recent years the flights are taking place rather regularly but especially in the early years there are considerable time gaps in-between. Depending on their purposes or which authority commissioned them, most aerial surveys covered only partially the List tidal basin. As the German-Danish border runs across the bay, aerial photographs for particular years are in general only available either for the German or the Danish part. Surveys of the two countries were not arranged or carried out at the same time. It has been only since 2003 that pictures can be obtained which cover the entire basin and are taken annually. For further details on the aerial photographs see Table 3.1.

**Table 3.1:** Metadata on the aerial photographs. The 'pixel size' is a scale for the digital resolution of the aerial photograph and gives the size of a ground pixel. OPM indicates if the photos were provided as digital Orthophotomosaics. Data source: ALR (Regional State Office for the Rural Areas), AWI (Alfred-Wegener-Institute for Polar and Marine Research), NPA (Regional Office of the Schleswig-Holstein Wadden Sea National Park), SJA (Sønderjyllands Amt) SWAP, GKSS (taken in the SWAP-project (Sylter Wattenmeer Austauschprozesse), provided by GKSS).

| Date | Colour | Pixel Size (in m) | Area | OPM | Data Source |
|---|---|---|---|---|---|
| 1928 | black-white | 0.64 | Sylt | yes | ALR |
| 27-Aug-1936 | black-white | 0.64 | Sylt | yes | ALR |
| 28-May-1945 | black-white | 1.4 | Danish part of List tidal basin | no | SJA |
| 1958 | black-white | 1.6 | German part of List tidal basin | yes | ALR |
| 25-May-1964 | black-white | 0.89 | Jordsand | no | SJA |
| 9-Sep-1968 | black-white | 0.83 | Danish part of List tidal basin | no | SJA |
| 28-May-1973 | black-white | 0.61 | Jordsand | no | SJA |
| 5-May-1975 | black-white | 0.32 | Danish part of List tidal basin | no | SJA |
| 27-Mar-1984 | black-white | 0.33 | Jordsand | no | SJA |
| 11-May-1988 | infra-red | 0.41 | Sylt | no | NPA |
| 15-May-1989 | black-white | 0.6 | Jordsand | no | SJA |
| 16-May-1989 | black-white | 0.6 | List tidal basin | no | ALR |
| 5-Jul-1989 | colour | 0.96 | Königshafen | no | SWAP, GKSS |
| 22-Aug-1989 | colour | 0.87 | Königshafen | no | SWAP, GKSS |
| 2-May-1990 | black-white | 0.53 | German part of List tidal basin | no | AWI |
| 15-Jul-1990 | colour | 0.56 | Königshafen | no | SWAP, GKSS |
| 14-Aug-1990 | colour | 0.9 | Königshafen | no | SWAP, GKSS |
| 25-Oct-1990 | colour | 0.83 | Königshafen | no | SWAP, GKSS |
| 29-Aug-1991 | colour | 0.86 | Königshafen | no | SWAP, GKSS |
| 19-May-1992 | colour | 0.86 | Königshafen | no | SWAP, GKSS |
| 17-Jun-1992 | colour | 1.39 | Königshafen | no | SWAP, GKSS |
| 20-Aug-1992 | colour | 0.93 | Königshafen | no | SWAP, GKSS |
| 11-May-1993 | colour | 0.33 | Jordsand | no | SJA |
| 8-Sep-1993 | colour | 0.62 | Königshafen | no | SWAP, GKSS |
| 10-Aug-1994 | colour | 0.49 | Königshafen | no | SWAP, GKSS |
| 22-Nov-1998 | black-white | 0.47 | German part of List tidal basin | no | ALR |
| 1999 | colour | 1.0 | Danish part of List tidal basin | yes | SJA |
| 7-Dec-2001 | colour | 0.85 | German part of List tidal basin | no | NPA |
| 16 to 29-Jul-2002 | colour | 0.25 | Danish part of List tidal basin | yes | SJA |
| 8-Dec-2002 | colour | 0.8 | German part of List tidal basin | no | NPA |
| 14-Oct-2003 | colour | 0.5 | List tidal basin | yes | AWI |
| 1-Oct-2004 | colour | 0.2 | Königshafen | yes | AWI |
| 13-Oct-2004 | colour | 0.85 | List tidal basin | no | AWI |
| 3-Apr-2005 | colour | 0.5 | List tidal basin | yes | AWI |
| 19-Aug-2005 | colour | 0.5 | List tidal basin | yes | AWI |
| 12-Sep-2006 | colour | 0.5 | List tidal basin | yes | AWI |

### 3.2.2 Georeferencing

The process of assigning map coordinates to an image is called georeferencing. All elements in a map get a specific geographic location and extent that enables to locate them on or near the earth's surface.

Some sets of aerial photographs were provided as digital Orthophotomosaics (OPM). This means that the photographs were already scanned, georeferenced, processed (e.g. colour adjustment, cutting of overlaps) and put together as a complete mosaic. All other aerial photographs were allocated as contact prints. They were scanned with a resolution of

800 dpi and saved as Tagged Image File Format (TIF) documents. The TIF files were imported into GIS using the ESRI software ArcGIS 9.1, ArcMap and georeferenced with it. The OPM of 2003 served as base map to which all other aerial photographs were georeferenced to. The OPM of 2003 was chosen because it has a high quality and accuracy, which was checked at numerous control points with the submeter GPS device Trimble GeoXT handheld. This GPS receiver was upgraded to a differential GPS (DGPS) by the use of the real-time differential correction receiver GeoXT Beacon-on-a-Belt. However, georeferencing was possible because an appropriate number of bench marks, mainly constructions like buildings, road intersections, harbours etc., which have been existing already since 1928, can be identified in the pictures. The accuracy of georeferencing was improved by DGPS field data. The total spatial error of the photographs (Total RMS Error) is mainly below 5 m in nearshore areas. Due to a lack of bench marks on the tidal flats, the spatial error increases to a maximum of 20 m with increasing distance from the shoreline, but it stays mainly below 10 m. In order to have one uniform coordinate system, all aerial photographs were georeferenced or converted to UTM 32 North, WGS 84.

### 3.2.3 Shoreline detection and digitising

Before a shoreline could be derived from the photos, at first it had to be defined as there are many different definitions (Boak and Turner 2005). The mean high water line is often used for sandy tidal beaches (Dolan et al. 1980, Thieler and Danforth 1994, Boak and Turner 2005) and was also chosen for this survey because it can be applied best to all different shores in the study area. In the following, the term ‘shoreline’ is synonymous with mean high tide line, except for the western and the southern shore of the island of Rømø. In this case, two lines were determined in order to get more significant results: the mean low tide line is regarded as the shoreline of Havsand, while the vegetation border separates the island proper from the high sand Havsand (Fig. 3.2).

The shorelines were derived from the georeferenced aerial photographs by visual analysis and manual on-screen digitising in ArcGIS 9.1, ArcMap. This is the most common technique (Boak and Turner 2005). Even though the shoreline was digitised by zooming close into the aerial photographs (scale 1:2000), the disadvantage of this 2D method is that a certain amount of information is lost during the scanning process. In case of doubts or to confirm existing results, 23.5 cm x 26 cm-large contact prints of the aerial photographs were further visually analysed via a stereo microscope as this reveals even more

information. However, due to the fractal structure of the shoreline, the digitised line had to be straightened and thus slightly generalised for practical reasons (see Fig. 3.4).

In the forerun of the digitising, field surveys with the DGPS were conducted on days with an average high tide water level (mean high tide level at the gauge List from 1995 to 2006: 586 cm). This was done in order to detect spatial pattern at the shore, which allow to determine the mean high tide line in the aerial photographs as well as to validate the digitised data. Therefore, exemplary shorelines were surveyed on the island of Sylt on June 26, 2004 (high tide level: 582 cm) and July 30, 2004 (581 cm) as well as on the island of Rømø on April 09, 2005 (584 cm).

The western shorelines of the two islands could be determined because sand bars are located just west of them (Table 3.2). The sandbars directly adjoin the shoreline and are only exposed during low tide. In the case of Rømø, the densely vegetated island proper was easily distinguished from the Havsand, which is almost unvegetated apart from some dunes.

**Table 3.2:** A list of criteria helping to determine different types of shorelines in the List tidal basin.

| Area | Features |
|---|---|
| mainland | seaward dyke bottom<br>Pleistocene cliff edge<br>salt marsh cliff edge |
| tidal flats<br>(including Jordsand) | sediment colour (brighter beach sand and darker tidal flat sediments)<br>seaward dyke bottom<br>salt marsh cliff edge<br>bottom of causeways<br>groynes (landward beginning is at beach) |
| Sylt | at List Deep: land-water transition<br>high tide line<br>at western shore: east of sand bars and runnels |
| Havsand | at List Deep: land-water transition<br>low tide line<br>at western shore: between swash bars and beach; swash bars run parallel to the beach and have ridges and runnels. The most landward runnel (darker sediment) is taken as boundary |
| Rømø proper | vegetation boundary |

The northern shore of Sylt and the southern shore of Havsand on Rømø borders directly the narrow and deep tidal inlet Lister Deep which has steep descending slopes. Here, different water levels have only minor horizontal effects and the shoreline could be taken as the observed land-water-transition.

On the eastern shores of the two islands as well as along the causeways, the mainland shores and for the islet of Jordsand, the transition between tidal flats and beaches or land could be found due to sediment colour changing from dark to light (Table 3.2).

### 3.2.4 Digital Elevations Models

For the Jordsand area and the northern part of Sylt, the 2D GIS shoreline data could be combined with 3D Digital Elevations Models (DEM) from different years. This allowed an upgrade from spatial analysis of changes in the shoreline position to the calculation of volume changes. Results had to be interpolated for the shorelines from those years for which a DEM was not available.

The basis of the DEMs is a dense grid of mostly equally distributed point data, whereas each point contains an x- and y-coordinate and a value for the elevation. These data points cover the entire List tidal basin as well as its terrestrial margins, the western shores of the island of Sylt and Rømø with parts of the North Sea and the complete northern half of the island of Sylt.

The elevation raw data from 1952 to 2002 was stored as ASCII files in the KIS- (coastal information system) data base and provided by the Regional State Office for the Rural Areas (ALR) in Husum. It originates from different field surveys which were conducted on foot on the beaches using a theodolite or GPS, by survey vessels using echo sounder or by plane carrying out laser scan flights. The surveys on foot and by ship took place at almost regular intervals. The most recent elevation data were taken in October 2004, covering the Königshafen whereby field measurements were supplemented by data derived from aerial photographs which were taken at the same time.

At first, the point data were edited in order to bring them in the correct format. Then they imported into ArcGIS 9.1, ArcMap and saved as shape-files. Then, the grids of data points were converted to the coordinate system UTM 32 North, WGS 84 in order to make them integrative to the aerial photographs and to the GIS files with the digitised features. These grids of data points show a high density as e.g. the grid of 1994 contains on average 476 data points $km^{-2}$ (total of 192 956 points). After that, the point data were loaded into ArcGIS 9.1, ArcScene, where Triangulated Irregular Networks (TINs) were calculated and the DEMs created (Fig. 3.3). The DEMs were improved by including break lines in order to display sharp edges properly. In order to check the results of the DEM, a comparison with nautical charts was undertaken.

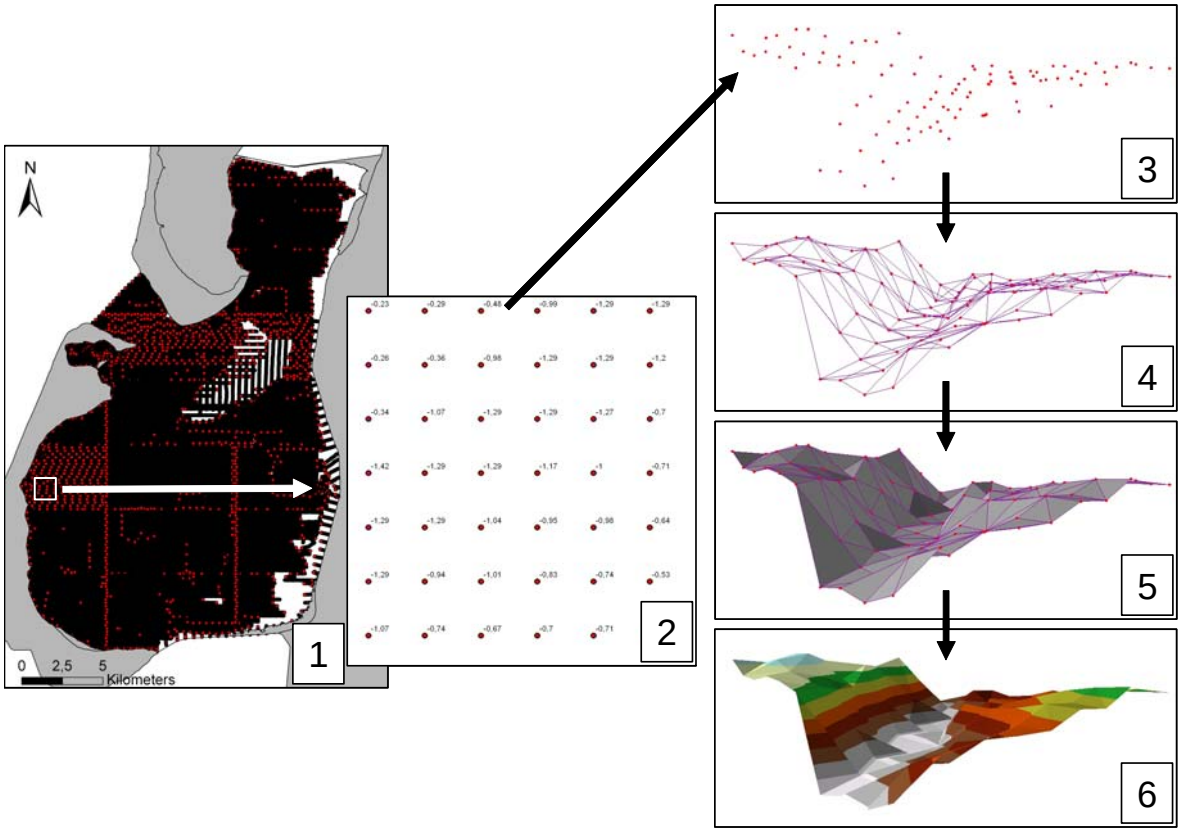


**Fig. 3.3:** Point files containing elevation data of the List tidal basin (1) and an enlarged detail of the area (2). Creating a Digital Elevations Model: according to their elevation value, the point data are brought into a 3D format (3), the elevated points get connected by a Triangulated Irregular Network (4), the areas get filled (5) and contour lines indicate the elevation.

A 2.2 x 3.6 km large area on Jordsands Flak with Jordsand in its centre was examined for volume changes. Regarding Jordsand in its larger vicinity allows to distinguishing between temporal shifts or relocations of material and real volume accessions or losses. Furthermore, the changes of the lengthwise elevated sand accretion of Jordsands Flak, on which Jordsand is located on top, can also be observed. Elevation profiles were compiled for different years with the 'Spatial Analyst' tool in ArcGIS 9.1, ArcMap.

Sylt is a rather large island compared to Jordsand and surveys for the whole northern part were not possible. Therefore, a 300 m wide nearshore zone along the shoreline was considered for observations in order to differentiate temporal sediment shiftings from real trends. This observation zone covers the sandy beaches with the onset of the adjoining belt of sand dunes as well as the nearshore marine area (Fig. 3.4). For a more detailed analysis of spatial and volume changes, the northern part of Sylt was divided into three subareas: west, north and east shore. They form morphological units as each subarea follows its own development trend.

Starting from the oldest shoreline available, spatial and volume changes were calculated in ArcGIS 9.1, ArcMap and ArcScene.

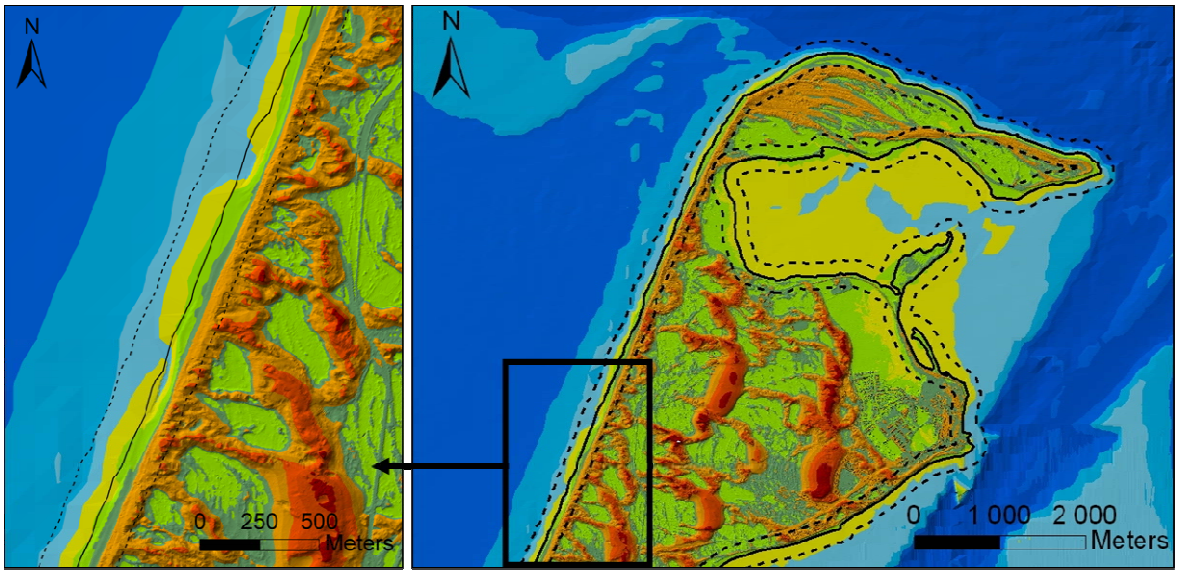


**Fig. 3.4:** The shoreline at the western shore of the island of Sylt (black line). The dotted lines indicate the extent of the observation zone covering the nearshore area as well as the dunes and cliffs.

### 3.2.5 Model data on 2D current velocities and water depths

In order to get information on the hydrodynamic conditions in the List tidal basin during a tide, model data on current velocities and water depths were brought into the GIS. All hydrographical and meteorological parameters significant for suspended sediment transport were collected within the framework of the MAST III project 'Pre-Operational Modelling In The Seas Of Europe (PROMISE)' from 1996 to 1997 (Riethmüller et al.1999). On the basis of these data a numerical model was designed to simulate the dynamics of 2D current velocities, flow directions and water depths within a complete tide in the List tidal basin. For the simulations different wind speeds (5, 10 and 20 m $s^{-1}$) and wind directions (N, NE, E, SE, S, SW, W and NW) were considered and the results for each combination presented at 14 phases of a tide. This corresponds to an average resolution of 50 minutes. The results are presented in coloured maps with a 100 m cell resolution.

The maps were provided by the GKSS. They were imported into the GIS software, georeferenced to the coordinate system UTM 32 North, WGS 84 and saved as rectified GIS-raster files (Fig. 3.5). As all maps have the same number of pixels and the same size, it was possible to automate the georeferencing with ArcGIS ModelBuilder. Each map was now composed of 2652 columns and 3156 rows whereby every cell has an x- and y-coordinate and a value for the water level. The calculated water level is a result of the

model simulation. Each cell has its own modelling result, which is displayed in the map by a distinctive defined colour. Thus, it was possible to allocate a numerical value to each cell according to the cells definite colour (Fig. 3.5). This allowed calculations of the raster files.

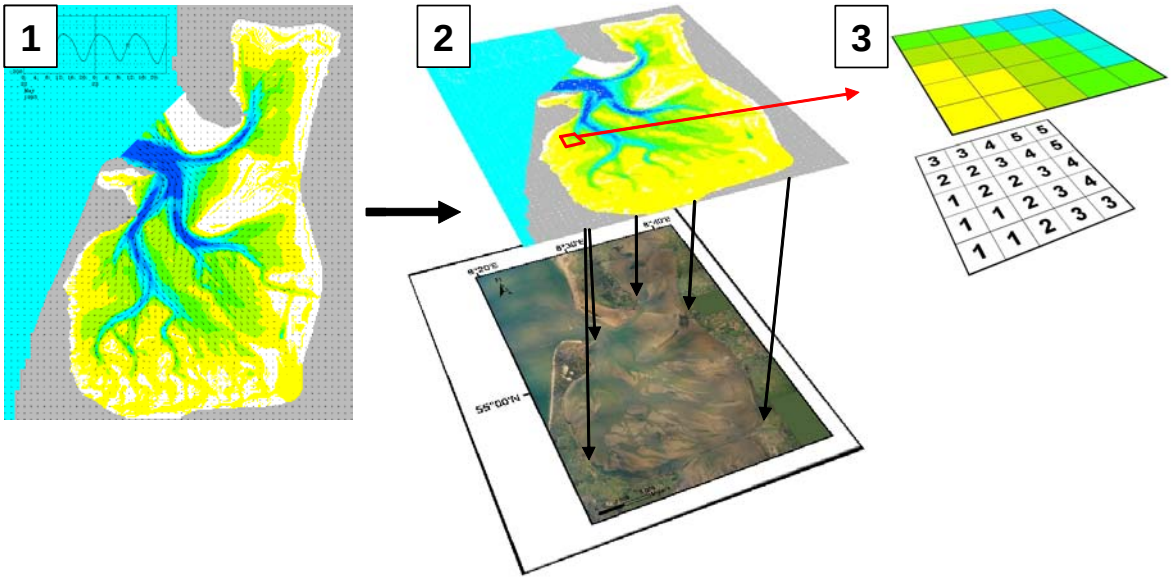


**Fig. 3.5:** A map with modelling data on water depths and current velocity (1) gets georeferenced in GIS on the base of a digital Orthophotomosaic (2). An enlarged detail of the area showing the coloured cells (3, above) and the same area displaying the numbers the colours are standing for (3, below).

To further complete the data set on water levels, records on high and low water levels from every tide collected at the gauge List (Sylt) from 1936 to 2007 were provided by the Waterways and Shipping Board (WSA) in Tönning.

## 3.3 Results

The shore of the mainland in the east of the List tidal basin is protected from the North Sea by the position of the two barrier islands Sylt and Rømø (Fig. 3.2). Furthermore, most of the mainland shore is stabilised by dikes and groyne fields. Therefore, there are hardly any ‘natural’ changes of this shoreline, but several man-made changes due to land claim occurred. ‘Natural’ changes are mainly affecting the salt marsh and the narrow beaches in front of the dikes.

### 3.3.1 Northern part of Sylt

The aerial photographs from 1928 only show the western and northern shore of the island of Sylt whereas the pictures from 1936 to 2003 cover the entire northern part of the island. Therefore, the spatial analysis for the western and northern shore can go further back in time.

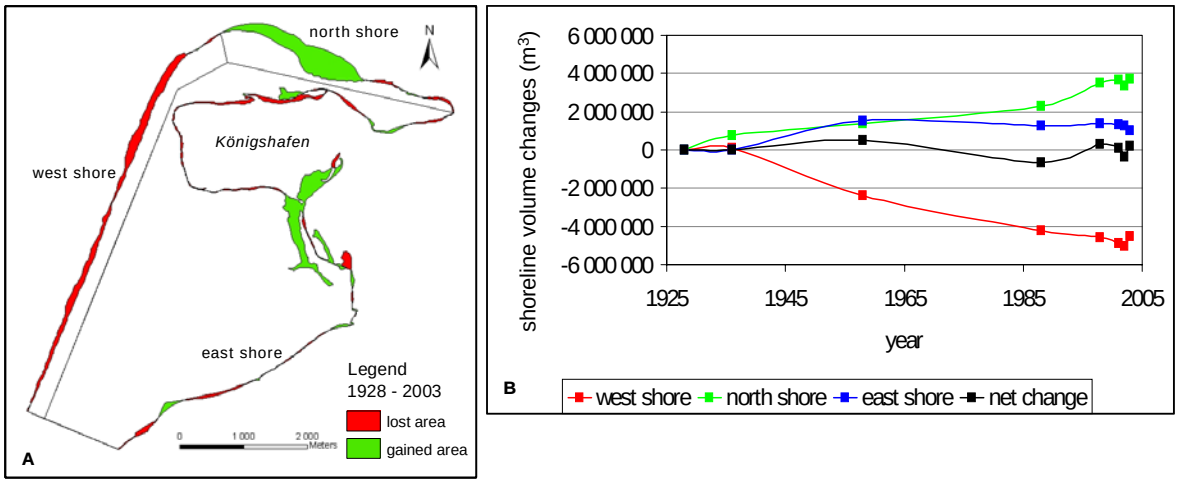


**Fig. 3.6:** The spatial development (A) and the changes in the sediment volumes (B, displayed as cumulative frequency curves) at the shores of northern Sylt from 1928 to 2003.

The west shore is strongly erosive. In this section, it lost 4 537 000 $m^3$ over the last 75 years (Fig. 3.6). Especially from 1936 to 1988 a steady, almost uniform and considerable retreat can be observed. However, for the last 15 years the loss of volume is much reduced. Regarding the position of the shoreline, it becomes obvious that the retreat was almost uniform in this section from 1928 to 1988, but since 1988 the shoreline is more or less stable in its position (Dolch 2006). The shoreline section in the north-west of the survey area is characterised by conspicuous stability over the entire observation period.

The north shore area is accumulating and gained 3 728 000 $m^3$ from 1928 to 2003. The gain of volume is almost steady but for the last 15 years it increased considerably. It can be seen that the spatial distribution of the accumulation is not equal along the shoreline but in particular focussed on the western half of the north shore area (Fig. 3.6). Regarding the course of the northern shoreline, a distinct bulge in the western half becomes obvious. From 1928 to 1998 it remained in its shape while it extended eastwards, but since 1998 the bulge becomes more and more integrated into the course of the shoreline which thus becomes smoother.

The east shore area increased in total by 1 007 000 $m^3$ from 1936 to 2003. From 1936 to 1958 a big gain of about 1 544 000 $m^3$ can be observed. No major changes can be recorded at the east shore since 1958, even though it is slightly erosive as it lost 537 000 $m^3$ until 2003. In comparison to the west shore this is rather little. No distinct erosion areas can be detected and the loss seems to be equally distributed. However, it can be observed that the shoreline got smoothened and small bays and sand spits were gradually incorporated.

The net change of the northern part of the island of Sylt presents the average of the changes of the three subareas. As the subareas develop different, their contrary development compensates each other. Therefore, only minor volume changes can be noticed in total for the northern part of the island of Sylt (Fig. 3.6).

It can be summarized that the overall course of the shoreline got levelled and straightened and that the west and the north shore are the most active areas where considerable changes can be noticed. This is worth a closer consideration. From 1928 to 2003 the west shore lost about 60 500 $m^3 yr^{-1}$ while the north shore showed an accumulation of 50 000 $m^3 yr^{-1}$. Having a more detailed look at smaller time intervals, a significant change in both, erosion rate and annual gain can be noticed. Two intervals were determined: 1928 to 1988 and 1988 to 2003. From 1928 to 1988 the considered western area decreased by approx. 70 500 $m^3$ per year. From 1988 to 2003 the annual retreat was about 20000 $m^3$. The north shore gained about 38 000 $m^3 yr^{-1}$ from 1928 to 1988. Regarding the period from 1988 to 2003 the accumulation increased considerably to 95 000 $m^3 yr^{-1}$. This means that the retreat rate at the west coast decreased by the factor 3.5 while the accumulation rate at the north coast increased by the factor 2.5.

### 3.3.2 Morphodynamic changes in the Königshafen

The Königshafen (Fig. 3.7) is located at the northern tip of the island of Sylt and is part of the subarea ‘east shore’. Apart from shoreline changes, interesting morphodynamic changes as well as constancies, which occur in the entire Wadden Sea area, can be observed here. Furthermore, the small-scale analysis in this area reveals the potential of the high-resolution aerial photographs. Therefore, a special focus was laid on this shallow bay.

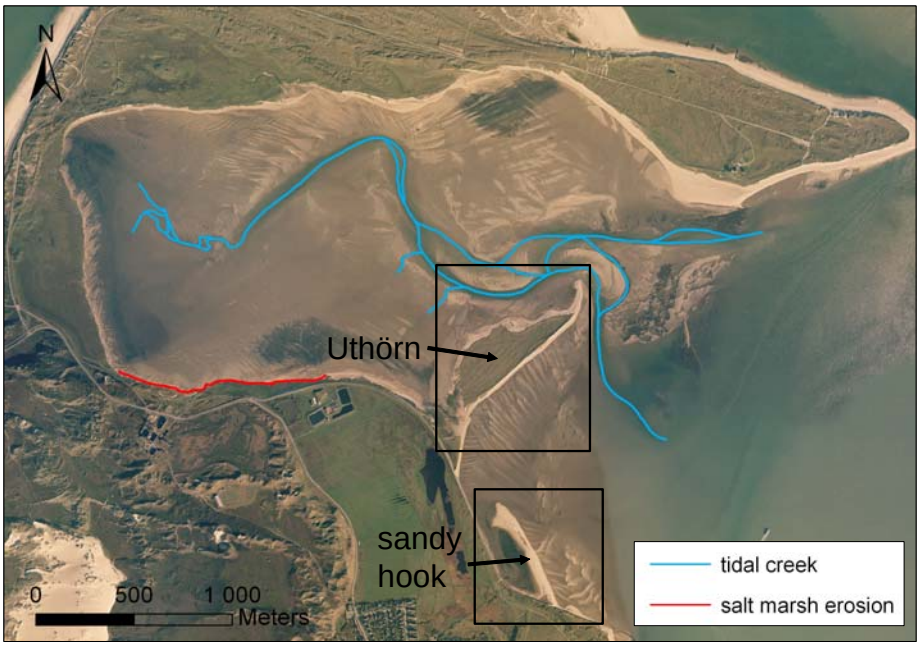


**Fig. 3.7:** The Königshafen with its central tidal creek (blue line) and the focus areas Uthörn and the sandy hook north of the village List. The red line indicates the surveyed section in the south-western Königshafen, where considerable salt marsh erosion is detected.

As mentioned above, the eastern shoreline is characterized by getting smoothed and levelled, even though there are only minor natural shifts in its position. Nevertheless, erosion of salt marshes, which are located at the south-western part of the Königshafen, can be observed. The long-term view (1936 – 2006) reveals that the salt marshes in the south of the inner Königshafen are particularly affected while only marginal erosion can be detected for the western ones. Therefore, the focus of the surveyed area lies in the south (Fig. 3.7). On average, salt marsh retreat amounts to 9.24 m (1936 – 2006, 0.13 m $yr^{-1}$) in this observed section, but the western and eastern part are differently affected. Considerable salt marsh retreat with an average of 15 m and a maximum of 26 m can be detected in the eastern half (0.2 m $yr^{-1}$) while only a minor retreat with an average of 4 m and a maximum of 5 m can be measured for the western part (0.06 m $yr^{-1}$) (Fig. 3.8). Regardless the erosion rates, field surveys reveal that all salt marshes in the surveyed area have a distinct erosion cliff with a maximum cliff height of 60 cm.

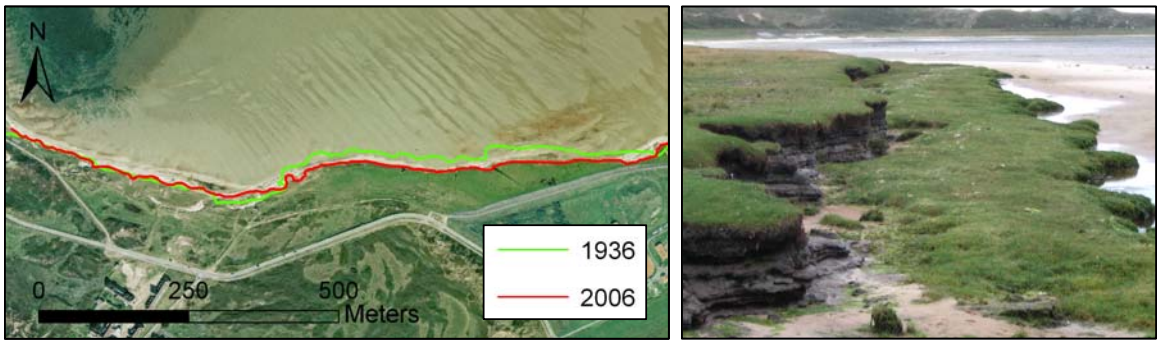


**Fig. 3.8:** The comparison of the courses of the salt marsh lines in 1936 and 2006 reveals a retreat, especially in the eastern half of the surveyed area. The photo to the right shows the salt marsh erosion cliff in the surveyed section in February 2008.

The course of the central tidal creek can also be determined by remote sensing (Fig. 3.7). It is characterized by a stable sinuous course and runs almost unchanged from 1936 to 2006.

The artificial island Uthörn shows an erosion cliff at its eastern shore which is facing the subtidal (Fig. 3.9). Retreat at this side shows rates of 0.4 m $yr^{-1}$ from 1958 to 2006. However, hardly any changes in the course of the shoreline and no net retreat (0.0 m $yr^{-1}$) can be detected at the eastern shore since 1989. Therefore, erosion does not seem to be dominant or a one-way trend here. The stable position of the entire island is remarkable anyway. Despite its rather exposed location, there are only minor changes, mainly in the form of little shoreline retreat or sediment redistributions at its western shore.

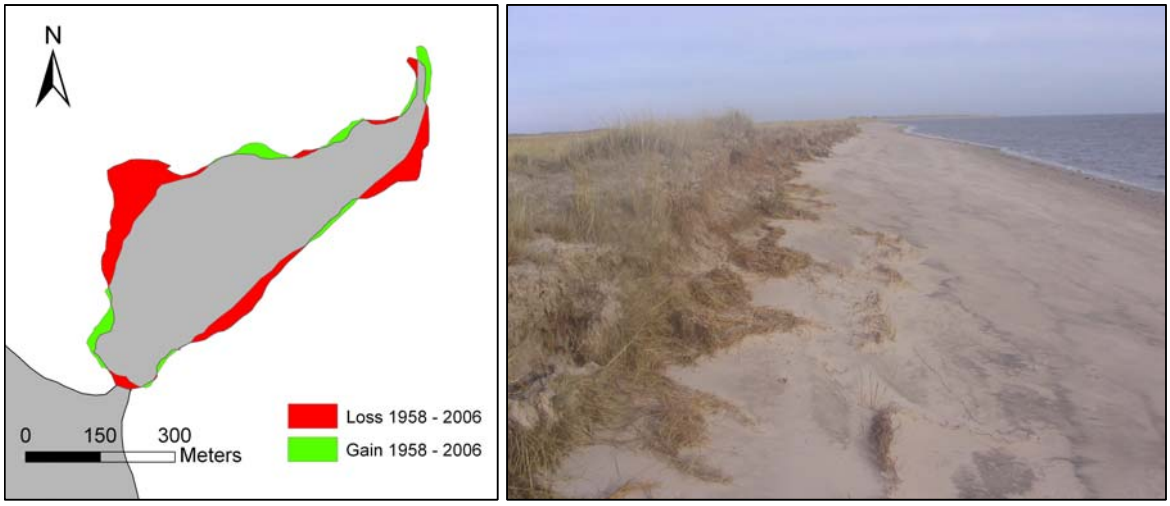


**Fig. 3.9:** Gain and loss in area as a result of shoreline changes of Uthörn from 1958 to 2006. The photo shows the erosion cliff at the eastern side (February 2008).

The most dynamic feature in Königshafen is a sandy hook which is situated south-east of Uthörn right at the entrance of the bay. From 1936 to 2006 this sandy hook changed from a bulge-shaped and compact to a narrow, long-stretched feature (Fig. 3.10). The length

increased from 360 to 580 m (3.1 m $yr^{-1}$) while its average width narrowed from 130 to 70 m (0.9 m $yr^{-1}$) and its area decreased constantly from 43 600 to 33 780 $m^2$ (140 $m^2$ $yr^{-1}$). At the same time the sandy hook moved steady and rapidly westwards by 260 m (3.7 m $yr^{-1}$), while its upper half bent in moving direction.

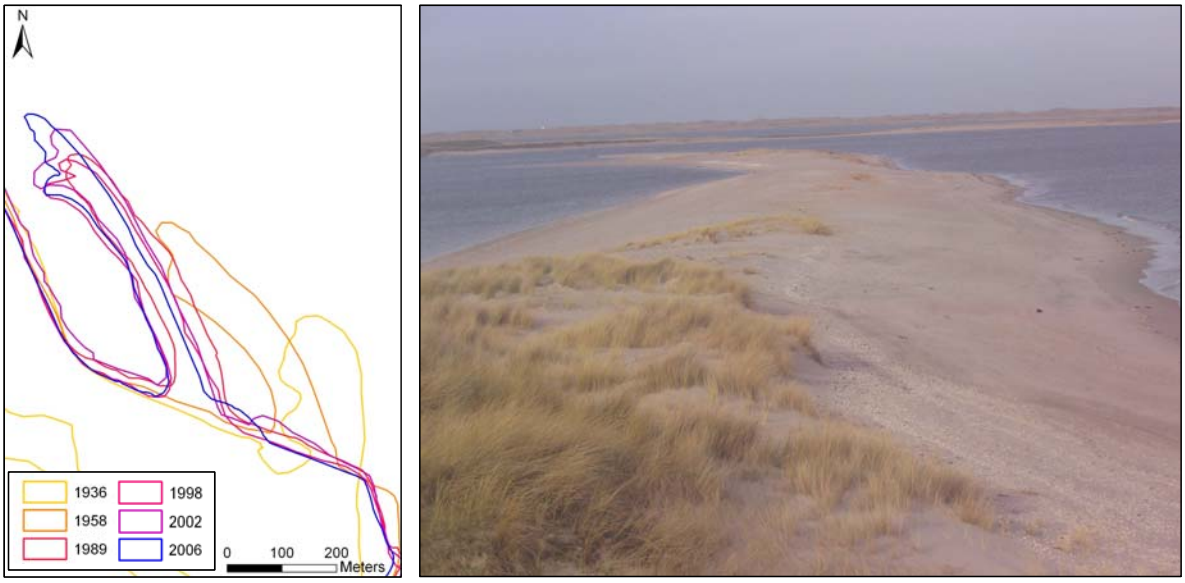


**Fig. 3.10:** Spatial development of the sandy hook north of the village List from 1936 to 2006. The photo shows the sandy hook at high tide in February 2008.

### 3.3.3 Southern half of Rømø

Due to data source, only 2D spatial changes could be calculated for the shoreline development of the southern half of the island of Rømø (Fig. 3.11).

The eastern and south-eastern shore of Rømø borders almost directly the tidal flats. Only minor changes and a rather stable position of the shoreline can be observed here. A notable development can be recorded for the southern and western shoreline.

Just south of Havneby harbour, the shoreline shifted about 100 to 150 m seawards from 1945 to 2006. However, at the southern tip, where Havsand is bordering the tidal inlet List Deep, a rather stable position of the shoreline occurs. This is followed by a 4 km long section in the southwest, where the shoreline retreated up to 200 m, while the next 3 km of shoreline extended seawards and accreted up to 300 m. The western shoreline of Havsand seems to be variable but in general it has mainly accreted about 75 to 100 m.

The island proper of Rømø is roughly expressed by the vegetation border. At the southern tip of Rømø the vegetated area is rather stable in its extent from 1945 to 2006, but in the western part the vegetation border extended mostly by 200 to 250 m towards the sea.

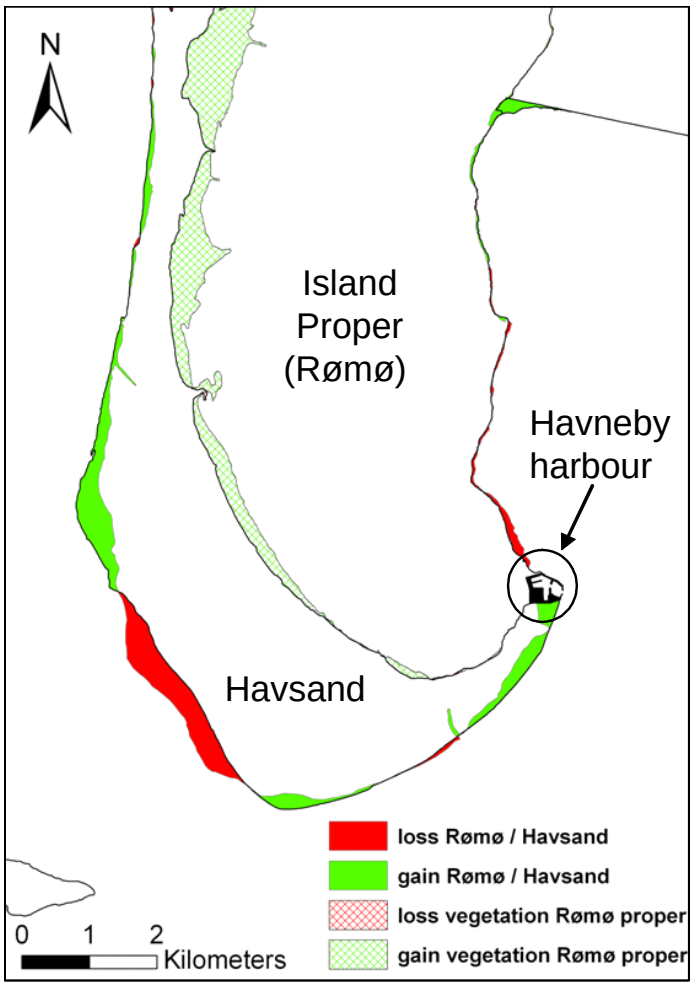


**Fig. 3.11:** Spatial development of the southern part of the island of Rømø from 1945 to 2006. The individual developments of Havsand and the vegetation boundary are displayed in the western and the southern part of island.

It can be summarised that the vegetation of the island proper of Rømø extended its boundaries by 330 m (5.5 m $yr^{-1}$) while the shoreline of Havsand advanced on average by 16 m (0.26 m $yr^{-1}$) from 1945 to 2006.

### 3.3.4 Jordsand

The development of Jordsand can be documented from 1936 to 2006. The aerial photographs of the period 1936 to 1999 show the disappearance of the island (Fig. 3.12) while from 1999 to 2006 Jordsand is a supratidal sand. With the total loss of the vegetation, presumably in the mid to late 1990s, the change from an island to a supratidal sand was completed.

From 1936 to 2006, Jordsand continuously decreased in size while its location shifted eastwards at the same time. The western front side was displaced by about 400 m towards the mainland (Fig. 3.12 A). The island decreased in volume from about 93 900 $m^3$ to

11 800 m³, which is a reduction of 87 % (Fig. 3.12 B). In average this means an annual loss of 1 300 m³.

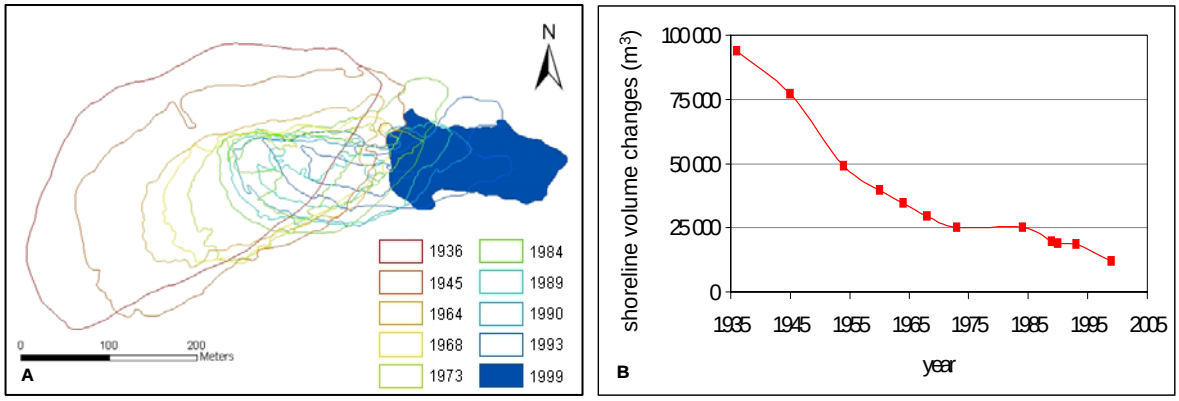


**Fig. 3.12:** The spatial development (left, A) and the changes of the sediment volume (right, B) of the island Jordsand from 1936 to 1999.

Digital Elevation Models (DEMs) from 1975 and 1994 and their cross-section profiles reveal that not only Jordsand itself but also Jordsands Flak, the elevated sand accumulation on which the island is located, has changed through the years (Fig. 3.13). The cross-sections show that Jordsands Flak decreased in width and height. At the same time, the tip of Jordsands Flak also retreated towards east-northeast. The elevation of the island Jordsand also changed. In 1975 it was about 1 m above sea level while in 1994 it was located only 20 to 30 cm above sea level.

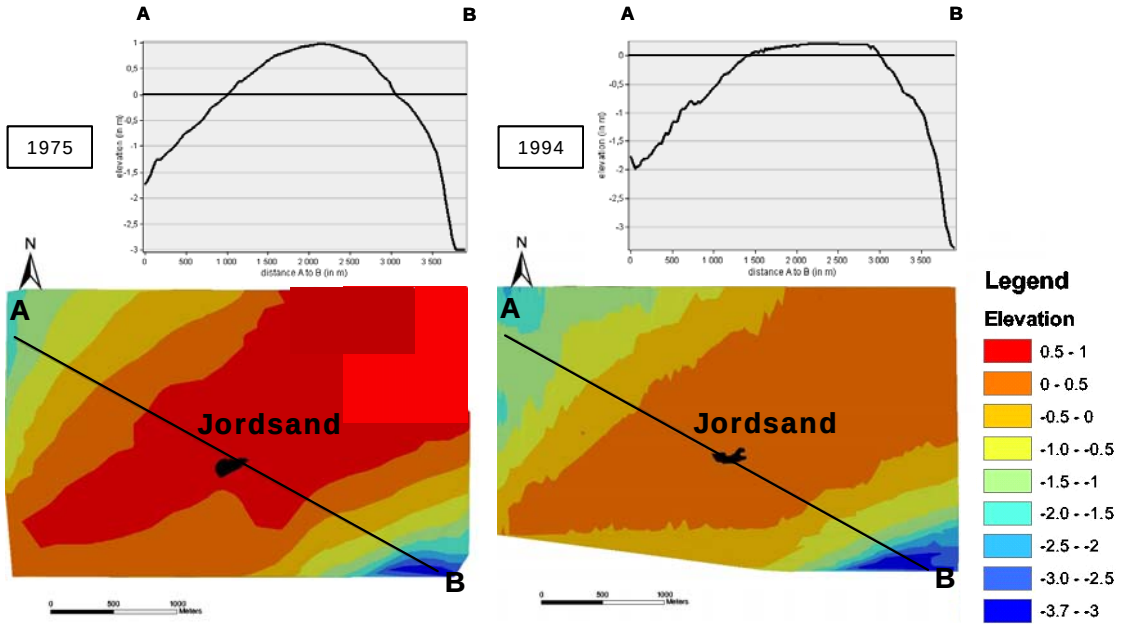


**Fig. 3.13:** Comparison of 2 Digital Elevation Models with cross-section profiles of Jordsand and Jordsands Flak (1975 and 1994, elevation in meter, negative values indicate below sea level).

## 3.4 Discussion

Chapter 3.2.3 addresses the methodical approach of the determination of shorelines in the study area. Shorelines at salt marsh and Pleistocene cliffs, at beaches adjoining tidal flats, at causeways and dykes can be reliable identified by the visual analysis of high-resolution aerial photographs. Initial field surveys are recommended but not essential at these features. However, field surveys are essential for the determination of shorelines at broad sandy area, like for example at the western shore of Sylt and Havsand.

### 3.4.1 Different coastal processes at the northern part of Sylt

Regarding the volume of the northern part of the island of Sylt, only minor changes can be observed from 1928 to 2003. However, having a look at the shape of this area and the position of the shorelines, clear shifts are obvious. The actual dynamics become apparent by the survey of the 3 coastal sections.

**Western shore**

Beach replenishment is carried out on the island of Sylt since 1972 and for this reason the survey period is divided into 2 time intervals. As the aerial photographs from 1988 are closest to that date, the time period was split in 1988 to show the ‘before’ and ‘after’ of sand replenishment and to check the efficiency of this coastal protection measure.

The artificial supply of sediment almost compensates the eroded material and stabilises the position of the western shoreline (Fig. 3.14). It explains why the annual negative net balance decreased from approx. 70 500 $m^3$ (1928 – 1988) to 20 000 $m^3$ (1988 – 2003) in this 6 700 m long coastal section. Sand replenishment is conducted almost annually at alternating sections at the western shore (ALR 2007). The annual replenishment is recommended because the average sand requirement is at minimum when the nourishment is continuous and it is more effective to fill smaller volumes at shorter intervals (Dette et al. 1994). The sand for beach replenishment is taken from an area about 10 km offshore of Sylt (CPSL 2005, ALR 2007) where the sand has a coarse grain size which is less vulnerable to erosion. The importance of the grain size for beach replenishment is shown by Eitner and Ragutzki (1992). Hamm et al. (2002) provide further information on experiences with beach nourishment.


**Fig. 3.14:** Sand replenishment at the west shore of Sylt. The sand gets transported by ship to the shore (a), and washed through pipelines to the beach, where it gets distributed by bulldozers (b and c).

For 2007, 3.5 million € were budgeted to supply only the beach of Sylt with 1.2 million $m^3$ of sand, but after the severe storms in the winter 2006-2007, 3 million € were additionally provided for the next 2 years. Altogether 14 million € are assured for beach replenishment on Sylt for the period 2007 to 2009 (ALR 2007, Landesregierung S-H 2007). Although beach replenishment is expensive and the effect last only for a limited time, in the case of Sylt there is no alternative solution for it (Ahrendt 1993, CPSL 2005). Solid structures such as dykes, tetrapodes, petrified shores etc. turned out to be inefficient (Ahrendt 1993) and are not compatible with tourism on the beach which is the most important economic factor for the island. Other dynamic sandy areas show conspicuous similarity to western Sylt and sand replenishment seems also to be the only solution, like e.g. the Skagen Spit in Denmark (Bruun 2000). However, sand replenishment also turned out to be the best environmental practice (CPSL 2005) and is carried out widely along the outer shore of sandy barrier islands in the entire Wadden Sea (CPSL 2001).

No sand replenishment is carried out in the stable shoreline section in the north-west of the survey area (Fig. 3.6). This area is stone petrified why no shoreline changes are detected here (see Fig. 3.1).

**Northern shore**

The northern shore is an area of prevailing sedimentation (Bayerl and Higelke 1994) and since the beginning of beach replenishments, the annual accumulation rate increased by the factor 2.5. The rather sudden and considerable increase can be explained by the availability of large quantities of unconsolidated sediments which are artificially supplied to the depositional system. Dette et al. (1994) showed that there is a positive correlation between the amount of material eroded and the sediment availability. The sand, which gets replenished at the west shore, gets loosened by waves and removed by long-shore currents.

Tidal currents divert a part of the sediment load into the List tidal basin where some of it is deposited at the northern shore of Sylt (Dolch 2006). Having a look at the more recent aerial photographs, the accumulation area can be identified as it is not or only sparsely covered with vegetation. This suggests that this area was recently gained.

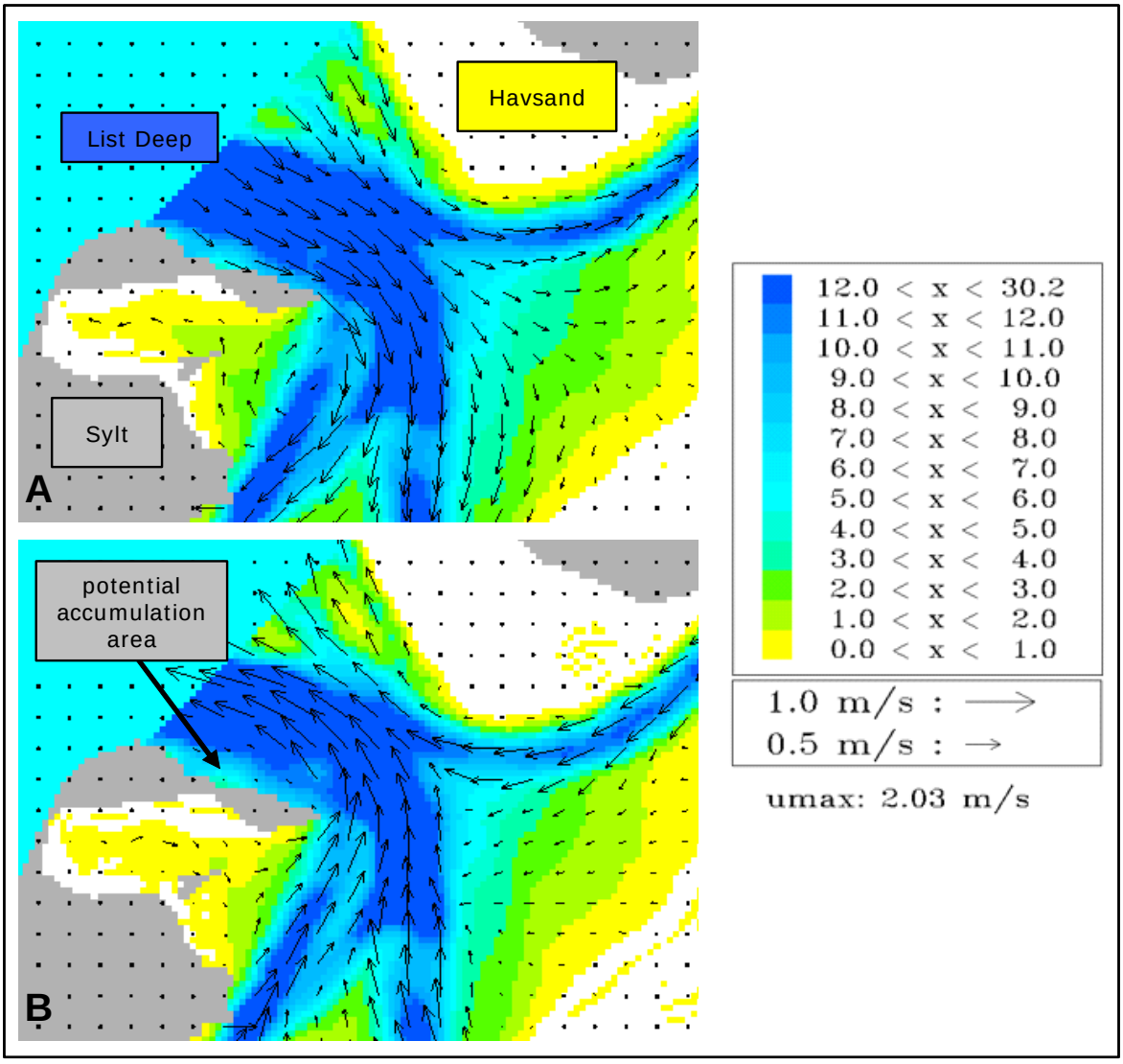


**Fig. 3.15:** Currents and water levels in the List tidal basin at northern Sylt and southern Rømø at rising (A) and falling (B) tide. Model data provided by GKSS.

The accumulation area could establish here despite the close vicinity to the tidal inlet List Deep with its strong currents. This can be explained by the different current patterns at rising and falling tides (Fig. 3.15). When the tides are rising, the incoming water causes high current velocities along the entire cross-section profile of the 2.8 km wide List Deep. When the tides are falling, the outgoing water gets deflected by the morphology and the shape of Sylt towards the centre and the north of the List Deep (Behrens et al. 1997). This results in slow currents at the northern shore just east of the bulge area where sediments

can accumulate. It can be assumed that these sediments are partly eroded with the following high tide but nevertheless, a positive net accumulation is clearly detected in the long-term view. However, the extent of the potential accumulation area is restricted by high current velocities and a further gain in area is limited. Nevertheless, this growing accumulation area is the reason for the eastward extension of the bulge until 1998 and from then on for its integration into a smoother shoreline (Fig. 3.6).

**Eastern shore**

The eastern shore shows a positive sediment net balance of 1 007 000 $m^3$ from 1936 to 2003. This can be mainly referred to the formation of the Lister Koog by the construction of a dyke in 1937 and the landfill of the island Uthörn in the early forties of last century (Fig. 3.1). Apart from this man made gain, slight erosion with an average annual loss of 11 900 $m^3$ can be observed since 1958 (Fig. 3.6). However, the sediment losses are not conspicuous as they are rather equally distributed and result mainly in a smoothening of the course of the shoreline. Compared to the western shoreline the losses are only minor, especially regarding the fact that the eastern shoreline is about 2.5 times longer. Nevertheless, erosion is clearly visible along the entire Wadden Sea side affecting marshes and cliffs (Ehlers 1988) and also the northern part of Sylt. However, the rather low erosion rates at the eastern shore can be explained by the existence solid coastal protection constructions, like dykes and petrified coastal sections (Landesregierung S-H 2001) as well as by its rather sheltered position, protected from wind and waves by the island of Sylt.

**Outlook**

Shoreline changes are often natural and a lot may happen during extreme events. Due to sea level rise and an increase of extreme events the rate of changes is accelerated, which can have devastating effects. Even though beach replenishment has altered the depositional regime considerably, the northern tip of the island of Sylt may get detached from the rest of the island within the next 40 to 50 years without it (Ahrendt and Thiede 2001). According to the recommendations of the CPSL (2005) sand nourishments successfully balance coastal erosion along the outer coastlines of barriers and should be applied wherever feasible. For these reasons, it is most likely that beach replenishment will be continued at the western shore and no major changes are expected here. Since a sea level rise of about 25 cm is expected for the Wadden Sea by 2050 (CPSL 2001), it is likely that the erosion rate and consequently the amount of sand needed for replenishment and the costs will increase considerably (Landesregierung S-H 2001). For the Dutch Wadden Sea it

is expected that the sand nourishment quantities will at least have to be doubled in the future (CPSL 2005).

The calculated volume of the potential accumulation area at the northern shore amounts to 900 000 to 1 000 000 $m^3$ and under current conditions this area would be filled up within the next 10 to 12 years. As currents and morphology are interacting, it is likely that the accumulation rates will decrease as the actual accumulation area approaches the zone of high current velocities. From this it follows that a cessation of the net accumulation at the northern shore of Sylt can be expected in approx. 20 years and that a dynamic equilibrium will establish. It remains to be seen where the sediments get transported then.

Regarding the further development of the east shore, no conspicuous changes are to be expected there as there are no hints for distinct erosive or accumulative areas.

Erosion and sediment deficiency can not only be observed at shores and beaches but also on the tidal flats. The fact that the tidal flats in the List tidal basin show a negative mass balance and their area was constantly decreasing during the last centuries is a combination of submersion due to rising sea level and erosion as a consequence of increased hydrodynamics (Higelke 1998, Reise 1998). In order to compensate this sediment deficiency and to maintain their area, Reise (2005) suggests replenishing sand also on the tidal flats. As the hydrodynamics are far less in the basin than at the outer western shore, erosion rates are also comparatively low. Therefore, sand replenishment would have a longer-lasting effect and the amount of sand as well as the frequency of the replenishment, in other words the costs, would be also comparatively low. For these reasons sand replenishment on the tidal flats should be considered.

### 3.4.2 Changes and dynamic equilibriums in the Königshafen

Salt marsh erosion occurs in the south-western corner of the Königshafen and it is dominant to the south. This is confirmed by Larsen et al. (1996) who also detected salt marsh erosion to the west. They estimated an average retreat of approx. 0.25 m $yr^{-1}$ with a maximum of 1.0 m $yr^{-1}$ for the Königshafen salt marsh from 1992 to 1994. Their average retreat rate is consistent with the results of this long-term survey but only for the salt marsh erosion to the south (0.2 m $yr^{-1}$). An extrapolation of Larson's results to my survey period (1936 to 2006) ends up in a total salt marsh retreat of about 17.5 m. This is concordant with the average total retreat of 15 m, which was measured in this long-term study (Fig. 3.8). However, this concordance does not apply to the maximum retreat rates measured by Larsen et al. (1996) and not to the salt marsh erosion to the west. It can be

assumed that these are more recent phenomena or the results were gained during an active period as erosion of salt marshes occurs predominantly during a sequence of storm conditions (Houwing 2000).

The course of the central tidal creek runs almost unchanged from 1936 to 2006. Even though variations of its course are observed throughout a year (own observations), there must be a dynamic equilibrium as the general pattern remains. The grain size composition of surface sediments indicates increased hydrodynamics in Königshafen (see chapter 4.4.1) but that does not seem to affect the course of the tidal creek. Even the fill up of the island Uthörn had obviously no impact on it. Uthörn was a natural island in the centre of the outer Königshafen and its size was considerably artificially increased by landfill in the early 1940s, which also connected it to the shore (Bayerl and Köster 1998). The extended island changed the morphology of the Königshafen and comes close to the tidal creek, but Uthörn seems to be situated in a way that it has no consequences for the course of the tidal creek.

Uthörn is characterised by its stable position even though its eastern shore shows a distinct erosion cliff. The long-term remote sensing data reveals some changes in the course of the shoreline from 1958 to 1989 (Fig. 3.9), but since then it seems that it has settled at a stable level. This can also be seen in the annual retreat rates of the eastern shoreline. After an adjustment period in the early years after the artificial landfill of the island, only minor changes in the position of the eastern shoreline, probably caused by sediment redistribution, and no annual net retreat can be detected since 1989. As the erosion cliff is most pronounced in winter (own observations) it can be assumed that there is a seasonality in the morphological processes. Sediments are most likely supplied to Uthörn in another season which prevents further cliff erosion. Seasonal morphological processes and dynamic equilibriums are also observed at other features in the Wadden Sea (Jacobsen 1986, Ricklefs and Neto 2005). Andersen et al. (2006) e.g. reports that in the Wadden Sea a certain amount of eroded material does not get exported to the open North Sea but is temporarily deposited in a nearby shallow tidal channel and later returned on the mudflat during calmer weather conditions. It is assumed that a similar form of this dynamic equilibrium also applies to the eastern shore of Uthörn.

A sandy hook is located east of the island Uthörn and constitutes an example for dynamics resulting in a steady development. It can be seen in the model data on current velocities that the morphology at the entrance of the Königshafen causes reversed currents at rising tides (Fig. 3.16). The deflected currents generate a vortex resulting in easterly currents for

the sandy hook. They are constantly pushing the sandy hook westwards and change its morphology (Fig. 3.10). It can be assumed that the currents exceeded a threshold and initiated the shifting. However, an average annual net movement of 3.7 m can be recorded for the sandy hook. At the same time, it elongated and narrowed and its area decreased by 22.5 %. Its upper half is bent in moving direction showing the pushing impact of the currents.

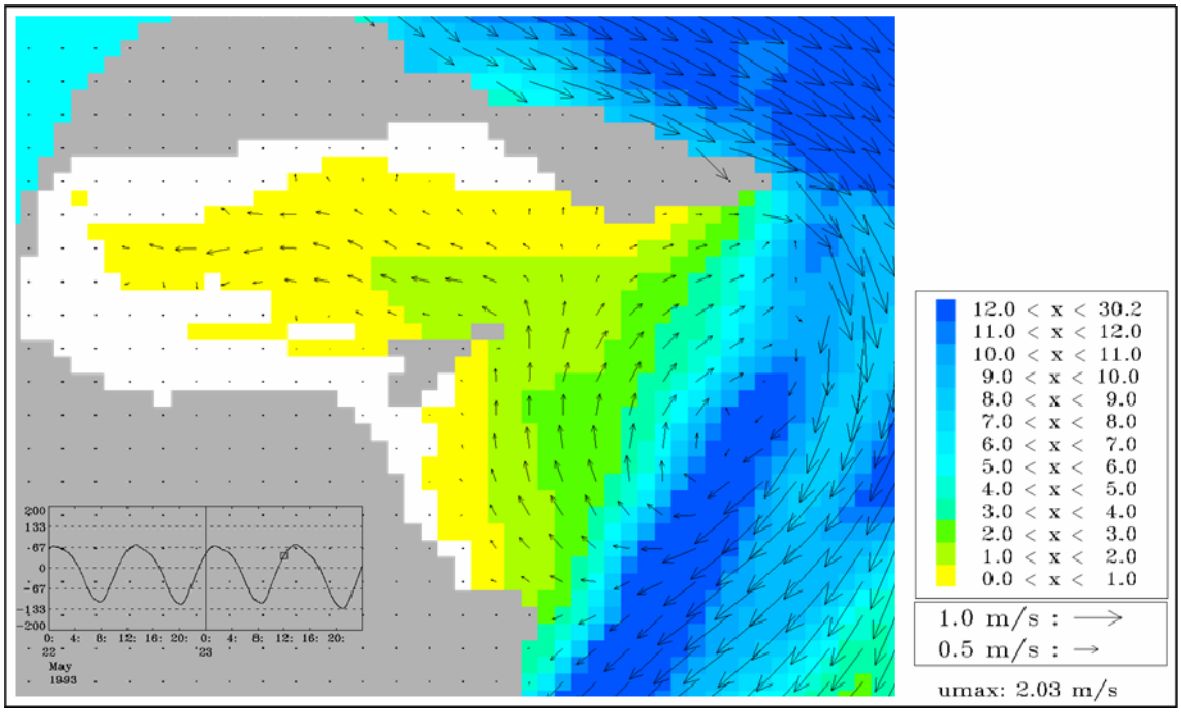


**Fig. 3.16:** Reversed currents at the entrance of the Königshafen at rising tides affecting the sandy hook. Model data provided by GKSS.

### 3.4.3 Expanding beaches and vegetation on Rømø

Only minor changes can be observed at the eastern and southern shore of the southern half of Rømø while the western coast shows all attributes of a dissipative beach.

Ehlers (1988) calculated an annual retreat of approx. 0.5 m at the Wadden Sea side of Rømø. This can not be generalised for the part of the eastern shoreline considered in this study as the long-term remote sensing show only a minor retreat. More pronounced erosion is recorded where the tidal channel approaches the shore exposing it to increased hydrodynamics.

A seaward expansion of the shoreline can be observed just south of Havneby harbour, where a small accumulation area established in the lee of the harbour. Otherwise, the southern shoreline of Rømø is characterized by a rather stable position which is due to a dyke. In contrast to the northern shore of Sylt, southern shore of Rømø is facing strong

currents at both, rising and falling tides by what no accumulation area could establish here (Fig. 3.15).

The western shore is variable but in general it has mainly accreted about 75 to 100 m from 1945 to 2006 (Fig. 3.11). Bartholdy and Pejrup (1994) observed that Rømøs western shore receives sediments from two sources. A certain amount of it gets eroded by hydrodynamics but for the net balance a surplus of sand remains allowing the shoreline to accrete. The analysis of the aerial photographs suggests an accretion of sand bars at the western shore as they are located very close to it and also merging the shore (Fig. 3.17). In calm weather when the swash is constructive, sand bars move closer to the shore and can become swash bars (Bird 2000). Bartholdy and Pejrup (1994) also observed cyclical depositions of relatively large sand bodies at the north-western corner of Rømø. The variability of the western shoreline can be explained by the stage of sand bar accretion or whether erosion or sediment accumulation was dominant at the time when the aerial photograph was taken.


**Fig. 3.17:** Swash bars at the western shore of the island of Rømø.

Regarding the amount of sediments supplied to the western shore, its accretion is rather minor. Beach profiles illustrate that the accretion is not only expressed in a seaward shift of the shoreline but also in an increase of the beach height which can be observed over the

entire cross-section profile (Bartholdy and Pejrup 1994). Due to this increase of the beach height, the seaward shift of shoreline is not as pronounced as expected.

The real accreting character can also be seen in the vegetation of the island proper. From 1945 to 2006, the southern vegetation boundary is rather stable in its position just like the shoreline. This can be explained by the dyke at the south-eastern shore of Rømø (Fig. 3.1). The western shore of the island consists of large sand areas and dunes. As there is no 'barrier' here, the vegetation extended steadily towards the sea and shows significantly higher rates than the western shoreline. The vegetation would not expand if the sea would have had too much impact or coastal degradation would prevail.

### 3.4.4 Loss of an island

The above mentioned rise of the mean high tide level in the List tidal basin is associated with an increased sediment hunger (Reise 2003, Reise and Lackschewitz 2003) and it can be assumed that the island Jordsand fell victim to it. The tidal flat area Jordsands Flak is located at the crotch of two tidal channels just as they diverge from the tidal inlet Lister Deep. Therefore, the north-west front of Jordsands Flak is facing the rather undamped currents from the tidal inlet. The water flowing in these tidal channels is attacking Jordsand and Jordsands Flak from the west, north and south. This results in the decrease of the size of the island and its eastward shift. Furthermore, the lengthwise elevated sand accretion on Jordsands Flak, where the island was located on, got levelled and eroded, in particular at the crotch of the two tidal channels (Fig. 3.13). The comparison of the DEMs reveals the same pattern of erosion that is also observed by Higelke (1998): erosion of intertidal flats is in particular taking place at their edge to the subtidal resulting in wider tidal channels and smaller intertidal flats.

It can be further assumed that the List tidal basin experiences an increased energy level through the reduction of the tidal catchment area due to embankments and the construction of the two causeways. This 'coastal squeeze' means less accommodation space resulting in increased hydrodynamics on the backbarrier tidal flats (Flemming and Nyandwi 1994, Mai 1999). The ascending high tide level in the List tidal basin also facilitates erosion. For further information see chapter 4.4.1.

According to historical documents, the island must have had a considerable size of 3 by 3 km in the late medieval times (Jespersen and Rasmussen 1989) but severe erosion especially during storm events degraded the island to a supratidal sand presumably in the mid to late 1990s. According to several historical documents, coastal erosion is a long

known problem for the island of Jordsand and was first mentioned in 1613 (Jepsen 1977, Jespersen and Rasmussen 1989). Nevertheless, no coastal protection measures were carried out for a long time. In 1976 an attempt to stop further degradation was made by setting groynes at the most affected front. By this time the size of the island had been so far decreased and above all the marsh basement so much depleted, that the disappearance of the island could only be retarded but not stopped (Fig. 3.18). The marsh formed a rather robust basement with an important stabilising effect but it decreased from approx. 43 ha in 1805 to 200 $m^2$ in 1982 (Jespersen and Rasmussen 1975, 1989).

Furthermore, the combination of a levelled Jordsands Flak and an ascending high tide level allowed sea water to have a greater impact on the island vegetation. Among erosion this also contributed to the conversion into a supratidal sand. Without stabilising vegetation the sandbank was shifted 100 m east towards the mainland within 6 years (1999 – 2005). Even though the size of the sand maintained during this time, it can be expected that the sand bank vanishes in the near future.

It can be assumed that only sand nourishments could have been preserved the islands. Unlike Sylt, however, Jordsand was not of economic importance and had no valuable objects to warrant expensive sand replenishment.

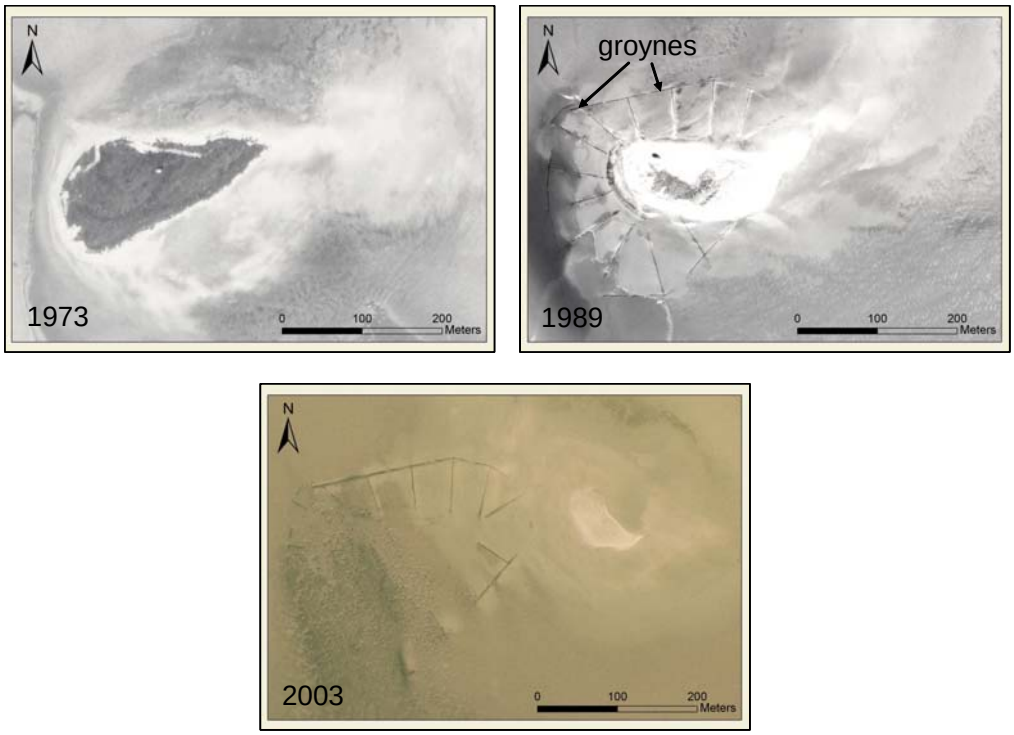


**Fig. 3.18:** Gradual disappearance of Jordsand. The size of the island and the extent of the vegetation were considerably reduced while the centre of the island was consistently shifted eastwards. The coastal protection measures (groynes) can be seen in the aerial photographs from 1989 and 2003 and it can also be detected that they had no significant effect.

## 3.5 Summary and conclusions

This study shows that different processes can be observed within a small coastal area. While the western shore of the island of Sylt as well as Jordsand and Jordsands Flak undergo severe erosion, the western shore of the island of Rømø and the northern shore of Sylt show prevailing sedimentation. Therefore, coastal morphology surveys have to be conducted with a high-resolution on a small scale. General assessments for larger areas are vague and can skew the real pattern.

The analysis of high-resolution aerial photographs with a Geographic Information System (GIS) proofed to be very suitable for the survey of morphological changes and developments. Furthermore, the combination of these remote sensing data with Digital Elevation Models and model data on current velocities allows understanding of interactions and coastal processes as well as making forecasts. An example is the increased accumulation rate at the northern shore of the island of Sylt due to the extra availability of large quantities of unconsolidated sediments because of sand replenishments at the western shore.

The analysis of aerial photographs also showed that beach replenishments successfully balance coastal erosion and stabilises shorelines. Regarding the difference of coastal processes and their intensities on a small spatial scale, this method can enable very efficient beach replenishments by the precise determination of the required amount of sand for defined coastal sections.

However, erosion and sediment deficiency is also detected on tidal flats, sand replenishment should also be considered here. Compared to the required amount of sand and the frequency of the replenishment at the highly erosive western shore, costs and efforts would be low here. Sand replenishment at the sheltered lee side of the barrier islands would have furthermore a longer-lasting effect. This is apparent from the high stability of the artificially created islet of Uthörn.

# 4 Long-term changes, dynamics and characteristics of intertidal surface sediments in a tidal basin in the northern Wadden Sea

## 4.1 Introduction

The Wadden Sea tidal flats of the sedimentary shore of the south-eastern North Sea are of multiple importances. They are among the most productive ecosystems in the world and exhibit a species community which is best adapted to this unique environment with its ever changing conditions. Tidal flats are serving as nursery grounds for crab, shrimp and fish as well as providing habitat to a rich benthic community, which is also an important food source, especially for shorebirds and migrating birds (Reise 1985, Dittmann 1999). Furthermore, tidal flats have a high capacity for coastal defence as they reduce the kinetic energy from open sea (Fan et al. 2006). Through this, they increase the deposition of sediments and are both quantitatively and qualitatively very important sinks, especially for muddy sediments (Andersen and Pejrup 2001).

The concentration of suspended, fine-grained material increases from the North Sea through the tidal inlets and reaches a maximum in the inner part of the tidal areas (Larsen et al. 1996). Most sediment supplied to the Wadden Sea originates from the North Sea, but the tidal flats also receive material from salt marsh erosion, atmospheric deposition, fluvial input and primary production in the form of unmineralized carbon (Postma 1981, Larsen et al. 1996, Pejrup et al. 1997, Pedersen and Bartholdy 2006).

The development of tidal flats by deposition of sediment is not only a result of hydrodynamic mechanisms, primarily settling/scour lag (Van Straaten and Kuenen 1957) and tidal asymmetry (Dronkers 1986), but also of biochemical processes, like flocculation and formation of faecal pellets (Pejrup 1988, Andersen and Pejrup 2002, Andersen et al. 2004). Furthermore, epibenthic structures like seagrass beds and mussel beds also enhance sedimentation and stabilise sediments (Ward et al. 1984, Fonseca and Fisher 1986, Heiss et al. 2000, Widdows et al. 2002) and high concentration of diatoms also increase the erosion shear stress of surface sediments (Riethmüller et al. 1998, Tolhurst et al. 1999, Austen et al. 1999, van de Koppel et al. 2001, Lanuru et al. 2007).

Sediments can also get resuspended either by wind-induced surface waves, internal waves or currents (Cacchione and Southard 1974, Sanford et al. 1991). Resuspension can be enhanced by organisms which destabilize sediments, e.g. by deposit feeding or

bioturbation (Widdows et al. 2002, Andersen et al. 2005, Paarlberg et al. 2005), like the lugworm *Arenicola marina* does (Wohlenberg 1937, Volkenborn and Reise 2006).

However, reworking of sediments is much larger than the net accumulation (Andersen and Pejrup 2001) and although mainly situated at sheltered sites, the sequence of sedimentation, resuspension and re-working makes tidal flat sediments highly dynamic with regard to both, their grain size composition as well as the spatial distribution of different sediment types.

Seasonal decline in biological production coupled with storms allows the sediment to be more easily eroded in winter while enhanced deposition of sediments is observed in summer (Dyer et al. 2000b). This often creates a seasonal cycle of erosion and deposition resulting in a mud drape in summer and more sandy sediments in winter (Andersen and Pejrup 2001, Chang et al. 2006). Dynamic equilibriums, like seasonality, are frequently found in this highly dynamic system but other changes are directional and lead to new conditions, like e.g. shoreline changes.

An example for permanent change is the considerable reduction of the tidal flat area in the European Wadden Sea by land claim and dyke construction over the past centuries (e.g. de Jonge et al. 1993, Reise 1998, Lotze et al. 2005, Reise 2005). The general net loss of sediments and tidal flat areas is furthermore associated with the depletion of fine-grained sediments (Higelke 1998, Bayerl et al. 1998). The reduction of a tidal catchment area leads to increased energy-levels in a tidal basin which results in a depletion of mud as it gets removed by waves and currents (Flemming and Nyandwi 1994, Mai and Bartholomä 2000). A coarsening of sediments may also be caused by mechanical cockle-dredging which increases resuspension and erosion of fine-grained sediments (Piersma et al. 2001). Cockle-dredging was intensively conducted in the Dutch Wadden Sea but is now forbidden. Flemming and Nyandwi (1994) assume that the coarsening has not only an impact on the sedimentary regime but also on the associated fauna.

A loss of tidal flat area and changes in the sediment composition are also observed in the northern Wadden Sea. In this study, intertidal surface sediments were therefore monitored in a semi-enclosed bay in the northern Wadden Sea at regular intervals of 6 to 8 weeks from November 2004 to December 2006. Changes in the sediment composition of tidal flats are often analysed but to my knowledge there is little information on area-wide spatial dynamics of sediment distribution patterns. Therefore, the aim of this time-series investigation was not only to survey the variability in sediment grain size composition but

also to analyse and quantify the spatial dynamics of the sediment types in order to determine the variability of this depositional system. In this regard, it was also checked if seasonality can be detected and what the main driving forces for sediment distribution patterns are.

The grain size composition of sediment allows conclusions on their origin but reflects also information on the prevailing hydrodynamics. In particular subtle changes in speed and force of the tidal currents leave traces in the granulometry of associated sediments. My hypothesis is that ongoing climate change and sea level rise leave a signal in surface sediments. Therefore, trends in the grain size composition were analysed for the period November 2004 to December 2006. In order to get also a long-term perspective of the depositional processes and to observe real trends in their development, the present survey was compared with former studies that have been undertaken by Wohlenberg (1937), Felix (1981) and Austen (1990).

## 4.2 Materials and methods

### 4.2.1 Survey areas and sampling

The List tidal basin is located in the northern Wadden Sea at the German-Danish border. Due to the multitude of coastal processes, which can be surveyed here, its well-defined borders and long and continuous history of research, this tidal basin is an ideal survey area for monitoring and research in the Wadden Sea (Reise and Gätje 1997). This study was conducted in the Königshafen, which is a semi-enclosed bay and part of the List tidal basin (Fig. 2.2). The List tidal basin und Königshafen underwent severe human modification (see Chapter 3.1). Reise (1998) estimates that over the last 500 years one third of the basin has been converted into land by embankment and its tidal flat area decreased from approx. 66 to 40 % within the 20$^{th}$ century. A coarsening trend in the sediments grain size composition can also be detected here and as no heavy mussel fishery occurs in the List tidal basin, there must be other reasons for it.

Sediment samples were taken from sampling stations which were determined in the run-up to the campaigns. The positions were selected based on aerial photographs and the coordinates of the sampling points calculated in a GIS shape-file using the ESRI software ArcGIS 9.1, ArcMap. Then, the GIS file was imported and transferred on the differential GPS (DGPS) GeoXT handheld via the Trimble software GPS Pathfinder Office 2.90. In the field, the sampling stations were located using the navigation task and as the DGPS device has a submeter accuracy, sampling was always conducted in the same spot. Each

time, two sediment samples were taken from the surface of each sampling location, one sediment sample (6 to 8 gram) for the analysis in the lab and one larger back-up sample (up to 50 gram).

**Königshafen (November 2004 - December 2006)**

In order to analyse the type and the development trend of surface sediments, a grid of 128 equally distributed sampling points with a distance of 200 m was designed for the entire intertidal area of the Königshafen (Fig. 4.1). The sampling was carried out during low tide from November 2004 until December 2006 with a sampling interval of 6 to 8 weeks depending on low water level (Table 4.1). All together, 15 samplings campaigns were carried out in which 1626 samples were taken. In 13 sampling campaigns, the entire area was surveyed. Two sampling campaigns cover only parts of the Königshafen because the aim was to do rapid, exemplary samplings as they were conducted immediately after change in weather with arising wind speeds of 26 m $s^{-1}$ (2004-47) and 14 m $s^{-1}$ (2006-12).

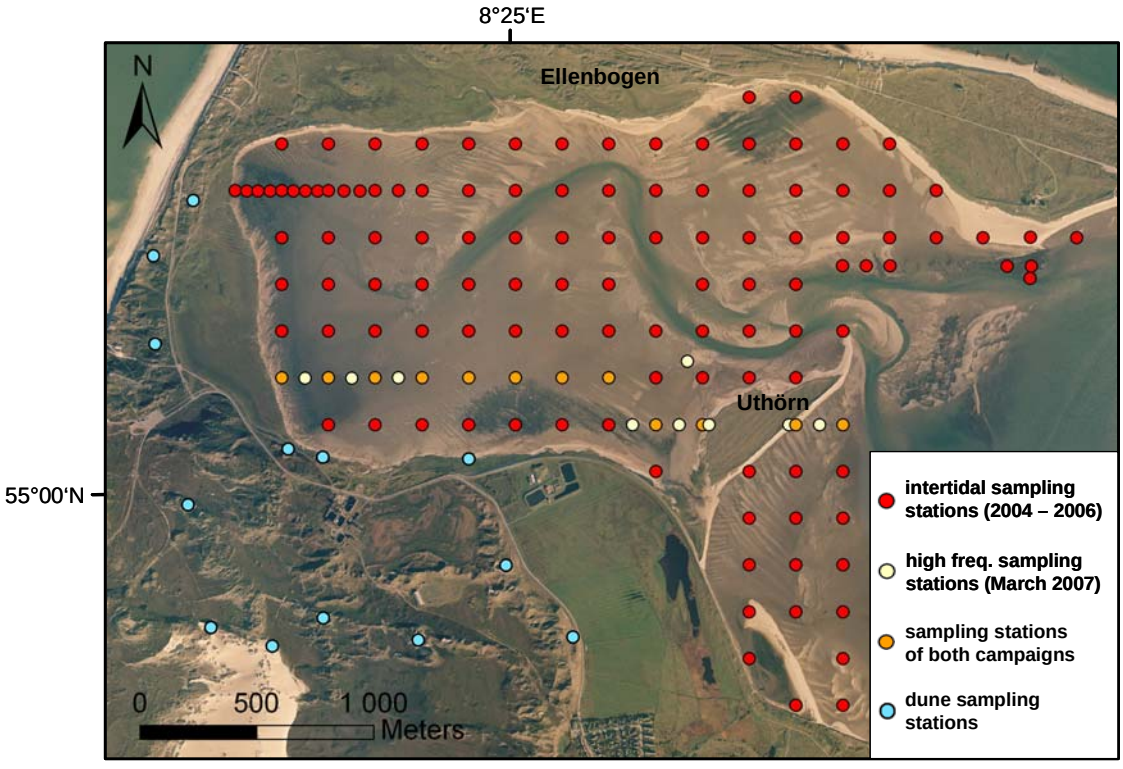


**Fig. 4.1:** Survey area Königshafen with the sampling stations for the different sampling campaigns.

**Table 4.1:** Sampling dates and number of collected sediment samples in Königshafen from November 2004 to December 2006.

| Year - week | Date | Number of samples |
|---|---|---|
| 2004-47 | 15 to 17-Nov-2004 | 118 |
| 2004-47 (partial) | 20-Nov-2004 | 24 |
| 2005-02 | 10 to 12-Jan-2004 | 78 |
| 2005-09 | 28-Feb to 02-Mar-2005 | 120 |
| 2005-16 | 18 to 20-Apr-2005 | 126 |
| 2005-25 | 26 to 27-Jun-2005 | 131 |
| 2005-33 | 18 to 21-Aug-2005 | 133 |
| 2005-46 | 18 to 21-Nov-2005 | 121 |
| 2006-01 | 07 to 08-Jan-2006 | 134 |
| 2006-09 | 03 to 04-Mar-2006 | 121 |
| 2006-12 (partial) | 25-Mar-2006 | 37 |
| 2006-18 | 01 to 02-May-2006 | 122 |
| 2006-32 | 08 to 09-Aug-2006 | 133 |
| 2006-38 | 21 to 23-Sep-2006 | 112 |
| 2006-51 | 19-Dec-2006 | 116 |

**High-frequency sampling in the Königshafen (March 2007)**

For the analysis of short-term changes in the sediment composition, a high-frequency sampling campaign along 2 east-west profiles was conducted in the Königshafen in March 2007 (Fig. 4.2). The first transect (18-65 to 25-65) was located in the inner Königshafen and had a length of 1400 m. It compromised 11 sampling stations with a 100 or 200 m spacing between them. Eight of theses sampling stations were also part of the sampling grid of the periodic sampling from November 2004 to December 2006 (Fig. 4.2). The second transect (25a-66 to 30-66) ran parallel to the first one and was located south of it. It stretched from the inner into the outer Königshafen and was 900 m long. The 9 sampling stations had a distance of 30 m or 100 m to each other and were located east and west of the artificial island Uthörn. At this transect 4 sampling stations were part of the large grid for the periodic sampling. One single sampling station (Tidal Creek) was located in the inner Königshafen near Uthörn in close vicinity to tidal creek. All together samples from 21 stations were taken during 5 consecutive low tides from March 4 to March 6, 2007 resulting in a total of 105 sediment samples.

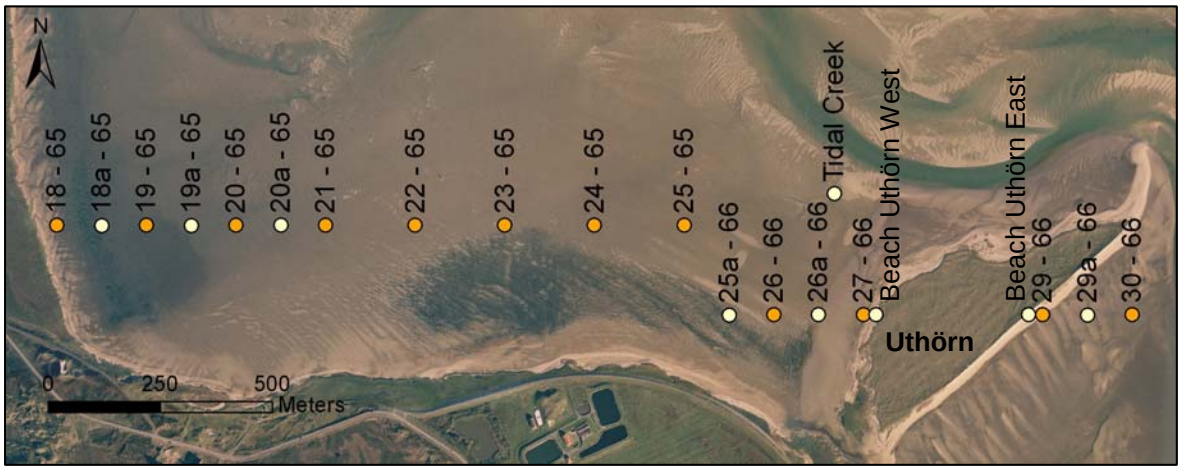


**Fig. 4.2:** Sampling stations of the high-frequency sampling campaign in March 2007.

### Dune sands

For the purpose of analysing the sediment input from surrounding sand dunes into the Königshafen, 13 sediment samples were taken in a one-time campaign on March 7, 2007. The sediment samples were taken from migrating or vegetated sand dunes which are located south and south-west of the Königshafen (Fig. 4.1). The sand dunes are either directly adjoining the Königshafen or its salt marshes or are situated in a distance of 600 to 900 m to the shallow embayment. In order to get a representative and unaffected sample of the real grain size composition of the dunes, the sediment was not taken directly from the surface but from a depth of 20 to 30 cm.

## 4.2.2 Analysis and classification of sediment samples

The grain size compositions were analysed of all sediment samples. For the preparation of the analysis, the samples were treated in the lab with acetic acid and hydrogen peroxide to destroy non-siliciclastic materials. Larger grains (> 2 mm) were removed by sieving because they were too large for the laser analyses. The grain size composition of the sediment < 2 mm was analysed with a 'CILAS 1180 Laser particle analyzer'. This instrument provides a measuring range of 14.6 to -1.4 φ (Phi) (0.04 to 2500 micrometers) with a class resolution of 0.1 φ. The resulting data sets were edited and further analysed using 'Gradistat', a grain size distribution and statistics package for the analysis of unconsolidated sediments (Blott and Pye 2001). The grain size statistics as well as the data on pebbles were brought into ArcGIS 9.1, ArcMap, allocated according to their sampling station and saved as point shape-files.

Two classification systems were used regarding the type of the sediments and the trend of their development (Table 4.2). In order to respond to the specific sediments in the

Königshafen and to show even subtle developments and changes in their composition, a new classification for sediment types was adopted. It was designed following the classification DIN 4022 (mud > 4 φ, sand 4 to -1 φ and gravel < -1 φ; these classes are further subdivided; for more information see Austen 1990). In order to increase resolution, mud was divided into mud and coarse mud. Unlike to the DIN 4022, coarse sand had to be determined < 1 φ according to the output of the already classified data by the 'CILAS 1180 Laser particle analyzer'.

**Table 4.2:** Classification of sediment types and the development trend of sediments.

| Sediment | Phi |
|---|---|
| mud (S 1) | > 6 |
| coarse mud (S 2) | 6 to 4 |
| fine sand (S 3) | 4 to 2.5 |
| medium sand (S 4) | 2.5 to 1 |
| coarse sand (S 5) | < 1 |

| Trend | Increase / decline of trend line |
|---|---|
| finer (T 1) | < -0.1 |
| slightly finer (T 2) | -0.02 to -0.1 |
| no trend (T 3) | -0.02 to 0.02 |
| slightly coarser (T 4) | 0.02 to 0.1 |
| coarser (T 5) | > 0.1 |

For the development trend of the sediments the average grain size (Mean) and the most frequent grain size (first Mode) were analysed and taken as parameters for sediment changes. As a dynamic equilibrium is assumed, the Mean value is supposed to show the dynamics while the first Mode represents the more stable overall status. Even though the focus was put on these two values it should be kept in mind that a sediment sample is composed of a broad range of grain size classes (Fig. 4.3a). For this classification, the grain size was considered in micrometers and not in Phi in order to avoid over- or underestimations caused by the logarithmic nature of the Phi-scale.

The trend shows if there is a steady development in the grain size composition at a certain location. For each sampling location the development of the Mean value and first Mode value were plotted over the entire sampling period from November 2004 to December 2006 (Fig. 4.3b). Then, each sampling location was classified according to the incline or decline of the trend line (Table 4.2).

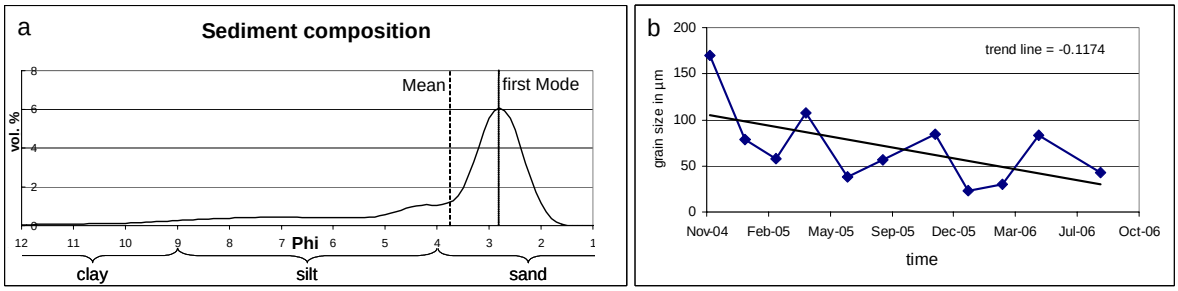


**Fig. 4.3:** The grain size composition graph of an exemplary sediment sample (a) and the development of a sample Mean value during the survey period (b).

### 4.2.3 Interpolation techniques

On the basis of the dense sampling grid, area-wide maps were interpolated for the Königshafen using the ArcGIS tool 'Geostatistical Analyst'.

Interpolations are methods to estimate unknown values on the basis of existing values, normally measurements. The interpolation techniques in the 'Geostatistical Analyst' are divided into two main types: deterministic and geostatistical methods.

Deterministic interpolation techniques have in common that unknown values are estimated on the base of the geometric distances of existing neighbouring values (Isaaks and Srivastava 1989). They can be divided into two groups, global and local. Global techniques calculate predictions using the entire data set. Local techniques calculate predictions from the measured points within neighbourhoods, which are smaller areas within the larger study area. The ArcGIS 'Geostatistical Analyst' provides amongst others the 'Radial Basis Functions' as a local interpolator which is an exact interpolator as it predicts a value that is identical to the measured value at a sampled location. An inexact interpolator predicts a value that is different from the measured value in order to avoid sharp peaks or troughs in the output surface.

Geostatistical techniques consider the spatial distribution of natural phenomena as a combination of geometrical distances and a statistical method. Geostatistics assume that at least some of the spatial variation of natural phenomena can be modeled by random processes with spatial autocorrelation. That means that unknown values are estimated by a weighted average of existing neighbouring values on the base of a statistical model in order to optimize weighting (Schlüter 1996). Geostatistical techniques produce not only prediction surfaces but also error or uncertainty surfaces, giving an indication of how good the predictions are (ESRI 2003). This makes it especially helpful for the interpolation of larger areas with data based on a not-designed, random sampling.

For this study the deterministic interpolation technique 'Radial Basis Functions' was chosen. Compared to the other interpolation methods it provided results which fit best to own field observations. It turned out to be most suitable because it considers small-scale variations and compared to other methods, especially geostatistical techniques like 'Kriging', it does not generalise too much which makes it most appropriate for the specific sediment characteristics in the Königshafen. Due to the dense sampling grid and the constant arrangement of sampling stations, error prediction was negligible for this study.

The results of 13 sampling campaigns from November 2004 to December 2006 were interpolated to area-wide maps of the Königshafen. In order to show even subtle changes and shifts in the grain size composition of the sediments, the maps were interpolated according to their more variable Mean value.

Two sampling campaigns were carried out after storm events and sediment samples were collected along transects or in sections of the Königshafen. In theses cases as well as for the high-frequency and the dune sampling, interpolations were abandoned because no area-wide data were available.

### 4.2.4 Comparison of sediment distribution patterns

For the detection of differences and similarities of the results of the 13 area-wide sampling campaigns, the interpolated sediment maps were compared with each other. The aim was to detect similarity in sediment distribution patterns as well as to assess seasonality and to find out what the driving parameters for sediment distribution are.

The work flow described below was done with the ArcGIS 'ModelBuilder'. With this tool, a model was generated which works like a macro and was used to automate a work flow.

At first, all interpolated maps were clipped to the shape of the intertidal Königshafen in order to make them congruent. After that the vector data maps were converted into raster data maps with a 10 m cell resolution (Fig. 4.4).

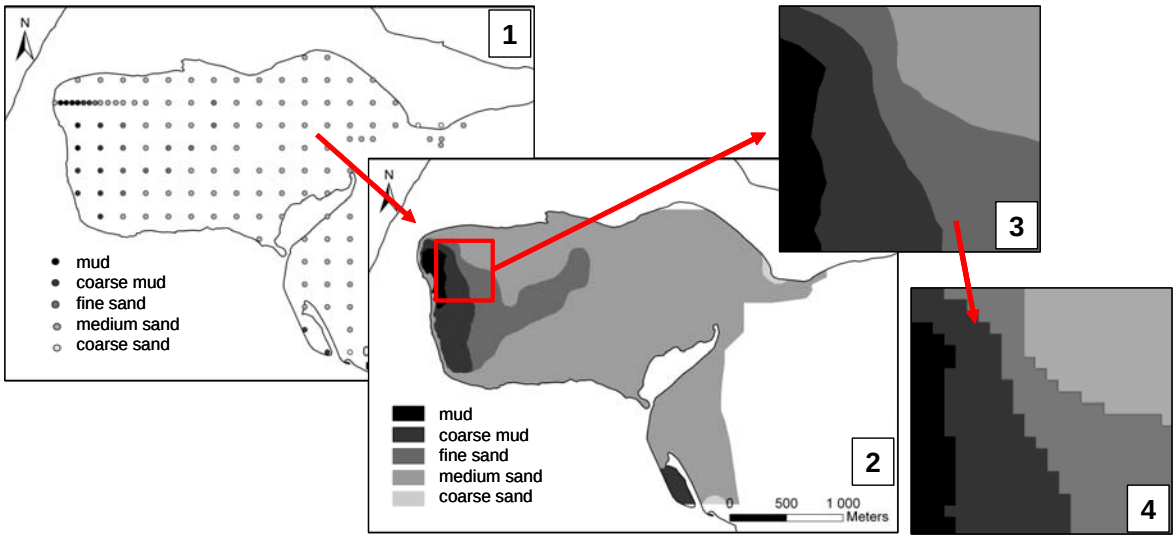


**Fig. 4.4:** Data points (1) are interpolated to area-wide maps (2). These maps are vector maps (3) which are converted to raster maps (4).

Then, the raster maps were reclassified so that each sediment type was identified by a prime number. For practical reasons due to the rareness of the sediment type 'coarse sand', it was included to the class 'medium sand', resulting in a total of 4 sediment types for the calculations. The prime numbers 1, 2, 3 and 5 were allocated to each raster cell according to the sediment type it represents. Now, it was possible to multiply these ID values of two raster maps on a cell by cell basis (Fig. 4.5). That means that two input raster maps were overlaid and the IDs of congruent cells multiplied resulting in a new output raster map with new ID values. This new map is a mathematical product of the two input maps and only those areas (raster cells) were considered, where the same sediment type is congruent in the two input maps. Therefore, these areas needed to be identified correctly. For this reason the raster cells were allocated with prime numbers because the multiplication of two raster cells from the same sediment type produces the unique IDs 1, 4, 9 and 25. In the new map, all areas with other IDs, i.e. locations in the Königshafen where sediments have changed from one sampling to the next, were excluded by another reclassification (Fig. 4.5). Then, the new reclassified raster maps were converted back into vector data maps. All areas with the same ID were merged to one polygon. In the next step the area of each polygon and its percentage on the entire Königshafen area were calculated. By this it could be determined to which percentage the sediments in the Königshafen remain or change and which sediments types are most affected.

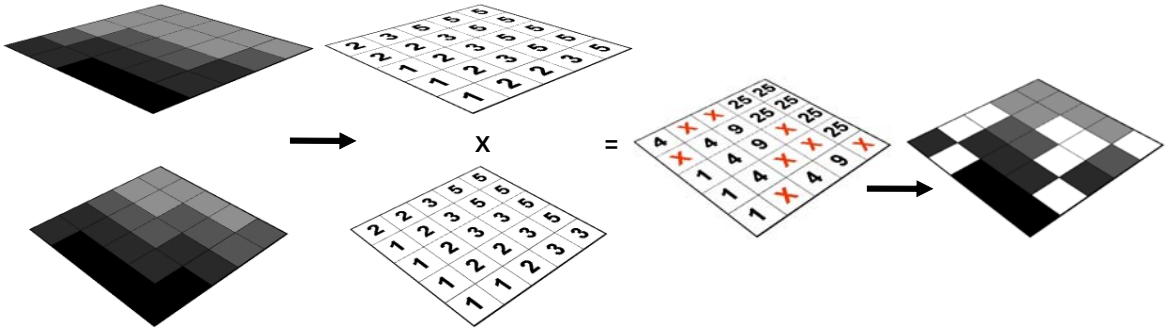


**Fig. 4.5:** Two raster layers, which show distribution of different sediment types, get reclassified to numbers so that every prime number represents the sediments type in its raster cell. These raster layers are multiplied and cells with sediment changes get deleted from the result layer. The result layer gets convert back to sediment colours. The white raster cells indicate where the sediment type has changed and are taken to express the dynamics in the sediment distribution pattern.

Two main comparisons were conducted with the interpolated maps of the sediment surveys. At first, each sampling was compared with the ensuing sampling starting in November 2004 yielding 12 comparative results. Then, the result of a sampling campaign was compared to the results of all other samplings. This was done for every single campaign resulting in 156 comparisons.

Furthermore, average values were calculated for the years 2005 and 2006 as well as for the entire sampling period. The average values from November 2004 to December 2006 were compared with surveys by Wohlenberg (1937), Felix (1981) and Austen (1990). These sediment data were presented in form of maps which were scanned with a resolution of 400 dpi, georeferenced and digitized in ArcGIS 9.1. As all former surveys used a coarser sediment classification system my data had to be reclassified and interpolated again in order to make the results comparable to earlier studies.

### 4.2.5 Mud content

Another sediment statistic calculated by the software 'Gradistat' is the mud content (> 4 φ) of a sediment sample. Sediments can be classified according to their Mean or first Mode value but also according to their mud content (Reineck and Siefert 1980). As this is a meaningful dynamic parameter, which reveals even subtle changes in the sediment composition, the mud content is also regarded in this study. Furthermore, it closely correlates to the sediment type.

For each of the 13 area-wide sampling campaigns the distribution of different mud content classes was interpolated for the intertidal Königshafen. This was also done in GIS using the 'Radial Basis Functions'. As the Königshafen is predominantly sandy, relatively low

mud contents were chosen for the classification (< 2.5 %, 2.5-5 %, 5-10 %, 10-25 %, 25-50 % and > 50 %) in order to detect also subtle changes in the grain size composition of sandy sediments. Finally, the area covered by each mud content class and its percentage to the entire Königshafen were calculated.

### 4.2.6 Sediment characteristics

Some sediment samples show in their grain size composition among a first Mode also a second or even third Mode which represents the second or third most frequently occurring particle class. These sediments are bimodal or trimodal which is caused by sediment input from different sources. On this account, polymodality is an important sediment parameter. For each sampling campaign, the positions of bi- and trimodal sediments were recorded and their spatial distribution pattern analysed.

The 'Sorting' and the 'Skewness' are further parameters to characterise sediments. The Sorting indicates the standard deviation, i.e. if a sediment sample is composed of a broad or narrow range of grain size classes. The Skewness is the degree of asymmetry of a frequency or cumulative curve. It indicates an excess of finer or coarser sediment particles (Blott and Pye 2001). Scatterplot graphs of Mean value and the Sorting or the Skewness were created in GIS. As the graph and the map of the Königshafen are interactive, it was not only possible to see the correlation between Mean value and Sorting or Skewness but also to detect the respective spatial position.

### 4.2.7 Weather data

Weather data as well as records on water levels (see chapter 2.2) were consulted for the detection of driving parameters in the sediment distribution. The Deutscher Wetterdienst (DWD) provided a multitude of long-term weather data from the weather station List (Sylt). For this study the daily data on minimum, average and maximum wind force as well as on the wind direction from November 2004 to March 2007 were of importance.

### 4.2.8 Statistics

All tests of statistical significance were conducted with the StatSoft software package STATISTICA 6.0. The p-level was determined at 0.05 and the standard deviation was used. The tests that were done are further specified in the following chapter 'Results'.

## 4.3 Results

### 4.3.1 Surface sediments in the Königshafen (2004 – 2006)

**Distribution of sediment classes**

The sediment classes in the Königshafen are ranging from mud (S 1) to coarse sand (S 5) (Fig. 4.6). Sediment compositions from November 2004 to December 2006 are displayed as average interpolated values of the sediments first Mode. The muddy sediments (S 1) cover the innermost western part of the Königshafen which is 1.5 % of the intertidal area. A strip of coarse mud (S 2; 5.5 %) adjoins it and stretches southwards, bordering a zone of fine sand (S 3). The fine sand forms a belt following the course of the tidal creek and covers 10.5 % of the intertidal. Medium sand (S 4) dominates in the Königshafen (80 %). In the sheltered location of a sandy hook in the south-eastern corner another zone of coarse mud (S 2; 1.5 %) established. Coarse sand (S 5) occurs in the outer Königshafen, in vicinity of steep sandy beaches and covers 1 % of the intertidal area.

It can be summarized that the finest sediments occur in the inner Königshafen while the rest of the survey area is dominated by medium sand.

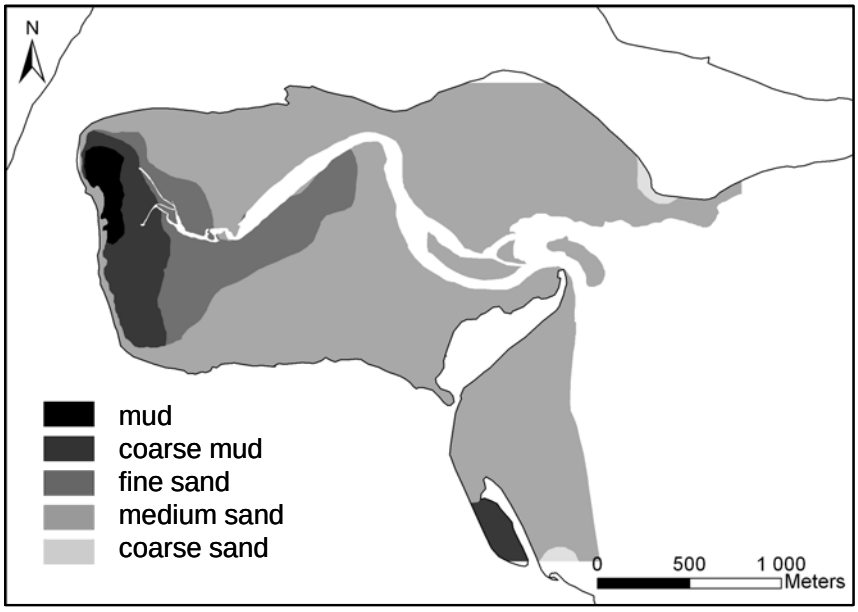


**Fig. 4.6:** The spatial distribution pattern of sediment types according to their average first Mode value from 2004 to 2006.

**Developmental trend of surface sediments (2004 – 2006)**

The temporal trend in the development of the grain size composition at each sampling location was classified into five groups ranging from a clear fining to a clear coarsening

trend. The trends shown here apply exclusively to the sampling period from November 2004 to December 2006.

The average grain size (Mean) is becoming finer in the innermost part of the Königshafen (Trend Mean (Tme) 1; Fig. 4.7). This area is almost congruent with the mud and coarse mud deposits and covers 8 % of the Königshafen intertidal area. Adjoining is a zone located where the mean grain size of the sediments is becoming slightly finer (Tme 2, covering 23 %). This zone also follows the course of the tidal creek similar to the occurrence of fine sands. Most sediments show no trend (Tme 3; 65 %), especially in the centre of the bay. In the north-eastern corner near intertidal mussel beds, the sediments are becoming slightly finer (Tme 2) and in the centre of the mussel beds even clearly finer (Tme 1). Nevertheless, the sediments are getting slightly coarser (Tme 4) outside the mussel beds at the transition to the subtidal. In the south-eastern corner with conspicuous megaripples the mean grain size also tends to become slightly coarser (Tme 4).

Compared to the Mean value the first Mode remains relatively stable and shows only few and weak trends (Fig. 4.7). There is mainly no trend in the first Mode (Trend Mode (Tmo) 3, coverage: 89 %). It is getting slightly finer (Tmo 2; 8 %) in two areas in the innermost part of the Königshafen and in the centre near the tidal creek. Similar to the Mean, the first Mode also becomes slightly coarser (Tmo 4; 3 %) in a few areas in the outer Königshafen.

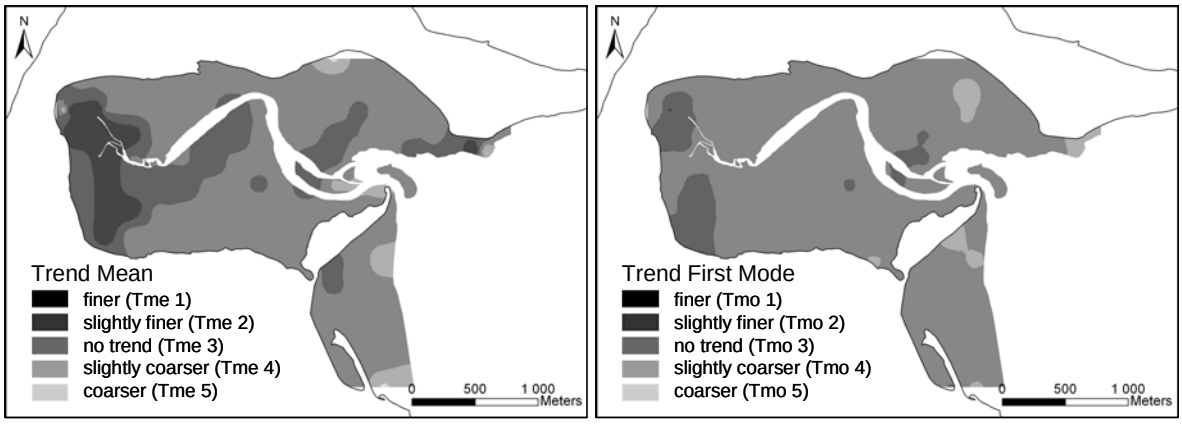


**Fig. 4.7:** Developmental trend of sediment Mean and first Mode value (2004 to 2006).

### 4.3.2 Comparison of sediment distribution patterns

The results of the 13 complete sampling campaigns from November 2004 to December 2006 were interpolated to area-wide sediment maps. The degree of change of the spatial distribution patterns of the different sediment types is displayed in maps and was calculated by direct comparison. Two sediment maps were overlayed and the extent of the

areas, where the sediment classes were not congruent, was determined (Fig. 4.9). The result given in percentage shows how much the surface sediments shifted in their position. It shows the spatial pattern of variability but not intensity.

First, the results consecutive surveys were compared. The aim was to assess the variability of the sediment distribution pattern within 6 to 8 weeks. This was regarded over two years in order to detect possible seasonality effects, i.e. if the magnitude of change is different in winter or summer. The 12 comparisons are displayed in chronological order in Table 4.3. The average magnitude of spatial change from one sampling to the next sampling covering a period from November 2004 to December 2006 is 26.3 %. The values are ranging from 15 % to a maximum of 36 % with a standard deviation of 5.6. The changes less than 20 % and more than 30 % are regarded to be exceptionally low and high, respectively. Eight comparisons are ranging in between 20 and 30 %, while 2 are exceptionally low and 2 are exceptionally high.

**Table 4.3:** Percentage of spatial changes of subsequent surveys (year – week).

| Comparing | % of spatial change |
|---|---|
| 2004-47 with 2005-02 | 26 |
| 2005-02 with 2005-09 | 29 |
| 2005-09 with 2005-16 | 32 |
| 2005-16 with 2005-25 | 28 |
| 2005-25 with 2005-33 | 25 |
| 2005-33 with 2005-46 | 15 |
| 2005-46 with 2006-01 | 19 |
| 2006-01 with 2006-09 | 36 |
| 2006-09 with 2006-18 | 28 |
| 2006-18 with 2006-32 | 25 |
| 2006-32 with 2006-38 | 23 |
| 2006-38 with 2006-51 | 30 |
| Average change | 26.3 |
| Standard deviation | 5.63 |

For the detection of differences and similarity in the sediment distribution patterns, each result of a sampling campaign was compared to the results of all other samplings (Table 4.4). The aim was to test the entire two year survey period for seasonality effects and to build a base for the detection of driving forces that are responsible for the spatial distribution of the sediments. The differences between two samplings are ranging from 15 to 51 %. The mean magnitude of change is 28.6 ± 7.5 %. In this case, the changes > 35 % are regarded to be exceptionally high and marked red while the changes < 20 % are marked green as exceptionally low.

A distinct spatial distribution pattern of the sediment types can be observed when regarding the average values for 2005 and 2006 (Fig. 4.9). The spatial changes of the distribution of sediment types (Table 4.4) followed this general pattern.

**Table 4.4:** Percentage of spatial changes of sediments resulting from the comparison of all samplings (year – week).

| | 2004-47 | 2005-02 | 2005-09 | 2005-16 | 2005-25 | 2005-33 | 2005-46 | 2006-01 | 2006-09 | 2006-18 | 2006-32 | 2006-38 | 2006-51 |
|---|---|---|---|---|---|---|---|---|---|---|---|---|---|
| 2004-47 | | 26 | 26 | 29 | 33 | 19 | 19 | 26 | 51 | 32 | 28 | 23 | 33 |
| 2005-02 | 26 | | 29 | 34 | 35 | 24 | 25 | 36 | 49 | 37 | 32 | 37 | 35 |
| 2005-09 | 26 | 29 | | 32 | 32 | 21 | 23 | 22 | 48 | 32 | 25 | 23 | 33 |
| 2005-16 | 29 | 34 | 32 | | 28 | 29 | 23 | 19 | 35 | 23 | 29 | 27 | 31 |
| 2005-25 | 33 | 35 | 32 | 28 | | 25 | 23 | 22 | 36 | 27 | 22 | 31 | 26 |
| 2005-33 | 19 | 24 | 21 | 29 | 25 | | 15 | 23 | 45 | 32 | 22 | 24 | 24 |
| 2005-46 | 19 | 25 | 23 | 23 | 23 | 15 | | 19 | 40 | 28 | 20 | 17 | 28 |
| 2006-01 | 26 | 36 | 22 | 19 | 22 | 23 | 19 | | 36 | 21 | 33 | 23 | 34 |
| 2006-09 | 51 | 49 | 48 | 35 | 36 | 45 | 40 | 36 | | 21 | 19 | 43 | 40 |
| 2006-18 | 32 | 37 | 32 | 23 | 27 | 32 | 21 | 21 | 28 | | 25 | 24 | 30 |
| 2006-32 | 28 | 32 | 25 | 29 | 22 | 22 | 20 | 19 | 33 | 25 | | 23 | 28 |
| 2006-38 | 23 | 37 | 23 | 27 | 31 | 24 | 17 | 23 | 43 | 24 | 23 | | 30 |
| 2006-51 | 33 | 35 | 33 | 31 | 26 | 24 | 28 | 34 | 40 | 30 | 28 | 30 | |

Furthermore, a successive comparison over the entire sampling period was conducted with the aim to detect the areas where the sediments remain in their class throughout the entire sampling period. The aim was to reveal the overall dynamics. Therefore, the differences were determined consecutively starting in November 2004. Within these 2 years, 75.6 % of the intertidal area has changed while in 24.4 % of it the sediments remained unchanged according to their class (Fig. 4.8). These 24.4 % are composed as follows: 22.5 % sand, 0.5 % fine sand, 1.2 % coarse mud and 0.2 % mud.

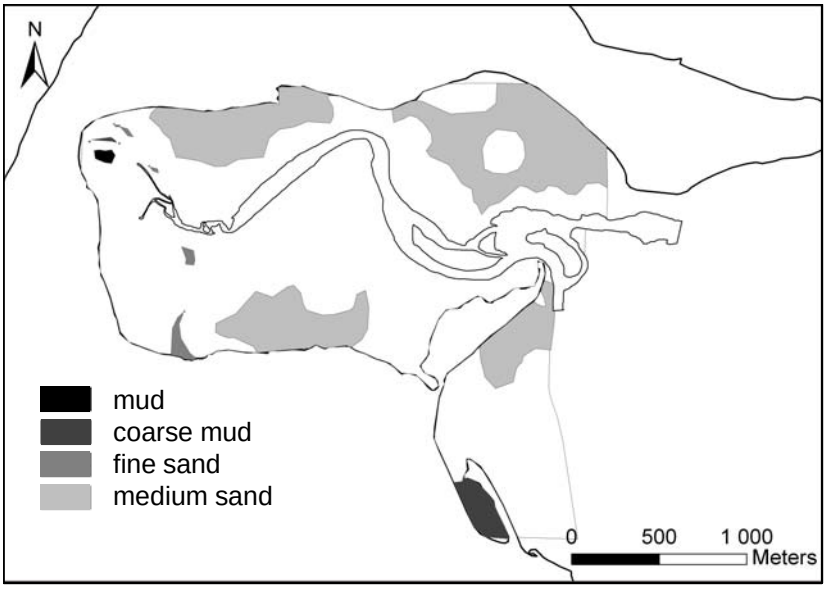


**Fig. 4.8:** Areas where the sediments remained unchanged during the entire survey period according to their Mean value (2004 – 2006).

In order to check for a dynamic equilibrium, the average sediment distributions on the base of all samplings from 2005 and 2006 were calculated and the results compared. The differences between the two years amount to 18 % of the intertidal Königshafen area (Fig. 4.9). This means that the same sediment types can be found in 82 % of the area (54 % sand, 23 % fine sand, 4.5 % coarse mud and 0.5 % mud).

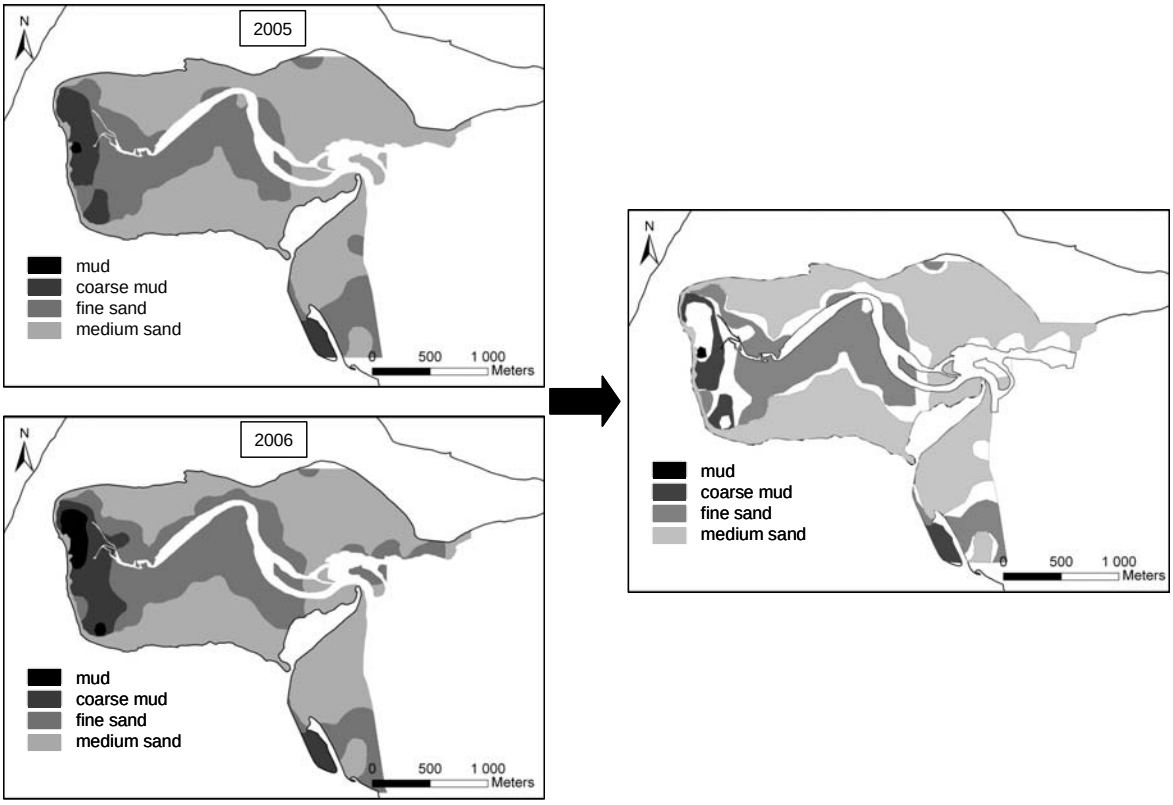


**Fig. 4.9:** Comparison of the average sediment distribution patterns of 2005 and 2006. The result shows where the same sediments are congruent in both years according to their Mean value.

### 4.3.3 Mud content

Among the variability of the spatial distribution of the sediments, the changes in the sediment composition at each sampling station were also quantified. The mud content was chosen in order to detect even subtle changes as it is a very dynamic factor. The relation of mud content and sediment type can be seen in the results of each sampling campaign as their spatial distribution shows very similar patterns.

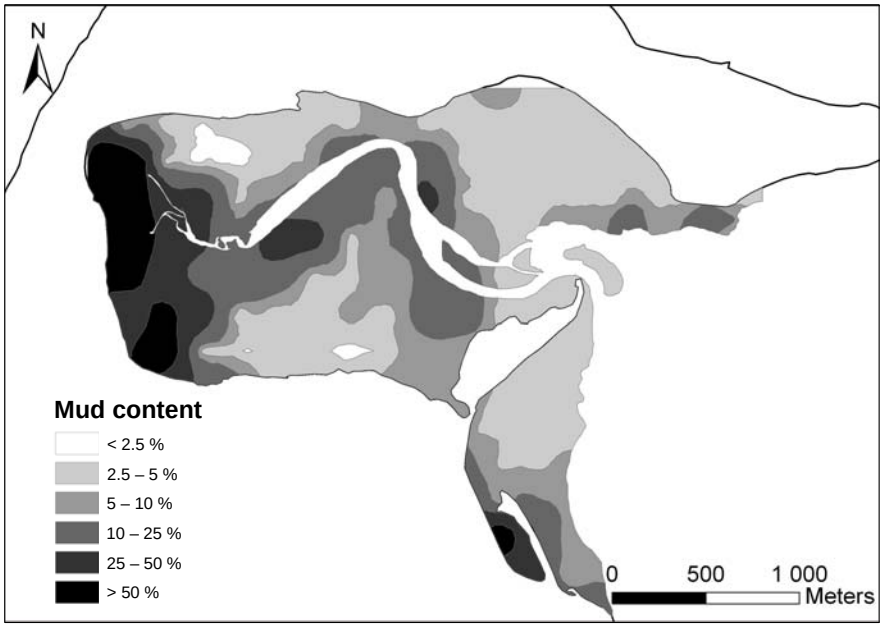


**Fig. 4.10:** The spatial distribution of the average mud content from 2004 to 2006.

The spatial distribution of the average mud content from November 2004 to December 2006 reveals that 1 % of the intertidal Königshafen has a mud content of less than 2.5 %, while 38 % of the area have a mud content between 2.5 and 5 % (Fig. 4.10). All these areas occur on sand-dominated tidal flats, primarily at the margins of the inner and in the outer Königshafen. Mud contents of 5 to 10 % cover 23 % of the intertidal and 21 % of it are characterised by a mud content of 10 to 25 %. These areas are mainly congruent with the occurrence of fine sand. They can be found close to the tidal creek in the inner half of the bay as well as in the southern outer Königshafen. 10 % show a mud content of 25 to 50 %, while the remaining 7 % have more than 50 %. Their distribution coincides with the occurrence of coarse mud and mud, which is especially in the innermost part of the Königshafen at the head of the creek.

The individual results of each sampling campaign are recorded in Table 4.5.

**Table 4.5:** Mud contents (in %) of each sampling campaign from November 2004 to December 2006 (year – week).

| Mud content | 2004-47 | 2004-47 (partial) | 2005-02 | 2005-09 | 2005-16 | 2005-25 | 2005-33 | 2005-46 |
|---|---|---|---|---|---|---|---|---|
| < 2.5 % | 14.9 | 17.0 | 30.8 | 0.1 | 0.3 | 1.5 | 22.0 | 6.1 |
| 2.5 - 5 % | 52.4 | 56.7 | 38.3 | 51.2 | 27.2 | 34.7 | 45.1 | 45.7 |
| 5 - 10 % | 12.0 | 6.5 | 11.0 | 22.8 | 31.4 | 24.1 | 15.4 | 23.2 |
| 10 - 25 % | 9.2 | 10.9 | 7.3 | 14.7 | 20.5 | 20.9 | 5.2 | 10.2 |
| 25 - 50 % | 5.7 | 3.8 | 4.6 | 6.8 | 15.5 | 13.4 | 4.7 | 7.5 |
| > 50 % | 5.8 | 5.1 | 8.0 | 4.5 | 5.1 | 5.3 | 7.6 | 7.2 |

| Mud content | 2006-01 | 2006-09 | 2006-12 (partial) | 2006-18 | 2006-32 | 2006-38 | 2006-51 |
|---|---|---|---|---|---|---|---|
| < 2.5 % | 0.1 | 0.2 | 3.7 | 0.1 | 15.6 | 7.3 | 18.4 |
| 2.5 - 5 % | 36.0 | 14.3 | 19.0 | 23.7 | 31.4 | 49.9 | 29.5 |
| 5 - 10 % | 28.7 | 26.6 | 26.6 | 29.9 | 21.6 | 15.8 | 14.9 |
| 10 - 25 % | 20.3 | 25.7 | 25.4 | 24.6 | 13.0 | 9.4 | 11.9 |
| 25 - 50 % | 11.2 | 23.1 | 8.1 | 13.0 | 9.0 | 10.8 | 12.1 |
| > 50 % | 3.6 | 10.3 | 17.2 | 8.7 | 9.4 | 6.9 | 13.2 |

### 4.3.4 High-frequency sampling

Sediment samples from 21 stations were collected during 5 consecutive low tides in order to analyse the short-term variability in their grain size composition. A high variability with considerable changes from tide to tide, which is primarily caused by supply or removal of mud, is detected.

The first east-west transect stretches along the inner Königshafen intersecting muddy and sandy areas. Therefore, the Mean values of this transect are ranging from 1.7 to 6.6 φ and the first Mode values from 1.8 to 4.6 φ during the entire sampling period. Due to the heterogeneity of the sediments grain size composition along the transect, the sampling points have to be regarded individually. The standard deviation of the Mean value for each sampling point ranges from a minimum of 0.03 φ to a maximum of 1.17 φ, with an average of 0.37 φ. The average standard deviation of the first Mode is 0.08 φ ranging from 0.0 to 0.29 φ (Table 4.6).

The second transect intersects mainly sandy tidal flats in the inner and outer Königshafen. Regarding the sampling period, the Mean values for each point of this transect are ranging from 1.9 to 2.3 φ and the values of the first Mode from 1.5 to 2.3 φ. Here, the average standard deviation of the Mean value is 0.17 φ with a minimum of 0.02 φ and a maximum of 0.89 φ. The average standard deviation of the first Mode amounts to 0.08 φ ranging from 0.0 to 0.18 φ.

The sampling station at the tidal creek was established to check the impact of the creek on the sediment dynamics. The results show Mean values from 3.2 to 3.9 φ while the first Mode values are ranging from 2.5 to 2.7 φ. Therefore, the average standard deviations are 0.32 and 0.08 φ, respectively which is in a normal range.

### 4.3.5 Sediment characteristics

**Polymodal sediments**

An average of 18 % of the sediment, sampled in the Königshafen from November 2004 to December 2006, show also a second and/or third Mode. This means that two or three grain size classes, which are rather different and not too close to each other, are most frequent in the sediments grain size composition. This may indicate that the sediment is supplied from different sources or the components were differently transported. 11 % are trimodal while 7 % are bimodal. There is no difference in their spatial distribution. For this analysis, the 13 area-wide sampling campaigns were considered. Sampling stations, where bi-or trimodal sediments occurred ≥10 times, were regarded as permanently polymodal while all others were classified as temporary. Permanently polymodal sediments occur mainly in the innermost part of the Königshafen and leewards of the sandy hook while the temporary ones are observed in the centre of the Königshafen in vicinity of the tidal creek (Fig. 4.11).

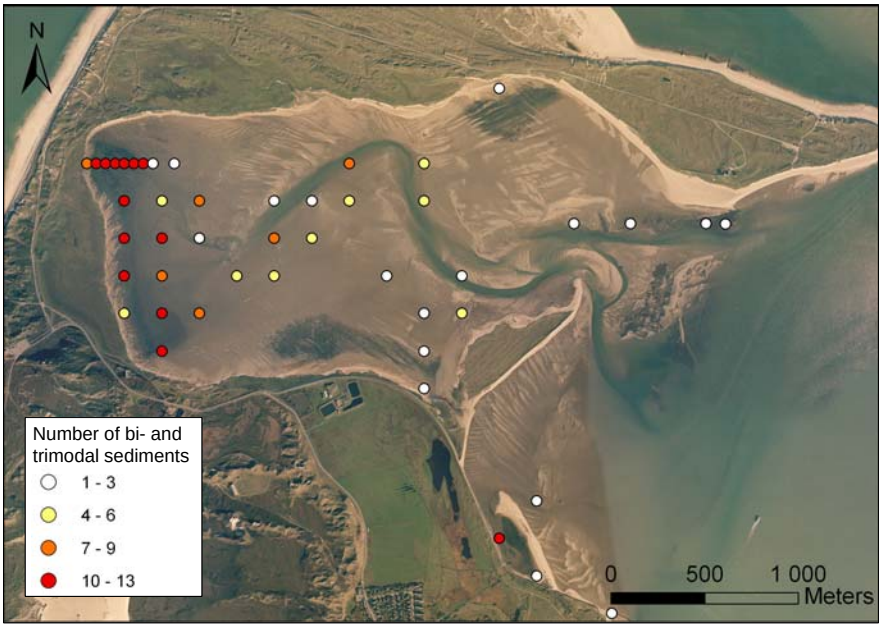


**Fig. 4.11:** Spatial distribution of polymodal sediments and number how often they were found at a sampling station from 2004 to 2006. All other sampling stations never showed mulitmodality during the sampling period.

**Sorting and Skewness**

Sorting indicates whether a sediment sample is composed of a narrow (well sorted) or broad (poorly sorted) range of grain size classes. Regarding the averages from November 2004 to December 2006, 1 % of all sampling stations show well sorted sediments, while 66 % are moderately sorted and 33 % are poorly sorted.

Skewness is the degree of asymmetry of a frequency curve (Blott and Pye 2001). Over the entire sampling period, no coarse skewed sediments could be found in the Königshafen. Only 6 % of all sampling stations exhibit symmetrical frequency curves. 67 % show 'fine skewed' sediments, while the sediments at 27 % of the sampling locations are 'very fine skewed'.

For both parameters, there are only minor differences between the averages of 2005 and 2006.

In order to analyse the sediment characteristics, Sorting and Skewness were plotted against the Mean value (Fig. 4.12 and 4.13). The moderately sorted sediments are mainly sand (1.5 to 2.5 φ) situated on the sandy tidal flats in the inner and outer Königshafen. The poorly sorted sediments are finer than sand (> 2.5 φ) and occur in the inner Königshafen, along the tidal creek and in the sheltered location of the sandy hook. There is a close positive correlation between Sorting and grain size: the finer the mean grain size the poorer the Sorting (Spearman R = 0.83, p = 0.00).

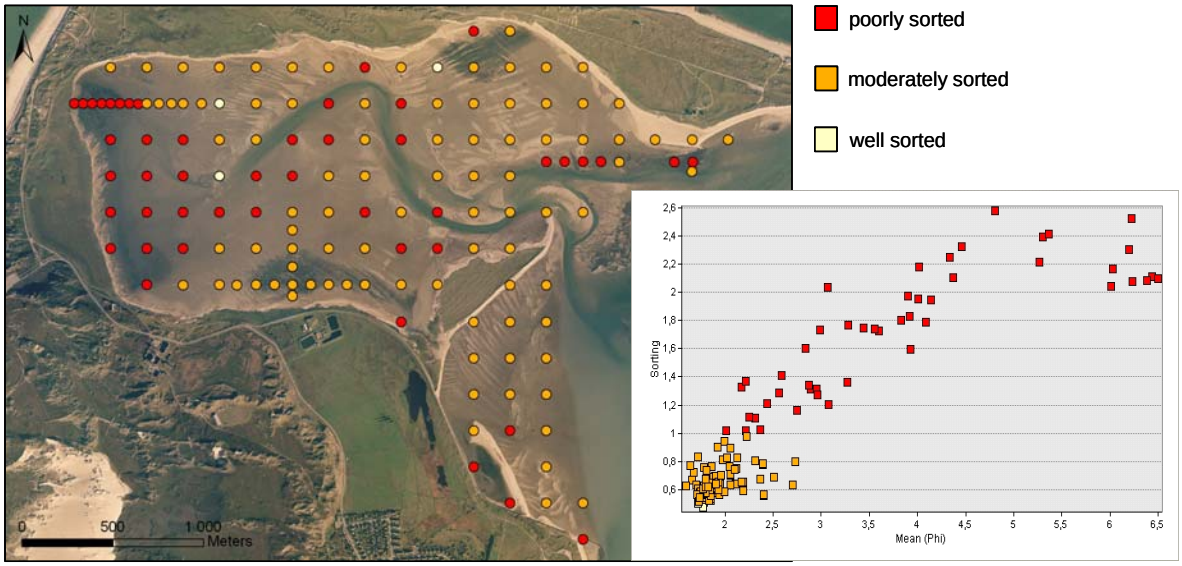


**Fig. 4.12:** Sorting is plotted against the Mean value and the map shows the spatial distribution of the results.

The sediment samples with symmetrical frequency curves have mainly a Mean value of 1.7 to 1.8 φ and can be found primarily on the margins of the sandy tidal flats in the inner Königshafen (Fig. 4.13). 'Fine skewed' cover a broad range from sand to mud (1.5 to 6.5 φ) with a clear concentration on sand (1.6 to 2.5 φ). They are located all over the Königshafen. 'Very fine skewed' sediments cover also a broad range from sand to mud (1.6 to 6.4 φ.) but their occurrence is especially focused on fine-grained areas, like along the tidal creek and at its head as well as near the sandy hook in the outer Königshafen.

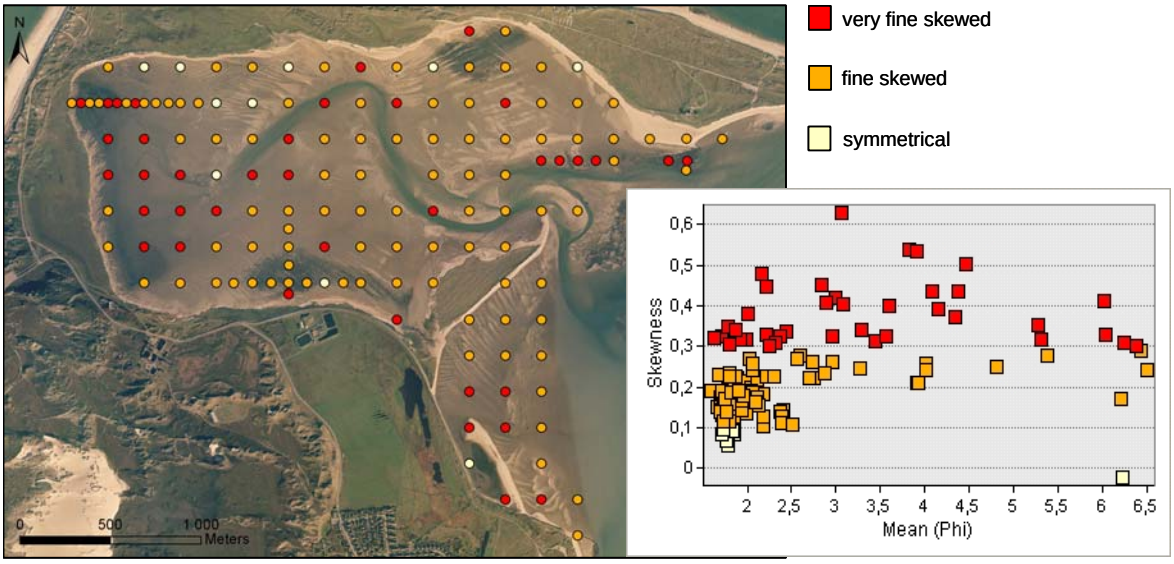


**Fig. 4.13** Skewness is plotted against the Mean value and the map shows the spatial distribution of the results.

### Dune sands

The 13 sediment samples from the sand dunes were analysed according to their grain size composition. Their Mean value ranges from 1.6 to 1.9 φ with an average of 1.7 φ. The values for their first Mode vary between 1.5 and 1.9 φ (average 1.7 φ). Regardless their distance to the Königshafen all grain size frequency curves offer considerable similarity. The mean standard deviation for all grain size classes (0.1 φ class resolution) and all 13 samples amounts to 0.12 φ.

## 4.4 Discussion

### 4.4.1 Development of intertidal surface sediments

In order to understand trends in the development of the Königshafen sediments, a long-term perspective is necessary. Therefore, this survey was compared with former studies conducted by Wohlenberg (1937), Felix (1981) and Austen (1990). Due to different sampling and analysis methods it is not possible to precisely quantify the changes. Nevertheless, a rough comparison is possible and gives a good idea how the former sediment situation in the Königshafen developed into the modern state.

**Long-term development of surface sediments from 1932/1933 to 2004/2006**

In 1932/1933 sand already dominated the intertidal, covering 68 % of the area, but the large share of finer sediments is remarkable: 21 % mud and 11 % mixed sediments (Fig. 4.14a). Coarse sand was not recorded. In 1981 coarse sand makes up 3% while medium sand covers 64 %, mixed sediments (including fine sand) 30 % and mud 3 % of the intertidal area (Fig. 4.14b). Between 1932/1933 and 1981 most of the mudflats already had disappeared. In 1989 sandy tidal flats covered 90 % (including 5 % coarse sand) of the intertidal, while mixed sediments make up 7 % and mud 3 % (Fig. 4.14c). Until today (2004/2006) the situation remained similar as the spatial share in the Königshafen is composed as follows: sandflats are covering 90 % while mixed sediments and mud are covering 8 % and 2 % (Fig. 4.14d). According to this classification system, coarse sand is also classified as sand and therefore is not itemised, although it occurs on the narrow beaches in the survey area. However, not many changes can be observed in the intertidal since 1989 because most of the mudflats have already been depleted.

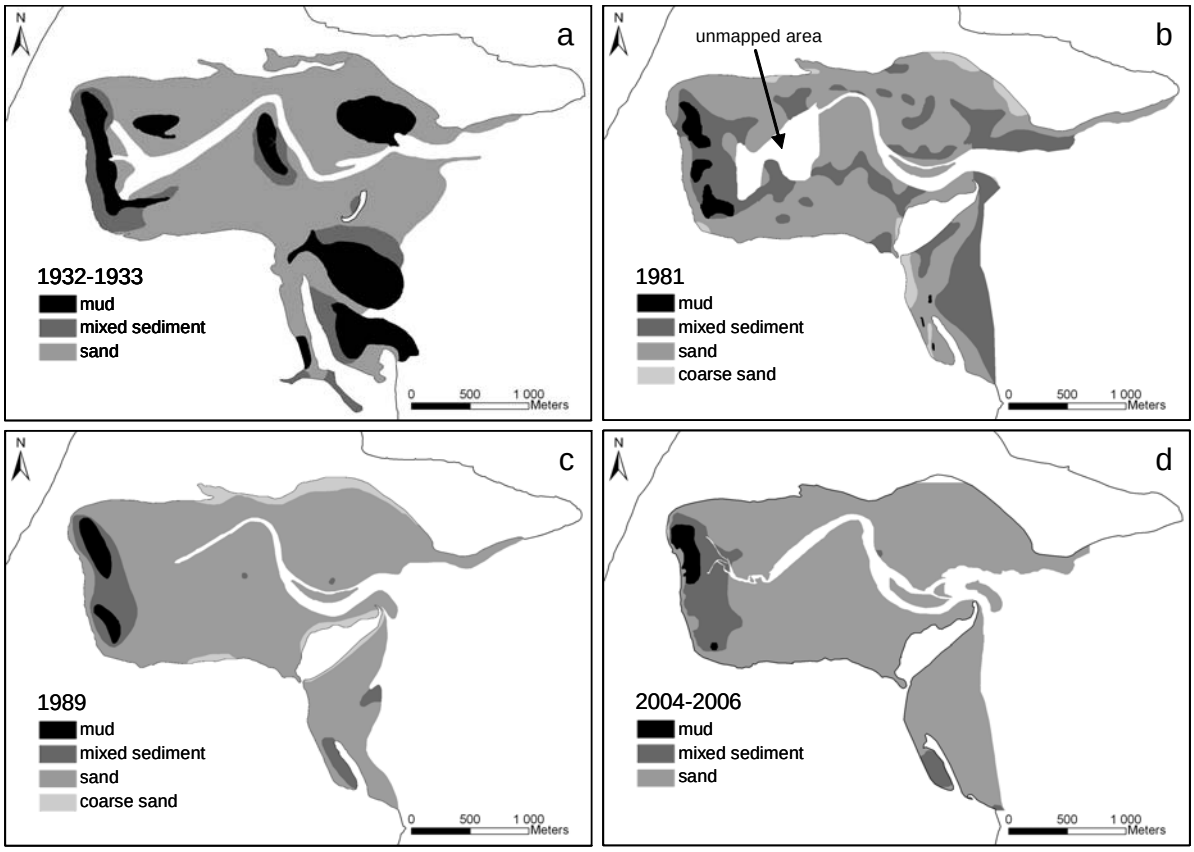


**Fig. 4.14:** The spatial distribution of sediment types in the Königshafen in 1932/1933 (a), 1981 (b), 1989 (c) and 2004/2006 (d).

Not only the spatial extent but also the spatial distribution of the sediments in the Königshafen changed. In 1932/1933 the mudflats occurred mainly in the outer Königshafen at the transition to the subtidal and still in 1981 large shares of mixed sediments and fine sands were found here and along the entire course of the tidal creek. Whereas in 1989 and today the muddy and mixed sediments vanished from the outer Königshafen except from a sheltered location bared by a sandy hook.

Altogether, a steady shift in the sediment composition and in the spatial extent of the different sediments can be observed over the years: Sandy tidal flats are becoming more and more dominant at the cost of areas with finer sediments. This general coarsening is so distinct that it affects the Mean and first Mode. It is suggested that the reason for this is not a reduced supply of fine-grained sediments but the depletion of fines. Pejrup et al. (1997) conclude that the net deposition of fine-grained sediment in a tidal basin is mainly a function of physiographical and hydrodynamical parameters and to a lesser degree of sediment availability. Since the "trapping" rate of fine-grained sediment out of North Sea water is very low in the List tidal basin compared to other tidal basins in the Wadden Sea, it can be assumed that the supply is not a limiting factor (Pejrup et al. 1997). Even though Pedersen and Bartholdy (2006) found a decreasing sediment availability from north to south for the three Danish tidal basins Grådyb, Knudedyb and Juvre, the Juvre tidal basin which is next to the List tidal basin and is located just a few kilometres north of it, still shows a considerably higher annual deposit of fine-grained material.

**Causes for mud depletion**

The depletion of mud has two main causes: biological and hydrodynamic factors. The loss of finer sediments goes along with a decline in the vegetation cover. Wohlenberg (1937) described that mudflats were very often associated with growing or decaying vegetation of *Fucus*, which grows on mussel beds, and seagrass (*Zostera*), especially in the outer Königshafen. The vegetation provided sheltered areas where mudflats could establish. Especially seagrass is known to stabilise sediments and enhance deposition of fine-grained sediments (Ward et al. 1984, Fonseca and Fisher 1986, Heiss et al. 2000). According to aerial photographs from 1936 the vegetation covered about 31 % of the intertidal while today's coverage is about 9 %. Reasons for the decline in seagrass cover can be increased hydrodynamics, sediment instability and eutrophication (Philippart et al. 1992, van Katwijk et al. 2000, Schanz and Asmus 2003, Reise and Kohlus 2008).

Similar phenomena and possible reasons for the development, observed in the Königshafen, are reported from other tidal flat areas. For example, Cardoso et al. (2004) observed that after a decline of seagrass, the former vegetated area was replaced by coarser unvegetated sediments. Preceding changes in the physical forcings might have lead to the decline of seagrass. Da Silva et al. (2004) found increasing tidal wave penetration inducing transport of coarser sandy sediment into a lagoon in northern Portugal. The increasing tidal wave penetration caused burial of seagrass beds with sand and a reduction in sediment stability. In response seagrass decreased substantially.

Wohlenberg (1937) further described that in 1932/1933 the muddy areas in the Königshafen were hardly walkable because of their extreme softness (sinking down to 1.2 m). The vegetation retained water which led to a slight water cover in large parts of the tidal flats during low tide and to an oversaturation of the sediment with water. The sediment density was also broken up by decaying seagrass and *Fucus* that was included into the sediment and also made it soft. This situation has changed. Today, the maximum penetration into the mud is about 0.4 m, the sediment is well drained and consolidated and the content of large organic particles is low (own observations). Obviously, the sediment characteristics changed from organic-rich, muddy tidal flat sediments to sandy siliclastic tidal deposits in less than 100 years. This goes along with a reduced vegetation cover in the bay because this also means a reduced availability of organic matter.

The other factor that plays an important role in the depletion of fine-grained sediments is the increase of hydrodynamics caused by a rising sea level and the reduction of the tidal catchment area. According to the CPSL (2001) the annual mean high water level rose by 2.5 mm $yr^{-1}$ in the Wadden Sea from 1890 to 1989 and even by 6.7 mm $yr^{-1}$ for the period 1971 to 1989. The data from the gauge List also shows a considerable increase in the high tide level as well as in the tidal range (see Chapter 2.2). A rising water level is associated with stronger currents that cause removal of fine-grained sediments. Furthermore, the reduction of the tidal catchment area leads to less accommodation space for the tidal flow which results in increased energy levels within the basin (Flemming and Nyandwi 1994, Mai 1999). The catchment area of the List tidal basin was mainly reduced by the construction of two causeways which connect the islands Sylt and Rømø with the mainland. The construction of the Hindenburg causeway in the south in 1927 had a direct effect and caused immediate changes in the sedimentary system (Wohlenberg 1953). In 1948 the construction of the Rømø causeway was finished and geomorphological changes as an immediate response were also observed (Jespersen and Rasmussen 1984).

Furthermore, the catchment area was reduced by land claim measures, which were undertaken along the Danish mainland shore from 1954 to 1972, and by the construction of a new dyke in 1979-1982 whereby the Margrethe-Koog was formed (Jespersen and Rasmussen 1989). In conclusion, Reise (1998) estimates that over the last 500 years one third of the List tidal basin has been converted into land by embankment and the tidal flat area decreased from approx. 66 to 40 % within the 20$^{th}$ century.

The tidal catchment area of the Königshafen was also reduced, which probably resulted in higher water levels and increased energy levels here as well. The construction of a dyke at the southern shoreline in 1937 and the artificial landfill of the island Uthörn in the early 1940s (Bayerl and Köster 1998) decreased the intertidal area by 0.24 km$^2$. The embankment also affected salt marshes, which are important flooding area, and taking them also into account the loss of the tidal catchment area amounts to 0.6 km$^2$ in the Königshafen.

Mud depletion as a result of the reasons outlined above can be observed in the entire Wadden Sea. Flemming and Nyandwi (1994), Flemming and Bartholomä (1997) and Mai and Bartholomä (2000) report it from the back-barrier tidal basin at the East Frisian Islands. Van Bernem (pers. comm.) found a coarsening trend in the Hörnum tidal basin south of the island of Sylt. In the Dutch Wadden Sea a landward-directed shift of mud resulting in less mud in the more offshore tidal flats but also in more mud in the sheltered coastal areas is detected (Zwarts 2003).

**Average spatial pattern of surface sediments from 2004 to 2006**

The distribution of the different sediment types shows a distinct spatial pattern with fine sediments in the inner part and coarse sediments towards the outer parts of the Königshafen (Fig. 4.6). Two factors contribute to the accumulation of the fine-grained sediments in the innermost part of the Königshafen: 1) low current velocities (Behrens et al. 1997, Backhaus et al. 1998) due to the sheltered position and 2) the morphology. The latter factor becomes apparent when draping in GIS the sediment layer over a Digital Terrain Model (Fig. 4.15). The areas of mud, coarse mud and fine sand are almost congruent with a morphological depression at the head of the tidal creek. This depression has a predominant elevation of -0.8 to -0.7 m while the sandy areas are considerably higher with mainly -0.3 to 0.2 m. As a consequence, the water residence time in this small basin is extended which enhances the settlement of fines. Fine-grained sediments are easily kept in suspension and they need time and calm conditions to settle from the water column to the

tidal flat. Gouleau et al. (2000) also report that the morphology plays an important role in sedimentation as he observed in an intertidal bay in France that the long-term sedimentation rate was four times higher in the lower part of the mudflat than in the upper part. Furthermore, the sheltered position in the inner Königshafen promotes establishment of these fine-grained sediments due to reduced resuspension whereby a gradient of increasing coarseness can be noticed towards the east. Another zone of coarse mud established in the sheltered lee side of the sandy hook in the south-east corner of the intertidal Königshafen where current velocities are usually low (Behrens et al. 1997).

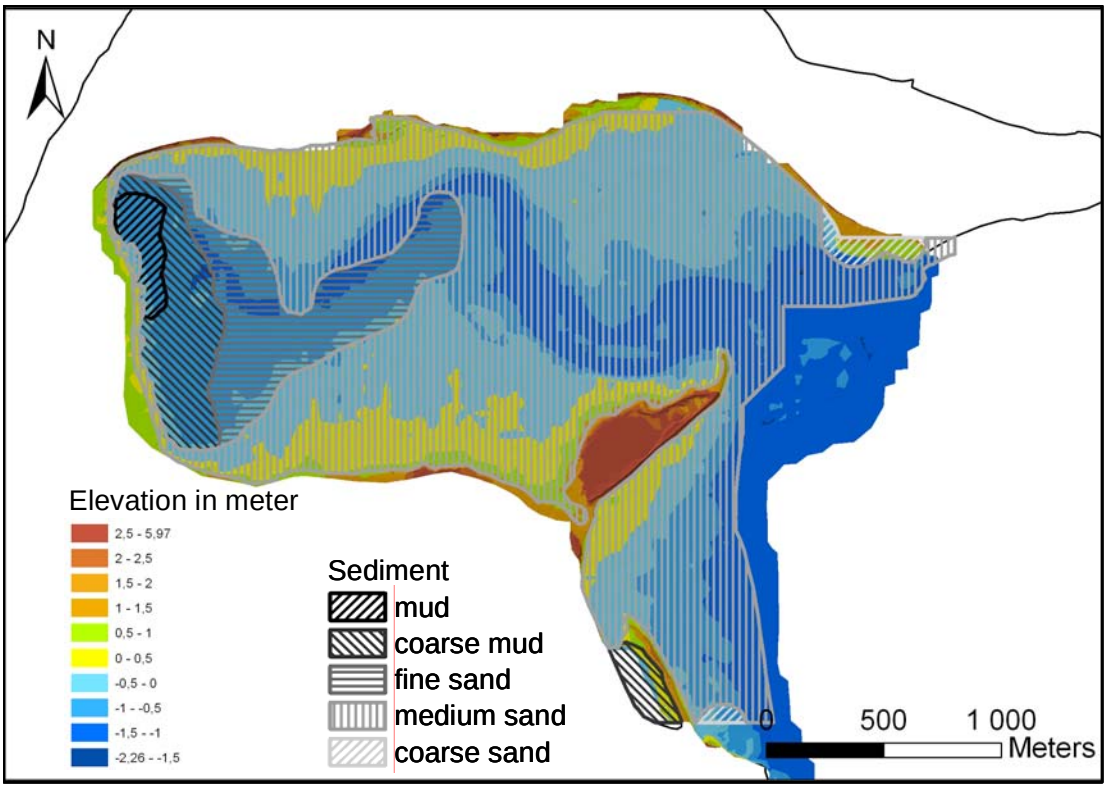


**Fig. 4.15:** The average sediment distribution according to the first Mode values from 2004 to 2006 laid over a Digital Terrain Model of the Königshafen.

Even though no particular grain size analysis was conducted for Uthörn, the sediments at its margins are very coarse and the amount of pebbles (> 2 mm) is conspicuous (own observation). Artificial landfill was conducted on the island of Uthörn in the early 1940s (Bayerl and Köster 1998) and increased its size considerably. As the sediment taken for the landfill is significantly coarser than the naturally occurring intertidal sediments, it can be assumed that the landfill affected the sediment composition in the outer Königshafen.

**Local trends in the development of surface sediments from 2004 to 2006**

The mean grain size of the sediments in the innermost part of the Königshafen is becoming finer or at least slightly finer from 2004 to 2006 (Fig. 4.7). Even though the spatial extent

of the area of fine-grained sediments did not increase, the sediment composition in this area became finer over the sampling period. In contrast, a general coarsening characterises the sediments of the more exposed outer part. This coarsening trend continues into the neighbouring subtidal where it can be also observed in the surface sediments (Dolch and Hass 2008). Despite the high variability of tidal flat surface sediments, it is assumed that these short-term trends are meaningful because in many cases the development was steady and there is a clear spatial distribution pattern of the trends which may not be a coincidence.

The trend of the first Mode follows the spatial pattern of the Mean but is far less pronounced (Fig. 4.7). The first Mode is much more stable. The distinctiveness as well as the spatial extent of its trends are far less compared to the trends of the Mean. With respect to the sediment grain size composition, this means that the bulk (first Mode) remains the same and the changes which are caused by the increased mud deposition in the innermost part and the removal of mud in the outer Königshafen can be seen in the varying Mean. These opposed developments can be explained by the different impacts of waves and currents. As mentioned above a considerable annual sea level rise is observed in the Wadden Sea (CPSL 2005). This is associated with stronger currents that may remove mud. This affects the outer Königshafen as it is located close to one of the main tidal channels of the List tidal basin. Furthermore, it can be assumed that a deposition of mud is hindered here due to more turbulent conditions in the water column.

In contrast to this, waves are more responsible for resuspension of fine-grained sediments than tidal currents in shallow terrain (French et al. 2000, Janssen-Stelder 2000, Green and Coco 2007) - like the inner Königshafen. Especially during storm events a lot of resuspension and erosion occurs (Janssen-Stelder 2000, Bartholdy and Aagaard 2001, Christiansen et al. 2006) at which wind-induced waves play an important role. Weisse et al. (2005) and Weisse and Plüß (2006) showed that storms decreased along the North Sea coast since the mid 1990's. It can be assumed that the innermost Königshafen is too shallow and sheltered so that – unlike in the outer Königshafen - the higher current velocities have no crucial impact yet. Furthermore, decreasing storm events (Weisse et al. 2005, Weisse and Plüß 2006) lead to a reduced resuspension through wave action so that the accumulated mud can establish and create a positive net balance in the innermost Königshafen (Larsen et al. 1996). Even though a lot of mud depletion has been detected over the last decades, these calmer years apparently enabled mud deposition.

Erosion and accumulation are opposite developments which are not only observed in the Königshafen but also in the entire List tidal basin. Pejrup et al. (1997) found out that the List tidal basin is in general a net sink for muddy sediments (< 4 φ) with an annual deposit of about 49 000 tons on the tidal flats. A positive annual net deposition of 1.4 tons is allotted to the Königshafen (Larsen et al. 1996). However, in the long-term view, the tidal flats of the List tidal basin show a negative mass balance since the loss or submersion of intertidal areas was dominant in the last centuries (Higelke 1998, Reise 1998). This affects mainly the tidal flats in the inner part of the bight which are more exposed. Therefore, it can be assumed that the deposition of fines in the List tidal basin is primarily restricted to the areas of mixed and muddy sediments which occur mainly in close vicinity to the coastline. These fine sediments form narrow stripes at the margins of the List tidal basin and cover 25 % and 3 % of the intertidal area, respectively (Bayerl et al. 1998). The phenomenon that deposition of fines occurs first of all in sheltered marginal areas coincides with our surveys in the Königshafen.

### 4.4.2 The riddle of the sands: grain size composition shifts between mud and sand

**Dynamics of the spatial distribution of intertidal surface sediments**

Dynamics of intertidal sediments are widely analysed (Dyer et al. 2000b, Andersen and Pejrup 2001 Chang et al. 2006, Andersen et al. 2006, Christiansen et al. 2006, Green and Coco 2007). However, in contrast to my study these surveys were conducted at a few individual sampling stations only. To my knowledge this study is the first analysis which is based on a dense sampling grid covering an entire intertidal bay over the period of two years. This study focuses on area-wide spatial dynamics of sediment distribution patterns and their quantification because there is little information on it so far.

The comparison of the spatial distribution of the sediments with the distribution pattern of the next subsequent survey revealed an average change rate of 26.3 %. The rate of change is high but the standard deviation of 5.6 is a surprisingly low. Many changes range between 25 and 28 % and the overall magnitude of change can be regarded as rather constant (Table 4.3). The comparison of each sediment distribution pattern with every other sediment distribution pattern confirms this (Table 4.4), as the average magnitude of change is 28.6 ± 7.5 % here. These changes are partly ascribable to net accumulation but primarily to reworking of the sediments as this happens to a much larger degree (Andersen and Pejrup 2001). Interestingly, the results of the sampling campaign 2006-09 show by far the least congruence to the results of all other samplings (Table 4.4). This can be explained

by a remarkable calm weather period prior to this sampling which resulted in an exceptional sediment distribution and also in a high mud content, especially for the mud content classes > 10 % (see Table 4.5).

Altogether 12 sampling stations were part of both sampling campaigns (Fig. 4.1), the high-frequency sampling in March 2007 and the medium-term sampling from November 2004 to December 2006 (Table 4.6). The medium- and short-term results reveal that muddy sediments are much more variable in their grain size composition than sandy sediments. Furthermore, it is detected that the minima and maxima of the Mean and the first Mode values as well as their standard deviations of these 12 stations were not significantly different comparing their medium- and the short-term variability (t-test, $p = 0.47$ (Mean), t-test, $p = 0.26$ ($1^{st}$ Mode)). The average values of the standard deviations reveal also only minor differences. This means that the ranges of the medium-term and short-term dynamics are very similar suggesting frequent reversals in the dynamics of tidal flat surface sediments. Sampling station 23-65 (Fig. 4.2, Table 4.6) represents a remarkable exception. The observed maximum Mean value in the high-frequency sampling is more than twice as high as in the medium-term sampling whereas the minimum values are almost the same. This means that a rapid significant input of mud must have occurred. This shows that considerable changes in the grain size composition of surface sediments are possible from tide to tide.

The sampling station ‘Tidal Creek’ (Fig. 4.2) revealed that the sediments in vicinity to the tidal creek are muddier than the adjacent sediments. This higher input of mud may be attributed to the creek and also, a significantly higher variability was expected as this is already indicated in the sampling from 2004 to 2006.

The dynamics of the Mean and first Mode values are within the normal range compared to the results from the other sampling stations.

**Table 4.6:** Comparison of the Mean and first Mode values of the medium-term (2004 to 2006) and high-frequency sampling campaign (March 2007).

| Sampling stations | 2004-2006 | | | March 2007 | | | 2004-2006 | | | March 2007 | | |
|---|---|---|---|---|---|---|---|---|---|---|---|---|
| | Min Phi | Max Phi | SD | Min Phi | Max Phi | SD | Min Phi | Max Phi | SD | Min Phi | Max Phi | SD |
| | **Mean** | | | **Mean** | | | **1st Mode** | | | **1st Mode** | | |
| **Transect 1** | | | | | | | | | | | | |
| 18 - 65 | 1.66 | 5.02 | 1.30 | 1.72 | 1.81 | 0.03 | 1.65 | 1.85 | 0.06 | 1.75 | 1.85 | 0.04 |
| 19 - 65 | 3.32 | 7.03 | 1.26 | 4.06 | 5.04 | 0.47 | 2.75 | 6.95 | 1.52 | 2.65 | 3.05 | 0.16 |
| 20 - 65 | 2.69 | 5.91 | 1.21 | 3.86 | 5.10 | 0.60 | 2.55 | 4.65 | 0.56 | 2.55 | 2.75 | 0.07 |
| 21 - 65 | 1.72 | 1.94 | 0.07 | 1.84 | 1.94 | 0.04 | 1.75 | 1.85 | 0.05 | 1.75 | 1.85 | 0.04 |
| 22 - 65 | 1.61 | 1.88 | 0.09 | 1.68 | 1.80 | 0.05 | 1.55 | 1.85 | 0.09 | 1.75 | 1.75 | 0.00 |
| 23 - 65 | 1.65 | 1.94 | 0.08 | 1.80 | 4.61 | 1.17 | 1.55 | 1.85 | 0.08 | 1.75 | 1.85 | 0.05 |
| 24 - 65 | 1.46 | 3.59 | 0.51 | 2.81 | 4.55 | 0.68 | 1.45 | 1.85 | 0.12 | 1.75 | 1.85 | 0.04 |
| 25 - 65 | 1.34 | 1.87 | 0.14 | 1.93 | 2.44 | 0.21 | 1.45 | 1.85 | 0.13 | 1.85 | 1.85 | 0.00 |
| **Average** | 1.93 | 3.65 | 0.58 | 2.46 | 3.41 | 0.41 | 1.84 | 2.84 | 0.33 | 1.98 | 2.10 | 0.05 |
| **Transect 2** | | | | | | | | | | | | |
| 26 - 66 | 1.77 | 4.06 | 0.58 | 1.96 | 2.13 | 0.07 | 1.75 | 1.85 | 0.04 | 1.85 | 1.95 | 0.04 |
| 27 - 66 | 1.90 | 2.45 | 0.17 | 2.01 | 2.20 | 0.09 | 1.75 | 2.35 | 0.21 | 1.85 | 2.15 | 0.16 |
| 29 - 66 | 1.57 | 2.04 | 0.13 | 1.65 | 1.99 | 0.12 | 1.35 | 1.95 | 0.21 | 1.45 | 1.85 | 0.18 |
| 30 - 66 | 1.74 | 1.95 | 0.07 | 1.83 | 2.00 | 0.07 | 1.65 | 1.85 | 0.06 | 1.75 | 1.85 | 0.05 |
| **Average** | 1.74 | 2.63 | 0.24 | 1.86 | 2.08 | 0.09 | 1.63 | 2.00 | 0.13 | 1.73 | 1.95 | 0.11 |

Andersen et al. (2006) also showed the high and rapid dynamics of intertidal sediments. It is a continuous alternation of erosion, transport and deposition. Rapid changes are possible because some of the eroded material from the tidal flat is not exported to the open North Sea but temporarily deposited in a nearby shallow tidal channel and later returned on the mudflat during calmer weather conditions (Andersen et al. 2006). There is a continuous exchange of silt between the bed of a tidal creek and the upper tidal flat during fair weather, which results in constantly changing sediment conditions (Dyer et al. 2000, Green and Coco 2007).

Changing sedimentary conditions may have an impact on the benthic fauna (Flemming and Nyandwi 1994). Tidal flats are home to rich and diverse benthic communities of macrofaunal and meiofaunal species, like snails, polychaetes, bivalves, amphipodes, ostracodes and copepodes (Reise 1985). They all live on and in the sediments, especially in the upper 5 cm, which is most affected by reworking (Andersen and Pejrup 2001). Therefore, only species that are best adapted to this changing environment can cope with these variable conditions. Significant long-term changes in the sediment composition, like coarsening, can also have selective effects on species by inhibiting or facilitating them (Reise et al. 2008).

**Test for seasonality effects and possible driving environmental parameters**

Even though the comparison of the average sediment distribution patterns of 2005 and 2006 shows only minor differences and suggests a dynamic equilibrium and a rather stable overall location of the sediment types, events with exceptional high and low rates of change were also found. The comparison of subsequent sediment distribution patterns reveals high rates of change from March to April 2005 and from January to March 2006 while the low rates of change were detected from August to November 2005 and November 2005 to January 2006 (Table 4.3). As exceptional high and low rates were both observed in winter and the other seasons showed no distinctive feature, this pattern does not indicate seasonality. The overall comparison of all sediment distributions confirms this as exceptional low and high change rates are obviously not linked to any season (Table 4.4).

Seasonality on intertidal flats, mainly in the form of erosion and the predominance of coarser sediments in winter and on the other hand prevailing sedimentation of mud in summer is worldwide observed (Andersen and Pejrup 2001, Ryu 2003, Yang et al. 2005, Chang et al. 2006). This can not be reported for the development of the surface sediments in the Königshafen. The analysis of sediment core data from the List tidal basin also did not reveal seasonality effects but it was suggested that wind has an effect (Bayerl 1992). Therefore, it was tested whether the wind and the associated water level, which prevailed 2 or 7 days before a sampling campaign, enhance the degree of change. However, no significant correlation could be detected between the degree of change and the wind direction, the average and maximum wind speed as well as the high and low tide water level (Spearmans rank correlation test). It was also analysed if similar conditions of these parameters result in similar spatial distribution patterns of the surface sediments. Statistical tests did not reveal a significant correlation in this case either. Nevertheless, these parameters have been found to leave a trace in the distribution of surface sediments (e.g. Jansen-Stelder 2000, Andersen and Pejrup 2001, Bartholdy and Aagaard 2001, Christiansen et al. 2006). However, in Königshafen there does not seem to be one dominant driving parameter or the interactions between several parameters do not leave a net effect. The depositional system is too complex and dynamic.

**Variable mud contents**

The mud contents are highest in the inner half of the bay in vicinity of the central tidal creek and at the head of it. Just like the sediment types (see Chapter 4.1.3) and for the same

reasons, the mud content is also related to the morphology. Areas with less than 10 % mud occur mainly in the more exposed outer Königshafen and on higher sand flats (0.2 to -0.4 m) which are at a distance of 150 – 300 m to the tidal creek. Areas with more than 10 % mud are located primarily in lower areas (-0.4 to -0.8 m), closer to the creek and in the sheltered inner part of the bay. The combination of a sheltered and low-lying position allows the establishment of permanently muddy sediments. Low-lying areas are characterized by an increased water residence time which gives fine sediment particles enough time to settle from the water column to the tidal flat and the sheltered position decreases resuspension. Water residence time is influenced by water levels. Therefore, the correlation between water levels (including high and low tides) and the spatial extent of different mud contents were tested at different time scales with a Spearmans rank correlation test. The water levels of the low tides and the high tides, which were prevailing 2 days and the entire week prior to a sampling campaign, were compared with the mud contents revealed by the sediment sampling (Table 4.7).

**Table 4.7:** Degree of significance for different mud content classes at low and high tides on different time scales prior to a sampling campaign.

| **Mud content** (spatial cover) | **p-values** low tides (2 days) | high tides (2 days) | low tides (1 week) | high tides (1 week) |
|---|---|---|---|---|
| > 2.5 % | 0.000281 | 0.01287 | 0.000011 | 0.000468 |
| > 5 % | 0.004474 | 0.007697 | 0.0092 | 0.004143 |
| > 10 % | 0.0517 | 0.0496 | 0.0462 | 0.0283 |

The comparison shows a strong negative correlation. The lower the water level, the higher the mud content and the larger the area covered by higher mud contents. This also applies vice versa and as the results in Table 4.7 show, there are no meaningful differences between the low and high tide water level. The modelling results of Behrens et al. (1997) show that high water levels of both, low and high tides, are primarily caused by strong westerly winds and that they are associated with stronger currents. The higher water turbulence causes increased resuspension which leads to less mud on the tidal flats and a high concentration of suspended matter in the water column (Bartholdy and Aagaard 2001, McCandliss et al. 2002). On the other hand, easterly offshore winds cause low water levels and calmer conditions which results in enhanced deposition of mud. This phenomenon is also observed by Andersen and Pejrup (2001).

The water levels an entire week before a sediment sampling lead to almost the same significance as the water levels only 2 days before the sampling. Therefore, the conditions,

which are prevailing just before the sampling campaign, lead to similar results. This means that short-term environmental conditions lead to a significant sediment status. This fits to the overall picture of very dynamic surface sediments. Significant results are gained for areas with a mud content of less than 10 %, i.e. for sandy tidal flats, and areas with a mud content of less than 5 % show even high significance (Table 4.7). The mud content of these tidal flats is so low that even small changes become obvious and significant. However, the effect is only temporary here. These sandy tidal flats are either high-lying or exposed and therefore, permanent deposition of mud is prevented by their position. Higher-lying sand flats primarily lack of constant mud supply while the mud at exposed tidal flats is easily resuspended.

Even though there is a strong correlation between the water level and the mud content of the surface sediments, the spatial distribution pattern of mud content classes is kept rather vague and only a very general picture can be derived from the water level.

### 4.4.3 Characteristics of intertidal surface sediments

In general, the Skewness of the sediments shows that there is a predominant excess of fine sediment particles in the grain size composition. The Sorting further reveals that the sediments are composed of a rather broad range of grain sizes. Two-thirds of the sediment samples are moderately sorted while one-third shows a poor sorting. Moderate to poor sorting suggests that the sediments come from different sources which have different grain size compositions or that the sediments were transported differently.

The analysis further revealed that 18 % of the sediments are bi- or trimodal, which indicates that the sediment is supplied from different sources. However, this can only be detected when the grain size composition of these sources differs.

The sediments in the innermost part of the Königshafen show a permanent bi- or trimodality while it is only temporary in the centre of the bay (Fig. 4.11).

Muddy sediments prevail in the innermost part. Their second Mode is formed by medium sand. It is assumed that the sand is blown in by wind because waves and currents are in general not enough to transport marine sand in this sheltered area. On the other hand it is suggested, that waves and currents are only during extreme events sufficient to transport the sand away which results in a rather permanent occurrence of sand here.

Another area where sediments are permanently bi- and trimodal is in the muddy area leewards the sandy hook in the outer Königshafen. The aeolian input reaches also sandy parts of the bay (own observations) but it can only be detected by this method when

deposited on a different sediment matrix. However, an aeolian input is confirmed by Austen (1994), who found evidence for it.

Temporary bi- and trimodal sediments occur in the centre of the Königshafen, predominantly in the area of fine sand. They are found in vicinity of the central creek. In these cases, the second or third Mode is formed by muddy sediments while the first Mode is created by sand. The tidal creek has a direct impact here as it deposits significant amounts of mud, sufficient to cause polymodality. The effect is not permanent due to resuspension. However, temporary bi- and trimodal sediments were found only after low water levels and easterly winds, e.g. observed in the sampling campaigns 2005-16, 2006-01, 2006-09 and 2006-18. It is shown in chapter 4.1.4 that fine-grained sediments are permanently deposited in the sheltered mud area at the head of the tidal creek but again this can not be proofed with this method as no second mode is formed.

Nevertheless, it can be concluded that this depositional system is supplied with sediment from two sources: a marine input of fine-grained sediments and an aeolian supply of sand from the surrounding dunes, which originated at a coarse-grained high energy beach.

According to Austen (1994), aeolian sand input into the Königshafen definitely takes place but is not of great quantity. So, it is remarkable that there is a strong dominance of sandy tidal flats and Bayerl and Higelke (1994) showed that beach and dune ridge sediments form up to 6 m thick layers. A marine input of sand is rather unlikely because the entire Königshafen is in a sheltered position. It has been an almost enclosed bay since the formation of the large sandy spit (Ellenbogen, see Fig. 4.1) at its north at least 1300 years ago (Lindhorst et al., in prep.). It can be assumed that the currents are rather slow since then. According to the correlation between the grain settling velocities and the maximum flow velocities (Flemming and Nyandwi 1994), the current velocities are not high enough to transport a significant amount of sand into the bay. Therefore, an aeolian input of sand is widely assumed (Nienburg 1927, Kolumbe 1933, Wohlenberg 1937, Austen 1994). Wohlenberg (1937) suggested that the high amount of sand can only be explained by migrating dunes. He presumes that the dunes originally migrated to the Königshafen and gushed and eroded into it. Bayerl and Higelke (1994) investigated a series of sediment cores from the Königshafen and detected that along a west-east profile the thickness of the layer of dune and beach ridge sediments constantly decreases towards the east, showing a major layer thickness in the innermost part of the Königshafen and a minor near Uthörn.

This indicates that this sand input must have come from the west, where the former migrating dunes are, and that the input is confined to the inner part of the Königshafen.

A comparison of the grain size frequency curves of tidal flat and dune sediments provides proof (Fig. 4.16). The sand from the surrounding formerly migrating dunes shows an average Mean value of 1.68 φ and a first Mode of 1.67 φ. Most remarkable is the high homogeneity of the samples as the grain size frequency curves of all dune samples are almost congruent. The distance of the dunes to the bay does obviously not cause different grain size compositions.

Some sandy tidal flats in the Königshafen show almost the same pattern in their grain size composition as the dunes (Fig. 4.17). This applies to the average grain size frequency curves of 49 sampling stations, which have Mean values ranging from 1.7 to 2.0 φ (average of 1.8 φ) and first Mode values varying between 1.7 and 1.9 φ (average 1.8 φ). Their mean standard deviation is 0.09 φ. Regarding dune and tidal flat sediments combined, their comparison reveals almost the same mean standard deviation (0.12 φ), showing that the differences in their grain size composition patterns are minor. 80 % of the intertidal Königshafen is covered with sand, but the 49 sampling stations, that have a similar grain size composition as the dunes, are restricted to the inner Königshafen (Fig. 4.17). The sands in the outer Königshafen do not show the typical grain size pattern which indicates that the input is confined to the inner part of the bay or the sediment composition in the outer Königshafen is altered due to exposure to stronger hydrodynamics. However, the fact that the grain size frequency curves of the dunes and the tidal flat sands are almost identical indicates that the dunes formerly migrated and eroded as a whole into the bay because no sorting by aeolian transport is observed. As the migrating dunes are nowadays stabelised by vegetation, the last input must have been a long time ago. This explains why muddy sediments could establish on top in the lower-lying sheltered innermost part of the bay. However, the stability of the grain size composition of the sand flats in the inner Königshafen is remarkable. The mud deposition from the sea onto the higher-situated sand flats has only temporary effects due to resuspension and no selective erosion of sand can be observed.

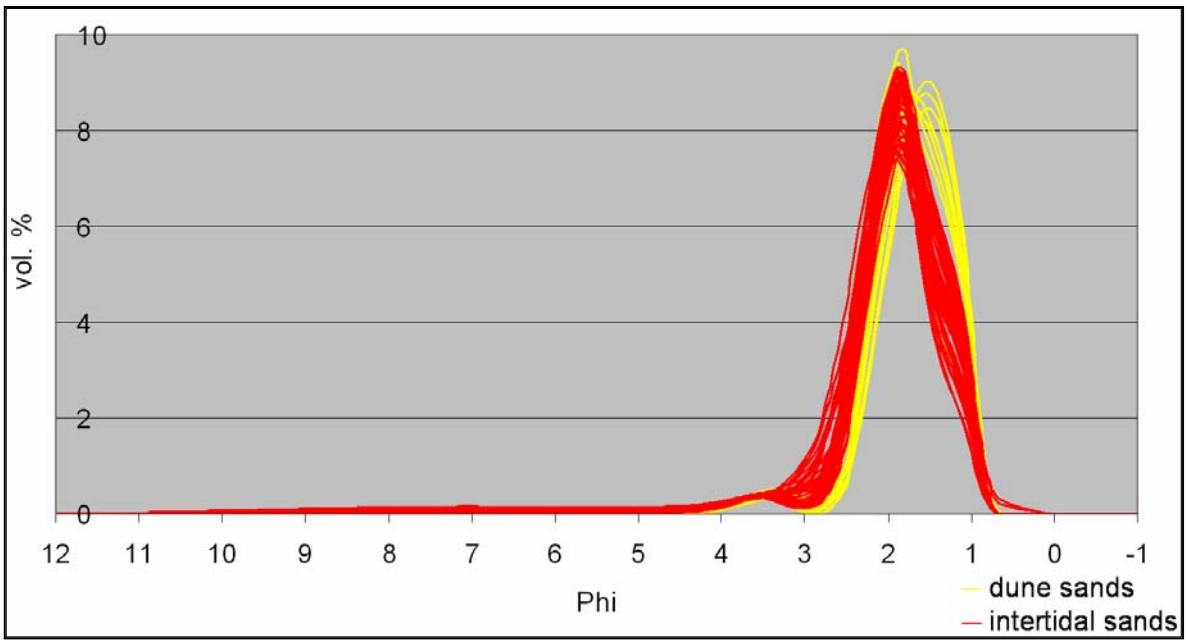


**Fig. 4.16:** The grain size frequency curves from 13 sand dune samples and 49 intertidal sampling stations.

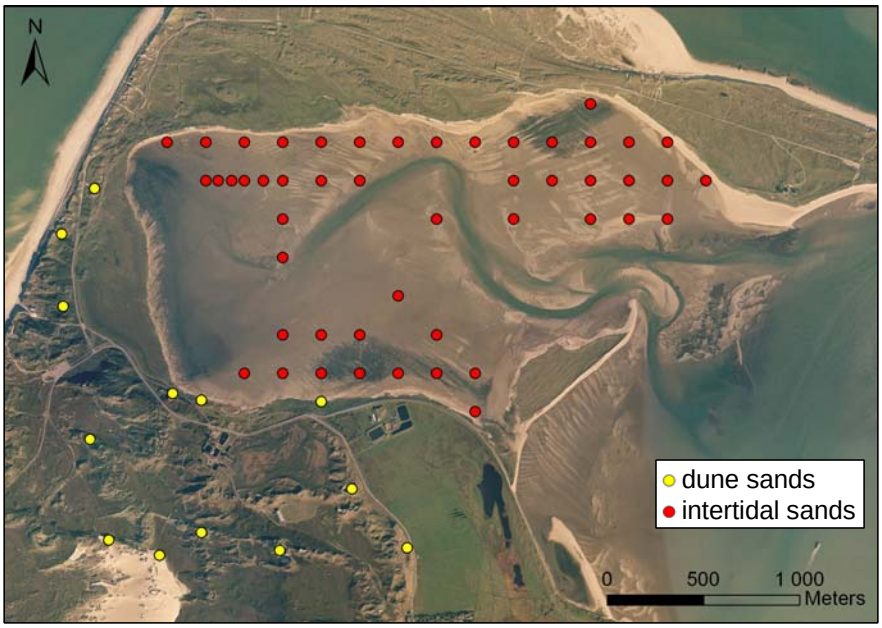


**Fig. 4.17:** The spatial distribution of dune and intertidal sands which have almost identical grain size frequency patterns.

## 4.5 Summary and conclusions

Coarsening of intertidal sediments as a result of severe, long-term depletion of mud can be observed in the entire European Wadden Sea. The primary reasons are increased hydrodynamics, which cause a selective removal of fine-grained sediments. This can be amplified when the vegetation cover becomes reduced over the years.

This study was carried out in a semi-enclosed bay in the northern Wadden Sea, where different sedimentary processes, which can be regarded as representative for the Wadden Sea, could be surveyed on a small scale. A distinct spatial pattern with a gradient of increasing grain size coarseness from sheltered to exposed areas is observed at the study site.

Diverging developments in a sheltered inner and an exposed outer area is apparent with accumulation of fines in the inner part and a coarsening in the outer part of the bay. This can be explained by the different impact waves and currents have on these locations.

The rate of change of the spatial distribution of sediment types is rather constant and affects 26 to 29 % of the survey area. These spatial changes in the sediment distribution occur within a few tides. This means that the associated tidal flat fauna must be adapted to such dynamic sedimentary conditions. However, the long-term stability of the general distribution pattern of the sediments suggests a dynamic equilibrium, at least on a medium-term scale.

Seasonality could neither be detected in the rate of change of surface sediments nor in their spatial distribution pattern. Instead, the status of the sediments is caused by short-term weather events. It could be shown that there is a strong negative correlation between water level and general mud content. A low water level is associated with decreased hydrodynamics which allow the deposition of mud. This effect is temporary as increased hydrodynamics which go along with rising water levels lead to resuspension and generally lower mud content on the tidal flats.

The depositional system of the survey area receives sediment from two sources: muddy sediments from marine sources and sand by aeolian input from surrounding dunes. The sandy tidal flats show the same grain size composition as the dunes. As no selective deposition can be detected, it can be assumed that past dunes migrated into the bay and became eroded by the sea.

# 5 Megaripple long and short-term dynamics on intertidal flats affecting biogenic structures

## 5.1 Introduction

Engineering and navigational projects require precise information about the shape and stability of the sea bed, especially in areas where the sea bed sediments are particularly mobile (Langhorne 1982). Therefore, dynamic transverse sedimentary bedforms are of great interest to engineers and geologists (Dalrymple et al. 1978). On tidal flats they are also interesting for biologists and ecologists because they can affect epibenthic structures, like e.g. seagrass beds (Marbà et al. 1994) and mussel beds. Epibenthic structures and their associated communities can get buried with sand when megaripples are migrating and overlay them.

There are three basic types of dynamic transverse sedimentary bedforms: morphology-ripples (small scale), megaripples (intermediate scale) and sand waves (large scale). They are distinguished by wavelength, height, steepness and morphological characteristics (Table 5.1) (Dalrymple et al. 1978). All these bedform types can be statistically related to power of currents, shear velocity, water depth and sediment grain size (Zarillo 1982).

**Table 5.1:** Main characteristics of the three basic types of dynamic transverse sedimentary bedforms (according to Dalrymple et al. 1978).

| Bedform type | Wavelength (L) in m | Heigth (H) in m | Steepness (L/H) | Morphological characteristics |
|---|---|---|---|---|
| ripples | < 0.3 | < 0.05 | ~ 10 | straight to linguoid in plan |
| megaripples (Type 1) | 0.1 - 25 | 0.05 - 0.5 | 10 - 150 | straight to smoothly sinuous, simple appearance, flat, constant crest height |
| megaripples (Type 2) | 0.05 - 14 | 0.05 - 0.7 | 6 - 34 | generally sinuous to lunate, complex appearance, steep profile, variable crest height |
| sandwaves | 10 - 215 | 0.15 - 3.4 | 17 - 210 | straight to smoothly sinuous in plain, constant crest height, megaripples can be superimposed |

Megaripples are the focus of this study. They are elevated, sandy accretions with a generally oblong structure (Fig. 5.1). Megaripples are 0.3 to 0.6 m high, 10 to 15 m long (McCave and Geiser 1978) and they usually form populations with a wavelength of 4 to 15 m (Zarillo 1982). They are widely observed and mainly found in sandy intertidal areas

like in the Wadden Sea or on tropical tidal flats (Larcombe and Ridd 1995) and in tidal eastuaries such as Rhine and Scheldt estuary (Bird 2000), in the Westerschelde (Boersma and Terwindt 1981) or in the Wash (McCave and Geiser 1978).

**Fig. 5.1:** Megaripples in the survey area Blidselbucht in May 2005.

Megaripples are primarily composed of medium sand as a high percentage of material coarser than 2.5 φ (phi) is required for their formation (Dalrymple et al. 1978). They show a good sorting in their grain size composition which gives them further stability. Among the adequate sediment, strong currents are also needed for the development of megaripples (Dalrymple et al. 1978, Larcombe and Jago 1996, Bird 2000).

According to Dalrymple et al. (1978), megaripples can be distinguished in Type 1 and Type 2. Type 1-megaripples form at weaker flow strength and therefore, are simple in appearance, straight to smoothly sinuous, rather flat and their height remains constant along the crestline. Type 2-megaripples are formed by stronger flow strength which results in a more complex appearance, a sinuous to lunate shape, a steep profile and their height is variable along the crestline (see Fig. 5.6).

The formation, orientation and migration of megaripples is not well understood (Gallagher et al. 1998). Megaripples are often aligned right-angled to the tidal flow, but this can not be generalised as they sometimes run diagonally or parallel to the current flow (Bird 2000). Rubin and Hunter (1987) found that bedforms can have any angle relative to the resultant transport direction. Bedforms that are transverse, oblique, and longitudinal are basically all

of the same kind as they do not require differing flow dynamics. On the other hand an infinite number of flow regimes can also produce the same bedform trend.

Megaripples are migrating, driven by tidal currents, and are important for sediment transport and bedform dynamics (Larcombe and Ridd 1995, Larcombe and Jago 1996). However, sediment transport directions can not be accurately determined by presuming the alignment of megaripples as they do not migrate in the direction of the vector sum of the currents. Megaripples are aligned so that the sediment transport normal to their crest is maximized (Rubin and Hunter 1987, Gallagher et al. 1998).

A great variety of measured megaripple migration rates is reported (e.g. Boothroyd and Hubbard 1975, McCave and Geiser 1978, Larcombe and Ridd 1995, Larcombe and Jago 1996, Gallagher et al. 1998). The rates are mostly ranging from 0.02 to 0.1 m $min^{-1}$ and net migrations of 1 to maximum 5 to 6 m per tide are observed. Current velocities of 0.5 to 0.6 m $s^{-1}$ were determined as a migration threshold (Boothroyd and Hubbard 1975, Larcombe and Ridd 1995, Larcombe and Jago 1996). Nevertheless, it is observed that the populations of megaripples are remarkably stable in their overall properties compared with the great variability shown by the tidal flows that activate them (Allen and Friend 1976, Zarillo 1982). This dynamic equilibrium is probably due to the reversed flow directions at ebb and flood tide.

Migrating megaripples can have an effect on seagrass beds and mussel beds. Tidal flats with megaripples are regarded to be highly dynamic areas which affect seagrass as it prefers stable sediment conditions (Phillipart et al. 1992, Reise and Kohlus 2008). Furthermore, Marbà et al. (1994) observed migrating megaripples which ran over seagrass and buried it. Seagrass as well as mussels can handle a certain degree of sediment accretion and react to it by vertical growing and moving respectively but negative effects could be observed at any rate (Okun 1999, Mills and Fonseca 2003, Cabaço and Santos 2007).

In this study, megaripples in the northern Wadden Sea near the island of Sylt were analysed by means of remote sensing and ground surveys.

The hypotheses, this study is based on, are:

1) The area of tidal flats with megaripples increases with increasing tidal range and high tide level,
2) Megaripples migrate in course of time,
3) Migrating megaripples interfere with biogenic habitat structures.

## 5.2 Material and methods

Data on megaripples were gained by field surveys and by derivation from aerial photographs, taken at low tide. This method was also used by McCave and Geiser (1978). The megaripples were identified in the field as well as in the aerial pictures by colour difference as they are brighter than their surrounding sediments and by their generally oblong structure. Furthermore, megaripples are elevated and thus stand out from ambient sediment.

### 5.2.1 Long-term development of megaripple populations (1936/1945 – 2003)

The spatial distribution of megaripple populations in the List tidal basin and the extent of the areas covered by them were examined for the period 1936/1945 to 2003. For this purpose georeferenced aerial photographs were visually analysed and the external boundaries of megaripple populations manually digitised on-screen with GIS using the ESRI software ArcGIS 9.1, ArcMap. The boundary was determined along the outermost occurrence of megaripples of a population (see Fig. 5.8). For further details on aerial photographs, georeferencing and digitising see Chapter 3.2.

This survey was divided into four periods: 1936/1945, 1955/1968, 1989/1990 and 2003. As the aerial photographs are showing different parts of the bay, those which are closest together in time were combined in order to cover the entire List tidal basin for the selected periods. For this analysis the general distribution of megaripples in the List tidal basin was recorded and the total area covered by them calculated for each period with the GIS software.

### 5.2.2 Medium-term development of individual megaripples (1998 – 2006)

To analyse the medium-term development of individual megaripples, the positions and shapes of 9 megaripples were manually digitised from aerial photographs from 1998 to 2006. Almost annually taken aerial photographs allow reconstructing a rather complete time series. Two study sites at the eastern shore of the island of Sylt were selected for this investigation: Blidselbucht and Königshafen.

Airborne data of 4 individual megaripples in the Blidselbucht (B 1 - B 4) and of 5 in the Königshafen (K 1 - K 5, Fig. 5.2) could be obtained in 7 remote sensing surveys. Besides the area and perimeter of each megaripple, the coordinates of the centroid were also calculated in ArcGIS 9.1, ArcMap. A centroid is the geometric centre of a polygon. In the case of irregularly shaped polygons, the centroid is derived mathematically and is weighted to approximate a sort of "center of gravity" (www.colorado.edu 1994). The migration of

the centroid was chosen as a scale for the dynamics of a megaripple as it takes both changes of its shape and changes of its position into account.

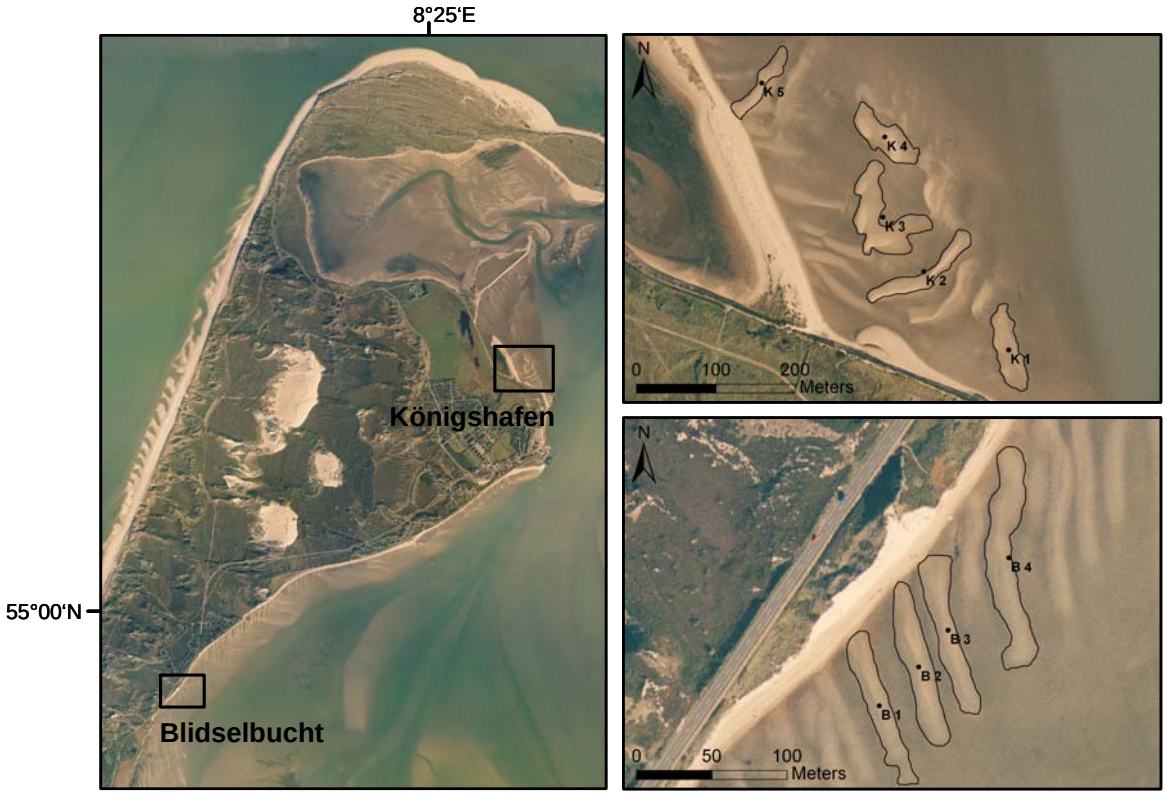


**Fig. 5.2:** The observed individual megaripples in the survey areas Königshafen and Blidselbucht in October 2003. The black points in the megaripples are their centroids.

### 5.2.3 Short-term variability of megaripples (May 2005 - August 2006)

In order to obtain data on the short-term dynamics of megaripples, the variability of their shape, position and height was analysed during a 16-months survey period. For this purpose, the same megaripples as for the medium-term investigation were surveyed in the Blidselbucht and in the Königshafen. Thirteen field surveys in almost regular intervals of 4 to 6 weeks were conducted with the submeter differential GPS (DGPS) device Trimble GeoXT handheld. While the shape and position of the megaripples were measured with the DGPS, the maximum height from ripple crest to ripple trough was determined for each megaripple with a measuring tape. The DGPS data were imported into the GIS software and the area covered by a megaripple, the perimeter and the position of the centroid calculated for each survey.

Megaripples show different extent and appearance within a year. In order to test if this is also reflected in a different grain size composition, sediment samples were taken at the study site Blidselbucht in May 5, 2005 and March 5, 2006. In May 2005, 29 sediment samples were taken along three parallel profiles running transverse over two megaripples

including the tidal flats area in front of, between and behind the two megaripples. In March 2006, 15 sediment samples were collected along three profiles. The sediment samples were treated and their grain size composition measured according to the method described in Chapter 4.2.2. Furthermore, one exemplary megaripple was determined which was surveyed in detail in these two campaigns and 3D-models were generated using ArcGIS 9.1, ArcScene.

### 5.2.4 Statistical analysis

The statistical analysis was conducted with the Statsoft software package STATISTICA 6.0. The p-level was determined at 0.05 and the standard deviation was used. The tests that were done are further specified in the following chapter 'Results'.

## 5.3 Results

### 5.3.1 Long-term development of the spatial distribution of megaripples in the List tidal basin (1936/1945 – 2003)

Megaripples show a specific pattern. In the areas where both requirements for their formation, strong hydrodynamics and sandy sediment, are met, not only a single megaripple is formed but whole populations of them. This can also be observed in the List tidal basin.

In the first period (1936/1945), populations of megaripples occur predominantly in Königshafen, on Havsand and on Jordsands Flak (Fig. 5.3). They can be found along the entire width of the List tidal basin (east-west direction), but their existence is focused on the centre of the bay as they do not reach its southern or northern part. Their main distribution is limited from 55°07.8' N to 54°59.1' N. Within this belt the megaripple groups can be often found in close vicinity to the tidal channels. They form mainly narrow stripes which often directly adjoin the shoreline. In total, the megaripples cover an area of 7.185 $km^2$, which is 5.4 % of the intertidal area of the List tidal basin.

Approx. 20 years later, minor changes can be observed in the spatial distribution pattern of the megaripple populations. Their occurrence is still limited to the centre of the List tidal basin. However, the area covered by them increased as the megaripple groups have extended their boundaries. In 1955/1968, 8.116 $km^2$ and 6.1 % of the intertidal area are covered by them respectively.

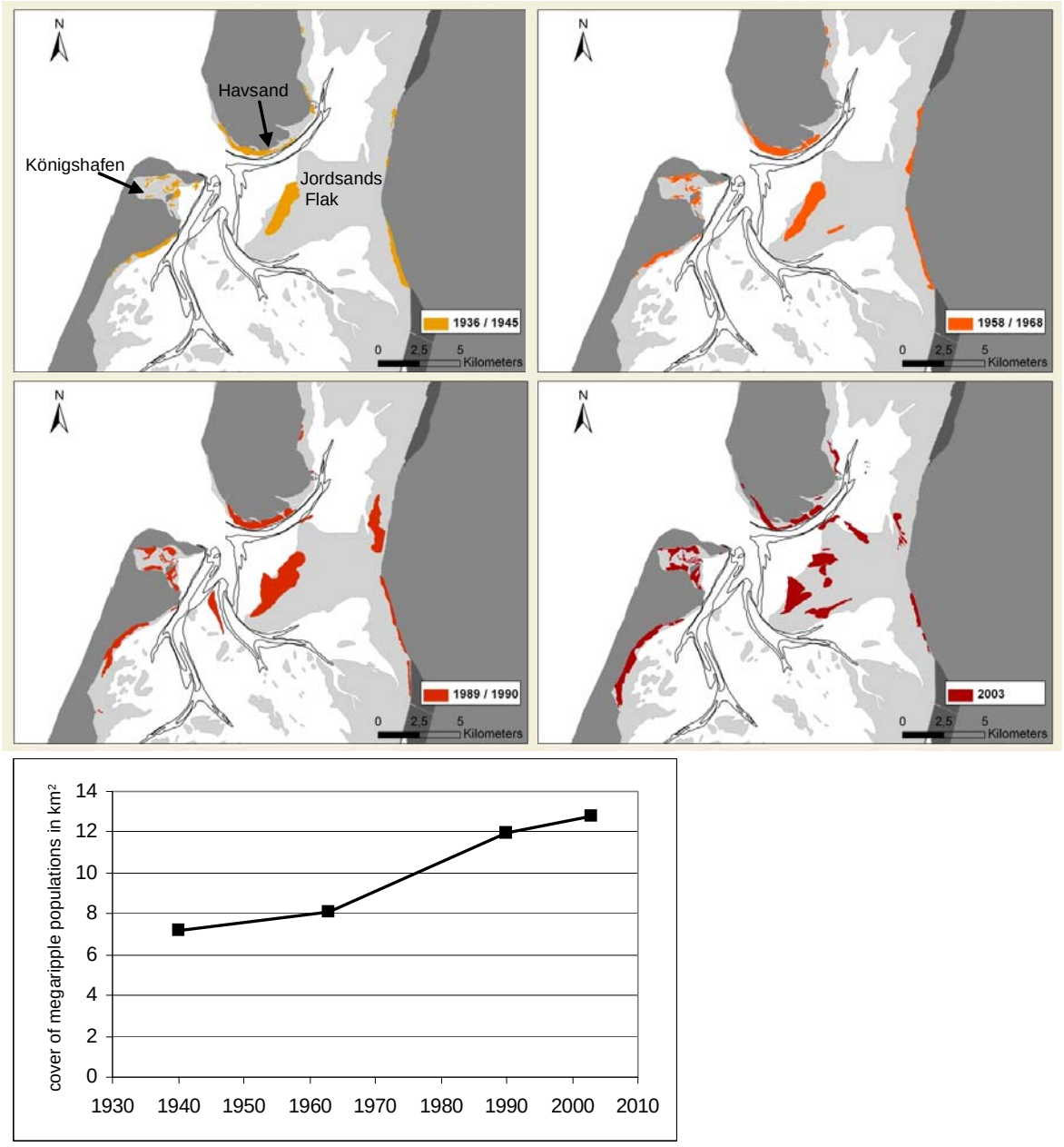


**Fig. 5.3:** Development of the spatial distribution and extent of megaripple populations in the List tidal basin (1936/1945 to 2003).

The pattern of the spatial distribution of the megaripples does not change much until 1989/1990. The fields formed by them are still strongly focused on the middle of the List tidal basin but they have extended further southwards. Starting from their established locations they further extended their distribution areas covering now 11.958 km$^2$ which means 8.9 % of the intertidal area.

By 2003 there are only minor changes in the general distribution pattern as the fields of megaripples are still in the same locations as the years before. Megaripples occur in Königshafen, on Havsand, on Jordsands Flak and east of the barrier islands. However, the

extension trend continues as they are now occurring from 55°06.4' N to 54°57.6' N. The 'band' of the main megaripple appearance kept almost its width but shifted about 2.7 km southwards. The megaripples now cover an area of 12.802 $km^2$ which is 9.6 % of the intertidal area of the List tidal basin. Compared to 1936/1945 a spatial gain of 178 % can be recorded for the megaripple populations until 2003.

It can be summarized that megaripples are characterized by their spatial distribution as well as by the persistence in the locations of individual populations. They occur along the entire width of the List tidal basin but are also limited to its centre in vicinity of the tidal inlet and the tidal channels. Over the years megaripple fields increased in size starting from their established locations and also extended their existence, especially southwards. On average the area covered by megaripples increased by 0.084 $km^2$ $yr^{-1}$.

### 5.3.2 Medium-term dynamics of megaripples (1998 – 2006)

From 1998 to 2006, 9 individual megaripples at the two study sites Blidselbucht and Königshafen were analysed with regard to the year-to-year variability of their positions, shapes and sizes.

The study site Blidselbucht represents a low current regime as the megaripples are located in a sheltered position. They are remote from stronger currents as the nearest tidal channel, which has a depth of only 7 m in this section, is 2300 m away. Backhaus et al. (1998) measured predominantly weak currents on the tidal flats with velocities often below 0.1 m $s^{-1}$. According to the classification by Dalrymple et al. (1978) the megaripples in the Blidselbucht are typical Type 1-megaripples as the shape is generally straight, the profile more flat and the height does not vary along the crestline.

These 4 surveyed megaripples run parallel to each other and are aligned in north north-west to south south-east direction, in an angle of 120 to 130° to the shoreline (Fig. 5.2). They are directly connected to the slope of the sandy beach and part of a large population consisting of 47 megaripples in 2006. Their shape varied slightly during the survey period and they can be always identified by their appearance. Furthermore, their migration is rather low and shows no trend in direction. From 1998 to 2006 the mean migration of the 4 centroids of the megaripple in the Blidselbucht was 16.0 ± 10.5 m (Fig. 5.4), which is a rate of 2.0 ± 1.3 m $yr^{-1}$. Here, their absolute migration distance (not the net distance) was regarded. The mean megaripple area amounts to 2444 ± 544 $m^2$ and the mean perimeter to 336 ± 77 m.

The study site Königshafen represents a high current regime. The megaripples which abound east of a sandy hook (Lister Haken) in the south-east Königshafen, are located 600 to 800 m away from a tidal channel. The channel is 15 to 20 m deep in this section and strong currents with maximum velocities of 0.6 m $s^{-1}$ are observed (Backhaus et al. 1998). However, there seems to be two populations of megaripples. Eight are more or less connected to the beach of the sandy hook and run eastwards in an angle of 110 to 120° to it. These resemble Type 1-megaripples. Another population of 9 megaripples is located seaward of the nearshore population with a partial overlap in area. These megaripples are highly irregular in size and shape. Their orientation is almost perpendicular to those of the nearshore population or no particular orientation can be identified. These offshore megaripples resemble Type 2-megaripples, and the five most conspicuous have been selected to study their morphodynamics (Fig. 5.2).

These 5 surveyed megaripples are characterised by a high variability, which is expressed in their migration and in merging and splitting of neighbouring megaripples which was observed 3 and 1 time respectively from 1998 to 2006. In this period, the mean migration of the megaripple centroids was 33.3 ± 14.7 m (Fig. 5.4), which is a rate of 4.2 ± 1.8 m $yr^{-1}$. Even though the migration is significantly higher than in the Blidselbucht (U-Test, p = 0.027), no trend in the moving direction could be detected. The mean area covered by the 5 megaripples is 2702 ± 1430 $m^2$ and the mean perimeter 393 ± 268 m.

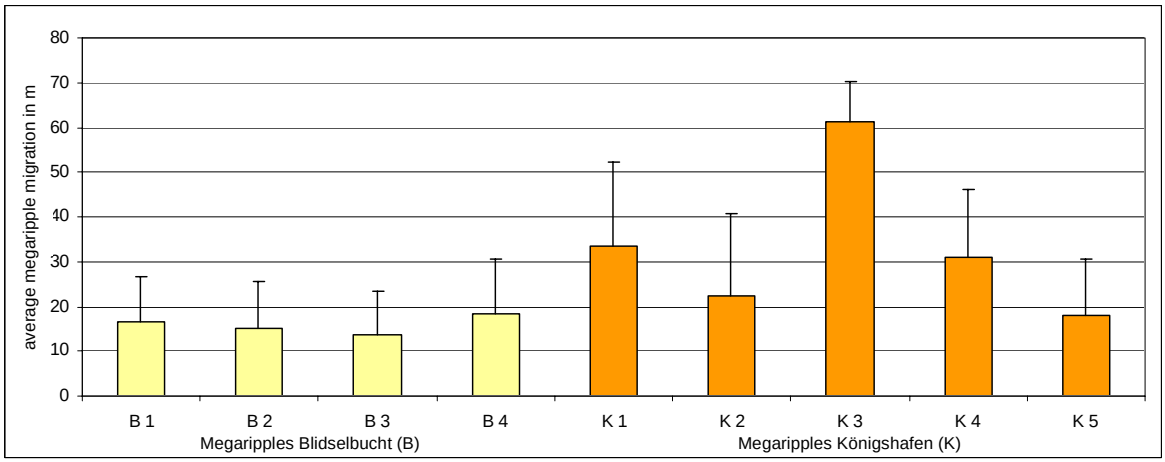


**Fig. 5.4:** Average spatial migration of megaripple centroids in the Blidselbucht (B 1 - B 4) and in the Königshafen (K 1 - K 5) from 1998 to 2006.

### 5.3.3 Short-term dynamics of megaripples (May 2005 – August 2006)

The morphodynamics of the 9 individual megaripples in the Blidselbucht and the Königshafen were recorded on a monthly interval for the period May 2005 to August 2006 in order to assess their variability.

In the Blidselbucht the megaripples were characterized by a rather stable position as the mean migration of the centroids was at 4.7 ± 2.2 m during the survey period (Fig. 5.5). Nevertheless, the megaripples changed their morphology as they varied in length, width and height. During this sampling period they covered a mean area of 1516 ± 424 $m^2$ while their mean perimeter was 266 ± 37 m and their mean maximum height amounted to 22 ± 6 cm.

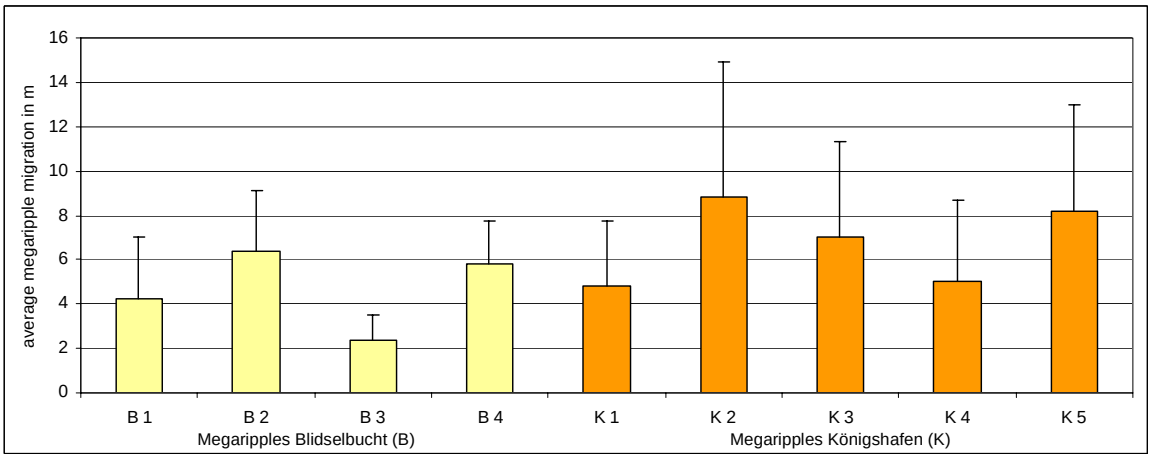


**Fig. 5.5:** Spatial migartion of megaripple centroids in the Blidselbucht (B 1 - B 4) and in the Königshafen (K 1 - K 5) from May 2005 to August 2006.

From May 2005 to August 2006, the megaripples in the Königshafen showed a mean migration of their centroids of 6.8 ± 4.4 m (Fig. 5.5), which is significantly higher than in the Blidselbucht (U-Test, p = 0.014). They also changed their morphology, mean area (2061 ± 626 $m^2$) and mean perimeter (296 m ± 55 m), and the higher standard deviations than in the Blidselbucht indicate higher dynamics. Their average maximum height was 42 ± 9 cm.

### 5.3.4 Grain size composition

It was observed that megaripples can have a different appearance during the year and in order to test the effect for the grain size composition, sediment samples were taken from 2 megaripples and their surrounding tidal flats in the Blidselbucht.

In May 2005, the megaripples were relatively high, stood out clearly from their environment and had distinct well-defined borders. The megaripple B 2 was regarded as representative for the population. This determination was possible because this population is characterised by a high homogeneity in the appearance of its megaripples. The exemplary megaripple was 105 m long and 16 m wide. It was 40 cm high at the north

north-west end and declined gradually to 20 cm at the south south-east end and had a volume of 220 $m^3$.

In March 2006, the megaripples were rather flat and had diffuse boundaries. The exemplary megaripple B 2 had a length of 92 m, a width of 11 m, a uniform height of 10 to 20 cm and a volume of only 73 $m^3$ then (Fig. 5.6).

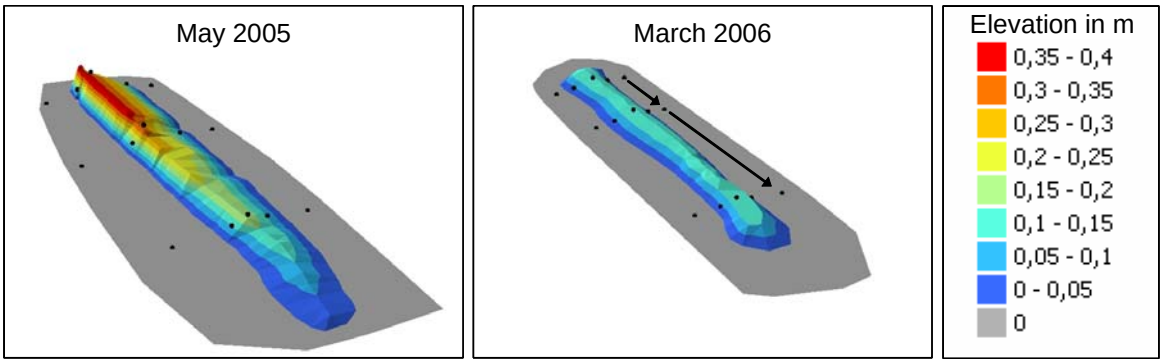


**Fig. 5.6:** The megaripple B 2 in its different occurrences. In May 2005 it represents a Type 2-megaripple while it shows typical Type-1 characteristics in March 2006. The black points mark the sampling locations for the sediment samples. The black arrows indicate that sediment samples that are in a line were combined to calculate averages presented in Fig. 5.7.

The average grain size compositions (Fig. 5.7) were calculated by combining the cross-sectional profiles. The averages were calculated out of 3 sampling stations which are located in each line (Fig. 5.6). This result in 9 average grain size compositions: 1 in front of megaripple W 2, 3 on megaripple W 2, 1 between the two megaripples, 3 on megaripple W 3 and 1 behind megaripple W 3 (Fig. 5.7).

In both surveys the megaripples were mainly composed of medium (50 – 70 %) and fine sand (20 – 35 %) whereas all other grain size classes contributed with less than 5 % to the grain size composition (Fig. 5.7). Despite their different occurrence, no significant differences could be detected in their grain size composition (U-Test, p = 0.34).

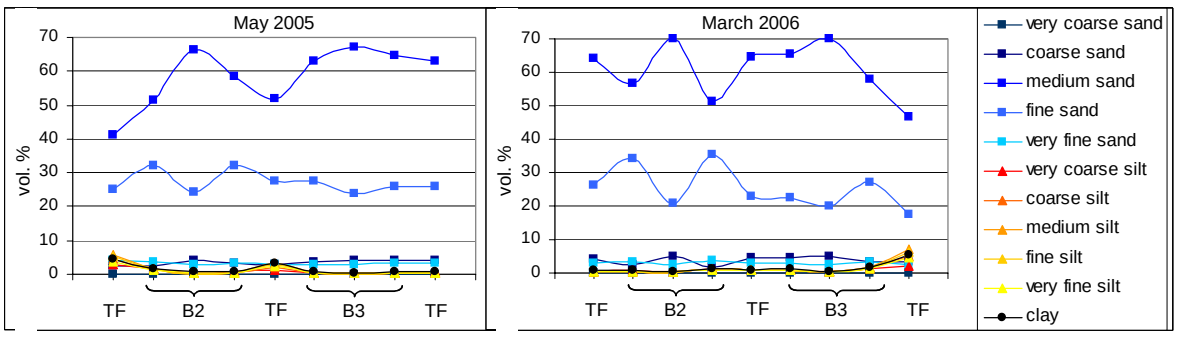


**Fig. 5.7:** The average grain size compositions of the sediment samples from the 3 cross-section profiles, which transected the megaripples B 2 and B 3 and the tidal flats (TF) in front of, between and behind them. Three sediment samples were taken along the width of each megaripple (W 2 and W 3).

Furthermore, it was analysed if the megaripples in the Blidselbucht show different grain size compositions than the tidal flats in their vicinity. The percentage of medium sand was in average slightly lower here (40 – 65 %) while fine sand amounted to 20 – 30 % and the other grain size classes to less than 5 % to the grain size composition. However, these are only minor changes and no significant difference in the grain size composition inside and outside the megaripples could be recorded in both surveys (U-Test, p = 0.25).

## 5.4 Discussion

### 5.4.1 Reasons for increasing megaripple populations

Intertidal megaripples are only found where the conditions of sandy sediment and strong currents are met. Therefore, their occurrence in the List tidal basin is limited to the centre, where sandy tidal flats are exposed to stronger currents. North and south of theses limits the sediments are too muddy and / or the strength of the currents is not sufficient.

However, the area covered by megaripple populations in the List tidal basin increased steadily from 718.5 ha in 1936/1945 to 1280.2 ha in 2003. This indicates that the conditions for their formation are enhanced. This can be due to a stronger current flow and / or a spatial increase of sand-dominated tidal flats. Basically, stronger currents can be regarded as the main cause for the increasing megaripple populations. Stronger currents are not only responsible for the formation of megaripples but also for a spatial expansion of sandy tidal flats because they induce a depletion of mud in the tidal flat sediment composition by removing fine-grained material.

A stronger current flow is associated with a rising sea level but can also be amplified by the reduction of the tidal catchment area. A constantly rising high tide level from 567.81 cm (1936 – 1945) to 585.23 cm (1996 – 2005) is recorded at the gauge List. Besides an increase in high tide level, there has been an increase in tidal range as well (Jensen et al. 1992). This should have a direct effect on current velocities. On the other hand, it can be assumed that wave action has also increased. As there is no strong evidence that the formation of megaripples is entirely attributed to strong currents, hydrodynamics should be considered as the driver. However, hydrodynamics are amplified not only by an increased tidal range but also by the reduction of the tidal catchment area. This leads to less accommodation space for the tidal flow which results in increased energy levels within the basin (Flemming and Nyandwi 1994, Mai and Bartholomä 2000). During the long-term survey period of this study (1936/1945 – 2003), the catchment area of the List tidal basin was almost completely closed by the construction of the Rømø causeways in 1948 which

connects the islands with the mainland. Further reductions occurred by land claim measures and dike constructions, like e.g. Mövenberg-Dike in 1937 and the Margrethe-Koog (1979-1982) (Wohlenberg 1953, Jespersen and Rasmussen 1984, Jespersen and Rasmussen 1989, Bayerl and Köster 1998) (see Fig. 3.1). However, considerable reduction of the tidal catchment area occurred also before 1936. Reise (1998) estimates that over the last 500 years one third of the List tidal basin has been converted into land by embankment and the tidal flat area decreased from approx. 66 to 40 % within the 20$^{th}$ century. Mud depletion is a result of the reasons mentioned above and can be observed in the entire Wadden Sea.

However, this pattern of increased current flow in the List tidal basin fits to the observed change in the grain size composition of surface sediments (see Chapter 4.4.1) as well as to the development of Jordsand and the sandy hook in the outer Königshafen (see Chapter 3.3.2).

Megaripples can be regarded as an indicator for increased hydrodynamics. I order to check if the detected increase of their populations is a regional phenomenon or only an exception occurring in the List tidal basin, I recommend conducting this long-term analysis also in other Wadden Sea areas. It is most likely that the number of reference areas is limited as the availability of long-term sets of high-resolution aerial photographs is a precondition for this study.

### 5.4.2 Megaripples and biogenic habitat structures: exclusion or coexistence?

Among the spatial expansion of the megaripple populations, a southward shift in the general occurrence was observed in the List tidal basin from 1936/1945 to 2003 (Fig. 5.3). In this regard, an interference of megaripples with mussel beds and seagrass beds was noticed, especially in the upper intertidal at the east shore of the island of Sylt. The question arises if megaripples are a threat to seagrass and mussel beds in the List tidal basin?

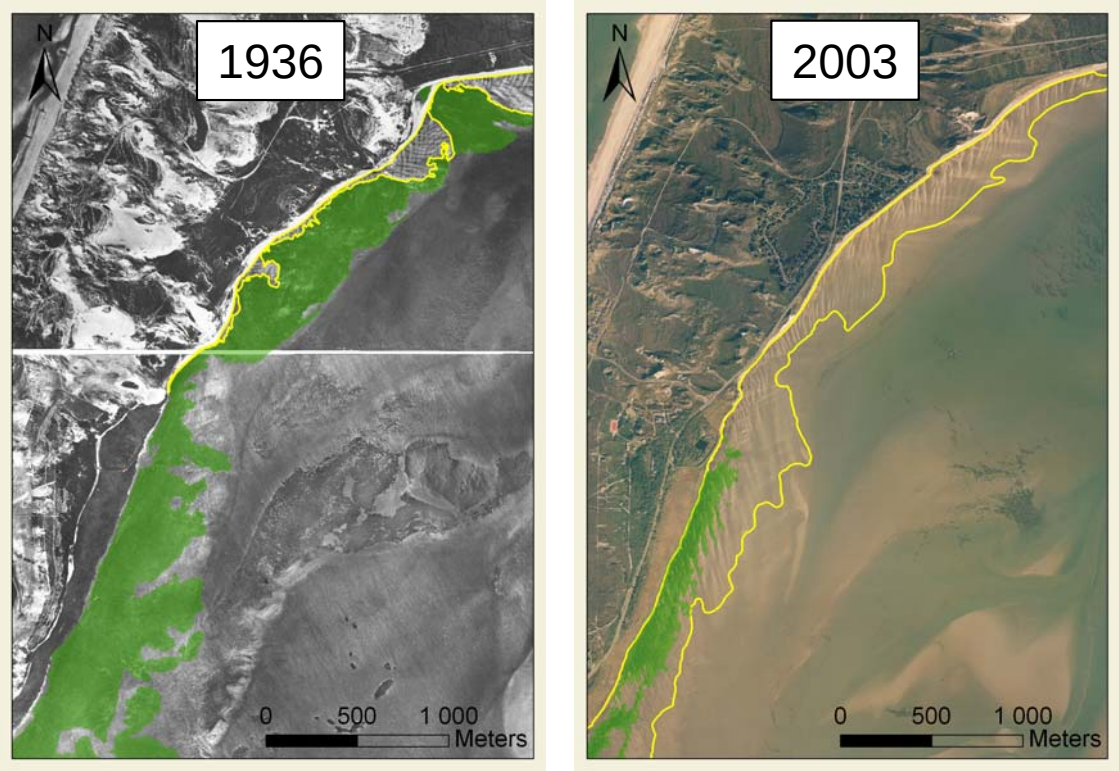


**Fig. 5.8:** The spatial distribution of seagrass (highlighted green) and megaripples (bordered yellow) at the eastern shore of the island of Sylt in 1936 and 2003. In 2003, the megaripples intrude into the seagrass bed.

Seagrass is sensitive to sediment instability as well as burial with sediment, e.g. by migrating megaripples (Philippart et al. 1992, Marbà et al. 1994, Cabaço and Santos 2007, Reise and Kohlus 2008). The long-term remote sensing data reveals that areas formerly inhabited by seagrass are now covered with megaripples. In the List tidal basin, an area of 1.825 $km^2$ which was formerly (1936/1945) covered with seagrass, is now (2003) unvegetated and occupied by megaripples. The eastern shore of the island of Sylt is predominantly affected by this (Fig. 5.8).

It can not be concluded whether the megaripples caused the disappearance of seagrass beds or only contributed to it. Perhaps megaripples formed after the decline of the seagrass and now inhibit its recolonization. A similar phenomenon is reported by Cardoso et al. (2004), who observed that after a decline of seagrass, the former vegetated area was replaced by coarser sediments which kept unvegetated.

Coexistence seems to be difficult. In addition to cases where megaripples exclude seagrass, there are also examples where they occur in a seagrass bed or intrude into it. In these cases the area covered by megaripples are seagrass free or in case of flat megaripples sparsely vegetated (Fig. 5.9). I hypothesise that the migration rate of the megaripples is the main

factor. Megaripples and seagrass beds can occur in the same location but only if megaripples are rather stationary after formation. A further evidence for this is the fact that these forms of coexistence are only found in very sheltered areas.

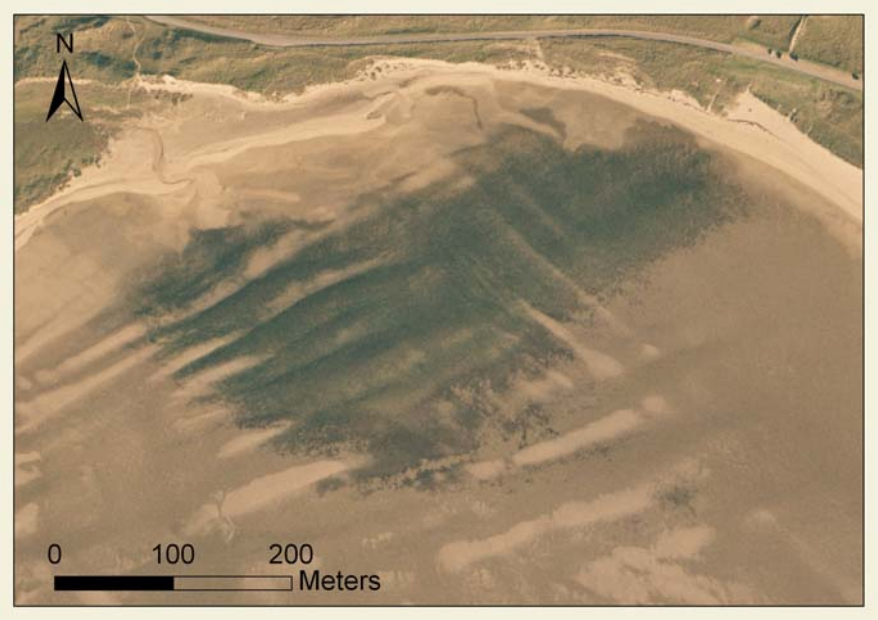


**Fig. 5.9:** Coexistence of seagrass and megaripples in the Königshafen in 2003.

Mussel beds seem to be more resistant towards sediment dynamics as they form more compact structures but they are also affected by burial with sediment. Mussels can actively escape from sedimentation but they cannot handle a continuous sedimentation and die when buried with a sediment layer thicker than 2 cm (Okun 1999). In the outer Königshafen distinct megaripples are found today in places where mussel beds existed in the mid 1990s (Fig. 5.10). In this case, the mussel beds have been scoured by ice in the severe winter 1995/96 (Strasser et al. 2001b). No recruitment of mussels occurred in the subsequent years and thus the few remnant beds faded away. It is interesting to see that oysters develop today in the northern part of the area but not in the part where megaripples exist. Even though mussel and oyster beds seem to be in general less sensitive to megaripples because they form more compact structures, this observation leads to the conclusion that their reestablishment can be inhibited or at least hampered by migrating megaripples.

However, it is observed that megaripples in the List tidal basin occur more often in the same places with seagrass beds than with mussel beds.

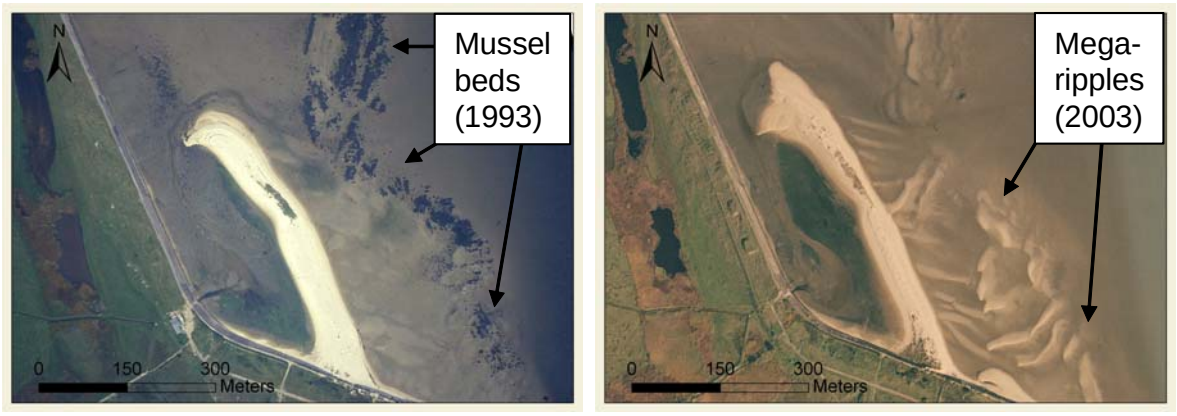


**Fig. 5.10:** Formation of distinct megaripples after the disappearance of mussel beds in the outer Königshafen.

### 5.4.3 Migration rates and appearance of megaripples

The analysis of the medium- and the short-term development of megaripples revealed significant differences between those in a low and those in a high current regime.

Comparing the medium-term development of the megaripples in the Blidselbucht and in the Königshafen it is observed that they have similar mean size and perimeter but the standard deviations of these parameters of the Königshafen megaripples is about 3 times higher. The higher variability is also indicated by the migration of the megaripple centroids which can be regarded as a scale for migration and morphology changes. In average, it is twice as high in the Königshafen as in the Blidselbucht. When regarding the migration of the centroids from May 2005 to August 2006, the differences between the megaripples in the high and in the low current regime were even more significant.

Nevertheless, the observed medium- and the short-term migration of the megaripples is rather low compared to migration rates reported in publications, e.g. about 1 m per tide at spring tide in North Wales (Larcombe and Jago 1996) or even 5 to 6 m per tide in Queensland, Australia (Larcombe and Ridd 1995). However, Asmus (pers. comm.) observed migration rates of several meters a day in the outer Königshafen in the mid 1990s. Consequently, there must be a form of dynamic equilibrium in megaripple migration which is also observed by Allen and Friend (1976) and Zarillo (1982). For the analysis of the medium-term development of the megaripples, aerial photographs were surveyed which were taken once a year and therefore, there is no knowledge on their short-term variability. However, the survey from May 2005 to August 2006 also does not reveal such high migration rates as reported by Reise (1985) and Asmus (pers comm) for the mid 1980s and mid 1990s. It can be assumed that the required hydrodynamic conditions for

high migration rates were not existent in 2005/2006. Weisse and Plüß (2006) and Weisse et al. (2005) showed that storms decreased along the North Sea coast since the mid 1990's which would give an explanation for the different megaripple dynamics.

The different appearance of the megaripples in the Blidselbucht in May 2005 and March 2006 results from different force of the current flows. The megaripples show characteristics of Type 2-megaripples in May 2005 and are typical Type 1-megaripples in March 2006. However, the grain size analysis revealed that the sediment composition is very similar and only the amount of sediment accumulated as megaripple is different. The volume difference of the exemplary megaripple amounted to 147 $m^3$. This can not be extrapolated to all megaripples in the List tidal basin due to their heterogeneity, but it can be estimated for the Blidselbucht population as the megaripples are rather uniform here. This entire megaripple population covers an area of 562 500 $m^2$ and the different occurrence of the megaripples means a relocation of about 6900 $m^3$ of sediment. The sediment which is normally homogenously distributed over a larger area is accumulated in the megaripples. This changes the tidal flat topography considerably and also affects overlying currents by introducing hydraulic roughness (Gallagher et al. 1998).

Furthermore, it was found in both campaigns that there are hardly any differences in the grain size composition of the megaripples and of the tidal flat sediments surrounding them. Even though they differ in colour as the megaripples are clearly brighter and the surrounding sediments seemed to be muddier, this impression could not be confirmed by the grain size analysis. I assume that the megaripples are better drained and have a lower water content because of their higher elevation. I further hypothesise that their place of origin and their place of occurrence is rather the same and that they do not migrate longer distances. It also seems that they are composed of the whole grain size spectrum of their location of origin and no grain size selection is taking place. Therefore, they are especially generated in places with well-sorted sediments.

## 5.5 Summary and conclusions

The occurrence of megaripples may be regarded as an indicator for sediment dynamics. A long-term analysis (1936/1945 – 2003) of megaripple populations in the List tidal basin reveals that the area affected almost doubled from 7.185 to 12.802 $km^2$ over the last six decades. It is suggested that this can be related to increased hydrodynamics which enlarge

the share of a sandy tidal area by mud depletion and there facilitate formation of megaripples.

It is further concluded that megaripples can be a threat to seagrass and mussel beds in the List tidal basin. Dynamic megaripples inhibit or at least hamper the reappearance of seagrass beds and mussel beds. Seagrass seems to be more affected. Mussels form resistant, compact structures, and megaripples are more often found in areas where seagrass occurs.

As expected, megaripples in the high current regime are significantly more dynamic than those in the low current regime. Presumably due to recently calmer weather conditions, high migration rates evident from the mid 1980s and mid 1990s were not observed again. In both regimes a dynamic equilibrium of megaripple migration could be noticed.

The different size and occurrence of megaripples is not reflected in a different grain size composition and can be related to different current flow. Furthermore, there is hardly any difference in the sediment composition of the megaripples and the surrounding tidal flats which indicates that their place of origin and their place of occurrence is the same.

I recommend conducting the long-term analysis of megaripple populations also in other Wadden Sea areas in order to examine if the detected increase is a regional phenomenon or only an exception occurring in the List tidal basin.

# 6 Development, dynamics and spatial pattern of intertidal seagrass beds analysed by remote sensing

## 6.1 Introduction

Seagrasses are flowering plants and the dominant vegetation of shallow sandy bottoms in coastal areas around the world (den Hartog 1970). They are of high ecological importance for coastal ecosystems as they are one of the most productive coastal vegetation types worldwide (Asmus and Asmus 2000, Cunha et al. 2005) and supply valuable ecosystem services (Constanza et al. 1997) (Fig. 6.1). Seagrass beds provide habitats and shelter from predators for a diversity of organisms and are spawning and nursery grounds for fish (Fonseca 1996, Polte et al. 2005, Polte and Asmus 2006). Furthermore, they are an important food source for waterfowl, especially for migrating birds like brent geese and wigeon (Ganter 2000, Nacken and Reise 2000), and support a complex detritus-based food chain (Cunha et al. 2005). Another important function is their ability to filter for nutrients as well as stabilising and trapping sediments by reducing the water flow with their leaf canopy (Fonseca 1996).

**Fig. 6.1:** Seagrass bed showing an abrupt boundary on Jordsands Flak in September 2004.

Seagrass requires good ecological conditions. It is sensitive towards eutrophication, turbidity / light limitation, hydrodynamics (currents and waves), sediment instability, tidal exposure / desiccation as well as changes in temperature and salinity (de Jonge and de Jong

1992, Philippart et al. 1992, Philippart 1994, Koch 2001, Schanz and Asmus 2003). Therefore, its spatial and temporal occurrence is determined by these factors.

Two species of seagrass occur in the European Wadden Sea: the dwarf eelgrass *Zostera noltii*, which grows mainly in the upper intertidal area, and the eelgrass *Zostera marina*, which occurs primarily in the lower intertidal (den Hartog 1970, Reise and Lackschewitz 1998). Their seasonal cycle is characterized by germination in May, a maximum extent and density in August and disappearance until December due to grazing by birds and leaf shed.

Especially since the early 20$^{th}$ century, a worldwide decline of seagrass beds, primarily due to human impact, can be observed (Hemminga and Duarte 2000, den Hartog and Phillips 2001, Green and Short 2003) and the European Wadden Sea is also affected (Kastler and Michaelis 1999). In the beginning of the 20$^{th}$ century, *Zostera marina* could also be found in the lower subtidal of the European Wadden Sea. From 1931 to 1934 the eelgrass pathogen *Labyrinthula zosterae* caused the so called 'wasting disease' and eliminated seagrasses at both coasts of the Atlantic Ocean (den Hartog 1987). While the *Zostera marina* beds recovered slowly at the neighbouring European coastal regions, it never returned into the subtidal of the Wadden Sea (de Jonge and de Jong 1992). This might have been caused by changing hydrodynamic conditions, too much turbidity, the loss of sheltered locations as well as the loss of seagrass itself (Giesen et al. 1990, Schanz and Reise 2006). Another dramatic decrease of seagrass has occurred since the 1960s/1970s, affecting the extant intertidal *Zostera* beds, especially in the southern Wadden Sea while the beds in the Northern Wadden Sea remained relatively stable (de Jonge et al. 1993, Kastler and Michaelis 1999, Reise 2006). This time anthropogenic eutrophication is regarded as the primary reason for the decline (van Katwijk et al. 1997, 1999) and level of eutrophication is higher in the southern than in the northern Wadden Sea (van Beusekom et al. 2005). However, since the 1990s an increase of seagrass beds can be observed in the Dutch and the Schleswig-Holstein Wadden Sea (Reise et al. 2005b).

Seagrass responds rather quickly to changed environmental conditions, resulting in a high variability of its spatial extent (Robbins 1997, Frederiksen et al. 2004a, 2004b). Therefore, seagrass is regarded as a good indicator for ecosystem health and an extensive seagrass monitoring is recommended for European coastal waters (Borum et al. 2004).

This study also deals with a monitoring approach of seagrass beds, carried out by remote sensing. A series of aerial photographs, which dates back to 1936, was analysed with a Geographic Information System (GIS). This method is widely applied and described in

literature, e.g. Bruce et al. 1997, Robbins 1997, Kowalski and Wilcox 1999, Pasqualini et al. 2001, Walker et al. 2001, Meehan et al. 2005.

In this study the focus is laid on

- the quantitative and qualitative long-term development of seagrass beds,
- their general spatial pattern,
- the dynamics of seagrass beds,
- the assessment of the potential of high-resolution aerial photographs for remote sensing of seagrass beds.

The survey area is the List tidal basin in the northern Wadden Sea, which is qualified for this study as tidal basins are the most suitable units for monitoring and research. Furthermore, this basin has well-defined borders as well as a long and continuous history of research (Reise and Gätje 1997). The List tidal basin is located in an area called Northfrisian Wadden Sea, which stretches from the Eiderstedt peninsula to the Danish-German border (54°16'N - 55°05'N).

## 6.2 Materials and methods

In order to calculate the long-term spatial development, of seagrass beds surface areas, most data were gained from georeferenced aerial photographs by on-screen digitising using the ESRI software ArcGIS 9.1, ArcMap. This remote sensing data was also completed by GPS field measurements and a historical survey from Nienburg (1927). Nienburgs survey was considered due to the accuracy of his mapping of the seagrass habitats. For further details on aerial photographs, georeferencing and digitising see Chapter 3.2.

### 6.2.1 Detection, definition and classification of seagrass beds

As the overground occurrence of seagrass beds is seasonal they can only be detected in aerial photographs which are taken in summer. Seagrass can be identified by visual analysis on the basis of certain features. They stand out from the tidal flats sediments by their greenish, darker colour. But colour is not a definite identifying feature because green algal mats have the same colour and dark-greenish is hard to detect when seagrass is growing on dark muddy sediments. It is more the combination of colour and texture that helps detection. Intertidal seagrass often forms patches and generate hummocks which give the bed a slightly dotted, heterogeneous texture. These patches are often either circular or irregular in shape (Reise and Kohlus 2008) and separated by small, shallow intertidal pools

and runnels. Furthermore, seagrass beds have preferred locations to grow. The analysis of the long-term series of aerial photographs reveals that in certain areas, mainly sheltered sites, seagrass beds are found permanently.

Seagrass beds were recorded by the on-screen digitising of their boundaries using GIS. The boundaries can be abrupt which facilitates detection. However, determination of the extent of the seagrass bed and the course of its boundary line gets difficult at a low cover or when seagrass gradually declines which both leads to fuzzy and diffuse boundaries. Especially in these cases, the quality of the aerial photographs is the limiting factor for the accuracy of the remote sensing. Therefore, ground-truth field surveys are essential in order to collect data for the validation of the remote sensing results. However, even though the identification of seagrass can be problematic, this method produces best possible results regarding the accuracy of the location and area of the beds.

Extensive field surveys with a Differential GPS device (DGPS) were carried out from July to August in 2004, 2005 and 2006, as ground surveying is feasible for mapping seagrass (Ierodiaconou and Laurenson 2002). As the DGPS is combined with a handheld computer, multiple attributes like species composition, density, epiphytes etc., could be immediately added in the field to the sampled data. This method is further described in chapter 7.2.1.

A comparison of field data and remote sensing data reveals that at least 20 % cover is required to detect seagrass in the aerial photographs. Anyway, data on seagrass beds with a density of > 20 % can be collected to a satisfying accuracy from the high resolution aerial photographs.

Field data was also consulted for the classification of digitised seagrass beds. Their degree of cover was estimated from the aerial photographs and classified as complete (> 80 %), dense (80-60 %), medium (60-30 %) or sparse (< 30 %). Seagrass beds can reach great extent and can also show heterogeneous density. Therefore, they were not classified in one piece but each bed divided into subareas according to their density (Fig. 6.2).

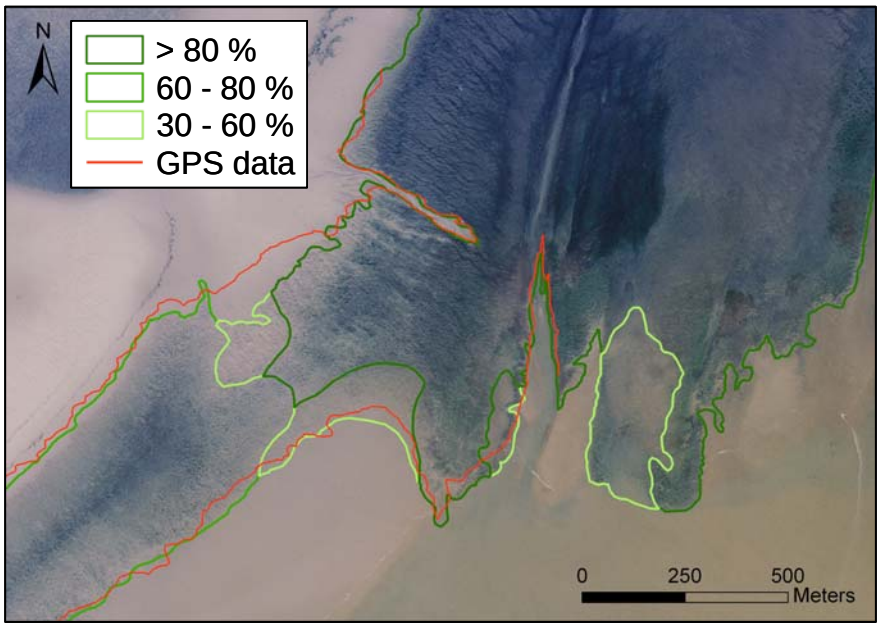


**Fig. 6.2:** An aerial photograph of the seagrass bed on Jordsands Flak in August 2004. The picture shows the boundaries of the bed and its classified cover densities assessed by remote sensing. The comparison with GPS field data reveals the accuracy of the digitised boundaries.

Field surveys were also conducted to find features to help distinguishing seagrass from green algae. In the aerial photographs, the texture is the major key for this. Green algae appear to be more homogeneous or, at a low cover, their texture is elongated and aligned in current direction. The comparison with aerial photographs taken in winter also provides cues: while the overground occurrence of seagrass is seasonal, green algae can be found during the entire year which helps to identify their locations.

### 6.2.2 Development of seagrass beds in the List tidal basin and its subareas

The areas of the seagrass beds were calculated with ArcGIS 9.1, ArcMap. For the complete List tidal basin the development of the quantity (number and size) and quality (degree of cover) of seagrass beds could be regarded from 2003 to 2006. Before 2003, aerial photographs cover the basin not area-wide but just partly. In order to also include these early taken photographs into the analysis and for a more detailed view, the List tidal basin was divided into 5 subareas (Königshafen, west, south, east and north, Fig. 6.3). These 5 subareas were analysed individually due to the temporal heterogeneity of the data base (aerial photographs). The longest time series in this study dates back to 1927 and refers to the subarea Königshafen.

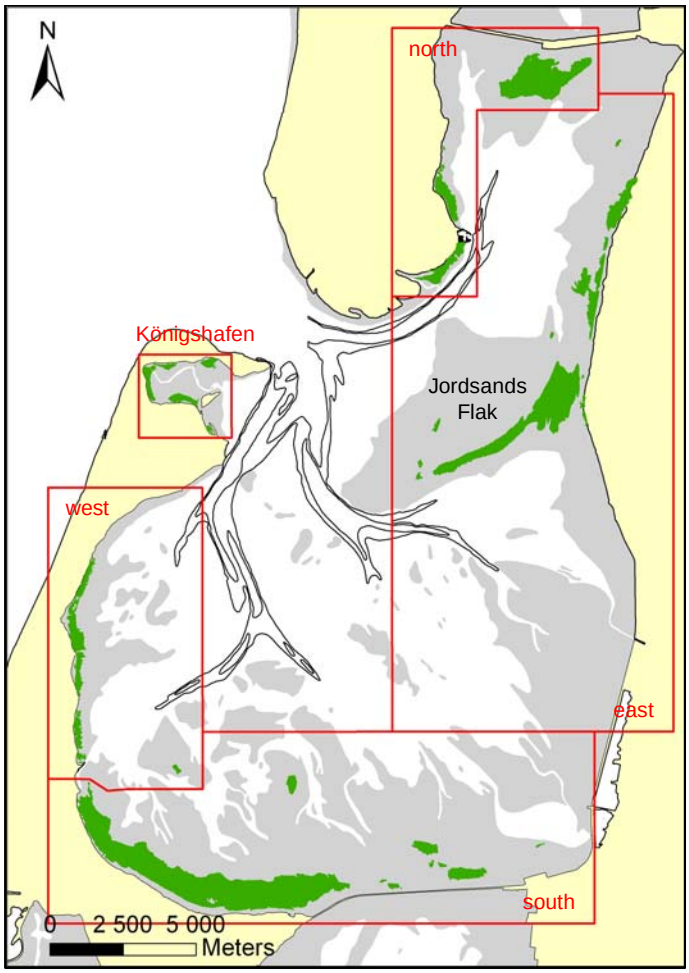


**Fig. 6.3:** The List tidal basin subdivided into 5 areas. The spatial distribution of the seagrass beds in 2003 and the tidal flat area 'Jordsands Flak', which protrudes into the basin, can be seen in the picture.

In GIS, the seagrass data was also integrated in the Digital Elevation Model (DEM) and in the results of the 'Model on 2D current velocities and water depths' (Behrens et al. 1997, see Chapter 3.2.5 for further information on the DEM and the model data). The needed information for the seagrass habitat requirements was extracted out of the models.

In order to get a more complete overview of the development, the Regional Office of the Schleswig-Holstein Wadden Sea National Park (NPA) in Tönning provided GIS shape files on the occurrence of seagrass beds (1996 to 2005) in the North-Frisian Wadden Sea.

### 6.2.3 Seasonal development of seagrass beds

The seasonal development of three seagrass beds in the Königshafen, i.e. growing and consolidation as well as their decline was also analysed. Therefore, multiple aerial photographs taken at different months from 1989 to 1994 were exploited. The images from May, June and August 1992 as well as August and October 1990 gave exemplary insight in the seasonal growth and decline of seagrass beds and therefore, were analysed in detail.

The GKSS provided these aerial photographs in a file format. They were taken in the framework of the SWAP-project (Sylter Wattenmeer Austauschprozesse) which was completed in 1995. For further details about the aerial photographs see Table 3.1 in chapter 3.2.1. The pictures were georeferenced and analysed as described in chapter 3.2.2.

## 6.3 Results

### 6.3.1 General location of seagrass beds in the List tidal basin

Seagrass beds in the List tidal basin occur all along the shoreline except for the southern half of the mainland shore. In general, they can be found in the shelter of the islands Sylt and Rømø, at both causeways, at the northern half of the mainland shore and in elevated locations on the tidal flat area Jordsands Flak (Fig. 6.3). The latter is the only location where seagrass beds expand into the centre of the bay. Otherwise the centre is without seagrass. The areas where seagrass beds potentially grow, are arranged like a narrow belt around the basin. As seagrass beds are characterised by a high variability regarding their spatial extent and the density of their cover, it is difficult to assign hotspot areas. In fact, potential seagrass areas are rather equally distributed at the bays margins which can be observed over the entire survey period.

Seagrass beds are primarily located in the upper intertidal in very close vicinity to the shoreline, often directly adjoining it. The general mean depth of seagrass occurrence in the List tidal basin is -0.1 m ranging from +0.6 to -1.1 m. Most seagrass beds have their landward edge within a distance of 0 to 50 m to the shoreline, except for areas where the distance is artificially enlarged by groin fields and for the seagrass beds on Jordsand.

### 6.3.2 Long-term development of seagrass in the List tidal basin

The aerial photographs from 2003 to 2006 cover the complete List tidal basin and thus allow an assessment and area-wide comparison of the conditions of seagrass beds in the entire basin at one point in time. The area covered by seagrass increased from 1987.5 ha in 2003 to 2875.6 ha in 2006, with a mean of 2485.8 ± 453.9 ha (Fig. 6.4). On average, 42 % of the seagrass beds show a complete cover (> 80 %), while 34 % have a dense (60 - 80 %), 23 % a medium (30 - 60 %) and 1 % a sparse cover (< 30 %). Regarding the average seagrass bed area from 2003 to 2006 subdivided into the 5 subareas, 2 % are allotted to the Königshafen, 5 % to the west, 53 % to the south, 30 % to the east and 10 % to the north of the List tidal basin.

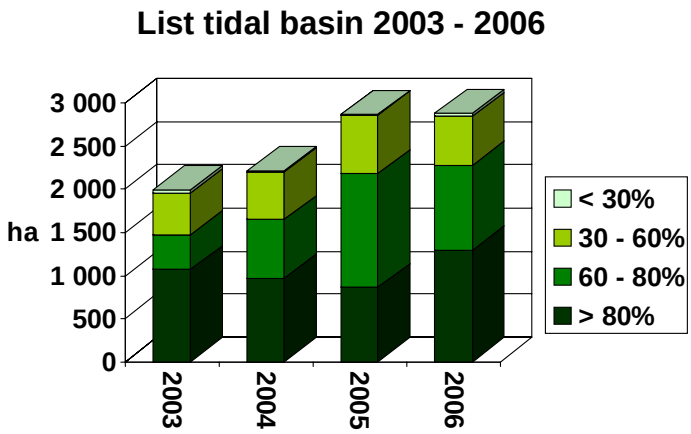


**Fig. 6.4:** The development of seagrass beds in the List tidal basin from 2003 to 2006.

### Königshafen (1927 – 2006)

In 1927, 40 % of the intertidal Königshafen were covered with seagrass. Nienburg (1927) reported a generally very dense cover and good conditions of the seagrass beds. They have their landward edge about 120 to 160 m away from the shoreline, border the tidal creek and are also found in the exposed outer parts. The seagrass cover drops down to 26 % by 1936 but according to the size and density of the intertidal seagrass beds, they are still in a good condition (Fig. 6.5). It can be observed, that the beds get displaced towards the margins of the inner Königshafen as their locations shifted closer to the shoreline and the beds decreased in the outer parts and in vicinity to the tidal creek. This trend continues as well as the steady decrease of the spatial extent, which declined from 129.8 in 1927 to 49.8 ha in 1989. The formerly extensive and almost continuous stock of seagrass shrank to 4 individual seagrass beds. From 1989 to 2004, the seagrass beds are rather stable in their size, shape and position and cover 11 to 14 % of the intertidal Königshafen. From 2003 to 2006 the cover further declines to 7 %, which is 29.1 ha, and since 2003 all seagrass beds are just 30 to 50 m away from the shoreline.

In general, a clear vanishing and degradation of the seagrass beds as well as their spatial shift towards the margins of the bay can be recorded from 1927 to 2006.

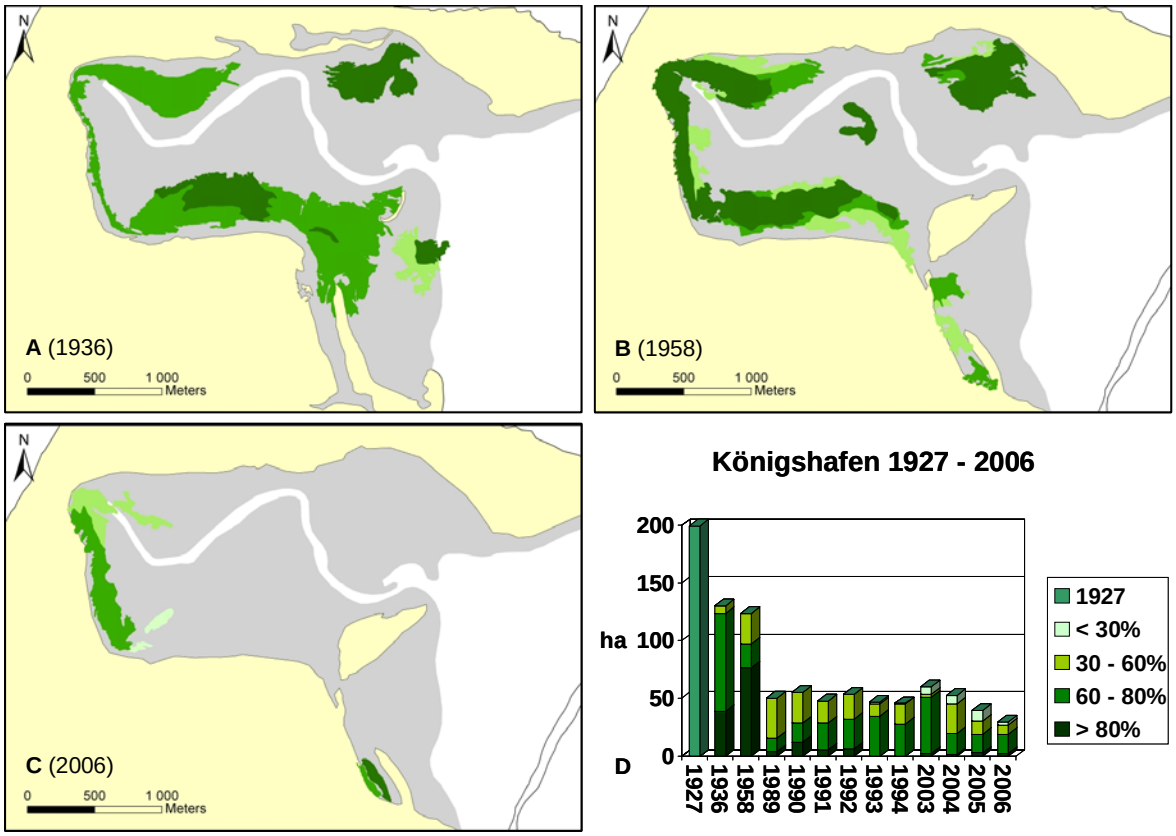


**Fig. 6.5:** The development of seagrass beds in the Königshafen (overview of the study area is given in Fig. 6.3). The spatial distribution in 1936 (A), 1958 (B) and 2006 (C) is shown exemplary in the maps while the development from 1927 to 2006 can be seen in the graph (D).

### Western part (1936 – 2006)

Regarding the seagrass beds in the western part of the List tidal basin, a spatial extent of 421.5 ha as well as a continuous and dense cover can be observed in 1936 (Fig. 6.6). The seagrass closely borders the shoreline where it forms a dense and continuous strip aligned in north-south direction. The width of this seagrass belt amounts to mainly 500 to 700 m with a maximum of 1200 m. In 1958, the seagrass bed still has a dense cover but a loss at the seaward edge results in a decreased width of primarily 400 m with a maximum of 1000 m. Furthermore, a starting disintegration can be observed in the northern range. The disintegration in the north continues and is the main cause for the spatial decrease from 326.3 ha in 1958 to 119.2 ha in 2003. By 2006 a lot of the seagrass bed in the north has vanished and just a 50 m wide stripe is left. The analysis of the aerial photographs from 2003 to 2006 revealed a pattern of decline: the affected parts of the seagrass bed show a considerable decrease in their cover density from one year to the next. This is followed by the loss of the sparser area in the next year in which this complete vanishing is almost

exactly confined to the thinned out area. This pattern of successive decline starts in a certain part of the seagrass bed and affects by and by the neighbouring areas.

However, even though the decline in the width is most pronounced in the northern part, where the seagrass bed approaches a tidal channel, the reduction of the width is a general phenomenon in this survey area. The central and the southern part are not as much affected but still the width narrows to 250 to 400 m here. It goes along with a considerable shift of the seagrass beds seaward boundary towards the land. Nevertheless, the average area covered by seagrass is rather stable with 127.5 ± 18.3 ha from 2003 to 2006. Furthermore and contrary to the degradation in the north, a densifying in the cover can be recorded for the southern part of the bed.

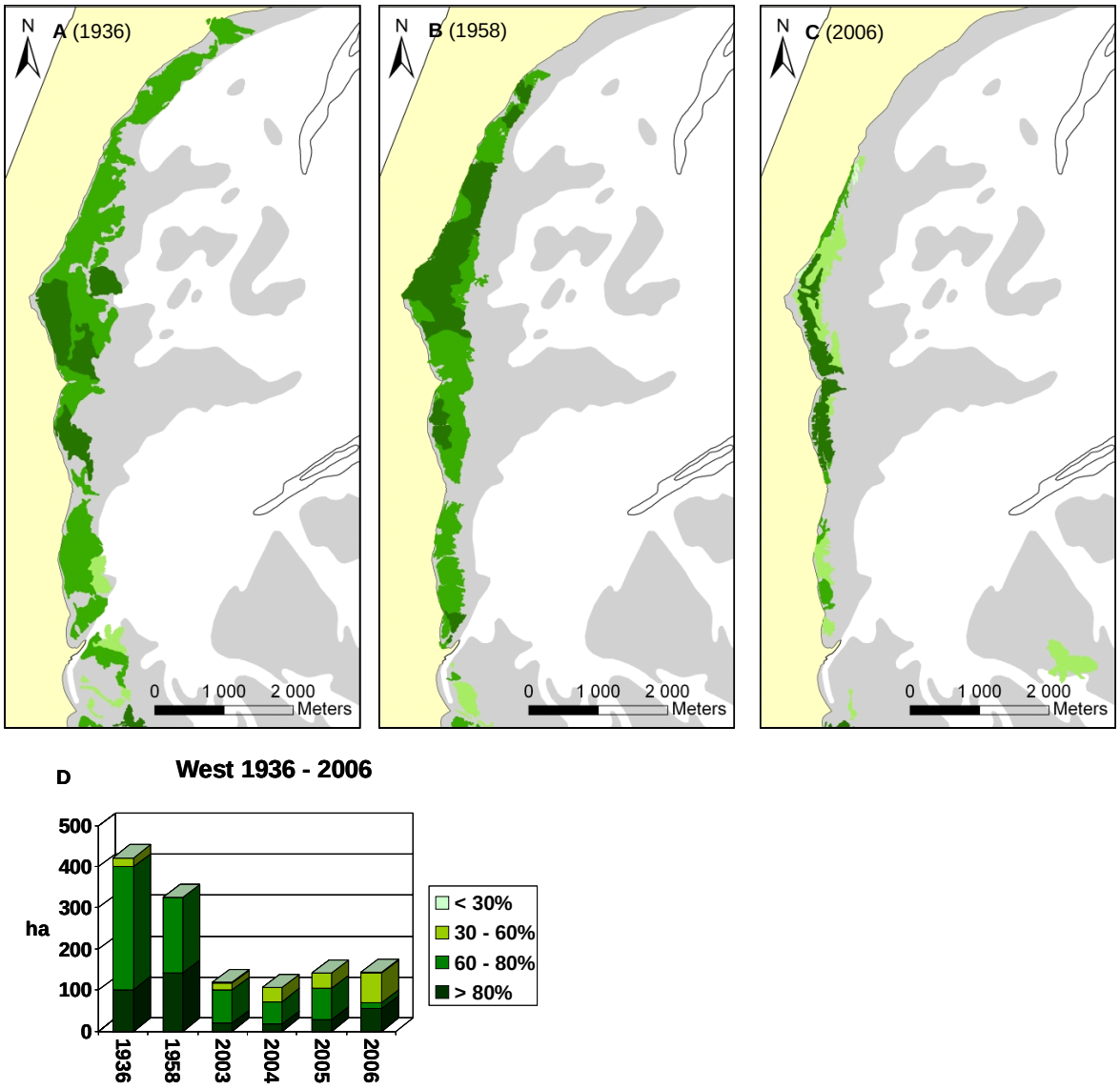


**Fig. 6.6:** The development of seagrass beds in the western part of the basin (overview of the study area is given in Fig. 6.3). The spatial distribution in 1936 (A), 1958 (B) and 2006 (C) is shown exemplary in the maps while the development from 1936 to 2006 can be seen in the graph (D).

**Southern part (1958 – 2006)**

In 1958, several larger seagrass beds are stretching from the island of Sylt along the causeway to the mainland (Fig. 6.7). They do not form a complete belt but a series of individual seagrass beds with unsteady shapes and widths varying from 200 to 1500 m. They are primarily dense and cover 1107.3 ha.

In 2003, a continuous dense seagrass bed can be observed in the western half of this subarea. It shows a width of 800 to 1200 m and is characterized by a dense cover. The seagrass stock in the eastern half consists of a few small and fragmentated beds. In total, the beds extend to 949.1 ha. Starting from the dense seagrass stock in the western half, the seagrass beds expand successively eastwards from 2003 to 2006. By 2006, a complete seagrass belt with a width of 600 to 1500 m stretches from Sylt to mainland and covers 1599.5 ha.

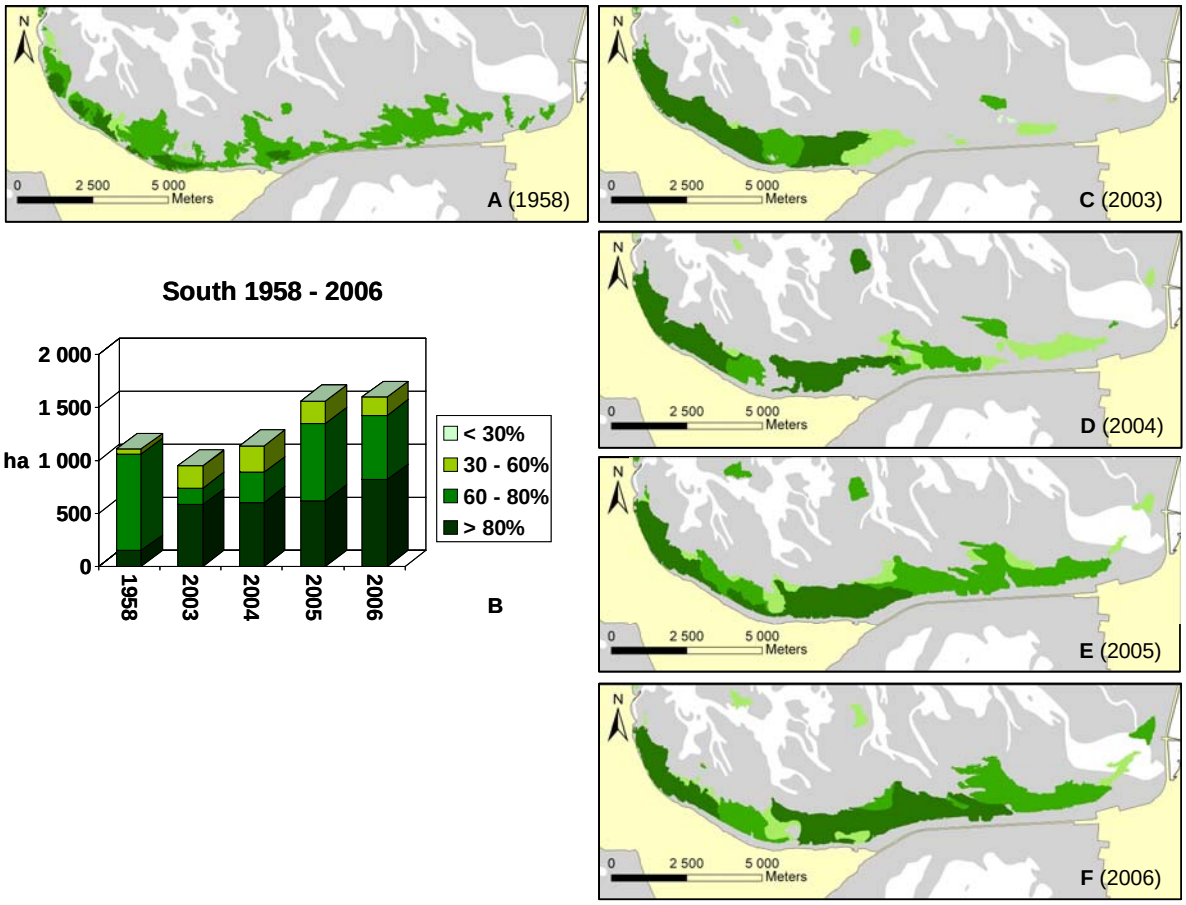


**Fig. 6.7:** The development of seagrass beds in the southern part of the List tidal basin (overview of the study area is given in Fig. 6.3). The spatial distribution in 1958 (A), 2003 (C), 2004 (D), 2005 (E) and 2006 (F) is shown in the maps while the development from 1958 to 2006 can be seen in the graph (B).

The expansion follows a certain pattern (Fig. 6.7 C to 6.7 F): a new gained seagrass area shows a sparse cover in its first year and densifies in the next 1 to 2 years. At the same time while it establishes, it further expands by accretion of another new and sparse seagrass area. Again this newly-accreted area densifies in the following year almost exactly within the boundaries of its first appearance. Through this, a successive eastward expansion happens. The pattern of expansion is inverse to the pattern of decline. Furthermore, the expansion, also like the decline, is not equally distributed. The growth of a seagrass bed starts from a denser part and is not spatially uniform but focuses on one major direction.

**Eastern part (1945 – 2006)**

Seagrass beds in the eastern part of the List tidal basin occur almost exclusively in the northern half of this subarea. Two major locations can be detected: on the tidal flat area Jordsands Flak and in the north of it at the mainland shore (Fig. 6.8).

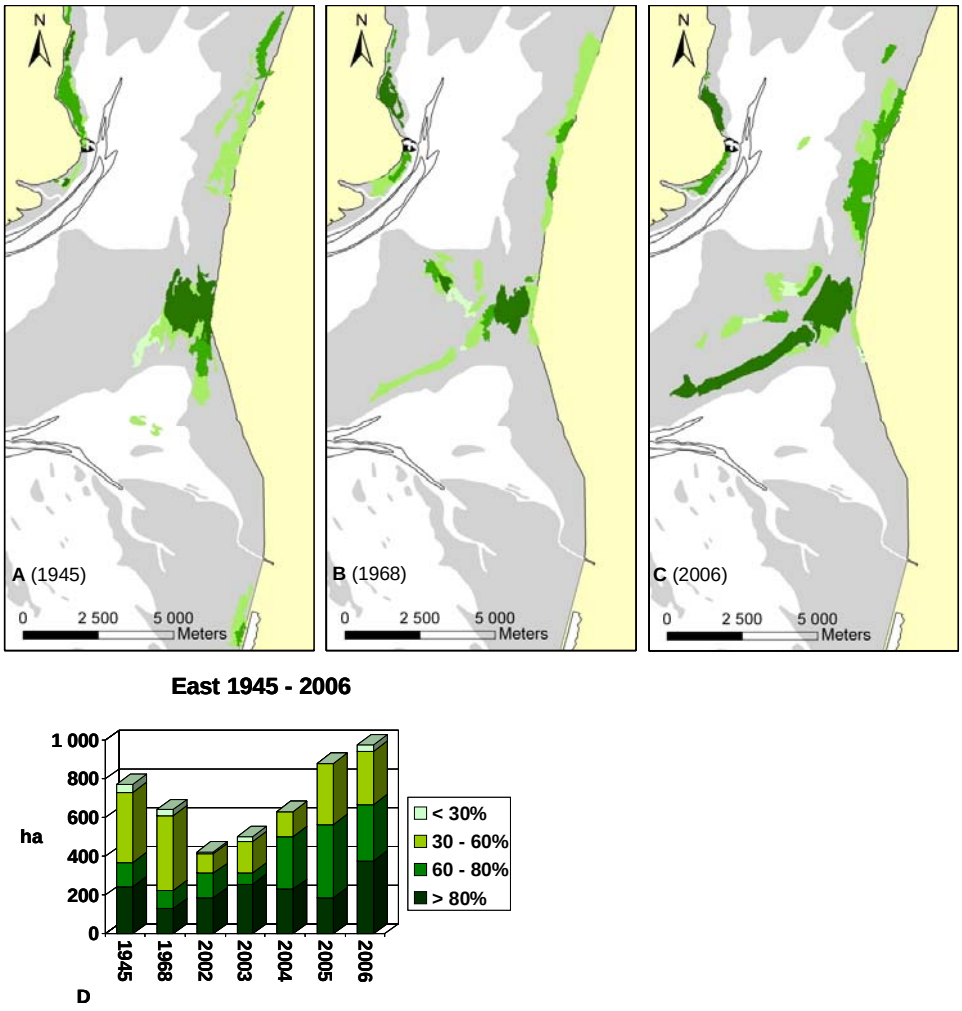


**Fig. 6.8:** The development of seagrass beds in the eastern part of the study area (overview of the study area is given in Fig. 6.3). The spatial distribution in 1945 (A), 1968 (B) and 2006 (C) is shown exemplary in the maps while the development from 1945 to 2006 can be seen in the graph (D).

In 1945, the seagrass beds occur mainly along the mainland shore. They cover an area of 772.2 ha and are characterised by an irregular shape and their width ranges from 300 to 700 m. In 1968, the seagrass beds are still located in vicinity to the shore but in addition a long stretch of seagrass established on Jordsands Flak protruding into the List tidal basin. The northern seagrass beds shifted southwards towards Jordsands Flak and their occurrence is less scattered as they form a rather complete belt. The minimum extent of the seagrass beds (424.4 ha) can be recorded for 2002 which is mainly because of the poor status of the northern seagrass beds which experienced severe degradation at their seaside. A period of growth and expansion followed from 2002 to 2006 (up to 975.2 ha) which is primarily caused by an increase of the existing northern beds as well as formation of new beds north of Jordsands Flak. The seagrass stock on Jordsands Flak hardly gained in area but strongly densified during this period.

**Northern part (1945 – 2006)**

The seagrass in the northern part of the List tidal basin occurs primarily at two locations, south of the Rømø causeway and east of the southern half of the island of Rømø in very close vicinity to its shoreline (Fig. 6.9).

The maximum spatial extent of the seagrass stock was 424.9 ha in 1945. In 1968, all seagrass beds have decreased in size amounting to a total 209.2 ha but a remarkably high percentage of a very dense cover can be observed (60 %). Their status in 2002 is characterised by a large spatial extent of 346.1 ha but also by a rather poor cover as 78 % are classified with a density of 30 to 60 %. From 2003 to 2006 a steady decline in the seagrass area from 358.1 to 128.8 ha is observed, primarily due to the decline of the seagrass bed at the Rømø causeway (Fig. 6.10). The typical pattern of decline, which has been already noticed in the western part of the bay, can also be observed here.

In general, the status of the northern seagrass beds is characterised by vanishing and degradation near the Rømø causeway while the beds near the island of Rømø are rather stable.

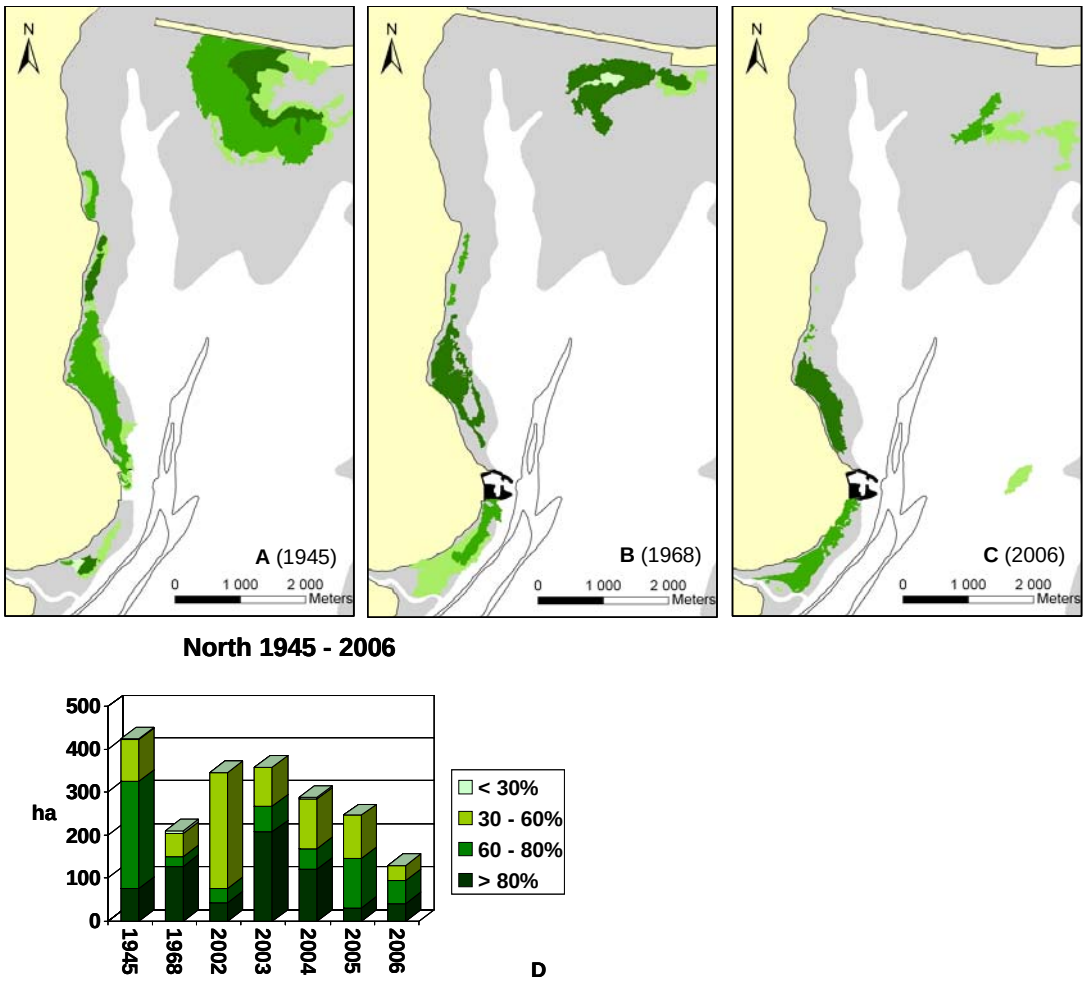


**Fig. 6.9:** The development of seagrass beds in the northern part of the basin (overview of the study area is given in Fig. 6.3). The spatial distribution in 1945 (A), 1968 (B) and 2006 (C) is shown exemplary in the maps while the development from 1945 to 2006 can be seen in the graph (D).

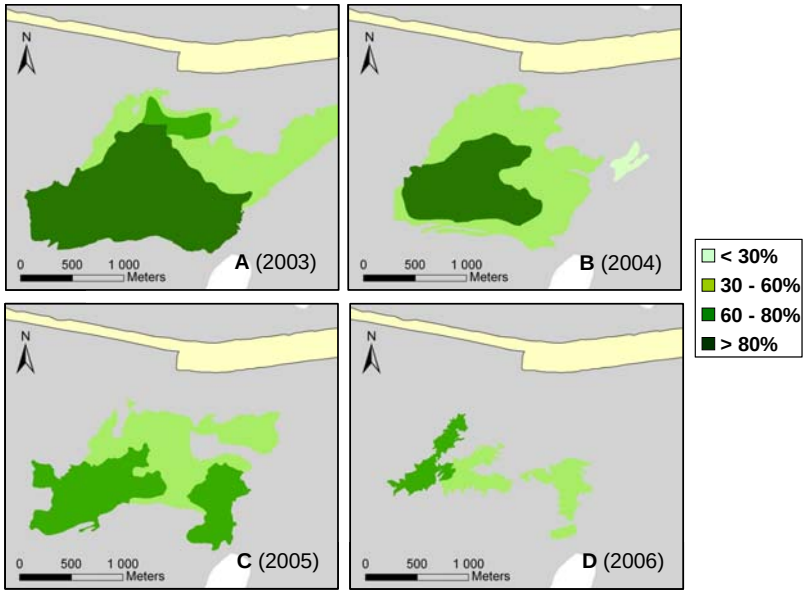


**Fig. 6.10:** The spatial development of seagrass bed at the Rømø causeway from 2003 (A) to 2006 (D). A pattern of successive decline can be observed.

### 6.3.3 Seasonal development of seagrass

Aerial photographs from May to August 1992 give exemplary insight in the seasonal growth of seagrass beds, while images from August to October 1990 show their seasonal decline. The analysis of this seasonal cycle was completed by the consideration of several other aerial photographs taken from 1989 to 1994.

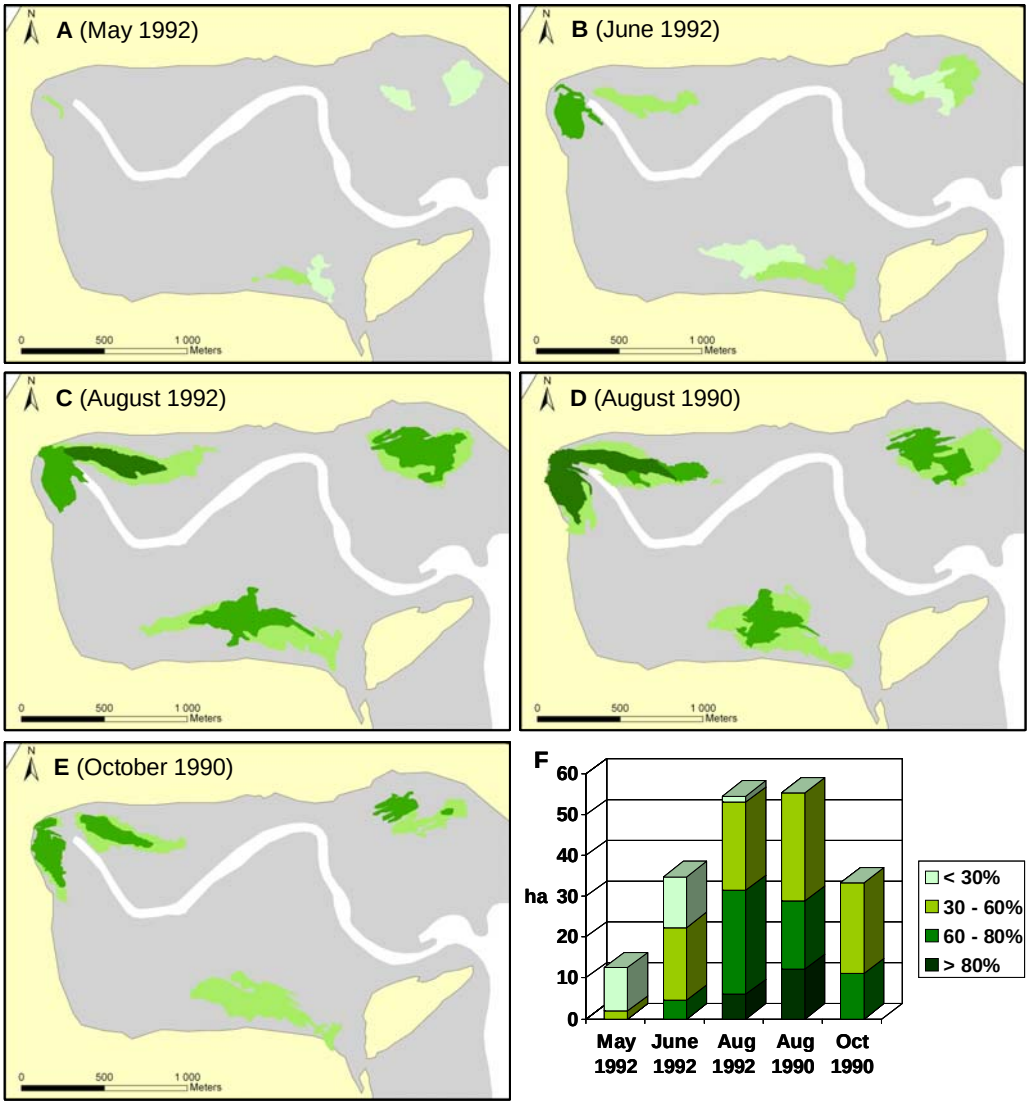


**Fig. 6.11:** The seasonal cycle of growth and decline of seagrass beds shown exemplary for 3 beds in the Königshafen. A – E show the spatial development while F gives surface area details.

Seagrass beds have their maximum extent and density in August (Reise and Kohlus 2008) and consequently this spatial extent is regarded as 100 % for the according year. Interestingly, the seasonal growth of seagrass beds follows the general pattern of expansion, which is described in chapter 6.3.2 (southern part). Seagrass can first be detected in the aerial photographs in May. They have formed 15 to 37 % of the maximum spatial extent then but their density of their cover is mainly < 30 % (Fig. 6.11). These areas

densify their cover until June while new areas with a sparse cover border them. In addition other new seagrass areas form in vicinity and until July they accrete to one bed. The maximum spatial extent of seagrass beds is almost attained in July while the densifying of cover is most pronounced from July to August. Interestingly, it could be observed in all surveyed seagrass beds that the areas that appeared first in May are not the densest in August. Other parts that germinate later can get a denser cover which indicates that densifying is not a continuous and constant process until the maximum is reached in August.

From August to October, the regarded seagrass beds lost 30 to 60 % of the extent in which the rate of decline can vary considerably for different parts of a seagrass bed. It was mainly observed that areas with a sparse cover vanished first which is according to the general pattern of decline. But it was also observed that some dense parts disappeared while more sparse parts remained.

## 6.4 Discussion

### 6.4.1 Long-term development of intertidal seagrass beds in the Wadden Sea

The decline of seagrass beds is a worldwide phenomenon. The reasons are multiple and for each area a different combination of factors is responsible. In general, increased human pressure in the form of eutrophication, siltation and mechanical disturbances, like dredging and bottom trawling, are regarded to be the main reasons (Short and Wyllie-Echeverria 1996, Hemminga and Duarte 2000, den Hartog and Phillips 2001, Green and Short 2003). Lotze et al. (2006) estimates that human impact destroyed > 65 % of the world's wetland and seagrass habitats.

The European Wadden Sea also experienced a strong decline in seagrass area. While the 'wasting disease' (1931 - 1934) eliminated seagrass from the subtidal (den Hartog 1987, de Jonge and de Jong 1992), intertidal *Zostera* bed were decreasing since the 1960s/1970s, at which the southern Wadden Sea was in particular affected. Starting in the Dutch Wadden Sea, this decline proceeded along the coast of Lower Saxony while the seagrass beds in the Northern Wadden Sea remained relatively stable except for some fluctuations (de Jonge et al. 1993, Kastler and Michaelis 1999, Reise 2006). In 1996, de Jonge et al. reported that less than 1 $km^2$ of the Dutch Wadden is covered with seagrass. Even though the cause for decline is still not clear for some Wadden Sea areas, it is assumed that anthropogenic eutrophication is the primary reason, but light limitation, changed hydrodynamic conditions, physical disturbance by shellfish fishery and even bioturbation are also

assumed (de Jonge and de Jong 1992, Philippart et al. 1992, Philippart 1994, Duarte 1995, van Katwijk et al. 1999, Schanz and Asmus 2003). Coastal eutrophication is primarily caused by the input of riverine nutrient loadings. This explains the severe decline of seagrass beds especially in the southern Wadden Sea as the rivers Ems, Weser and Elbe are discharging into it. Therefore, a north-south gradient is expected for the northern Wadden Sea, at which more healthy seagrass beds are estimated in the north as this area is more remote from the Elbe estuary. This spatial pattern is confirmed by aerial surveys conducted from 1994 to 2006 (Reise and Kohlus 2008).

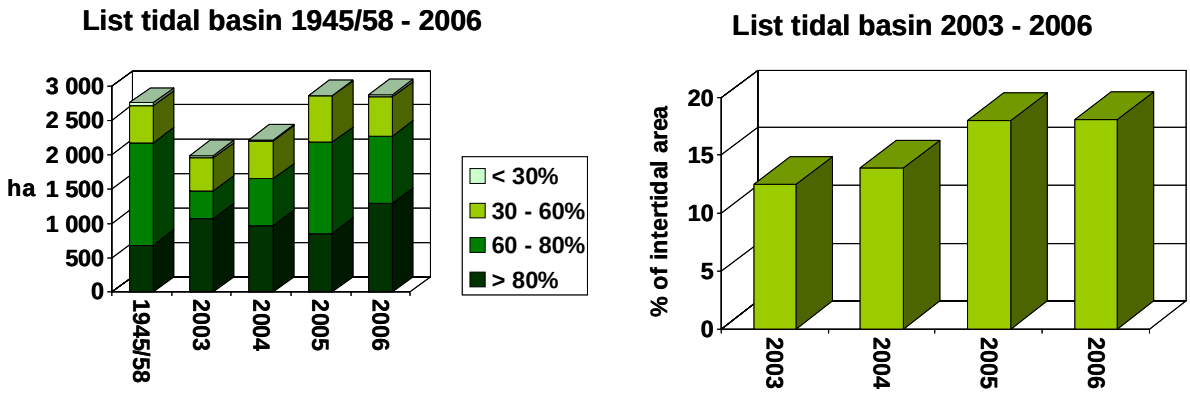


**Fig. 6.12:** The development of seagrass beds in the List tidal basin from 2003 to 2006 compared to the situation in 1945/58 (left) and the development of the seagrass bed area (2003 to 2006) expressed as percentage of the intertidal area (right).

However, the seagrass beds in the southern Wadden Sea are slightly and slowly recovering since the 1990s (Reise et al. 2005b). The beds in northern Wadden Sea even show a 3 to 4-fold increase in area from 1994 to 2006. Especially in the last 6 years a notable gain can be recorded (Reise and Kohlus 2008). Observations made in the List tidal basin for this study confirm this trend. The bed area in the bay increased from 1987.5 ha in 2003 to 2875.6 ha in 2006 which is a plus of 145 %. The comparison of the 2006 seagrass status with the one from 1945/58 (2754.8 ha), which was before the general decline that started in the 1960s/1970s, shows that today the bed area in the List tidal basin even exceeds the former extent (Fig. 6.12, left). Furthermore, the proportion of the highest density (> 80 %) increased from 25 to 45 %. Seagrass beds in the List tidal basin covered on average 16.7 % of the intertidal area from 2003 to 2006, while their development showed a steady increase from 12.5 % in 2003 to 18.1 % in 2006 (Fig. 6.12, right). Reise and Kohlus (2008) suggest that this general positive trend in the European Wadden Sea is mainly because of a decrease in storm surge levels since the mid 1990s (Weisse et al. 2005, Weisse and Plüß

2006) and the decline of human pressure: riverine nutrient loads have been decreasing for the last 20 years (van Beusekom et al. 2005) and mechanical disturbances have been reduced since large areas are closed for cockle dredging (Dankers et al. 1999).

### 6.4.2 Short-term dynamics of intertidal seagrass beds

Besides the long-term developmental trends, seagrass also shows considerable dynamics on smaller time scales.

The annual aerial survey in the Northfrisian Wadden Sea (1994 – 2006) reveals that only 12 % of the total seagrass area consisted of permanent beds while further 12 % showed seagrass beds for more than 8 years during this 13-year survey. 76 % of the total seagrass area are rather dynamic (Reise and Kohlus 2008). Frederiksen et al. (2004a, 2004b) also report highly variable seagrass beds from the Danish Wadden Sea as a considerable decline with reductions of about 60 % within 6 years, but also a recovery at a similar time scale, were observed.

Dynamic seagrass can also be observed in the List tidal basin, especially when regarding individual beds. For example the seagrass bed in the southern part of the bay increased within just 4 years (2003-2006) from 950 ha to 1600 ha, which is a plus of 169 % (Fig. 6.7). In the same period, the seagrass bed in the northern part near the causeway decreased by 81 %, from 260 ha to 49 ha (Fig. 6.10). These two examples also show that seagrass beds within the same area can develop in opposite direction and that seagrass responds rather quickly to changing conditions. In the List tidal basin seagrass beds in the Königshafen, western and northern part are declining while the habitats in the southern and eastern part show a considerable increase which compensates the losses.

Besides high spatial and temporal variability, seagrass is also characterised by a seasonal cycle (Fig. 6.11). It sprouts in May and June. Even though the cover is sparse, the maximum spatial extent of a bed is almost achieved by late June, while densifying primarily happens from July to August. The young seagrass plants are especially vulnerable and sensitive to sediment instability. It is likely that a severe storm during that phase can have a long-lasting effect on the appearance and extent of seagrass. If certain tidal flat areas with sprouting seagrass are particularly affected by a storm, this could be an explanation for different development of beds within the same region and also the high variability of seagrass occurrence. Further research is required to test this hypothesis.

### 6.4.3 Spatial pattern of intertidal seagrass beds

In the Northfrisian Wadden Sea and the List tidal basin spatial patterns in the occurrence of seagrass beds are observed, which can be regarded to have general validity for intertidal *Zostera*.

Seagrass occurs only at sheltered sites because it is directly sensitive to strong hydrodynamics (de Jonge et al. 1996, Fonseca and Bell 1998, Schanz and Asmus 2003) as well as to sediment instability which often results from it (Philippart et al. 1992, van Katwijk et al. 2000). Both, burial and erosion have strong negative effects on seagrass (Mills and Fonseca 2003, Cabaço and Santos 2007) and Philippart et al. (1992) found that *Zostera marina* and *Zostera noltii* are equally sensitive to sediment dynamics. Seagrass is so sensitive that it can not even handle sediment dynamics on a small scale, in form of bioturbation (Townsend and Fonseca 1998). For that reason, the sediment-reworking lugworm *Arenicola marina* and seagrass are spatially seperated (Philippart 1994, own obs.).

Anyway, while eutrophication seems to be the key factor for the spatial pattern of seagrass in the southern Wadden Sea (van Katwijk et al. 1997, 1999), Reise and Kohlus (2008) hypothesize that it is sediment stability for the Northfrisian Wadden Sea. Seagrass avoids strong hydrodynamics in the form of currents or wind-induced waves, for it does neither appear in the fetch of the prevailing south-westerly wind nor on exposed and lower tidal flats. This pattern can also be found in the List tidal basin. Seagrass is strongly focussed on the upper intertidal at the sheltered leeside of the islands and along the two causeways remote from the tidal channels. It is remarkable how closely the beds are approaching the shoreline. Compared to the spacious tidal flats, south of the island of Sylt, the tidal flat area in the compact List tidal basin is rather limited which explains why the occurrence of seagrass is ‘squeezed’ to the margins of the bay. Jordsands Flak is the only area where seagrass beds are protruding into the centre of the basin. But it can be assumed that seagrass habitats could only establish here because of its sheltering elevation. The areas on Jordsands Flak, where seagrass occurs (Fig. 6.3), show an elevation of mainly +0.3 m to +0.5 m while adjacent areas with no seagrass have an elevation of ≤ -0.1 m. In general in the List tidal basin, no or very few seagrass beds appear in the vicinity of tidal channels on low-lying tidal flats as well as along the mainland shore in the south-eastern part of the basin. In the latter area considerable land claim measures were carried out (Jespersen and Rasmussen 1989), which cause sediment accretion rates that are too high for seagrass to handle the burial (Reise and Kohlus 2008). The absence or lack of seagrass in close

vicinity to dikes along the mainland shore is not only observed in the Northfrisian but also in the Dutch Wadden Sea (Philippart and Dijkema 1995).

### 6.4.4 Long-term spatial development of seagrass beds in the List tidal basin

Regarding the long-term spatial development of seagrass beds it can be observed that they are shifting away from tidal channels or vanish in their vicinity and concentrate close to shores or watersheds such as the Jordsands Flak and the two causeways between the islands and the mainland.

Especially in the Königshafen and the western part of the List tidal basin seagrass beds are shifting entirely away from tidal channels and towards the shore and/or beds are declining at their seaside part. Furthermore, general degradation of seagrass beds which are in close proximity to a tidal channel are also observed, especially when there is no alternative space to shift to. This can be explained by the seagrass sensitivity to strong hydrodynamics (de Jonge et al. 1996, Fonseca and Bell 1998, Schanz and Asmus 2003) and sediment instability (Philippart et al. 1992, van Katwijk et al. 2000). Data records from the gauge List from 1936 to 2007 reveal a considerable increase of the high tide water level as well as of the tidal range (see Chapter 2.2) which increases current velocities. The increasing current flow occurs primarily in the tidal channels. This may be why seagrass avoids their vicinity.

On the other hand, increasing seagrass beds can be found in the southern and eastern part of the basin, where the main tidal channels are remote. It is suggested that seagrass could increase in these sheltered sites during the last years, because it is unaffected by the increasing current flow and benefits from the decrease in storm surge levels since the mid 1990s (Weisse et al. 2005, Weisse and Plüß 2006).

In some areas, seagrass beds show a cycle of appearance, vanishing and reappearance. After degradation or complete vanishing of a seagrass bed, it recovers and reappears almost exactly in the same area. This could be observed, e.g. for the seagrass bed in the southern part which was present along the entire causeway in 1958, had vanished in large parts in 2003 and reappeared along the entire causeway by 2006 (Fig. 6.7). The same applies to the seagrass bed in the north-eastern part on Jordsands Flak, where they were absent in 1945, present in 1968, again absent in 2002 and reappeared until 2006. These fluctuations also indicate the dynamics of seagrass. Causes for fluctuations can be internal, like for example the old age of the rhizome or a lack of seeds, while seagrass also responds

rather quickly to external conditions like recurrent infections or changed environmental conditions (Robbins 1997, Hemminga and Duarte 2000, Green and Short 2003).

## 6.5 Summary and conclusions

After decades of severe decline of seagrass habitats in the European Wadden Sea, a recovery and increase can be observed since the 1990s. This can be primarily traced back to the decline of human pressure, mainly in the form of decreasing riverine nutrient loadings. Furthermore, it can be assumed that the decrease in storm surge levels since the mid 1990s has also a positive effect on a regional scale. However, seagrass beds in the List tidal basin do not change in synchrony. From 2003 to 2006 seagrass beds in the west and north decreased in area while those in the south and central part increased. It is hypothesized that differential effects of storms during sprouting season may account for such opposite developments. Losses and gains compensated each other in this period. Compared to the 1940s/1950s, the areal extent of seagrass beds in 2005-2006 is very similar. The same applies to the spatial pattern. Beds may vanish but reoccur at the same site some years later.

On the other hand, it is also observed that seagrass habitats in vicinity to tidal channels are degrading at that side which faces the channel or the beds are shifting entirely away from them. This indicates increased hydrodynamics, which are caused by increasing tidal range and a reduction of the catchment area. It can be assumed that for the future increasing hydrodynamics and associated sediment instability will be an increasing problem for seagrass habitats.

Seagrass requires good ecological conditions, is sensitive to a variety of factors and responds rather quickly to changing environmental conditions. It is neither possible to name an exclusive factor for recent developmental trends nor to make a prediction regarding the future development. Therefore, regular monitoring will be essential. In this regard, the analysis of high-resolution aerial photographs with GIS proofed to be an accurate method for the assessment of the quantitative and qualitative status of seagrass beds. This method is especially suitable to survey larger areas, which are not easy to access.

# 7 Remote sensing analysis of development, dynamics and spatial pattern of intertidal mussel beds

## 7.1 Introduction

Blue mussels (*Mytilus edulis*) are sessile suspension feeding bivalves that live in estuaries and coastal environments (Widdows et al. 2002), where they occur from the mid intertidal to the subtidal. In the intertidal, mussels occur predominantly in the lower intertidal as tidal submergence, which also means availability of food, is considered to be one of the most important factors for growth (Reise and Lackschewitz 1998, Buschbaum and Saier 2001, Saier 2001).

Mussels form beds with densities of up to 4000 individuals per $m^2$ (Buschbaum and Nehls 2003) (Fig. 7.1). The individuals bind themselves to other mussels, associated flora and fauna or hard substrate using byssal attachment (Ruth 1998), resisting storms, currents and waves (Buschbaum and Saier 2003). These beds are of high ecological importance as they are hotspots of biodiversity and productivity. They provide habitat for various species that seek shelter, organic enriched sediment or simply permanent water pools at low tide or hard substrate. Furthermore, mussel beds are an important food source e.g. for crabs, birds, seastars and man (Riesen and Reise 1982, Asmus 1987, Dittmann 1990, Nehls et al. 1998, Buschbaum and Saier 2003).

**Fig. 7.1:** Mussel bed in the Königshafen in July 2004. The picture shows that the mussels are heavily overgrown with oysters.

Mussels feed on phytoplankton, bacteria and detritus by filtration and at this they also take up a considerable amount of suspended sediments (Dame and Dankers 1988). They are important for the transport of material and energy from the pelagic to the benthic system and furthermore for the control of phytoplankton biomass (Dolmer and Frandsen 2002). In other words, they also clear the water and it is assumed that a single mussel can filter up to 15 litres per day on average (Buschbaum and Saier 2003, Buschbaum and Nehls 2003). Accordingly, Dankers and Koelemaij (1989) estimate, that the entire volume of the Wadden Sea could be filtered by its existing *Mytilus edulis* population within a period of 8 to 9 days. Among the clearance of water, another important function of mussels is their ability to increase sedimentation of suspended matter. The particles, which are filtered out of the water column, are agglutinated in faeces and pseudofaeces, which get deposit in and around mussel beds. A lot of fine-grained material is trapped in these faecal pellets, which have a higher settling velocity than the individual particles. This enhances sedimentation. Through this input of organic mud, mussel beds provably affect the sediment composition (Kröncke 1994) and Reise et al. (1994) further state that a bay's trapping efficiency of fine-grained material is connected to benthic filter feeders.

The recruitment of blue mussels happens by the settlement of juvenile on established mussel beds. As recruitment is more successful after severe winter, the annual mussel stock (numerical abundances and biomass) is characterized by substantial year-to-year variability in the Wadden Sea (Strasser et al. 2001a, 2003, Beukema et al. 2001).

During severe winters existing mussel beds can also be heavily damaged by scouring ice floes (Obert and Michaelis 1991, Strasser et al. 2001b) and severe winter storms (Nehls et al. 2002). For example, the number of mussel beds in the Schleswig Holstein Wadden Sea decreased by half due to severe winter storms from 1989 to 1990. Especially mussel beds in the exposed Wadden Sea were predominantly affected and can be regarded as highly dynamic in their occurrence. Remaining mussel beds after this storm period were only found in sheltered areas and are characterised by persistency over decades (Reise et al. 1989, Nehls and Thiel 1993).

Mussel fishery has also a significant effect on mussel beds. Intertidal mussel beds almost disappeared from the Wadden Sea in the 1980s due to fishery combined with a period of low spatfall. The impact of fishery became obvious in the 1990s when mussel beds were increasing and recovering in Denmark and in Schleswig-Holstein after the closing of large

areas for fishery. Mussel beds in Lower Saxony beds were still under fishery pressure and further declined dramatically (Dankers et al. 1999).

However, even today a strong decrease in blue mussel bed area can be observed in most places of the Wadden Sea. For example in the German part of the List tidal basin the area covered with blue mussels decreased from 140.5 ha in 1998 to 45.0 ha in 2005 (Nehls and Büttger 2006). This is related to the long period of mild winters since 1995/96 which has led to a low recruitment of blue mussels (Nehls et al. 2006).

Until the end of the 19$^{th}$ century, extensive subtidal beds of the European oyster *Ostrea edulis* were also present in the Wadden Sea. The constant and high fishery pressure resulted in a dramatic decline in the native oyster population, which became extinct in the northern Wadden Sea (Hagmeier and Kändler 1927, Reise 1982). In 1986, the Pacific oyster *Crassostrea gigas* was introduced to the Northern Wadden Sea for aquaculture (Diederich 2006). Blue mussel beds and oyster reefs are the only major secondary hard substrate in the Wadden Sea and, therefore, they do not only serve as a settlement surface for juvenile blue mussels but also for other sessile organisms. The first oyster that dispersed as a larva and settled on a blue mussel bed was discovered in 1991, 5 years after oyster farming has commenced. Today, mussel beds are undergoing a dramatic change as they are heavily colonized by the Pacific oyster *Crassostrea gigas*. Until 2003 a large population of several millions oysters with abundances of more than 300 oysters $m^{-2}$ became established on blue mussel beds (Diederich et al. 2005). This massive increase of oyster abundance was enabled by three consecutive warm summers because warm summers promote oyster recruitment while warm winters hamper successful recruitment of blue mussels (Strasser et al. 2001a, Diederich et al. 2005). Today, even numbers of 1800 oysters $m^{-2}$ can be found (Reise 2008, unpublished data).

By now the survey of the occurring change in the mussel beds species composition became a major aspect in the blue mussel monitoring, which was originally created due to the multiple ecological importance of mussel beds for the Wadden Sea ecosystem. Mussel monitoring is admitted to the Trilateral Monitoring and Assessment Program (TMAP) and conducted by a composition of remote sensing of aerial photographs and field survey (Nehls and Ruth 2004).

This study also deals with a remote sensing monitoring approach of mussel beds. A series of aerial photographs, which dates back to 1936, was analysed with a Geographic Information System (GIS). This remote sensing method is also used in other studies that

deal with mussel bed monitoring, e.g. Michaelis et al. 1995, Millat and Herlyn 1999, Nehls et al. 2002, Stoddard 2003, Herlyn 2005.

In this study the focus is laid on

- the quantitative and qualitative long-term development of mussel beds,
- their general spatial pattern.

The survey area is the List tidal basin in the northern Wadden Sea. Tidal basins are the most suitable units for monitoring and research and furthermore, this basin has well-defined borders as well as a long and continuous history of research (Reise and Gätje 1997).

## 7.2 Materials and methods

The data on surface areas of mussel beds to calculate their spatial development were exclusively gained from georeferenced aerial photographs by on-screen digitising using the ESRI software ArcGIS 9.1, ArcMap. This remote sensing data was also completed by GPS field measurements and historical data. Surveys by Nienburg (1927) on the occurrence of blue mussel beds in the Königshafen were considered in respect of their position and distribution but not for spatial analysis as the mapping accuracy is not reliable. For further details on aerial photographs, georeferencing and digitising see Chapter 3.2.

### 7.2.1 Detection, definition and classification of mussel beds

In the text below, when ‘mussel beds’ are mentioned one has to be aware that since the beginning of the 21$^{st}$ century these beds are not exclusively formed by the blue mussel *Mytilus edulis* but also by the spreading Pacific oyster *Crassostrea gigas*. Actually, the beds are today mixed beds but in order to maintain a uniform terminology in this long-term study, the term ‘mussel beds’ is retained.

Mussel beds were detected in the aerial photographs by a combination of attributes: in general, they have a darker colour than their surrounding sediments. But colour by itself is not always a safe indicator, especially not when the contrast is missing, e.g. when mussel beds are located on dark muddy sediments or the quality of aerial photographs is limited. Mussel beds are further characterised by their rough, uneven and cleft surface. The structured surface and their mainly distinct elevation help to distinguish them from their flat and level surrounding.

The determination of the borderline of mussel beds was carried out according to the 25 m-rule. This means that mussel occurrences, which are within a distance of 25 m to each

other, were combined within one border including the gaps between them (Nehls and Büttger 2006). Large gaps were only excluded when their size exceeded the actual size of the mussel beds. Extensive fields of small scattered mussel clusters in close vicinity to mussel beds were observed in field surveys. However, as they are no mussel beds in the narrow sense and bias the results towards an overstatement of the spatial coverage, they were not considered for the analysis. The ratio of mussel shells to living mussels can not be evaluated by visual analysis of aerial photographs. Furthermore, the species composition of a mussel bed can also not be discovered by this method. Oysters settle on established mussel beds, where they grow over and between blue mussels. Therefore, the currently ongoing transformation in the List tidal basin from mussel beds into oyster reefs could not be examined.

Ground truthing in order to validate the digitised features as well as to estimate the degree of coverage of mussel beds was conducted in extensive field surveys with the differential GPS (DGPS) device 'Trimble GeoXT handheld' from July to August in 2004, 2005 and 2006. As this DGPS receiver is combined with a handheld computer, multiple attributes could be immediately added in the field to the sampled spatial data. The attributes, e.g. date, time, species composition, coverage density etc., were determined in the run-up to the sampling campaign. An attribute table was created on a PC using the software GPS Pathfinder Office 2.90 and transferred to the GPS receiver. In the field, the list of attributes was implemented and the respective value to each attribute allocated. This ground truthing provided guidelines for the classification of mussel bed densities and was beneficial for the later evaluation of densities which were detected in the aerial photographs. The created GPS files were exported into GIS shape-files and loaded into GIS, where a direct comparison of field data with remote sensing data was conducted.

Field survey data from 1998 to 2004 was provided by BioConsult SH in the form of GPS track files and taken for validation of remote sensing data from older aerial photographs. This data was sampled in the framework of the Trilateral Monitoring and Assessment Program (TMAP). The Regional Office of the Schleswig-Holstein Wadden Sea National Park (NPA) in Tönning also supplied GIS shape files on the occurrence of mussel beds in the North-Frisian Wadden Sea (1996 to 2001) for validation.

The digitised mussel beds were classified according to their density. As mussel beds are small and rather homogenous compared to seagrass beds (see Chapter 6.2.1) they were

classified as a whole. The degree of coverage was estimated from the aerial photographs and classified as dense (> 60 %), medium (30 – 60 %) or sparse (< 30 %) (Fig. 7.2).

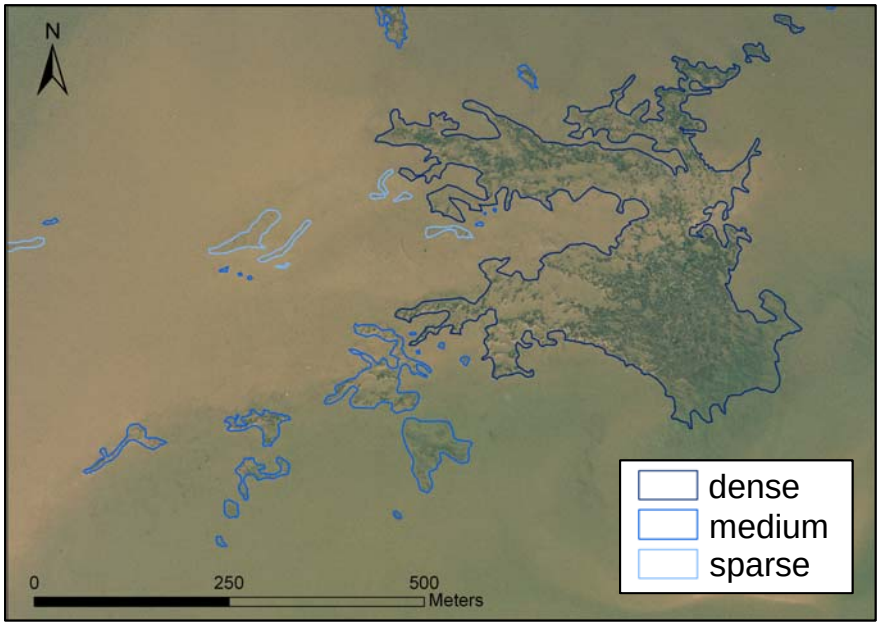


**Fig. 7.2:** An aerial photograph of mussel beds in the Blidselbucht in October 2003. The picture shows the borders of the beds and the classified different cover densities assessed by remote sensing.

### 7.2.2 Development of mussel beds in the List tidal basin and its subareas

The areas of the mussel beds were calculated with the GIS software ArcGIS 9.1, ArcMap. For the entire List tidal basin the development of the quantity (number and size) and quality (degree of cover) of mussel beds could be recorded for the period 1999/2001 to 2006. Before 1999/2001, aerial photographs cover the basin not area-wide but only in part. In order to also include these early taken photographs into the analysis and for a more detailed view, the List tidal basin was divided into 5 subareas (Königshafen, west, south, east and north, Fig. 7.3). These 5 subareas were analysed individually due to the temporal heterogeneity of the data base (aerial photographs). The longest time series dates back to 1936.

In GIS, the mussel bed data was also integrated in the Digital Elevation Model (DEM) and in the results of the ‘Model on 2D current velocities and water depths‘ (Behrens et al. 1997, see Chapter 3.2.5 for further information on the DEM and the model data). The needed information for the blue mussel habitat requirements were extracted out of the models.

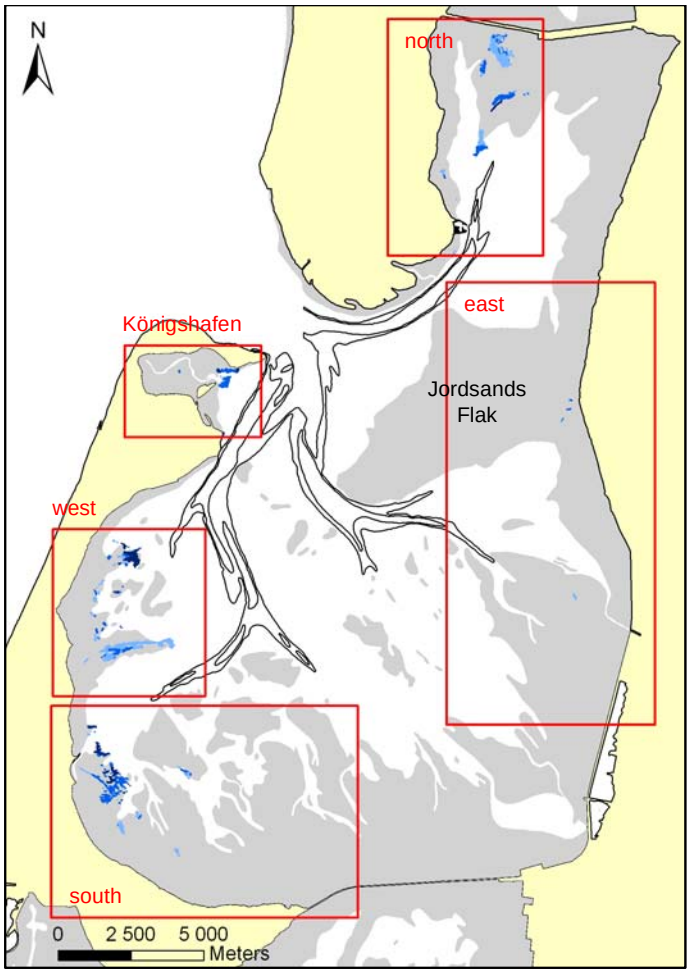


**Fig. 7.3:** The List tidal basin subdivided into 5 areas. The spatial distribution of the mussel beds in 2003 and the tidal flat area 'Jordsands Flak', which protrudes into the basin, can be seen in the picture.

## 7.3 Results

### 7.3.1 General location of mussel beds in the List tidal basin

The mussel beds in the List tidal basin can be found almost exclusively on the tidal flats in the shelter of the islands Sylt and Rømø, where they are confined close to their eastern shorelines (Fig. 7.3). Their occurrence is especially focussed on the south-western quarter of the List tidal basin, as 68 % of the mussel beds are located there. The tidal flats east of Sylt can be regarded as a mussel hotspot for the bay. Mussel beds are absent from exposed tidal flats and can hardly be found in vicinity to the mainland. This spatial pattern was observed in all aerial photographs from 1936 to 2006.

Mussel beds are primarily located between island shorelines and the tidal channels which run close to them. Here, they occur at the lower low tide level. The mean depth of the mussel beds in the List tidal basin is -0.9 m with a depth ranging from -0.3 to -1.5 m.

Most mussel beds at the eastern shore of Rømø have their landward edge within a distance of 250 to 500 m to the shoreline. There are only two larger mussel beds in vicinity to the delta of the tidal channel (Rømø Dyb), which are 1500 m away. East of Sylt the landward edge of the mussel beds is in general within a distance of 1000 m to the shoreline, except for the mussel beds which are located in the tidal basin Königshafen.

### 7.3.2 Development of intertidal mussel beds in the List tidal basin

For the period 1999/2001 to 2006, the development of the size and status of the intertidal mussel beds can be recorded not just for the subareas but also for the entire List tidal basin. Their spatial distribution is as described above. Mussel beds in the List tidal basin are characterised by a rather stable position. Even though they vary in their extent, most mussel beds show persistence and can be surveyed in the same location from 1936 to 2006.

The average mussel bed area from 1999/2001 to 2006, derived from the aerial photographs, amounts to 111.6 ± 12.7 ha (Fig. 7.4). Thereof, 16 % are dense mussel beds while, 37 % show a medium density and 47 % are sparse. Subdividing the average mussel bed area into the 5 subareas, 8 % are allotted to the Königshafen, 39 % to the west, 21 % to the south, 1 % to the east and 31 % to the north of the List tidal basin. As some mussel beds are persistent while others vanish, it is suggested not to observe the development of individual beds but rather to consider all beds in a defined area.

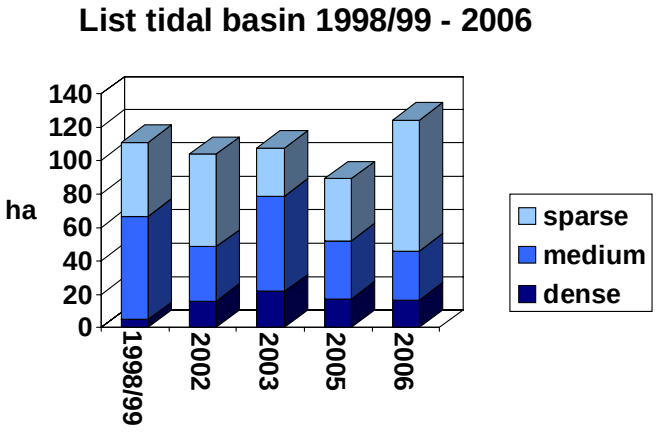


**Fig. 7.4:** The development of mussel beds in the List tidal basin from 1998/99 to 2006.

#### Königshafen (1927 – 2006)

In the Königshafen, the existence of mussel beds can be traced back until 1927. The data on mussel beds in 1927 are derived from a map and cannot be used for spatial calculations but it can be seen that they already occurred at present locations. The mussel beds are

found primarily in the outer Königshafen close to the subtidal. When they occur in the inner Königshafen, they are mainly closely located to the central tidal creek.

In 1936, their extent and status was rather poor (2.99 ha) but increased to a maximum appearance in 1993 (24.1 ha) (Fig. 7.5). A decline in the mussel bed area can be observed after 1994. This is primarily caused by the vanishing of two larger mussel beds, which could be both recorded over a period of 2 decades before. The bed in the centre of the Königshafen and the one in the outer Königshafen gradually declined and totally disappeared by 2001. Nevertheless, both beds started to reform in 2005 and 2006 as oyster beds.

In general, the observed mussel beds in the Königshafen are persistent in their position. Four locations could be determined where mussel beds were observed for decades or even for the entire survey period (1927 – 2006): one is located in the central Königshafen in close vicinity to the tidal creek while the other three can be found at the opening of the Königshafen, close to the subtidal. The mussel beds show primarily a medium coverage.

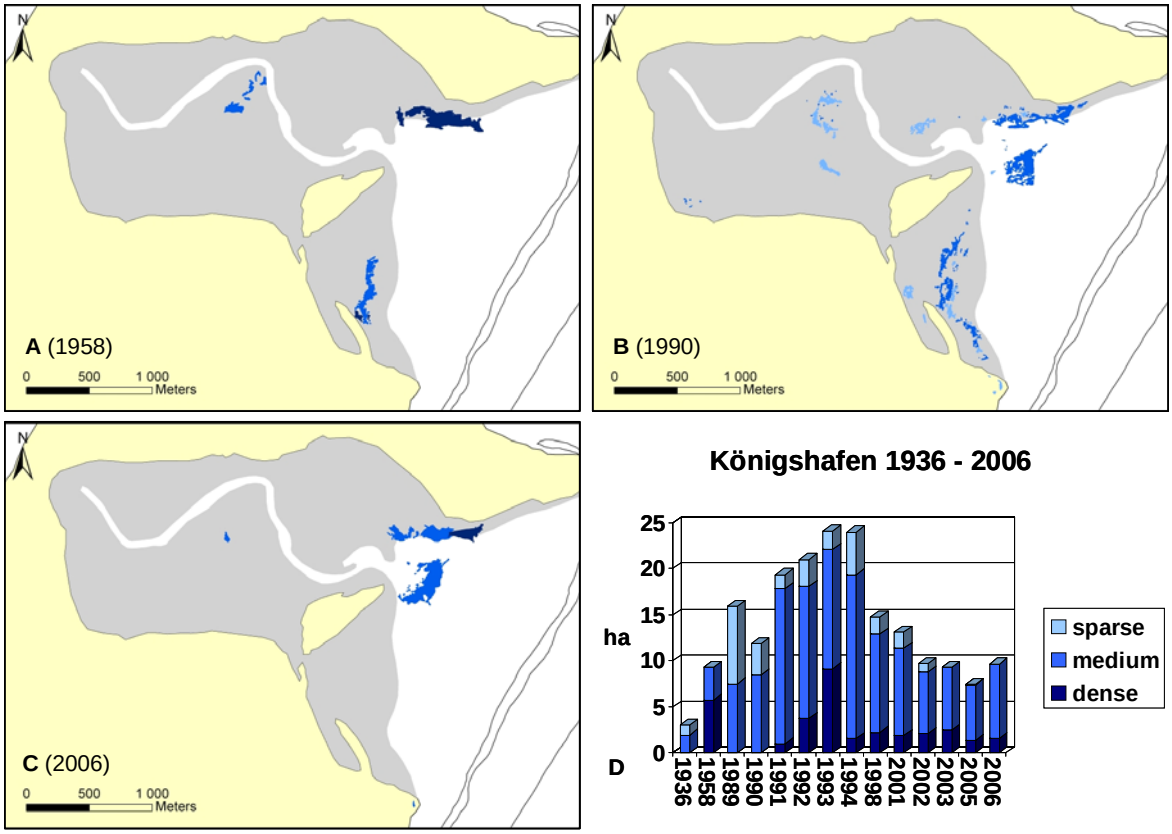


**Fig. 7.5:** The development of mussel beds in the Königshafen (overview of the study area is given in Fig. 7.3). The spatial distribution in 1958 (A), 1990 (B) and 2006 (C) is shown exemplary in the maps while the development from 1936 to 2006 can be seen in the graph (D).

**Western part (1936 – 2006)**

There are two main mussel beds in this subarea: a rather circular-shaped mussel bed in the north (Blidselbucht) and a long-stretched, band-shaped bed (Leghörn) in the south (Fig. 7.6). They are characterised by their persistence while the occurrence of smaller and scattered beds, which are mainly located between them, is more variable.

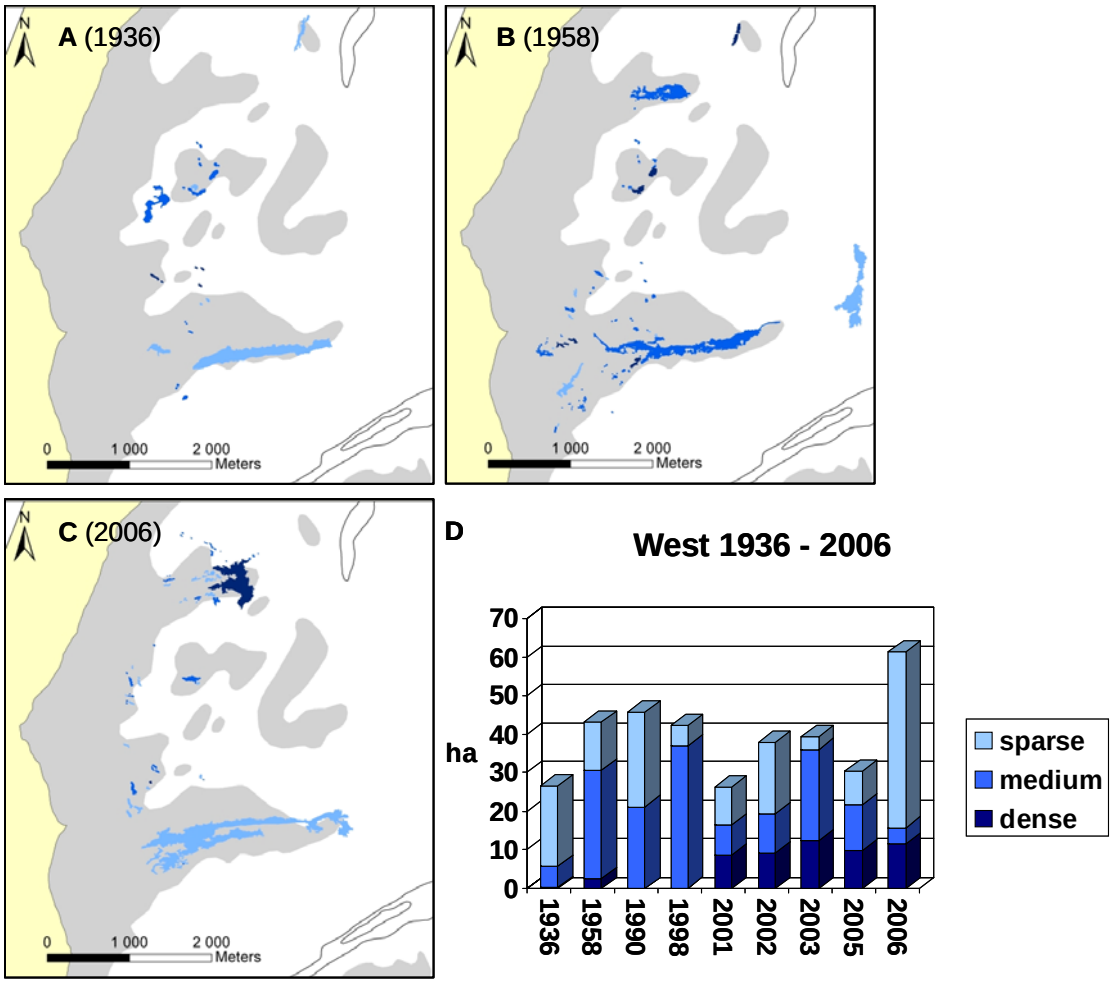


**Fig. 7.6:** The development of mussel beds in the western part of the basin (overview of the study area is given in Fig. 7.3). The spatial distribution in 1936 (A), 1958 (B) and 2006 (C) is shown exemplary in the maps while the development from 1936 to 2006 can be seen in the graph (D).

In 1936, there are only few mussel beds in the western part of the List tidal basin. Even though they cover an area of 26.8 ha they are characterised by a sparse coverage. In 1958, the mussel beds gained in size and became denser but can be found in the same locations as in the 1936. Additionally, new mussel beds appeared, by which the general spatial distribution pattern, that can be observed until today, is achieved for this subarea. The aerial photographs from 1990 and 1998 reveal only minor changes in the spatial extent and distribution of the mussel beds.

The variations in area observed from 1998 to 2006 are primarily caused by the Leghörn mussel bed. The loss in area from 1998 to 2001 is due to its poor condition as this formerly continuous bed became sparse and fragmented during that time. The gain in area from 2001 to 2002 and 2005 to 2006 are also found in the Leghörn mussel bed as it recovers. The latter gain in area is already indicated in 2005 but at that stage too sparse to identify it as a mussel bed, now actually dominated by oysters.

In general, the area covered by mussels and their distribution pattern are relatively stable from 1958 to 2006 and the density mainly sparse and medium.

**Southern part (1936 – 2006)**

All mussel beds in the southern part of the List tidal basin are confined close to the island of Sylt (Fig. 7.7). Most beds are stretched, narrow and have a band-shaped appearance. The main mussel bed complex is distinguished by its stability in size and shape over the entire survey period. The changes occurred mainly south and east of it.

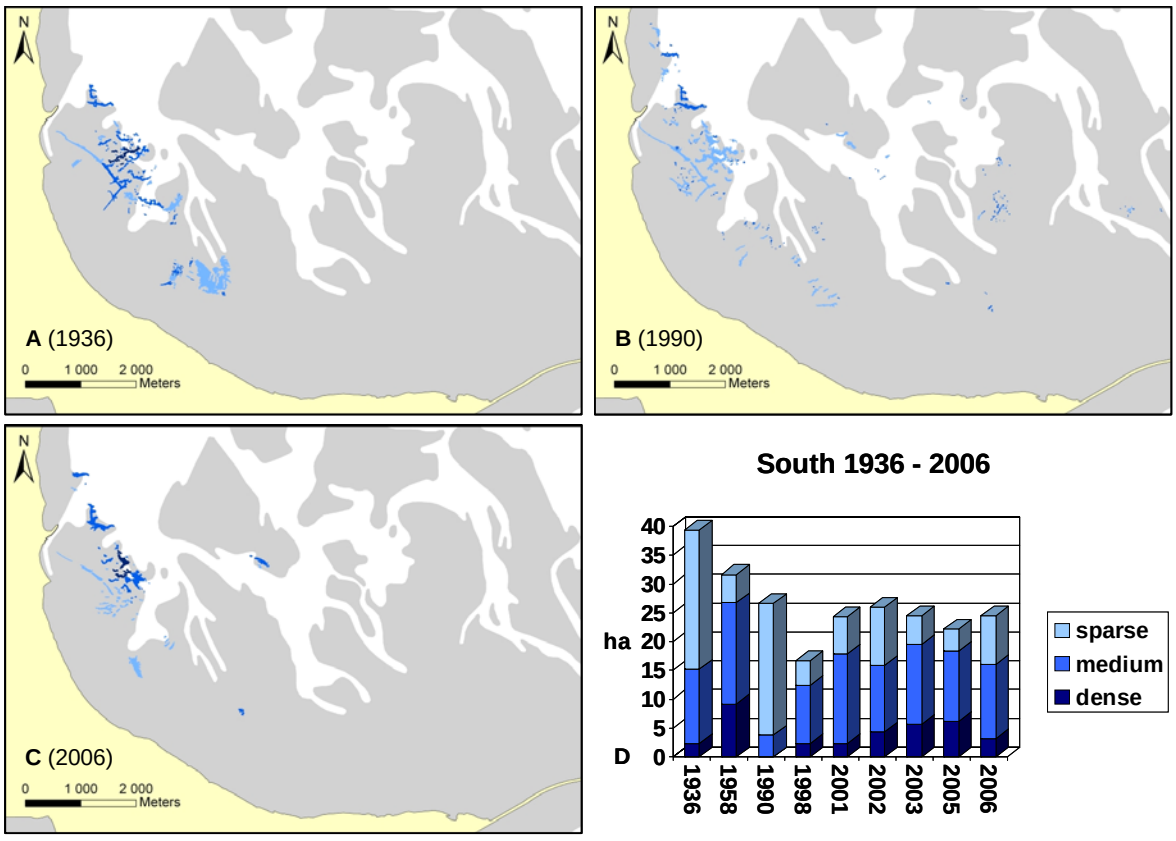


**Fig. 7.7:** The development of mussel beds in the southern part of the study area (overview of the study area is given in Fig. 7.3). The spatial distribution in 1936 (A), 1990 (B) and 2006 (C) is shown exemplary in the maps while the development from 1936 to 2006 can be seen in the graph (D).

In 1936, a larger but sparse mussel accumulation formed south of the main complex which resulted in the maximum spatial extent (40 ha) observed in this subarea. A steady decline

in mussel bed area is recorded until 1990 as the sparse mussel accumulation in the south vanished. Among the main mussel bed locations, many small and scattered beds can be observed in the rather exposed east in 1990. Between 1990 and 1998 many beds in these exposed locations disappeared and even the individual mussel beds of the main complex decreased in their width even though they maintained their shape. From 2001 on, the spatial distribution as well as the densities of the mussel beds are rather stable but oysters are taking over.

**Eastern part (1945 – 2006)**

There are only very few mussel beds in the eastern part of the List tidal basin (Fig. 7.8). They are located at a gully between Jordsands Flak and the mainland.

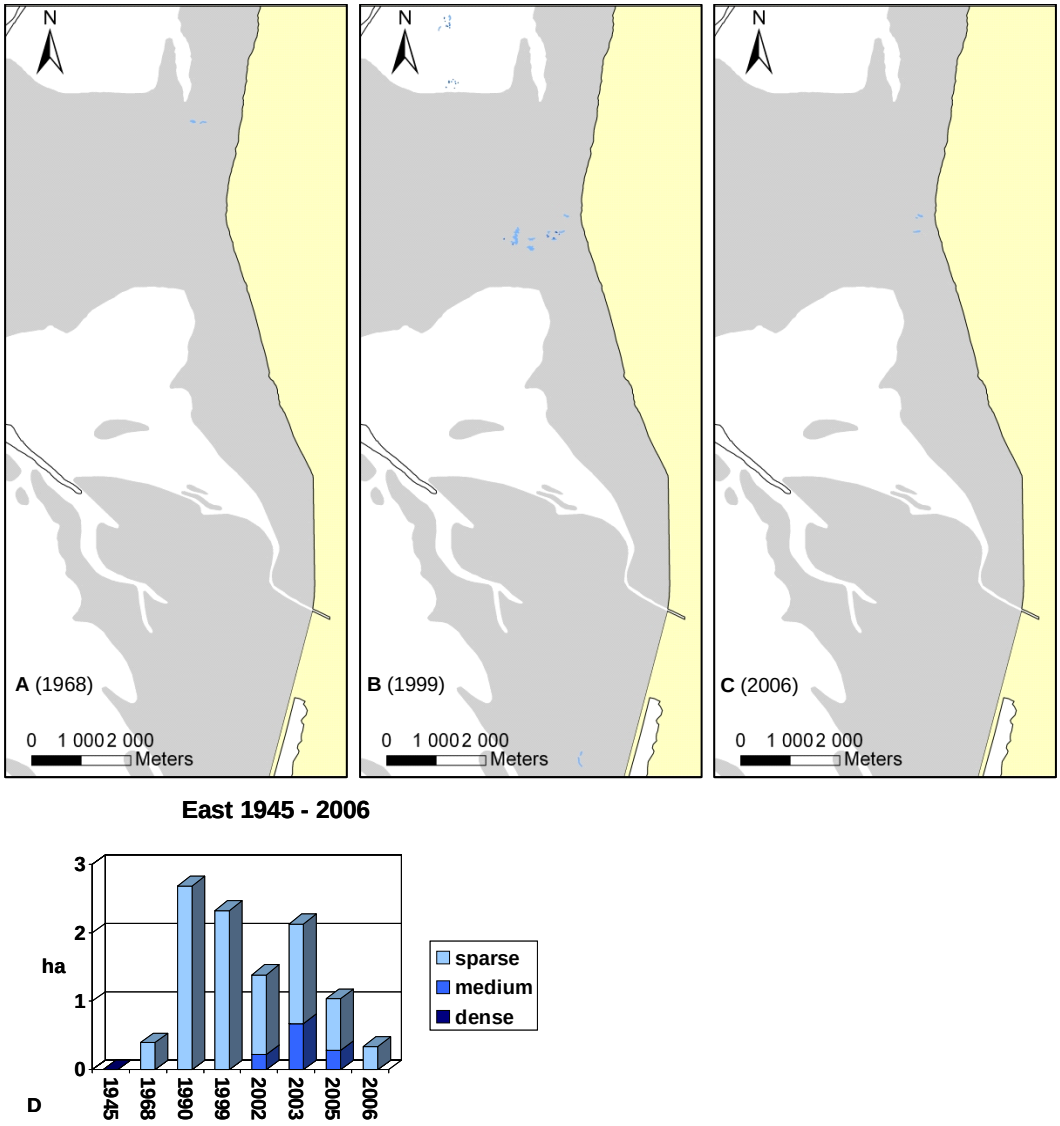


**Fig. 7.8:** The development of mussel beds in the eastern part of the basin (overview of the study area is given in Fig. 7.3). The spatial distribution in 1968 (A), 1999 (B) and 2006 (C) is shown exemplary in the maps while the development from 1945 to 2006 can be seen in the graph (D).

No mussel beds could be observed in 1945 and 1968, and very few small and sparse beds were present there after. The maximum spatial extent of 2.7 ha for this subarea is reached in 1990 as very small and scattered mussel beds formed in the exposed north of Jordsands Flak. These beds vanished almost completely from 1990 to 1999. Only the beds in vicinity to the mainland remained. A further decrease from 2003 to 2006 affects the mussel beds near the mainland and leads to an almost complete vanishing of beds in this area.

In general: mussel beds show the poorest stability and constancy in this subarea and are characterised by a sparse coverage.

**Northern part (1945 – 2006)**

The mussel beds in the northern part of the List tidal basin are located all along the eastern shore of the island of Rømø up to the Rømø causeway (Fig. 7.9).

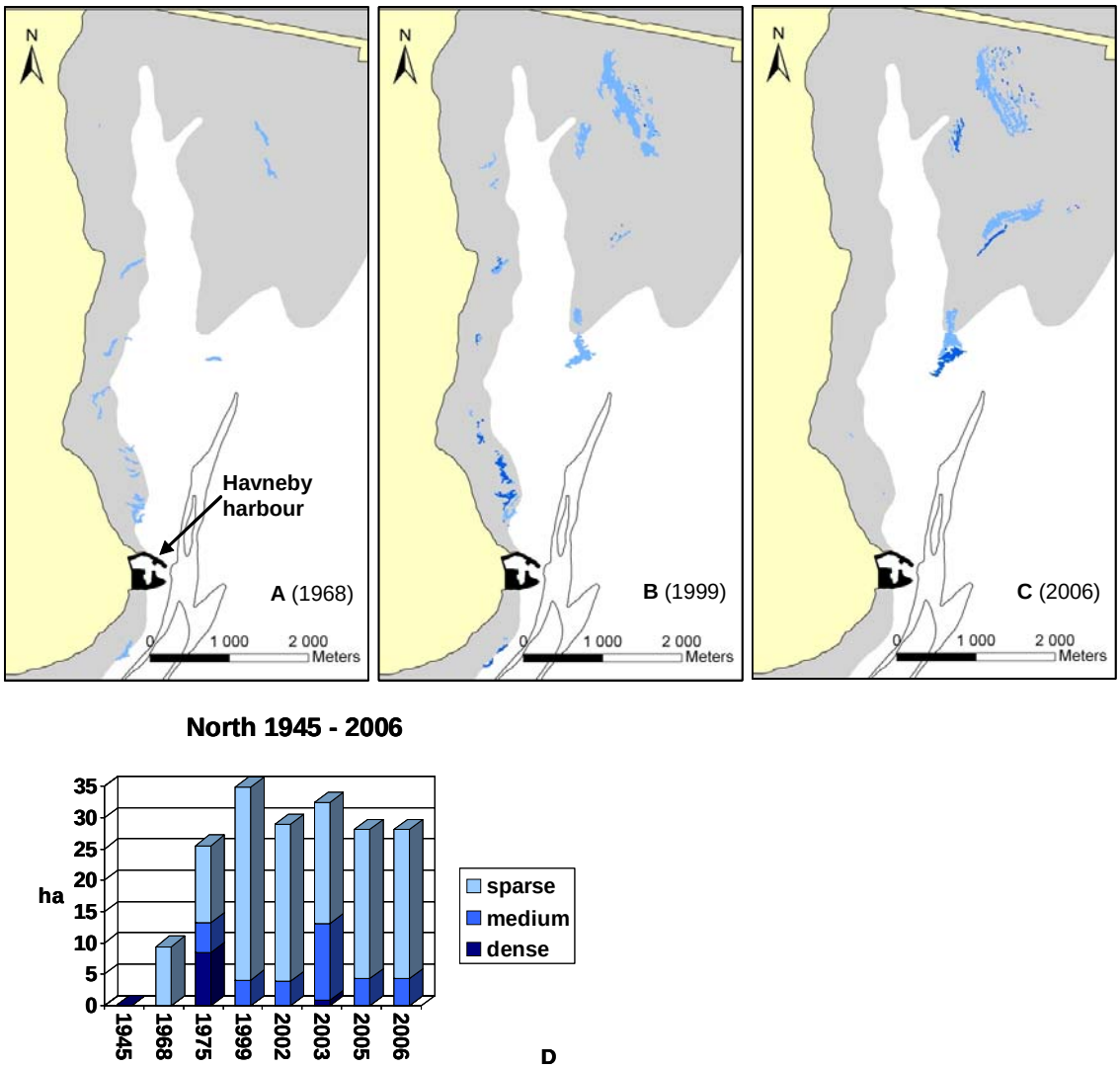


**Fig. 7.9:** The development of mussel beds in the northern part of the List tidal basin (overview of the study area is given in Fig. 7.3). The spatial distribution in 1968 (A), 1999 (B) and 2006 (C) is shown exemplary in the maps while the development from 1945 to 2006 can be seen in the graph (D).

In 1945, no mussel beds could be observed in the aerial photographs. They are first detected in sparse coverage in 1968, but the base of their spatial distribution pattern, which they show through the entire survey period, is already realised then. Starting from this pattern, the mussel beds gradually increased in number and size from 9.4 ha in 1968 to 35.2 ha in 1999. During this time, a new and large mussel bed formed near the causeway while on the other hand mussel beds on Havsand south of Havneby harbour strongly declined. There are only minor changes in the beds from 1999 to 2002 but the narrow band-shaped mussel beds north of Havneby harbour decreased in density and area and are almost completely gone by 2005. This is compensated by an increase of beds, which are located more in the centre of the northern part. Nevertheless, this location can still be regarded as sheltered due to the position of the island protecting against the prevailing south-westerly fetch. However, a spatial shift of the main mussel bed locations can be recognized.

Even though the mussel beds have a considerable spatial extent in the northern part amounting to 31 % of the total, they are characterised by a rather sparse coverage.

## 7.4 Discussion

### 7.4.1 Spatial pattern of intertidal mussel beds

Mussel beds are a regular but not ubiquitous faunal feature of back-barrier tidal flats of the European Wadden Sea (Hertweck and Liebezeit 2002). They also occur in the List tidal basin where they are mostly located at the lee side of the two barrier islands. Mussel beds need shelter from fetch as they are sensitive to storms (Nehls and Thiel 1993, Nehls et al. 2002) as well as to ice scouring (Obert and Michaelis 1991, Strasser et al. 2001b).

Mussels are suspension-feeders and they are situated at the mid intertidal to the subtidal because the longer they are covered with water the longer they have access to food. On tidal coasts, the duration of air exposure is considered to be one of the most important factors limiting growth of mussels (Buschbaum 2001) and hardly any beds can be found where the emersion time is above 50 % (Brinkmann et al. 2002). Furthermore, mussels live longer on beds that are exposed only for a short time at low tide (McGrorty and Goss-Custard 1991). No distinct and large subtidal mussel beds occur in the List tidal basin because they were overexploited and so far re-establishment has not occurred (Saier 2001, Buschbaum and Saier 2003).

Mussel beds are rather massive structures which can resist strong currents alongside tidal channels. However, very high current speeds may have negative effects on filtration rates

(Newell 1999, Brinkmann et al. 2002). Their resistance also allows mussel bed formation in wave exposed areas, but there they may not persist for long (see Fig. 7.12). The occurrence of mussel beds is more dynamic there compared to those in sheltered sites, particularly severe winter storms and ice scouring can lead to their disappearance (Nehls and Thiel 1993, Strasser et al. 2001b). However, such mussel beds may reappear at sites from where they once vanished, even though this requires time and favourable conditions. This can be seen e.g. in the central and outer Königshafen. However, it is also observed in other parts of the Wadden Sea that mussel beds show irregular cycles of appearance, disappearance and reappearance at preferred distinct locations (Hertweck and Liebezeit 2002).

Mussel beds in the List tidal basin can be divided into temporary beds in exposed areas, which are the minority, and persistent beds in sheltered locations which are the rule. Most of the persistent beds can be observed over the entire observation period (1936 – 2006). These beds form a very constant spatial distribution pattern because they mostly remain where they once established at their sheltered sites. Dankers and Koelemaij (1989) also observed in the Dutch Wadden Sea that the spatial distribution pattern of intertidal mussel beds is relatively stable over decades.

Interestingly, it can be often observed that mussel beds form narrow and band shaped structures (Fig. 7.10). This is the result of self organisation. Mussel beds show regularly spaced banding patterns perpendicular to the water flow. The competition for algae on the one hand as well as the mutual protection from waves and currents on the other hand has led to this pattern which enhances productivity, resistance and resilience against disturbance (van de Koppel et al. 2005). However, occasionally also large coherent beds with only some small gaps develop (see Fig. 7.10: lower right).

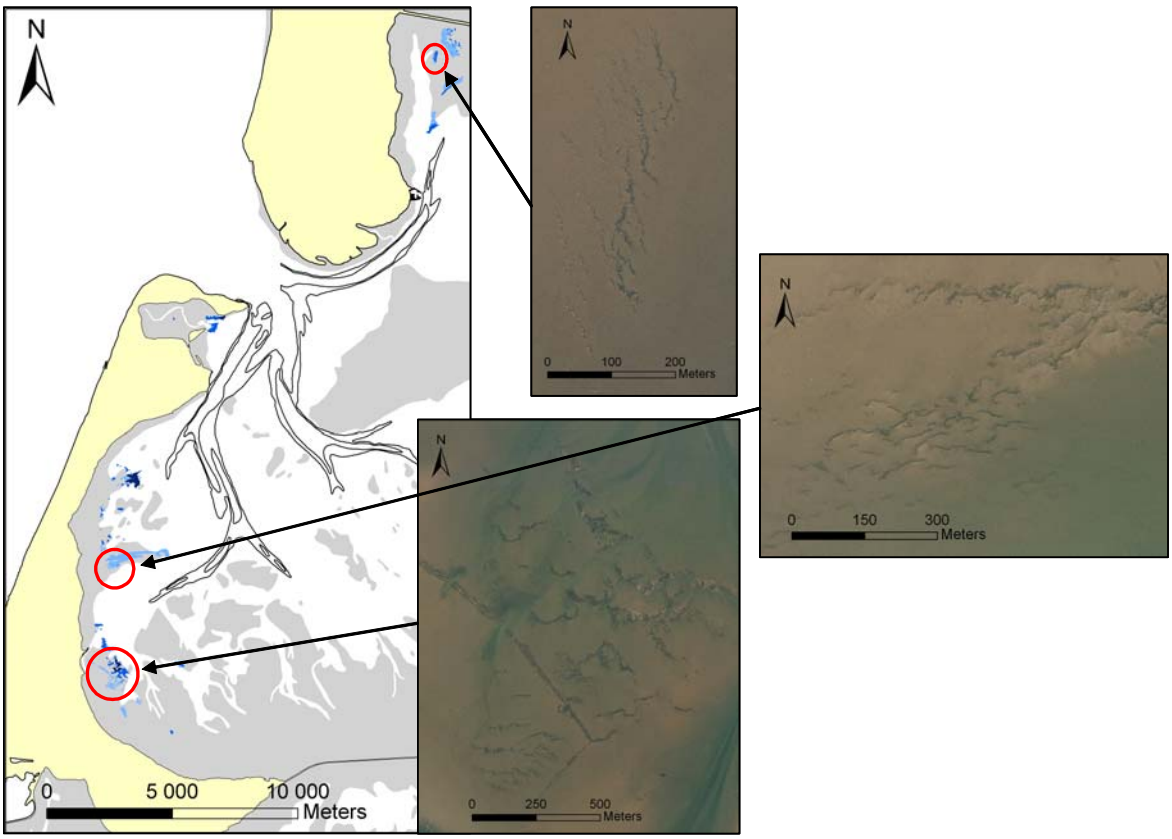


**Fig. 7.10:** Narrow and band shaped mussel beds in the List tidal basin (2003).

### 7.4.2 Long-term development of intertidal mussel beds in the Wadden Sea

Dankers and Koelemaij (1989) confirmed the consistency of the spatial distribution pattern of intertidal mussel beds over decades. Nevertheless, they also found that their surface area can vary greatly which has high influence on the ecosystem especially in terms of water filtering capacity. In the List tidal basin it is also detected that changes in bed area are in general due to expansion or contraction of established mussel beds and to a lower rate because of vanishing and new formation.

In 1945/58 the mussel beds in the List tidal basin only covered 84.0 ha. In the German part of the List tidal basin an intensive exploitation of mussel beds commenced shortly after World War II and lasted into the 1950s (Reise, pers. comm.). This may have contributed to the rather low mussel bed area observed in 1945/58. An agreement to refrain from dredging intertidal mussel beds in the National Park of Schleswig-Holstein is implemented since 1997 (CWSS 2002). Nevertheless, traces of dredging on mussel beds close to low water level have been repeatedly observed (Reise, pers. comm.). The effects can be rather similar to those of ice scouring. However, the mussel bed area in the List tidal basin increased up to 124.0 ha by 2006, which is 147.5 % compared to 1945/58 (Fig. 7.11). It

can be assumed that the ban of dredging intertidal mussel beds significantly contributed to this increase. It is also likely that the increase of the mussel population is to some extent induced by eutrophication (Nehls and Thiel 1993), which results in a higher food availability for mussels. However, mussel beds in the List tidal basin covered 0.78 % of the intertidal area in 2006, while it was 0.56 % in 2005, which agrees with the 2005 value Nehls and Büttger (2006) detected for the German part of the basin.

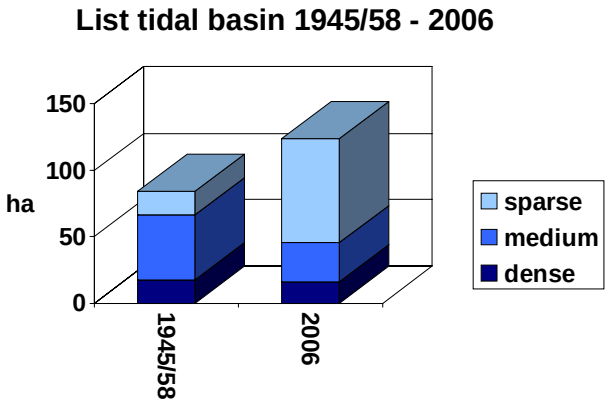


**Fig. 7.11:** The status and area of mussel beds in the List tidal basin in 1945/58 and 2006.

However, intensive mussel fishery lead to a strong decline of intertidal mussel beds until they almost disappeared from the entire Wadden Sea in the 1980s (Dankers et al. 1999). Therefore, the Wadden Sea in Denmark, Schleswig-Holstein and The Netherlands was totally or partly closed for fishery which resulted in an increasing mussel bed area. In Lower Saxony the beds are still under fishery pressure (Dankers et al. 1999). Herlyn and Millat (2000) observed that the areal loss of mussel beds in Lower Saxony was nearly 95 % and the loss of biomass 98 % from 1989 to 1996 and that the major reason for this is mussel fishery. This strong decline constantly continues and the area of blue mussel beds further decreased from 2900 ha in 1999 to 1300 ha in 2004 (de Vlas et al. 2005). The development is different in other parts of the European Wadden Sea. In the Dutch Wadden Sea the surface area of intertidal mussel beds varied from 1994 to 2003 but in general increased considerably from 2000 to 2003. In Schleswig-Holstein, the area was reduced almost by two-third from 952 ha in 1999 to 353 ha in 2005 (Nehls and Büttger 2006). For the Danish Wadden Sea there is also a considerable decrease in the estimated biomass observed from 1989 to 2002 (de Vlas et al. 2005). The reasons for the prevailing decline of the native blue mussels is mainly caused by failing spatfall due to mild winters (Nehls and

Büttger 2006). Mild winters result in a lower recruitment because of higher predation pressure by crabs and shrimps.

Compared to the development in Schleswig-Holstein, the overall situation of mussel beds in the List tidal basin seems to be rather stable. A decline in bed area can be observed in the Königshafen and the eastern part but the mussel bed area in the eastern part is rather insignificant. Same applies for the southern and northern part. The impact of winter storms were most obvious in the south and a shift in the major location of mussel beds is observed in the north. The western part is characterised by mainly stable conditions but a considerable increase occurred from 2005 to 2006. This areal gain is already suggested in 2005 as a new large mussel started to form but was too sparse then. It was a matter of classification to regard it as a mussel bed in 2006. This gain had a significant impact on the total mussel bed area of the entire basin and led to the assessment of rather stable conditions even though the proportion of mussel beds classified as ‘sparse’ is rather high. Visiting those mussel beds at the ground revealed a dominance of Pacific oysters. There may be a potential of this invading species to establish beds of a larger size than mussel beds have ever been (see Fig. 7.6, the long-stretched bed Leghörn in the lower right).

As mussel beds form massive structures, they show no impact by increased hydrodynamics as it can be observed for seagrass beds (see chapter 6.4.4). However, mussel beds are sensitive to severe ice drift and storms (Obert and Michaelis 1991, Nehls and Thiel 1993, Strasser et al. 2001b), which can considerably influence their development or even existence.

Strong winters with ice scouring damaging severely all intertidal mussel beds in the northern Wadden Sea occurred in 1962/63 and 1978/79, and more moderate disturbances affected mussel beds in winters during the mid 1980s (Reise, pers. comm.). Until today, the last winter with considerable ice scouring, which had long-lasting negative effects on mussel beds, was in 1995/1996 (Strasser et al. 2001b). Unfortunately, no aerial photographs are available for a direct comparison of the mussel bed situation before and after this winter. However, the comparison of the spatial distribution of mussel beds in 1990 and 2006 reveals a conspicuous pattern of selective vanishing (Fig. 7.12). Primarily, mussel beds in exposed locations in the fetch of the prevailing wind-direction vanished. This indicates that most likely the interactions between ice and storm may have generated this pattern of loss (Fig. 7.12). Disturbance by ice and storms may remove or severely

damage intertidal mussel beds, and if subsequent recruitment fails to revive those beds, they may vanish completely. This course of events has been directly observed for the field of mussel beds in the south-eastern Königshafen subsequent to the strong ice winter in 1995/96 (Reise, pers. comm.). These beds were completely gone by 2001.

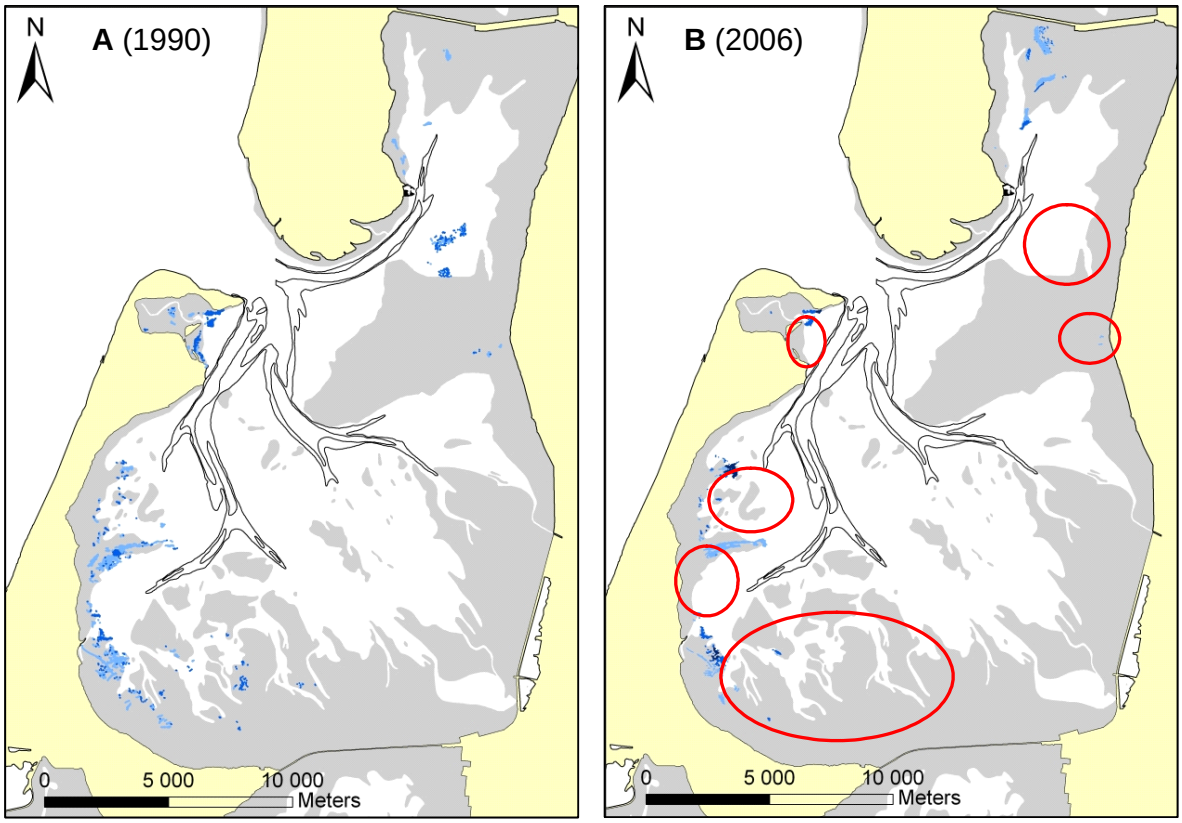


**Fig. 7.12:** The spatial distribution of mussel beds in the List tidal basin in 1990 and 2006. The highlighted areas show where mussel beds vanished in particular.

Mussel beds are currently undergoing a dramatic change as they are colonized by the Pacific oyster *Crassostrea gigas*. The native blue mussels and the introduced oysters can not be distinguished by visual analysis of aerial photographs. Therefore, this shift in the species composition can not be detected by this method even though the oyster invasion is getting to huge dimensions, not only in the List tidal basin but also in the entire Wadden Sea (Diederich et al. 2005, Reise et al. 2005a, Nehls and Büttger 2006, Wehrmann 2007). However, even though blue mussels and oysters appear at the same sites, there is no evidence that the Pacific oysters are causing the decline of blue mussels, which can be mainly ascribed to an indirect effect of mild winters (Nehls et al. 2006).

## 7.5 Summary and conclusions

Mussel beds are a common feature on back-barrier tidal flats in the European Wadden Sea. They can be divided into persistent and temporal beds. Persistent beds are located at sheltered sites. They form stable features with consistent spatial distribution patterns, which can be observed over several decades. Temporal beds can form in rather exposed areas. There, they are vulnerable to extreme events, like storms, severe ice scouring and especially interactions of both, which may let them disappear abruptly. From 1946 to 1997 also dredging of intertidal mussels for human consumption may have contributed to losses in mussel bed area.

Changes in bed area are not only caused by vanishing and formation of mussel beds. Permanent beds dominate and account for the largest share. Therefore, changes in surface area are mainly due to expansion or contraction of persistent mussel beds. These beds keep their basic spatial pattern when changing in surface area.

# 8 General discussion

An attempt has been made to analyze and quantify some change in coastal morphology and biogenic habitats in a tidal basin of the northern Wadden Sea, mainly from the second half of the last century until today. The obtained knowledge on variability and trends may serve to better understand what is likely to happen in the future. This is a much debated issue because IPCC (2007) and Rahmstorf (2007) predict an accelerated sea level rise for the 21st century and this will affect the coastal processes studied here. The development of specific scenarios is beyond the scope of the present study and should be a next step. However, the quantified observations on past changes do offer the chance to make some general projections and to discuss sensible human adaptations.

An accelerated sea level rise is one of the most certain consequences of global warming (Zhang et al 2004). It is due to thermal expansion of water, input of water into the ocean from glaciers and ice sheets, and changed water storage on land. Melting ice sheets have the largest potential effect and the global sea level rose about 2 mm $yr^{-1}$ from 1880 to 1990 (Rahmstorf 2007). In this regard, regional differences have to be considered as for example the annual mean high water level in the Wadden Sea rose by 2.5 mm $yr^{-1}$ from 1890 to 1989 and even by 6.7 mm $yr^{-1}$ for the period 1971 to 1989 (CPSL 2001). However, a further global sea level rise of 0.5 to 1.4 meters above the 1990 level, which is equivalent to 4.5 to 12.7 mm $yr^{-1}$, is projected until 2100 (Rahmstorf 2007). An increased storminess, which is accompanied with climate change, comes on top of the rising sea level. Even though we are experiencing a calmer weather period now (Weisse et al. 2005, Weisse and Plüß 2006), storm surges may increase along the North Sea coast towards the end of the 21st century (Woth et al. 2006). This is consistent with other model predictions, according to which extreme wave heights in the southern and eastern North Sea may increase by about 5 to 8 % at the same time period (Grabemann and Weisse 2007). An exacerbation of sandy beach erosion is expected (Zhang et al. 2004).

The response of the Wadden Sea on the rising sea level depends on the scenario of the rate of rise. Oost et al. (2005) expect tidal flats to be able to keep up with a sea level rise due to faster sedimentation up to a critical limit of 3 mm $yr^{-1}$ (for large tidal basins) to 6 mm $yr^{-1}$ (for small tidal basins). CPSL (2001) regards a sea level rise of up to 5 mm $yr^{-1}$ for the most realistic scenario in the Wadden Sea. The Wadden Sea is expected it be able to adapt to such a rise without substantial changes and prevent inundation by internal redistribution of tidal flat sediments. Internal redistribution is especially essential for the Northfrisian Wadden Sea

because no important sediment input from the North Sea is expected here. The depots of Pleistocene sediment which were available during most of the Holocene development of the northern Wadden Sea area are now depleted (Thiede and Ahrendt 2000). Furthermore, approx. 33 % of Holocene sediments are embanked today and therefore, missing in the sediment budget (Eppel and Ahrendt 2005). However, redistribution is expected to occur in the form of erosion in tidal channels and sedimentation on tidal flats. This would result in increased height differences, steepening of the topography and coarsening of the tidal flat sediments (Hofstede 1999, 2002, Eppel and Ahrendt 2005). An increase in the cross-sectional areas of tidal channels and an estimated loss of 2.5 to 7.5 % of the tidal flat surface area as well as a general sediment deficit are expected under the scenario of 5 mm $yr^{-1}$ sea level rise (CPSL 2001, 2005). However, it is assumed that the structure and function of the Wadden Sea ecosystem would remain more or less unchanged (Hofstede 1999, 2002). However, only if rates of sea level rise do not exceed a certain "breakpoint". The excess of such a breakpoint will result in the development of the Wadden Sea in the direction of tidal lagoons, which primarily means a severe areal reduction of intertidal flats. However, the exact level of such a breakpoint is not known and differs from basin to basin (CPSL 2001, 2005).

Based on this study I do not share the assessment that the Wadden Sea will adapt to sea level rise without substantial changes. These assumptions were made based on an expected sea level rise of 5 mm $yr^{-1}$. However, the rate of sea level rise was already 6.7 mm $yr^{-1}$ in the Wadden Sea for the period 1971 to 1989. Severe coastal problems witnessed in the 20$^{th}$ century will be exacerbated in the 21$^{st}$ century under plausible global warming (Zhang et al. 2004). Eppel and Ahrendt (2005) also expect the current state of the Wadden Sea to be threatened on a medium time scale. Hofstede (1999) assumes that the Wadden Sea ecosystem can handle a moderate sea level rise but only if this is not accompanied by a significant change of wind- or wave-climate. Otherwise, it is presumed that erosion of tidal flats and salt marshes will be dominant. However, an increase of storm surges and extreme wave heights is expected in the southern North Sea for the end of the 21$^{st}$ century (Woth et al. 2006, Grabemann and Weisse 2007). Furthermore, loss and submersion of intertidal areas are no recent phenomena as they are observed for example in the List tidal basin over the last centuries (Higelke 1998, Reise 1998). This trend is expected to exacerbate under an accelerated sea level rise.

The five study objects of this survey are all sensitive to an accelerated sea level rise, or more precisely to increased hydrodynamics. Hydrodynamics can not only be increased by an

accelerated sea level rise but also on a local level by the reduction of the catchment area of a tidal basin. This leads to less accommodation space for the water which further results in increased energy levels within the basin (Flemming and Nyandwi 1994, Mai 1999). For the List tidal basin, Reise (1998) estimates that one third of it has been converted into land by embankment over the last 500 years and that the tidal flat area decreased from approx. 66 to 40 % within the 20$^{th}$ century.

Increased hydrodynamics also accelerate erosion and the rate of shoreline changes, especially when storms and waves occur in combination with high water levels (Larson et al. 1999). The overall damage potential as a result of sea level rise and increased erosion is estimated for Germany at 330 to 410 billon €, in which the impact is greater on the North Sea coast than on the Baltic Sea coast due to more low-lying areas (Sterr et al. 2000a, Sterr 2002). On a global scale, Zhang et al. (2004) estimate that apart from the existence of some island states and deltaic coasts, at least 100 million people, who live within one meter of mean sea level, are threatened in the coming decades.

The observed loss of intertidal areas is associated with a depletion of mud. Even though Andersen et al. (2006) argues that fine-grained tidal flats in the Danish Wadden Sea are not seriously threatened by the expected sea level rise in the 21$^{st}$ century, it may be assumed that this is a rather local phenomenon. This study indicates an ongoing coarsening of sediments and as this is also reported from other parts of the Wadden Sea (Flemming and Nyandwi 1994, Flemming and Bartholomä 1997, Mai and Bartholomä 2000, Zwarts 2003, van Bernem, pers. comm.), it may be considered as a large scale process. It is caused by an accelerating, long-term depletion of mud due to resuspension and removal of the fine-grained sediments by increased hydrodynamics. It is expected that this process will continue and mud flats further decrease. The depletion of fines will be amplified so that grain sizes coarser than mud are affected in the future as well. Changes in grain size composition implicate changes in the composition of benthos, changing from a dominance of mud dwelling surface deposit feeders and diatom grazers to a dominance of sand dwelling subsurface deposit feeders with polychaetes and agile peracarid crustaceans (Lackschewitz and Reise 1998, Reise 1998, Reise et al. 2008).

It is observed that the area covered by megaripple populations almost doubled in the List tidal basin over the last six decades. This may also be related to increased hydrodynamics which facilitate formation of megaripples. This trend can be expected to continue as well as an

increase of sediment dynamics, for which the occurrence of megaripples are regarded as an indicator.

Seagrass is directly sensitive to strong hydrodynamics (de Jonge et al. 1996, Fonseca and Bell 1998, Schanz and Asmus 2003) as well as to sediment instability which often results from it (Philippart et al. 1992, van Katwijk et al. 2000). Increased hydrodynamics particularly occur in tidal channels which is why seagrass habitats degrade in their vicinity or shift entirely away from them. Today, degradation is limited to the vicinity of tidal channels because we are experiencing a calmer weather period now (Weisse et al. 2005, Weisse and Plüß 2006), which may have caused the general increase of seagrass bed area in the northern Wadden Sea (Reise and Kohlus 2008). However, it can be assumed that this situation will change. Degradation is expected to expand to other seagrass occurrences due to the predicted sea level rise as well as the increase of the storm surges and extreme wave heights (Woth et al. 2006, Grabemann and Weisse 2007). Hydrodynamics are regarded to become a serious threat to seagrass habitats in the Wadden Sea in the long run.

Mussel beds are rather massive structures. Therefore, they can resist strong currents and are less vulnerable to increased hydrodynamics, although very high current speeds may have negative effects on filtration rates (Newell 1999, Brinkman et al. 2002). However, mussels are also sensitive to burial by sediment (Okun 1999, Widdows et al. 2002) which can be enhanced by increased hydrodynamics. Furthermore, they can be affected by severe storms (Nehls and Thiel 1993, Nehls et al. 2002) which are predicted for the end of the 21$^{st}$ century (Woth et al. 2006, Grabemann and Weisse 2007). However, apart from this physical external interference, climate change can also be detected in changes in species composition of mussel beds. Under scenarios of global warming, the ongoing massive increase of oyster abundance, which is promoted by warm summers (Diederich et al. 2005), is expected to proceed and to be the most extensive effect for mussel beds.

The five study objects are closely linked and interactions between them even increase the effects of sea level rise and increased hydrodynamics.

Shoreline changes alter the morphology but changes in the morphology can also affect shorelines, e.g. when tidal channels alter their course as it was realized after the completion of the Rømø dam (Jespersen and Rasmussen 1984).

However, the grain size composition, developmental trend and the deposition of sediments can also be linked to the morphology. The long-term depletion of fine-grained intertidal sediments

primarily occurs in exposed areas while sheltered low-lying areas with extended water residence times experience enhanced settlement of fines on a medium time scale (Fig. 4.15), a phenomenon also reported from other intertidal areas (Gouleau et al. 2000). However, the coarsening of sediments can be regarded as dominant as it is widely observed in the Wadden Sea (Flemming and Nyandwi 1994, Flemming and Bartholomä 1997, Mai and Bartholomä 2000, Zwarts 2003, van Bernem, pers. comm.). It enlarges the share of a sandy tidal area.

Sandy tidal flats, as well as strong hydrodynamics, are required for the formation of megaripples (Dalrymple et al. 1978) and a direct link between the increasing share of a sandy tidal area and an increasing megaripple population can be assumed.

The coarsening of sediments is amplified by a reduced vegetation cover, primarily seagrass, which usually inhibits resuspension and enhances sedimentation of mud (Ward et al. 1984, Gacia et al. 1999, Heiss et al. 2000, Gacia et al. 2003). However, as seagrass is also affected by increased hydrodynamics and sediment instability (Philippart et al. 1992, de Jonge et al. 1996, Fonseca and Bell 1998, van Katwijk et al. 2000, Schanz and Asmus 2003), this results in a decreasing bed area which means fewer sheltered areas where mudflats could establish. This promotes an increasing share of sandy tidal flats where megaripples can form. Again, megaripples interfere with the occurrence of seagrass as their migration threatens these epibenthic structures (Marbà et al. 1994) (Fig. 8.1).

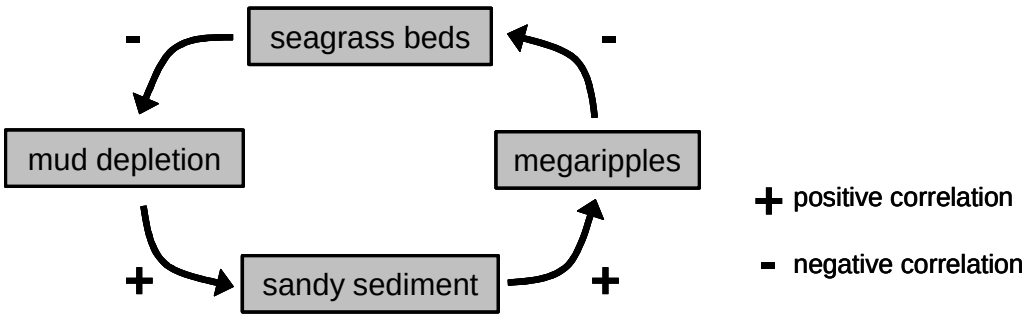


**Fig. 8.1:** A schematic overview of the interactions of seagrass beds, mud depletion, sand and megaripples.

Mussels are also sensitive to burial (Okun 1999, Widdows et al. 2002) and may be threatened by migrating megaripples as well. On the other hand they can also prevent erosion of sediments by protecting them from hydrodynamics (Widdows et al. 2002), but the bed area of native mussels have been constantly decreasing in the Wadden Sea over the last years (de Vlas et al. 2005). However, the invading Pacific oysters are considerably larger than mussels and tend to form large aggregates of heavy weight. They also eventually occupy an area larger

than what is presently covered by mussel beds. Thus one may expect that beds dominated by Pacific oysters could exert a stronger stabilising effect than native mussels did. Nevertheless, regarding the fact that in 2003 intertidal mussel beds covered in many places of the Wadden Sea only 1 % of the intertidal area (de Vlas et al. 2005), one has to be aware that the stabilising effect is rather localised. However, apart from providing shelter, mussels and oyster also affect the sediment composition by the input of organic mud (Kröncke 1994).

I assume that the observed morphodynamic and biodynamic processes will accelerate and the surveyed features will be characterised by increased variability. The reason for this will be an accelerated sea level rise and increased hydrodynamics. All these morphological and biological features are strongly linked to each other and the developmental trend of one can significantly drive the development of another. Therefore, it is recommended to monitor a combination of selected abiotic and biotic factors in order to assess the complex Wadden Sea ecosystem. The methods introduced in this study proofed to be highly suitable for a monitoring, especially as the survey of high-resolution aerial photographs with GIS allows a multi-purpose data collection from one data source and an analysis within one system. However, a continuous monitoring programme is recommended in order to assess variability and to detect developmental trends early, especially in consideration of aggravated conditions accompanied by climate change.

# References

Ahrendt, K. (1993). Sedimentdynamik an der Westküste Sylts (Deutsche Bucht/Nordsee). Meyniana 45: 161-179.

Ahrendt, K., Thiede, J. (2001). Naturräumliche Entwicklung Sylts - Vergangenheit und Zukunft. In: Daschkeit, A., Schottes, P. (Eds.). Klimafolgen für Mensch und Küste am Beispiel der Nordseeinsel Sylt. Springer, Berlin, Heidelberg, New York: 69-112.

Allen, J. R. L., Friend, P.F. (1976). Changes in intertidal dunes during two spring-neap cycles, Lifeboat Station Bank, Wells-next-the-Sea, Norfolk (England). Sedimentology 23: 329-346.

Andersen, T. J., Pejrup, M. (2001). Suspended sediment transport on a temperate, microtidal mudflat, the Danish Wadden Sea. Marine Geology 173: 69-85.

Andersen, T. J., Pejrup, M. (2002). Biological Mediation of the Settling Velocity of Bed Material Eroded from an Intertidal Mudflat, the Danish Wadden Sea. Estuarine, Coastal and Shelf Science 54: 737-745.

Andersen, T. J., Jensen, K.T., Lund-Hansen, L.C., Mouritsen, K.N., Pejrup, M. (2004). Measurements of Erodibility and Settling Velocity of Intertidal and Subtidal Cohesive Sediments in a Coastal Lagoon, The Danish Wadden Sea. Journal of Coastal Research 41: 170.

Andersen, T. J., Lund-Hansen, L.C., Pejrup, M., Jensen, K.T., Mouritsen, K.N. (2005). Biologically induced differences in erodibility and aggregation of subtidal and intertidal sediments: a possible cause for seasonal changes in sediment deposition. Journal of Marine Systems 55: 123-138.

Andersen, T. J., Pejrup, M., Nielsen, A.A. (2006). Long-term and high-resolution measurements of bed level changes in a temperate, microtidal coastal lagoon. Marine Geology 226: 115-125.

Andres, F. J., Byrnes, M.R. (1991). Accuracy of Shoreline Change Rates as Determined from Maps and Aerial Photographs. Shore and Beach (January): 17-26.

ALR (Amt für ländliche Räume, Husum) (2007). Küstenschutzmaßnahmen Westküste Sylt 2007. Husum.

Asmus, H. (1987). Secondary production of an intertidal mussel bed community related to its storage and turnover compartments. Marine Ecology Progress Series 39: 251-266.

Austen, I. (1990). Geologisch-sedimentologische Kartierung des Königshafens (List auf Sylt) und Untersuchung seiner Sedimente. Diploma thesis.

Austen, I. (1994). The surficial sediments of Königshafen - variations over the past 50 years. Helgoländer Meeresuntersuchungen 48: 163-171.

Austen, I., Andersen, T.J., Edelvang, K. (1999). The Influence of Benthic Diatoms and Invertebrates on the Erodibility of an Intertidal Mudflat, The Danish Wadden Sea. Estuarine, Coastal and Shelf Science 49: 99-111.

Backhaus, J., Hartke, D., Hübner, U., Lohse, H., Müller, A. (1998). Hydrographie und Klima im Lister Tidebecken. In: Gätje, C., Reise, K. (Eds.). Ökosystem Wattenmeer - Austausch-, Transport- und Stoffumwandlungsprozesse. Springer, Berlin, Heidelberg, New York: 39-54.

Bartholdy, J., Pejrup, M. (1994). Holocene Evolution of the Danish Wadden Sea. Senckenbergiana maritima 24: 187-209.

Bartholdy, J., Aagaard, T. (2001). Storm surge effects on a back-barrier tidal flat of the Danish Wadden Sea. Geo-Marine Letters 20: 133-141.

Bayerl, K., Austen, I., Köster, R., Pejrup, M., Witte, G. (1998). Dynamik der Sedimente im Lister Tidebecken. In: Gätje, C., Reise, K. (Eds.). Ökosystem Wattenmeer - Austausch-, Transport- und Stoffumwandlungsprozesse. Springer, Berlin, Heidelberg, New York: 127-159.

Bayerl, K., Köster, R. (1998). Morphogenese des Lister Tidebeckens. In: Gätje, C., Reise, K. (Eds.). Ökosystem Wattenmeer - Austausch-, Transport- und Stoffumwandlungsprozesse. Springer, Berlin, Heidelberg, New York: 25-29.

Bayerl, K.-A. (1992). Zur jahreszeitlichen Variabilität der Oberflächensedimente im Sylter Watt nördlich des Hindenburg Damms. Berichte aus dem Forschungs- und Technologiezentrum Westküste der Universität Kiel 2. Büsum.

Bayerl, K.-A., Higelke, B. (1994). The development of northern Sylt during the Latest Holocene. Helgoländer Meeresuntersuchungen 48: 145-162.

Behrens, A., Gayer, G., Günther, H., Rosenthal, W. (1997). Atlas der Strömungen und Wasserstände in der Sylt-Romo-Bucht. Geesthacht, GKSS Forschungszentrum.

Beukema, J. J., Dekker, R., Essink, K., Michaelis, H. (2001). Synchronized reproductive success of the main bivalve species in the Wadden Sea: Causes and consequences. Marine Ecology Progress Series 211: 143-155.

Bird, E. C. F. (Ed.) (2000). Coastal Geomorphology - An Introduction. Wiley, Chichester.

Blott, S. J., Pye, K. (2001). Gradistat: A grain size distribution and statistics package for the analysis of unconsolidated sediments. Earth Surface Processes and Landforms 26: 1237-1248.

Boak, E. H., Turner, I.L. (2005). Shoreline Definition and Detection: A Review. Journal of Coastal Research 21(4): 688-703.

Boersma, J. R., Terwindt, J.H.J. (1981). Neap-spring tide sequences of intertidal shoal deposits ina mesotidal estuary. Sedimentology 28: 151-170.

Boothroyd, J. C., Hubbard, D.K. (1975). Genesis of bedforms in mesotidal estuaries. Estuarine Research 2: 217-234.

Borum, J., Duarte, C.M., Krause-Jensen, D., Greve, T.M. (2004). European seagrasses: an introduction to monitoring and management. A publication by the EU project Monitoring and Managing of European Seagrasses (M&MS) EVK3-CT-2000-00044.

Brinkman, A. G., Dankers, N., van Stralen, M. (2002). An analysis of mussel bed habitats in the Dutch Wadden Sea. Helgoland Marine Research 56: 59-75.

Bruce, E. M., Eliot, I.G., Milton, D.J. (1997). Method for Assessing the Thematic and Positional Accuracy of Seagrass Mapping. Marine Geodesy 20: 175-193.

Bruun, P. (2000). The Coastal Geomorphological Development of the Skagen Spit, Jutland, Denmark. Its Fate During the Next Century. Coastal Erosion and Accretion. Journal of Coastal Research 16(4): 1094-1099.

Buschbaum, C., Saier, B. (2001). Growth of the mussel *Mytilus edulis* L. in the Wadden Sea affected by tidal emergence and barnacle epibionts. Journal of Sea Research 45: 27-36.

Buschbaum, C. (2001). Selective settlement of the barnacle *Semibalanus balanoides* (L.) facilitates its growth and reproduction on mussel beds in the Wadden Sea. Helgoland Marine Research 55: 128-134.

Buschbaum, C., Saier, B. (2003). Ballungszentrum Muschelbank - Biodiversität und nachhaltige Nutzung. Biologie unserer Zeit 33(2): 100-106.

Buschbaum, C., Nehls, G. (2003). Effekte der Miesmuschel- und Garnelenfischerei. In: Lozán, J., Rachor, E., Reise, K., Sündermann, J., von Westernhagen, H. (Eds.). Warnsignale aus Nordsee & Wattenmeer. Geo, Hamburg: 250-255.

Cabaço, S., Santos, R. (2007). Effects of burial and erosion on the seagrass *Zostera noltii*. Journal of Experimental Marine Biology and Ecology 340: 204-212.

Cacchione, D. A., Southard, J.B. (1974). Incipient sediment movement by shoaling internal gravity waves. Journal of Geophysical Research 79(15): 2237-2242.

Cardoso, P. G., Pardal, M.A., Lillebo, A.I., Ferreira, S.M., Raffaelli, D., Marques, J.C. (2004). Dynamic changes in seagrass assemblages under eutrophication and implications for recovery. Journal of Experimental Marine Biology and Ecology 302: 233-248.

Chang, T. S., Bartholomä, A., Flemming, B.W. (2006). Seasonal Dynamics of Fine-Grained Sediments in a Back-Barrier Tidal Basin of the German Wadden Sea (Southern North Sea). Journal of Coastal Research 22(2): 328-338.

Chen, S., Chen, L., Liu, Q., Li, X., Tan, Q. (2005). Remote sensing and GIS-based integrated analysis of coastal changes and their environmental impacts in Lingding Bay, Pearl River Estuary, South China. Ocean & Coastal Management 48: 65-83.

Christiansen, C., Volund, G., Lund-Hansen, L., Bartholdy, J. (2006). Wind influence on tidal flat sediment dynamics: Field investigations in the Ho Bugt, Danish Wadden Sea. Marine Geology 235: 75-86.

Costanza, R., d'Arge, R., de Groot, R., Farber, S., Grasso, M., Hannon, B., Limburg, K., Naeem, S., O'Neill, R.V., Paruelo, J., Raskin, R.G., Sutton, P., van den Belt, M. (1997). The value of the world's ecosystem services and natural capital. Nature 387: 253-260.

CPSL (Coastal Protection and Sea Level Rise) (2001). Final Report of the Trilateral Working Group on Coastal Protection and Sea Level Rise. Wadden Sea Ecosystem No. 13. Common Wadden Sea Secretariat, Wilhelmshaven, Germany.

CPSL (Coastal Protection and Sea Level Rise) (2005). Coastal Protection and Sea Level Rise – Solutions for sustainable coastal protection in the Wadden Sea region. Wadden Sea Ecosystem No. 21. Common Wadden Sea Secretariat, Trilateral Working Group on Coastal Protection and Sea Level Rise (CPSL), Wilhelmshaven, Germany.

Cunha, A. H., Santos, R.P., Gaspar, A.P., Bairros, M.F. (2005). Seagrass landscape-scale changes in response to disturbance created by the dynamics of barrier islands: A case study from Ria Formosa (Southern Portugal). Estuarine, Coastal and Shelf Science 64: 636-644.

CWSS (Common Wadden Sea Secretariat) (2002). Shellfish Fisheries. An Overview of Policies for Shellfish Fishing in the Wadden Sea. Common Wadden Sea Secretariat, Wilhelmshaven, Germany.

CWSS (Common Wadden Sea Secretariat) (2008). Nomination of the Dutch-German Wadden Sea as World Heritage Site. Common Wadden Sea Secretariat - World Heritage Nomination Project Group (WHNPG), Wilhelmshaven, Germany

da Silva, J. F., Duck, R.W., Catarino, J.B. (2004). Seagrasses and sediment response to changing physical forcing in a coastal lagoon. Hydrology and Earth System Sciences 8(2): 151-159.

Dalrymple, R. W., Knight, R.J., Lambiase, J.J. (1978). Bedforms and their hydraulic stability relationships in a tidal environment, Bay of Fundy, Canada. Nature 275: 100-104.

Dame, R. F., Dankers, N. (1988). Uptake and release of materials by a Wadden Sea mussel bed. Journal of Experimental Marine Biology and Ecology 118: 207-216.

Dankers, N., Koelemaij, K. (1989). Variations in the mussel population of the Dutch Wadden Sea in relation to monitoring of other ecological parameters. Helgoländer Meeresuntersuchungen 43: 529-535.

Dankers, N., Brinkman, A.G., Meijboom, A., Zegers, J. (1999). Recovery of intertidal mussel beds in the Wadden Sea after large-scale destruction. Journal of Shellfish Research 18(2): 713.

de Jong, F., Bakker, J.F., van Berkel, C.J.M., Dankers, N.M.J.A., Dahl, K., Gätje, C., Marencic, H., Potel, P. (1999). 1999 Wadden Sea Quality Status Report. Wadden Sea Ecosystem No.9, Common Wadden Sea Secretariat, Trilateral Monitoring and Assessment Group, Quality Status Report Group. Wilhelmshaven, Germany.

de Jonge, V. N., de Jong, D.J. (1992). Role of tide, light and fisheries in the decline of *Zostera Marina* L. in the Dutch Wadden Sea. Netherlands Institute for Sea Research Publication Series 20: 161-176.

de Jonge, V. N., Essink, K., Boddeke, R. (1993). The Dutch Wadden Sea: a changed ecosystem. Hydrobiologia 265: 45-71.

de Jonge, V. N., de Jong, D.J., van den Bergs, J. (1996). Reintroduction of eelgrass (*Zostera marina*) in the Dutch Wadden Sea; a review of research and suggestions for management measures. Journal of Coastal Conservation 2: 149-158.

de Vlas, J., Brinkman, B., Buschbaum, C., Dankers, N., Herlyn, M., Kristensen, P.S., Millat, G., Nehls, G., Ruth, M., Steenbergen, J., Wehrmann, A. (2005). Intertidal Blue Mussel Beds. In: Essink, K., Dettmann, C., Farke, H., Laursen, K., Lüerßen, G., Marencic, H., Wiersinga, W. (Eds.). Wadden Sea Quality Status Report 2004. Common Wadden Sea Secretariat, Wilhelmshaven, Germany: 190-200.

den Hartog, C. (Ed.) (1970). The sea-grasses of the world. North-Holland Publ Comp, Amsterdam, London.

den Hartog, C. (1987). Wasting disease and othe dynamic phenomena in *Zostera* beds. Aquatic Botany 27: 3-14.

den Hartog, C., Phillips R.C. (2001). Common structures and properties of seagrass beds fringing the coasts of the world. In: Reise, K. (Ed.). Ecological Comparisons of Sedimentary Shores. Springer, Berlin, Heidelberg, New York: 195-212.

Dette, H.-H., Fuehrboeter, A., Raudkivi, A.J. (1994). Interdependence of Beach Fill Volumes and Repetition Intervals. Journal of Waterway, Port, Coastal and Ocean Engineering 120(6): 580-593.

Diederich, S. (2005). Differential Recruitment of introduced Pacific oysters and native mussels at the North Sea coast: coexistence possible? Journal of Sea Research 53: 269-281.

Diederich, S., Nehls, G., van Beusekom, J.E.E., Reise, K. (2005). Introduced Pacific oysters (*Crassostrea gigas*) in the northern Wadden Sea: invasion accelerated by warm summers? Helgoland Marine Research 59: 97-106.

Diederich, S. (2006). High survival and growth rates of introduced Pacific oysters may cause restrictions on habitat use by native mussels in the Wadden Sea. Journal of Experimental Marine Biology and Ecology 328: 211-227.

Dittmann, S. (Ed.) (1999). The Wadden Sea Ecosystem - Stability, Properties and Mechanisms. Springer, Berlin, Heidelberg, New York.

Dolan, R., Hayden, B.P., May, P., May, S. (1980). The Reliability of Shoreline Change Measurements from Aerial Photographs. Shore and Beach (October): 22-29.

Dolan, R., Fenster, M.S., Holme, S.J. (1991). Temporal Analysis of Shoreline Recession and Accretion. Journal of Coastal Research 7(3): 723-744.

Dolch, T. (2006). The use of high-resolution aerial photographs and Digital Elevation Models for spatial analyses and 3D-quantification of coastline changes at dynamic shores. In: Bungenstock, F., Riexinger, S., Bittmann, F. (Eds.). Beiträge der 24. Jahrestagung des Arbeitskreises „Geographie der Meere und Küsten“, Forschungszentrum Terramare Berichte 16, Wilhelmshaven: 16-21

Dolch, T., Hass, H.C. (2008). Long-term changes of intertidal and subtidal sediment compositions in a tidal basin in the northern Wadden Sea (SE North Sea). Helgoland Marine Research 62: 3-11.

Dolmer, P., Frandsen, R.P. (2002). Evaluation of the Danish mussel fishery: suggestions for an ecosystem management approach. Helgoland Marine Research 56: 13-20.

Drinkwaard, A. C. (1999). Introductions and developments of oysters in the North Sea area: A review. Helgoländer Meeresuntersuchungen 52(3-4): 301-308.

Dronkers, J. (1986). Tidal asymmetry and estuarine morphology. Netherland Journal of Sea Research 20(2-3): 117-131.

Duarte, C. M. (1995). Submerged aquatic vegetation in relation to different nutrient regimes. Ophelia 41: 87-112.

Ducrotoy, J.-P., Elliott, M., de Jonges, V.N. (2000). The North Sea. Marine Pollution Bulletin 41(1-6): 5-23.

Dyer, K. R., Christie, M.C., Feates, N., Fennessy, M.J., Pejrup, M., van der Lee, W. (2000). An Investigation into Processes Influencing the Morphodynamics of an Intertidal Mudflat, the Dollard Estuary, The Netherlands: I. Hydrodynamics and Suspended Sediment. Estuarine, Coastal and Shelf Science 50: 607-625.

Ehlers, J. (1988). Morphologische Veränderungen auf der Wattseite der Barriere-Inseln des Wattenmeeres. Die Küste 47: 3-30.

Eitner, V., Ragutzki, G. (1992). The effect of artificial beach nourishment on the sediment dynamics of a mesotidal barrier island (Norderney, southern North Sea, Germany). Modern and ancient clastic tidal deposits. B. W. E. Flemming: 26-27.

Eitner, V. (1996). Geomorphological response of the East Frisian barrier islands to sea-level rise: an investigation of past and future evolution. Geomorphology 15: 57-65.

Eppel, D., Ahrendt, K. (2005). Wattenmeersedimente: Sedimentinventar Nordfriesisches Wattenmeer. Abschlussbericht 03KIS037, Kiel.

ESRI (Ed.) (2003). ArcGIS 9 - Using ArcGIS Geostatistical Analyst. Redlands.

Essink, K., Dettmann, C., Farke, H., Laursen, K., Lüerßen, G., Marencic, H., Wiersinga, W. (2005). Wadden Sea Quality Status Report 2004. Wadden Sea Ecosystem No.19, Common Wadden Sea Secretariat, Trilateral Monitoring and Assessment Group, Quality Status Report Group. Wilhelmshaven, Germany.

Fan, D., Guo, Y., Wang, P., Shi, J.Z. (2006). Cross-shore variations in morphodynamic processes of an open-coast mudflat in the Changjiang Delta, China: With an emphasis on storm impacts. Continental Shelf Research 26: 517-538.

Felix, K.-M. (1981). Sedimentologische Kartierung und Untersuchung des Königshafens und der Gaten, Tiefs und Rinnen des Wattenmeeres von List/Sylt. Diploma thesis.

Flemming, B. W., Nyandwi, N. (1994). Land reclamation as a cause of fine-grained sediment depletion in backbarrier tidal flats (southern North Sea). Netherlands Journal of Aquatic Ecology 28(3-4): 299-307.

Flemming, B. W., Bartholomä, A. (1997). Response of the Wadden Sea to a Rising Sea Level: a Predictive Empirical Model. Deutsche Hydrographische Zeitschrift 49(2/3): 343-353.

Fonseca, M. S., Fisher, J.S. (1986). A comparison of canopy friction and sediment movement between four species of seagrass with reference to their ecology and restauration. Marine Ecology Progress Series 29: 15-22.

Fonseca, M. S. (1996). The role of seagrasses in nearshore sedimentary processes: a review. Estuarine shores: evolution, environments, and human alterations. K. F. Nordstrom, Roman, C.T. (Eds.). Chichester, Wiley: 261-186.

Fonseca, M. S., Bell, S.S. (1998). Influence of physical settings on seagrass landscapes near Beaufort, North Carolina, USA. Marine Ecology Progress Series 171: 109-121.

Frederiksen, M., Krause-Jensen, D., Holmer, M., Laursen, J.S. (2004a). Long-term changes in area distribution of eelgrass (*Zostera marina*) in Danish coastal waters. Aquatic Botany 78: 167-181.

Frederiksen, M., Krause-Jensen, D., Holmer, M., Laursen, J.S. (2004b). Spatial and temporal changes in eelgrass (*Zostera marina*) landscapes: influences of physical settings. Aquatic Botany 78: 147-165.

French, C. E., French, J.R., Clifford, N.J., Watson, C.J. (2000). Sedimentation-erosion dynamics of abondoned reclamations: the role of waves and tides. Continental Shelf Research 20: 1711-1733.

Gacia, E., Granata, T.C., Duarte, C.M. (1999). An approach to measurement of particle flux and sediment retention within seagrass (*Posidonia oceanica*) meadows. Aquatic Botany 65: 255-268.

Gacia, E., Duarte, C.M., Marba, N., Terrados, J., Kennedy, H., Fortes, M.D., Tri, N.H. (2003). Sediment deposition and production in SE-Asia seagrass meadows. Estuarine, Coastal and Shelf Science 56: 909-919.

Gallagher, E. L., Elgar, S., Thornton, E.B. (1998). Megaripple migration in a natural surf zone. Nature 394: 165-168.

Ganter, B. (2000). Seagrass (*Zostera* spp.) as food for brent geese (*Branta bernicla*): an overview. Helgoland Marine Research 54: 63-70.

Gätje, C., Reise, K. (Eds.) (1998). Ökosystem Wattenmeer - Austausch-, Transport- und Stoffumwandlungsprozesse. Springer, Berlin, Heidelberg, New York.

Giesen, W. B. J. T., van Kartwijk, M.M., den Hartog, C. (1990). Eelgrass condition and turbidity in the Dutch Wadden Sea. Aquatic Botany 37: 71-85.

Gouleau, D., Jouanneau, J.M., Weber, O., Sauriau, P.G. (2000). Short- and long-term sedimentation on Montportail-Brouage intertidal mudflat, Marennes-Oléron Bay (France) Continental Shelf Research 20: 1513-1530.

Grabemann, I., Weisse, R. (2007). Impact of climate change on extreme wave conditions in the North Sea. ICESM Abstracts 1.

Green, E. P., Short, T.F. (Ed.) (2003). World Atlas of Seagrasses, University of California Press.

Green, M. O., Coco, G. (2007). Sediment transport on an estuarine intertidal flat: Measurements and conceptual model of waves, rainfall and exchange with a tidal creek. Estuarine, Coastal and Shelf Science 72: 553-569.

Hagmeier, A., Kändler, R. (1927). Neue Untersuchungen im nordfriesischen Wattenmeer und auf den fiskalischen Austernbänken. Aus der Biologischen Anstalt auf Helgoland und deren Zweiglaboratorium in List auf Sylt 16.

Hamm, L., Capobianco, M., Dette, H.H., Lechuga, A., Spanhoff, R., Stive, M.J.F. (2002). A summary of European experience with shore nourishment. Coastal Engineering 47: 237-264.

Hapke, C. J. (2005). Estimation of regional material yield from coastal landslides based on historical digital terrain modelling. Earth Surface Processes and Landforms 30: 679-697.

Heiss, W. M., Smith, A.M., Probert, P.K. (2000). Influence of the small intertidal seagrass *Zostera novazelandica* on linear water flow and sediment texture. New Zealand Journal of Marine and Freshwater Research 34: 689-694.

Hemminga, M. A., Duarte, C.M. (Eds.) (2000). Seagrass Ecology. Cambridge University Press, Cambridge.

Herlyn, M., Millat, G. (2000). Decline of the intertidal blue mussel (*Mytilus edulis*) stock at the coast of Lower Saxony (Wadden Sea) and influence of mussel fishery on the development of young mussel beds. Hydrobiologia 426: 203-210.

Herlyn, M. (2005). Quantitative assessment of intertidal blue mussel (*Mytilus edulis* L.) stocks: combined methods of remote sensing, field investigation and sampling. Journal of Sea Research 53: 243-253.

Hertweck, G., Liebezeit, G. (2002). Historic mussel beds (*Mytilus edulis*) in the sedimentary record of a back-barrier tidal flat near Spiekeroog Island, southern North Sea. Helgoland Marine Research 56: 51-58.

Higelke, B. (1998). Morphodynamik des Lister Tidebeckens. In: Gätje, C., Reise, K. (Eds.). Ökosystem Wattenmeer - Austausch-, Transport- und Stoffumwandlungsprozesse. Springer, Berlin, Heidelberg, New York: 103-126.

Hofstede, J. L. A. (1997). Process-Response Analysis for the North Frisian Supratidal Sands (Germany). Journal of Coastal Research 13(1): 1-7.

Hofstede, J. L. A. (1999). Mögliche Auswirkungen eines Klimawandels im Wattenmeer. Petermanns Geographische Mitteilungen 143(4): 305-314.

Hofstede, J. L. A. (2002). Morphologic responses of Wadden Sea tidal basins to a rise in tidal water levels and tidal range. Zeitschrift für Geomorphologie 46(1): 93-108.

Houwing, E.-J. (2000). Morphodynamic development of intertidal mudflats: consequences for the extension of the pioneer zone. Continental Shelf Research 20: 1735-1748.

IPCC (Intergovernmental Panel on Climate Change) (2007). Climate Change 2007: Synthesis Report. Contribution of Working Groups I, II and III to the Fourth Assessment Report of the Intergovernmental Panel on Climate Change. Core Writing Team, Pachauri, R.K and Reisinger, A. (Eds.). IPCC, Geneva, Switzerland.

Isaaks, E. H., Srivastava, R.M. (Eds.) (1989). An Introduction to Applied Geostatistics. Oxford University Press, New York, Oxford.

Jacobsen, N. K. (1986). The intertidal sediments. Geografisk Tidsskrift 86: 46-62.

Jacobsen, N. K. (1998). The High Sands of the Danish Wadden Sea - Especially in the Ebb-Tide Delta, Soren Jessens Sande, and its Incorporation with the Island of Fano. Journal of Coastal Research 14(1): 175-184.

Janssen-Stelder, B. (2000). The effect of different hydrodynamic conditions on the morphodynamics of a tidal mudflat in the Dutch Wadden Sea. Continental Shelf Research 20: 1461-1478.

Jensen, J., Mügge, H.-M., Schönfeld, W. (1992). Analyse der Wasserstandsentwicklung und Tidedynamik in der Deutschen Bucht. Küste 53: 211-275.

Jepsen, P. U. (Ed.) (1977). Jordsand - Vogelinsel im Wattenmeer. Bygd, Esbjerb.

Jespersen, M., Rasmussen, E. (1975). Jordsand - Erosion und Akkumulation einer Hallig. Geografisk Tidsskrift 75: 13-23.

Jespersen, M., Rasmussen, E. (1984). Geomorphological effects of the Romo Dam: development of a tidal channel and collapse of a dike. Geografisk Tidsskrift 84: 17-24.

Jespersen, M., Rasmussen, E. (1989). Jordsand - ein Bericht über die Vernichtung einer Hallig im dänischen Wattenmeer. Seevögel - Zeitschrift Verein Jordsand 10(2): 17-25.

Kastler, T., Michaelis, H. (1999). The Decline of Seagrasses, *Zostera marina* and *Zostera noltii*, in the Wadden Sea of Lower Saxony. Senckenbergiana maritima 29 (Suppl.): 77-80.

Kelletat, D. (1989). Physische Geographie der Meere und Küsten - Eine Einführung. Teubner, Stuttgart.

Kelletat, D. (1995). Atlas of coastal geomorphology and zonality. Journal of Coastal Research(Special Issue No. 13 CERF): 286 pp.

Koch, E. W. (2001). Beyond Light: Physical, Geological, and Geochemical Parameters as Possible Submersed Aquatic Vegetation Habitat Requirements. Estuaries 24(1): 1-17.

Kolumbe, E. (1933). Ein Beitrag zur Kenntnis der Entwicklungsgeschichte des Königshafens bei List auf Sylt. Wiss. Meeresuntersuchung. N. F. Abt. Kiel 21: 116-130.

Kowalski, K. P., Wilcox, D.A. (1999). Use of historical and geospatial data to guide the restoration of a Lake Erie coastal marsh. Wetlands 19(4): 858-868.

Kroencke, I. (1994). Impact of biodeposition on macrofaunal communities in intertidal sandflats. Marine ecology 17(1-3): 159-174.

Lackschewitz, D., Reise, K. (1998). Macrofauna on flood delta shoals in the Wadden Sea with an undeground association between the lugworm *Arenicola marina* and the amphipod *Urothoe poseidonis*. Helgoländer Meeresuntersuchungen 52: 147-158.

Landesregierung S-H (- Ministerium für ländliche Räume, Landesplanung, Landwirtschaft und Tourismus des Landes Schleswig-Holstein) (2001). Generalplan Küstenschutz - Integriertes Küstenschutzmanagement in Schleswig-Holstein. Kiel.

Landesregierung S-H (- Minister für Landwirtschaft, Umwelt und ländliche Räume) (2007). Haushaltsmittel für den Küstenschutz. Drucksache 16/1203, Schleswig-Holsteinischer Landtag, Kiel.

Langhorne, D. N. (1982). A Study of the Dynamics of a Marine Sandwave. Sedimentology 29(4): 571-594.

Lanuru, M., Riethmüller, R., van Bernem, C, Heymann, K. (2007). The effect of bedforms (crest and trough systems) on sediments erodibility on a back-barrier tidal flat of the East Frisian Wadden Sea, Germany. Estuarine, Coastal, and Shelf Science 72: 603-614.

Larcombe, P., Ridd, P.V. (1995). Megaripple dynamics and sediment transport in a mesotidal mangrove creek: implications for palaeoflow reconstructions. Sedimentology 42: 593-606.

Larcombe, P., Jago, C.F. (1996). The morphological dynamics of intertidal megaripples in the Mawddach Estuary, North Wales, and the implications for palaeoflow reconstructions. Sedimentology 43: 541-559.

Larsen, M., Pejrup, M., Edelvang, K. (1996). A Fine-grained Sediment Budget for a small Tidal Area, Königshafen, Sylt, Germany. Danish Journal of Geography 96: 1-10.

Larson, M., Hanson, H., Kraus, N., Newe, J. (1999). Short- and Long-term Responses of Beach Fills Determined by EOF Analysis. Journal of Waterways, Port, Coastal, and Ocean Engineering 125(6): 285-293.

Li, R., Keong, C.W., Ramcharan, E., Kjerfve, B., Willis, D. (1998). A Coastal GIS for Shoreline Monitoring and Management - Case Study in Malysia. Surveying and Land Information Systems 58(3): 157-166.

Lindhorst, S., Fürstenau, J., Hass, C.H., Betzler, C. (in prep.). Anatomy of a hooked spit.

Lotze, H., Lenihan, H.S., Bourque, B.J., Bradbury, R.H., Cooke, R.G., Kay, M.C., Kidwell, S.M., Kirby, M.X., Peterson, C.H., Jackson, J.B.C. (2006). Depletion, Degredation, and Recovery Potential of Estuaries and Coastal Seas. Science 312: 1806-1809.

Lotze, H. K., Reise, K., Worm, B., van Beusekom, J.E.E., Busch, M., Ehlers, A., Heinrich, D., Hoffmann, R.C., Holm, P., Jensen, C., Knottnerus, O.S., Langhanki, N., Prummel, W., Vollmer, M., Wolff, W.J. (2005). Human transformations of the Wadden Sea ecosystem through time: a synthesis. Helgoland Marine Research 59: 84-95.

Lotze, H. K. (2005). Radical changes in the Wadden Sea fauna and flora over the last 2,000 years. Helgoland Marine Research 59: 71-83.

Mai, S. (1999). Die Sedimentverteilung im Wattenmeer: Ein Simulationsmodell. Berichte aus dem Fachbereich Geowissenschaften der Universität Bremen 142. Bremen.

Mai, S., Bartholomä, A. (2000). The missing mud flats of the Wadden Sea: a reconstruction of sediments and accommodation space lost in the wake of land reclamation. In: Flemming, B.W., Delafontaine, M.T., Liebezeit, G. (Eds.). Muddy Coast Dynamics and Resource Management: 257-272.

Marba, N., Cebrián, J., Enríquez, S., Duarte, C.M. (1994). Migration of large-scale subaqueous bedforms measured with seagrasses (*Cymodocea nodosa*) as tracers. Limnol. Oceanogr. 39(1): 126-133.

McCandliss, R. R., Jones, S.E., Hearn, M., Latter, R., Jago, C.F. (2002). Dynamics of suspended particles in coastal waters (southern North Sea) during a spring bloom. Journal of Sea Research 47: 285-302.

McCave, I. N., Geiser, A.C. (1978). Megaripples, ridges and runnels on intertidal flats of the Wash, England. Sedimentology 26: 353-369.

McGrorty, S., Goss-Custard, J.D. (1991). Population dynamics of the mussel *Mytilus edulis*: spatial variations in age-class densities of an intertidal estuarine population alon environmental gradients. Marine Ecology Progress Series 73: 191-202.

Meehan, A. J., Williams, R.J., Watford, F.A. (2005). Detecting Trends in Seagrass Abundance Using Aerial Photograph Interpretation: Problems Arising with the Evolution of Mapping Methods. Estuaries 28(3): 462-472.

Menn, I. (2001). Ecological comparison of two sandy shores with different wave energy and morphodynamics in the North Sea. PhD Thesis.

Menn, I. (2002). Beach morphology and food web structure:comparison of an eroding and an accreting sandy shore in the North Sea. Helgoland Marine Research 56: 177-189.

Michaelis, H., Obert, B., Schultenkoetter, I., Boecker, L. (1995). Die Miesmuschelbestände der niedersächsischen Watten, 1989-1991. Ber. Forschungsstelle Küste 40: 55-70.

Millat, G., Herlyn, M. (1999). Documentation of Intertidal Mussel Bed (*Mytilus edulis*) Sites at the Coast of Lower Saxony. Senckenbergiana maritima 29 (Suppl.): 83-93.

Mills, K. E., Fonseca, M. (2003). Mortality and productivity of eelgrass *Zostera marina* under conditions of experimental burial with two sediment types. Marine Ecology Progress Series 255: 127-134.

Moore, L. J. (2000). Shoreline Mapping Techniques. Journal of Coastal Research 16(1): 111-124.

Moore, L. J., Griggs, G.B. (2002). Long-term cliff retreat and erosion hotspots along the central shores of the Monterey Bay National Marine Sanctuary. Marine Geology 181: 265-283.

Nacken, M., Reise, K. (2000). Effects of herbivore birds on intertidal seagrass beds in the northern Wadden Sea. Helgoland Marine Research 54: 87-94.

Nehls, G., Thiel, M. (1993). Large-scale distribution patterns of the mussel *Mytilus edulis* in the Wadden Sea of Schleswig-Holstein: Do storms structure the ecosystem? Netherlands Journal of Sea Research 31(2): 181-187.

Nehls, G., Diederichs, A., Stoddard, P. (2002). Miesmuschelmonitoring im Nationalpark Schleswig-Holsteinisches Wattenmeer 2001. Bericht an das Landesamt für den Nationalpark Schleswig-Holsteinisches Wattenmeer. Hockensbüll.

Nehls, G., Ruth, M. (2004). Miesmuschelmonitoring und Miesmuschelmanagement im Nationalpark Schleswig-Holsteinisches Wattenmeer - Berichtszeitraum 1997 - 2002. Bericht an das Landesamt für den Nationalpark Schleswig-Holsteinisches Wattenmeer. Hockensbüll.

Nehls, G., Büttger, H. (2006). Miesmuschelmonitoring im Nationalpark Schleswig-Holsteinisches Wattenmeer 1998 - 2005. Bericht an das Landesamt für den Nationalpark Schleswig-Holsteinisches Wattenmeer. Hockensbüll.

Nehls, G., Diederich, S., Thieltges, D.W., Strasser, M. (2006). Wadden Sea mussel beds invaded by oysters and slipper limpets: competition or climate control? Helgoland Marine Research 60: 135-143.

Newell, C. R. (1999). The effect of current speed and particle concentration on mussel (*Mytilus edulis*) filtration rate: A recirculating flume study. Journal of Shellfish Research 18(1): 300.

Nienburg, W. (1927). Zur Ökologie des Wattenmeeres - 1. Teil: Der Königshafen bei List auf Sylt. Wiss. Meeresunters. (Abt. Kiel) 20: 146-196.

Obert, B., Michaelis, H. (1991). History and ecology of the mussel beds (*Mytilus edulis* L.) in the catchment area of a Wadden Sea tidal inlet. In: Elliott, M., Ducrotoy, J.-P. (Eds.). Estuaries and coasts. Spatial and Temporal Intercomparisons. Olsen & Olsen: 185-194.

Okun, N. (1999). Einfluß der Sedimentation auf die Miesmuschel (*Mytilus edulis* L.). Diploma thesis.

Oost, A., Becker, G., Fenger, J., Hofstede, J., Weisse, R. (2005). Climate.In: Essink, K., Dettmann, C., Farke, H., Laursen, K., Lüerßen, G., Marencic, H., Wiersinga, W. (Eds.). Wadden Sea Quality Status Report 2004. Common Wadden Sea Secretariat, Wilhelmshaven, Germany: 75-82.

Paarlberg, A. J., Knaapen, M.A.F., de Vries, M.B., Hulscher, S.J.M.H., Wang, Z.B. (2005). Biological influences on morphology and bed composition of an intertidal flat. Estuarine, Coastal and Shelf Science 64: 577-590.

Pasqualini, V., Pergent-Martini, C., Clabaut, P., Marteel, H., Pergent, G. (2001). Integration of Aerial Remote Sensing, Photogrammetry, and GIS Technologies in Seagrass Mapping. Photogrammetric Engineering & Remote Sensing 67(1): 99-105.

Pedersen, J. B. T., Bartholdy, J. (2006). Budgets for fine-grained sediment in the Danish Wadden Sea. Marine Geology 235: 101-117.

Pejrup, M. (1988). Suspended sediment transport across a tidal flat. Marine Geology 82: 187-198.

Pejrup, M., Larsen, M., Edelvang, K. (1997). A fine-grained sediment budget for the Sylt-Romo tidal basin. Helgoländer Meeresuntersuchungen 51: 253-268.

Philippart, C. J. M., Dijkema, K.S., van der Meer, J. (1992). Wadden Sea Seagrasses: Where and Why? Netherland Institute for Sea Research 20: 177-191.

Philippart, C. J. M. (1994). Interactions between *Arenicola marina* and *Zostera noltii* on a tidal flat in the Wadden Sea. Marine Ecology Progress Series 111: 251-257.

Philippart, C. J. M., Dijkema. K.S. (1995). Wax and wane of *Zostera noltii* Hornem. in the Dutch Wadden Sea. Aquatic Botany 49: 255-268.

Piersma, T., Koolhaas, A., Dekinga, A., Beukema, J.J., Dekker, R., Essink, K. (2001). Long-term indirect effects of mechanical cockle-dredging on intertidal bivalve stocks in the Wadden Sea. Journal of Applied Ecology 38: 976-990.

Pilkey, O. H., Cooper, J.A.G. (2004). Society and Sea Level Rise. Science 303: 1781-1782.

Polte, P., Schanz, A., Asmus, H. (2005). The contribution of seagrass beds (*Zostera noltii*) to the function of tidal flats as a juvenile habitat for dominant, mobile epibenthos in the Wadden Sea. Marine Biology 147: 813-822.

Polte, P., Asmus, H. (2006). Intertidal seagrass beds (*Zostera noltii*) as spawning grounds for transient fishes in the Wadden Sea. Marine Ecology Progress Series 312: 235-243.

Postma, H. (1981). Exchange of materials between the North Sea and Wadden Sea. Marine Geology 40: 199-213.

Postma, H. (1996). Sea-Level Rise and the Stability of Barrier Islands, with special reference to the Wadden Sea. In: Milliman, J.D., Haq, B.U. (Eds.). Sea-Level Rise and Coastal Subsidence, Kluwer Academic Publishers, Dordrecht: 269-280.

Rahmstorf, S. (2007). A Semi-Empirical Approach to Projecting Future Sea-Level Rise. Science 315: 368-370.

Rankey, E. C., Morgan, C. (2002). Quantified rates of geomorphic change on a modern carbonate tidal flat, Bahamas. Geology 30(7): 583-586.

Reineck, H.-E., Siefert, W. (1980). Faktoren der Schlickbildung im Sahlenburger und Neuwerker Watt. Die Küste 35: 26-51.

Reise, K. (1982). Long-term changes in the macrobenthic invertebrate fauna of the Wadden Sea: are polychaetes about to take over? Netherland Journal of Sea Research 16: 29–36.

Reise, K. (Ed.) (1985). Tidal Flat Ecology - An Experimental Approach to Species Interactions. Springer, Berlin, Heidelberg, New York.

Reise, K. (1998). Coastal Change in a Tidal Backbarrier Basin of the Northern Wadden Sea: Are Tidal Flats Fading Away? Senckenbergiana maritima 29: 121-127.

Reise, K. (Ed.) (2001). Ecological Comparisons of Sedimentary Shores. Ecological Studies 151. Springer, Berlin, Heidelberg, New York.

Reise, K. (2003). More sand to the shorelines of the Wadden Sea. In: Wefer, G., Lamy, F., Mantoura, F. (Eds.). Marine Science Frontiers for Europe. Springer, Berlin, Heidelberg, New York: 203-216.

Reise, K. (2005). Coast of change: habitat loss and transformations in the Wadden Sea. Helgoland Marine Research 59: 9-21.

Reise, K. (2006). Vorkommen von Grünalgen und Seegras im Nationalpark Schleswig-Holsteinisches Wattenmeer 2005. Forschungsbericht im Auftrag des Landesamtes für den Nationalpark Schleswig-Holsteinisches Wattenmeer, Tönning: 17 pp.

Reise, K., Herre, E., Sturm, M. (1989). Historical changes in the benthos of the Wadden Sea around the island of Sylt in the North Sea. Helgoländer Meeresuntersuchungen 43: 417-433.

Reise, K., Herre, E., Sturm, M. (1994). Biomass and abundance of macrofauna in intertidal sediments of Königshafen in the northern Wadden Sea. Helgoländer Meeresuntersuchungen 48: 201-215.

Reise, K., Gätje, C. (1997). The List tidal basin: a reference area for scientific research in the northern Wadden Sea. Helgoländer Meeresuntersuchungen 51: 249-251.

Reise, K., Lackschewitz, D. (1998). Benthos des Wattenmeeres zwischen Sylt und Romo. In: Gätje, C., Reise, K. (Eds.). Ökosystem Wattenmeer - Austausch-, Transport- und Stoffumwandlungsprozesse. Springer, Berlin, Heidelberg, New York: 55-64.

Reise, K., Lackschewitz, D. (2003). Combating habitat loss at eroding Wadden Sea shores by sand replenishment. In: Wolff, W.J., Essik, K., Kellermann, A., van Leeuwe, M.A. (Eds.). Challenges of the Wadden Sea. Proceedings of the 10th International Scientific Wadden Sea Symposium. Groningen 2000, Ministry of Agriculture, Nature Management and Fisheries, University of Groningen.

Reise, K., Dankers, N., Essink, K. (2005a). Introduced species. In: Essink, K., Dettmann, C., Farke, H., Laursen, K., Lüerßen, G., Marencic, H., Wiersinga, W. (Eds.). Wadden Sea Quality Status Report 2004. Common Wadden Sea Secretariat, Wilhelmshaven, Germany: 155-161.

Reise, K., Jager, Z., de Jong, D., van Katwijk, M., Schanz, A. (2005b). Seagrass. In: Essink, K., Dettmann, C., Farke, H., Laursen, K., Lüerßen, G., Marencic, H., Wiersinga, W. (Eds.). Wadden Sea Quality Status Report 2004. Common Wadden Sea Secretariat, Wilhelmshaven, Germany: 155-160.

Reise, K., Herre, E., Sturm, M. (2008). Mudflat biota since the 1930s: Change beyond return? Helgoland Marine Research 62: 13-22.

Reise, K., Kohlus, J. (2008). Seagrass recovery in the Northern Wadden Sea? Helgoland Marine Research 62: 77-84.

Ricklefs, K., Neto, N.E.A. (2005). Geology and Morphodynamics of a Tidal Flat Area along the German North Sea Coast. Die Küste 69: 93-128.

Riesen, W., Reise, K. (1982). Macrobenthos of the subtidal Wadden Sea: Revisited after 55 years. Helgoländer Meeresuntersuchungen 35(4): 409-423.

Riethmüller, R., Behrens, A., Gassenmaier, G., Gayer, G., Günther, H., Puls, W., Rosenthal, W., Rybaczok, R., Witte, G., Ziemer, F., Herbers, D., Baumert, H. (1999). The PROMISE/Sylt-Romo data set - a comprehensive bench-mark data set to test and evaluate numerical models for suspended sediment transport in shallow tidal lagoons. GKSS 99/E/53, Geesthacht.

Robbins, B. D. (1997). Quantifying temporal change in seagrass areal coverage: the use of GIS and low resolution aerial photography. Aquatic Botany 58: 259-267.

Röber, B., Rudolphi, H. (2004). Impacts of sea level changes on coastal regions: a local study for SEAREG. In: Schernewski G., Löser, N. (Eds.). Managing the Baltic Sea. Coastline Reports 2: 185 - 194.

Robinson, E. (2004). Coastal changes along the coast of Vere, Jamaica over the past two hundred years: data from maps and aerial photographs. Quaternary International 120: 153-161.

Rogers, S. S., Sandweiss, D.H., Maasch, K.A., Belknap, D.F., Agouris, P. (2004). Coastal change and beach ridges along the northwest coast of Peru: Image and GIS analysis of the Chira, Piura, and Colan beach-ridge plains. Journal of Coastal Research 20(4): 1102 - 1125.

Rubin, D. M., Hunter, R.E. (1987). Bedform Alignment in Directionally Varying Flows. Science 237: 276-278.

Ruth, M. (1998). Wadden Sea ecosystem research - sub-project Wadden Sea of Schleswig-Holstein. Investigations on the biology and fishery of blue mussels in the National Park Schleswig-Holstein Wadden Sea 73. Umweltbundesamt, Berlin.

Ryu, S. O. (2003). Seasonal variation of sedimentary processes in a semi-enclosed bay: Hampyong bay, Korea. Estuarine, Coastal and Shelf Science 56: 481-492.

Saier, B. (2001). Direct and indirect effects of seastars *Asterias rubens* on mussel beds (*Mytilus edulis*) in the Wadden Sea. Journal of Sea Research 46: 29-42.

Sanford, L. P., Panageotou, W., Halka, J.P. (1991). Tidal resuspension of sediments in northern Chesapeake Bay. Marine Geology 97(1-2): 87-103.

Schanz, A., Asmus, H. (2003). Impact of hydrodynamics on development and the morphology of intertidal seagrasses in the Wadden Sea. Marine Ecology Progress Series 261: 123-134.

Schanz, A., Reise, K. (2005). Seegras-Monitoring im Schleswig-Holsteinischen Wattenmeer - Forschungsbericht zur Bodenkartierung ausgewählter Seegraswiesen im Schleswig-

Holsteinischen Wattenmeer 2003. Bericht an das Landesamt für Natur- und Umwelt des Landes Schleswig-Holstein, Flintbek.

Schanz, A., Reise, K. (2006). Referenz und Klassifizierungsansatz für die Makrophytenvegetation des Nordfriesischen Wattenmeeres gemäß der Vorgaben der EG-Wasserrahmenrichtlinie (EGWRRL). Bericht an das Landesamt für Natur- und Umwelt des Landes Schleswig-Holstein, Flintbek.

Schlüter, M. (Ed.) (1996). Einführung in geomathematische Verfahren und deren Programmierung. Enke, Stuttgart.

Short, A. D. (Ed.) (1999). Handbook of Beach and Shoreface Morphodynamics. Wiley, Chichester, New York, Weinheim, Brisbane, Singapore, Toronto.

Short, F. T., Wyllie-Echeverria, S. (1996). Natural and human-induced disturbances of seagrasses. Environmental Conservation 23(1): 17-27.

Sterr, H., Ittekkot, V., Klein, R.J.T. (2000a). Weltmeere und Küsten im Wandel des Klimas. Petermanns Geographische Mitteilungen 143: 24-31.

Sterr, H., Klein, R., Reese, S. (2000b). Climate Change and Coastal Zones: An Overview of the State-of-the-Art on Regional and Local Vulnerability Assessment. In: FEEM Working Paper Series 38: 1-24.

Sterr, H. (2002). Climate Change Impacts on the Coastal Regions of Germany. In. Ewing L., Wallendorf, L. (eds.): Proceedings of Solutions to Coastal Disasters Conference 2002, Reston: 511-525.

Sterr, H. (2003). Geographische Charakterisierung der Nordseeregionen. In: Lozán, J., Rachor, E., Reise, K., Sündermann, J., von Westernhagen, H. (Eds.). Warnsignale aus Nordsee & Wattenmeer. Geo, Hamburg: 40-46.

Stoddard, P. (2003). Reconstruction of Blue Mussle Beds Using Aerial Photographs from 1989 and 2002 of the Northern Frisian Wadden Sea, Germany. Unpublished Report, BioConsult SH, Hockensbüll.

Strasser, M., Reinwald, T., Reise, K. (2001). Differential effects of the severe winter of 1995/96 on the intertidal bivalves *Mytilus edulis*, *Cerastoderma edule* and *Mya arenaria* in the Northern Wadden Sea. Helgoland Marine Research 55: 190-197.

Strasser, M., Hertlein, A., Reise, K. (2001). Differential recruitment of bivalve species in the northern Wadden Sea after the severe winter of 1995/96 and of subsequent milder winters. Helgoland Marine Research 55: 182-189.

Strasser, M., Dekker, R., Essink, K., Gunther, C.-P., Jaklin, S., Kroncke, I., Madsen, P.B., Michaelis, H., Vedel, G. (2003). How predictable is high bivalve recruitment in the Wadden Sea after a severe winter? Journal of Sea Research 49(1): 47-57.

Thiede, J., Ahrendt, K. (2000). Klimaänderung und Küste - Fallstudie Sylt. Teilprojekt: Klimabedingte Veränderung der Gestalt der Insel Sylt, BMBF 01LK9526. Abschlussbericht. Kiel.

Thieler, E. R., Danforth, W.W. (1994). Historical Shoreline Mapping (I): Improving Techniques and Reducing Positioning Errors. Journal of Coastal Research 10(3): 549-563.

Tolhurst, T. J., Black, K.S., Shayler, S.A., Mather, S., Black, I., Baker, K., Paterson, D.M. (1999). Measuring the in situ Erosion Shear Stress of Intertidal Sediments with the Cohesive Strength Meter (CSM). Estuarine, Coastal and Shelf Science 49: 281-294.

Townsend, E. C., Fonseca, M. (1998). Bioturbation as a potential mechanism influencing spatial heterogenity of North Carolina seagrass beds. Marine Ecology Progress Series 169: 123-132.

van de Koppel, J., Rietkerk, M., Dankers, N., Herman, P.M.J. (2005). Scale-Dependent Feedback and Regular Spatial Patterns in Young Mussel Beds. American Naturalist 165(3): E66-E77.

van de Koppel, J., Herman, P.M.J., Thoolen and H. P., C.H.R. (2001). Do alternate stable states occur in natural ecosystems? Evidence from a tidal flat. Ecology 82(12): 3449-3461.

van Katwijk, M. M., Vergeer, L.H.T., Schmitz, G.H.W., Roelofs, J.G.M. (1997). Ammonium toxicity in *Zostera marina*. Marine Ecology Progress Series 157: 159-173.

van Katwijk, M. M., Schmitz, G.H.W., Gasselink, A.P., van Avesaath, P.H. (1999). Effects of salinity and nutrient load and their interaction on *Zostera marina*. Marine Ecology Progress Series 190: 155-165.

van Katwijk, M. M., Hermus, D.C.R., de Jong, D.J., Asmus, R.M., de Jonge, V.N. (2000). Habitat suitability of Dutch Wadden for restoration of *Zostera marina* beds. Helgoland Marine Research 54: 117-128.

van Straaten, L. M. J. U., Kuenen, P.H. (1957). Accumulation of fine grained sediment in the Dutch Wadden Sea. Geol. Mijnb. 19: 329-354.

Volkenborn, N., Reise, K. (2006). Lugworm exclusion experiment: Responses by deposit feeding worms to biogenic habitat transformation. Journal of Experimental Marine Biology and Ecology 330: 169-179.

Walker, D. I., Hillman, K.A., Kendrick, G.A., Lavery, P. (2001). Ecological significance of seagrasses: Assessment for management of environmental impact in Western Australia. Ecological Engineering 16: 323-330.

Ward, L. G., Kemp, W.M., Boynton, W.R. (1984). The influence of waves and seagrass communities on suspended particulates in an estuarine embayment. Marine Geology 59: 85-103.

Wehrmann, A., Markert, A., Schmidt, A. (2007). Miesmuschelbank: ein verlorener Lebensraum? Die Einwanderung der Pazifischen Auster in das Wattenmeer und ihre Folgen. Natur- und Umweltschutz (Zeitschrift Mellumrat) 6(1): 10-14.

Weisse, R., von Storch, H., Feser, F. (2005). Northeast Atlantic and North Sea Storminess as Simulated by a Regional Climate Model during 1958-2001 and Comparison with Observations. Journal of Climate 3: 465-479.

Weisse, R., Plüß, A. (2006). Strom-related sea level variations along the North Sea coast as simulated by a high-resolution model 1958-2002. Ocean Dynamics 56: 16-25.

Widdows, J., Brinsley, M. (2002). Impact of biotic and abiotic processes on sediment dynamics and the consequences to the structure and functioning of the intertidal zone. Journal of Sea Research 48: 143-156.

Widdows, J., Lucas, J.S., Brinsley, M.D., Salkeld, P.N., Staff, F.J. (2002). Investigation of the effect of current velocity on mussel feeding and mussel bed stability using an annular flume. Helgoland Marine Research 56: 3-12.

Wohlenberg, E. (1937). Die Wattenmeer-Lebensgemeinschaften im Königshafen von Sylt. Helgoländer wissenschaftliche Meeresuntersuchungen 1: 1-92.

Wohlenberg, E. (1953). Sinkstoff, Sediment und Anwachs am Hindenburgdamm. Die Küste 2(2): 33-94.

Woth, K., Weisse, R., von Storch, H. (2006). Climate change and North Sea storm surge extremes: an ensemble study of storm surge extremes expected in a changed climate projected by four different regional climate models. Ocean Dynamics 56: 3-15.

Yang, B. C., Dalrymple, R.W., Chun, S.S. (2005). Sedimentation on a wave-dominated, open-coast tidal flat, south-western Korea: summer tidal flat - winter shoreface. Sedimentology 52: 235-252.

Zarillo, G. A. (1982). Stability of bedforms in a tidal environment. Marine Geology 48: 337-351.

Zhang, K., Douglas, B.C., Leatherman, St.P. (2004). Global Warming and Coastal Erosion. Climatic Change 64(1-2): 41-58.

Zwarts, L. (2003). Bodemgesteldheid en mechanische kokkelvisserij in de Waddenzee. RIZA Rapport. RIZA Lelystad.

## Web pages

www.colorado.edu (1994). The Geographer's Craft, Department of Geography, University of Colorado at Boulder, Glossary.
http://www.colorado.edu/geography/gcraft/gloss/glossary.html

www.syltinfo.de (2008). Orte auf Sylt.
http://www.syltinfo.de/content/view/286/42/

www.romo.dk (2008). Rømø – Tønder.
http://www.romo.dk/tyskland/de-de/menu/turist/regionen/roemoe/roemoe.htm

# Acknowledgements

I wish to thank Prof. Dr. Horst Sterr for taking on the supervision and for support but also for giving me the freedom I had in this study.

I am in particular deeply grateful to Prof. Dr. Karsten Reise for encouraging guidance and lots of valuable comments. Thanks for always taking your time helping me, for inspiration and for sharing your enthusiasm.

Thanks to Christian Hass who actually made this PhD position possible and obtained materials and equipment. I am thankful for getting insights in sedimentology, for support whenever I needed it and for all the possibilities I have got.

I owe particularly a great thanks to Christian Buschbaum for being the best office mate I could imagine. Thanks for reading and correcting lots of drafts of this thesis, for interesting insights on tidal flat biology, for statistical support and especially for inspiring talks on life and science while sharing litres of coffee.

Prof. Dr. Michael Schlüter is thanked a lot for his interest in my study and his generous and ungrudging help in geostatistical analysis. For further support in all kind of questions on GIS, I am grateful to Chris Cogan, Kerstin Jerosch and Christina Morchner.

I also wish to thank Justus van Beusekom for very constructive comments on two drafts and Nils Volkenborn for helping me with the first steps in statistics.

The secretariat, namely Kristin Kessenich and Gurdy Bardt, always helped with formal matters.

This study would not have been possible without the valuable data I received from external sources. Jörn Kohlus (Regional Office of the Schleswig-Holstein Wadden Sea National Park, Tönning), Lutz Christiansen (Regional State Office for the Rural Areas, Husum), Jens Sund Laursen (Sønderjyllands Amt, Tønder / Denmark) as well as Roland Doerffer (GKSS) and Desmond Murphy (Brockmann Consult) are acknowledged for providing aerial photographs. I am also thankful to Arfst Hinrichsen (Regional State Office for the Rural Areas, Husum) who supplied data files for the Digital Elevation Models and Gerhard Gayer (GKSS) for model data on current velocities and water depths. Ingrid Austen and Karl-Michael Felix are thanked for providing results and data of their sediment surveys. Georg Nehls (BioConsult SH) allocated GPS track files of mussel beds surveys, Dietlind Reuter (Deutscher Wetterdienst) long-term weather data, the Federal Maritime and Hydrographic Agency in Hamburg provided ice data and the Waterways and Shipping Board in Tönning supplied long-term data from the gauge List.

Field and lab work was supported by indispensable helpers. Thanks to Jan Fermer, Katrin Prinz, Patricia Graf, Johann Klages, Volker Wagner and Lars Konen. Thanks a lot!

In four years on Sylt, I have seen many people coming and leaving and the list of those who enriched live on the island is long. I can only give an abstract, but I would like to name a few: Sylvia (for a most appreciated warm welcome), Imme, Iris, Judith, Christian, Anke, Patrick, Moritz, Florian, Michael, Lars, Susanne, Tina … and especially Dina (for so much!).

My family is thanked for constant support during my whole studies and my friends on the mainland for understanding that I was so rarely available the last years.

Hiermit versichere ich, dass die vorliegende Dissertation selbständig von mir angefertigt wurde und dass sie nach Form und Inhalt meine eigene Arbeit ist. Sie wurde keiner anderen Stelle im Rahmen eines Prüfungsverfahrens vorgelegt. Dies ist mein einziges und bisher erstes Promotionsverfahren. Die Promotion soll im Fach Physische Geographie erfolgen. Des Weiteren erkläre ich, dass ich Zuhörer bei der Disputation zulasse.

Kiel, den 01. April 2008

Tobias Dolch